PNNL-37067
NREL/TP-6A40/92512

West Coast Offshore Wind Transmission Study

2025

T. Douville, K. Arkema, E. Boos, M. Daly, K. Oikonomou, C. Qin,
A. Rahman, E. Schweitzer, S. Siddiqui, B. Vyakaranam, K. Wilson
Pacific Northwest National Laboratory (PNNL)

G. Brinkman, S. Bredenkamp, R. Fuchs, C. Gschwend, J. Jorgenson,
T. Mai, C. Nguyen, B. Roberts, A. Rose, P. Sharma, H. Sun, G. Zuckerman
National Renewable Energy Laboratory (NREL)

Prepared for the U.S. Department of Energy
under Contract DE-AC05-76RL01830

PACIFIC NORTHWEST NATIONAL LABORATORY
operated by
BATTELLE
for the
UNITED STATES DEPARTMENT OF ENERGY
under Contract DE-AC05-76RL01830

Printed in the United States of America

Available to DOE and DOE contractors from
the Office of Scientific and Technical Information,
P.O. Box 62, Oak Ridge, TN 37831-0062
www.osti.gov
ph: (865) 576-8401
fox: (865) 576-5728
email: reports@osti.gov

Available to the public from the National Technical Information Service
5301 Shawnee Rd., Alexandria, VA 22312
ph: (800) 553-NTIS (6847)
or (703) 605-6000
email: info@ntis.gov
Online ordering: http://www.ntis.gov

PNNL-37067
NREL/TP-6A40/92512

West Coast Offshore Wind Transmission Study

Cover image reproduced with permission from Equinor

January 2025

T. Douville, K. Arkema, E. Boos, M. Daly, K. Oikonomou, C. Qin, A. Rahman, E. Schweitzer, S. Siddiqui, B. Vyakaranam, K. Wilson
Pacific Northwest National Laboratory (PNNL)

G. Brinkman, S. Bredenkamp, R. Fuchs, C. Gschwend, J. Jorgenson, T. Mai, C. Nguyen, B. Roberts, A. Rose, P. Sharma, H. Sun, G. Zuckerman
National Renewable Energy Laboratory (NREL)

Prepared for
the U.S. Department of Energy
under Contract DE-AC05-76RL01830

Pacific Northwest National Laboratory
Richland, Washington 99354

National Renewable Energy Laboratory
Golden, Colorado 80401

Acknowledgments

The authors would like to acknowledge the valuable guidance and input provided during this report. The authors are grateful to the following list of contributors. Their feedback, guidance, and review proved invaluable.

> Michael Abdelmalak, Fernando Bereta dos Reis, Cameron Bracken, Casey Burleyson, Allison Campbell, Holly Campbell, Tse-Chun Che, Sohom Datta, Kishan Prudhavi Guddanti, Kevin Harris, Li He, Jason Hou, Alicia Mahon, Sameer Nekkalapu, Tony Nguyen, Meghana Ramesh, Patrick Royer, Orestis Vasios, Shaobu Wang, Jan Westman, PNNL
>
> Mike Bannister, Dave Corbus, Paul Pinchuk, Clara Houghteling, Rebecca Green, Leonardo Rese, Lanaia Carveth, Shahil Shah, NREL
>
> Elaine Hart, Ana Mileva, Sylvan Energy Analytics
>
> Jeff Barton, Dmitry Kosterev, Richard Schafer Jr., Bonneville Power Administration
>
> Jeff Billinton, Ebrahim Rahimi, California Independent System Operator
>
> Scott Beyer, Fangfang Du, PacifiCorp
>
> Cindy Bothwell, Jian Fu, Jocelyn Brown-Saracino, Hannah Taylor, Liz Hartman, Wind Energy Technologies Office
>
> Alissa Baker, Katie Segal, Grid Deployment Office
>
> All members of the West Coast Offshore Wind Transmission Study Advisory Committee

This report was prepared by the Pacific Northwest National Laboratory and the National Renewable Energy Laboratory for the U.S. Department of Energy, Grid Deployment Office.

Acronyms and Abbreviations

AC	Alternating Current
ADS	Anchor Data Set
AOSWTS	Atlantic Offshore Wind Transmission Study
AS	Ancillary Services
BA	Balancing Authority
BESS	Battery energy storage systems
BOEM	Bureau of Ocean Energy Management
BPA	Bonneville Power Administration
BPAT	Bonneville Power Administration Transmission Balancing Authority
BTM	Behind the meter
CA	California
CAISO	California Independent System Operator
CC	Combined cycle turbine
CCS	Carbon Capture and Storage
CEM	Capacity expansion model
CIPB	Pacific Gas & Electric Bay Area Balancing Authority
COI	California-Oregon Intertie
C-PAGE	Chronological Alternating Current Power Flow Automated Generation
CT	Combustion turbine (peaking unit)
CV	Cross-validation
DC	Direct Current
DCAT	Dynamic Contingency Analysis Tool
DDVM	Data Development and Validation Manual
DoD	Department of Defense
DOE	Department of Energy
dPV	Distributed photovoltaic
DR	Demand response
EGRASS	Electrical Grid Resilience and Assessment System
ELCC	Effective Load Carrying Capability
ESI	Environmental Sensitivity Index
FERC	Federal Energy Regulatory Commission
FOR	Forced outage rate
GEO	Geothermal
GHG	Greenhouse gas
GIS	Geospatial Information System

GODEEEP	Grid Operations, Decarbonization, Environmental and Energy Equity Platform
GW	Gigawatt
H2	Hydrogen
H2-CT	Hydrogen-fueled combustion turbine
HMS	Highly migratory species
HVAC	High Voltage Alternating Current
HVDC	High Voltage Direct Current
IBR	Inverter-based resource
InVEST	Integrated Valuation of Ecosystem Services and Tradeoffs
IO	Input-Output
LCOE	Levelized cost of energy
LBW	Land-based wind
LMP	Locational marginal price
LOLE	Loss of Load Expectation
MAPE	Mean Absolute Percentage Error
ML	Machine learning
MLP	Multi-layered perceptron
MPA	Marine Protected Area
MTDC	Multi-Terminal, Direct Current
MW	Megawatt
MWh	Megawatt-hour
NERC	North American Reliability Corporation
NIFC	National Interagency Fire Center
NMS	National Marine Sanctuary
NOAA	National Oceanic and Atmospheric Administration
NPV	Net Present Value
NREL	National Renewable Energy Laboratory
NSRDB	National Solar Radiation Data Base
NTP	National Transmission Planning Study
NW	Northwest
O&M	Operations and maintenance
ORNL	Oak Ridge National Laboratory
OSW	Offshore Wind
PAC	PacifiCorp
PACE	PacifiCorp East Balancing Authority
PACW	PacifiCorp West Balancing Authority
PCDS	Production Cost Data Subcommittee

PCM	Production cost models
PDCI	Pacific Direct Current Intertie
PESGM	Power & Energy Society General Meeting
PNNL	Pacific Northwest National Laboratory
PNW	Pacific Northwest
POI	Points of Interconnection
PSH	Pumped storage hydropower
PSLF	Positive Sequence Load Flow
PV	Photovoltaic
QGIS	Quantum Geographic Information System
RA	Resource Adequacy
ReEDS	Regional Energy Deployment System
TEAM	Transmission Economic Assessment Methodology
TELL	Total ELectricity Loads
TGW	Thermodynamic Global Warming
TLP	Tension leg platforms
USACE	United States Army Corps of Engineers
USGS	United States Geological Survey
VMS	Vessel Monitoring System
VRE	Variable Renewable Energy
WA	Washington state
WECC	Western Electricity Coordinating Council
WI	Western Interconnection
WiRES	Wildfire Risk Estimation for Energy Systems
WRF	Weather Research and Forecasting

Executive Summary

Fueled by strong ocean winds, transmission of offshore wind (OSW) power on the U.S. West Coast holds the potential to deliver electricity when and where it is needed and reduce overall costs of electricity supply to western states. However, capturing these benefits requires intentional planning and the maturation of burgeoning technologies. It is the overarching ambition of this study to inform such efforts for system planners, industry, and energy policymakers at Federal, Tribal, state, and local levels. For this reason, the work was guided by an Advisory Committee of over 100 active members and five focused subgroups on the topics of planning, system operations, environment and siting, technology, and community values.

Approach

The study addressed the following knowledge gaps, identified through review of work to date:

- **Optimization of generation and transmission capacity** was conducted, spanning the Western Interconnection over the years 2025–2050. These models accounted for state energy legislation, national electricity emissions reductions of 90% by 2035 and 100% by 2045 (advised by the Advisory Committee and consistent with the core scenarios of the National Transmission Planning Study), restrictive siting of future land-based renewable energy, and the projected cost of all technologies. The resulting least-cost systems included **15 GW of West Coast OSW in 2035** (13 in California, 2 in Oregon) **and 33 GW in 2050** (25 in California, 6 in Oregon, 2 in Washington)**.** Total generation expansions of approximately 200 GW by 2035 and 400 GW by 2050 were also incorporated.
- **Geospatial analysis across the West Coast** guided the creation of five plausible offshore wind generation and transmission topologies to deliver this energy to onshore Points of Interconnection (POIs). Plans of system operators, projected interconnection capacity, federal lease activities, floating OSW technology readiness, and ocean co-use were incorporated in potential generation and transmission footprints, such as shown in Figure ES. 1. These topologies corresponded to alternate strategies for OSW development that could be pursued.
- **Pathways for development** were defined and compared. In 2035, the Concentrated Topology

Figure ES. 1. Excerpt of 2050 Interregional Topology interconnected through five POIs and the Distributed Topology utilized nine POIs. In 2050, Radial, Intraregional, and Interregional Topologies were developed with the prior POIs, generation footprints, and power injections but incorporated distinct strategies for transmission coordination, demonstrating how the system could develop over time. The 2050 Radial Topology may be non-optimal but represents a potential future without coordinated planning. Together both the 2035 topologies and the three potential 2050 topologies represented **six discrete pathways for OSW development from 2035 to 2050** (Figure ES. 2). Models of these topologies were created to assess the least-cost dispatch of future generation and transmission resources to reliably serve future electricity demand. Costs of each topology were estimated and economic value of OSW transmission within and between regions was examined.

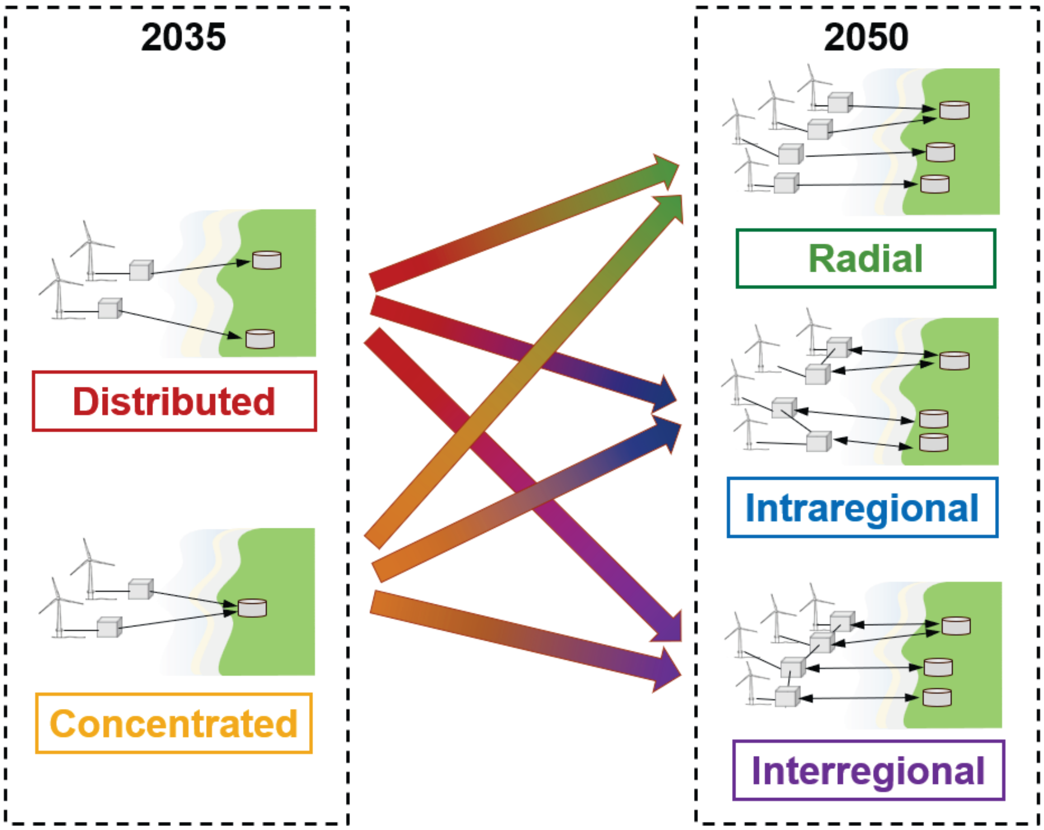

Figure ES. 2. Six development pathways, 2035-2050, examined in this study

- **Reliability and resilience of each transmission topology** were assessed. Critical contingencies, informed by system operators along the West Coast, were simulated across 50 representative hours of the annual dispatch solutions. System reinforcements and redispatch solutions were identified to support acceptable system response. Critical wildfire contingencies were assessed. Short circuit ratios were analyzed at POIs.
- **Community perspectives** were considered by evaluating the potential influence of OSW topologies on ecosystem services. An advisory group prioritized three services for this study. Natural capital models were developed to characterize coastal risk, energy resilience, and fisheries.

In addressing these gaps, this study indicates that **West Coast OSW transmission could deliver not only OSW energy but valuable contributions to a reliable, resilient, cost-effective, and clean Western Interconnection**.

Key Findings

Coordinated West Coast OSW transmission holds strong economic value.

Six development pathways were evaluated. Pathways leading to Interregional and Intraregional Topologies in 2050 have significant benefits-cost advantages over those leading to the Radial Topology in 2050, as seen in Figure ES. 3. These four pathways indicated net benefits exceeding $14 billion in net present value (NPV). Production cost benefits exceeded the combined costs of offshore transmission development and the costs of onshore system reinforcements to maintain reliability. The main source of the benefits accruing through the 2050 topologies was the use of the transmission to share lower-cost generation across regions. The least cost pathway observed was the 2035 Distributed Topology to 2050 Interregional Topology, which delivered $25B (2024$) in net present value over the 2050 Radial Topology.

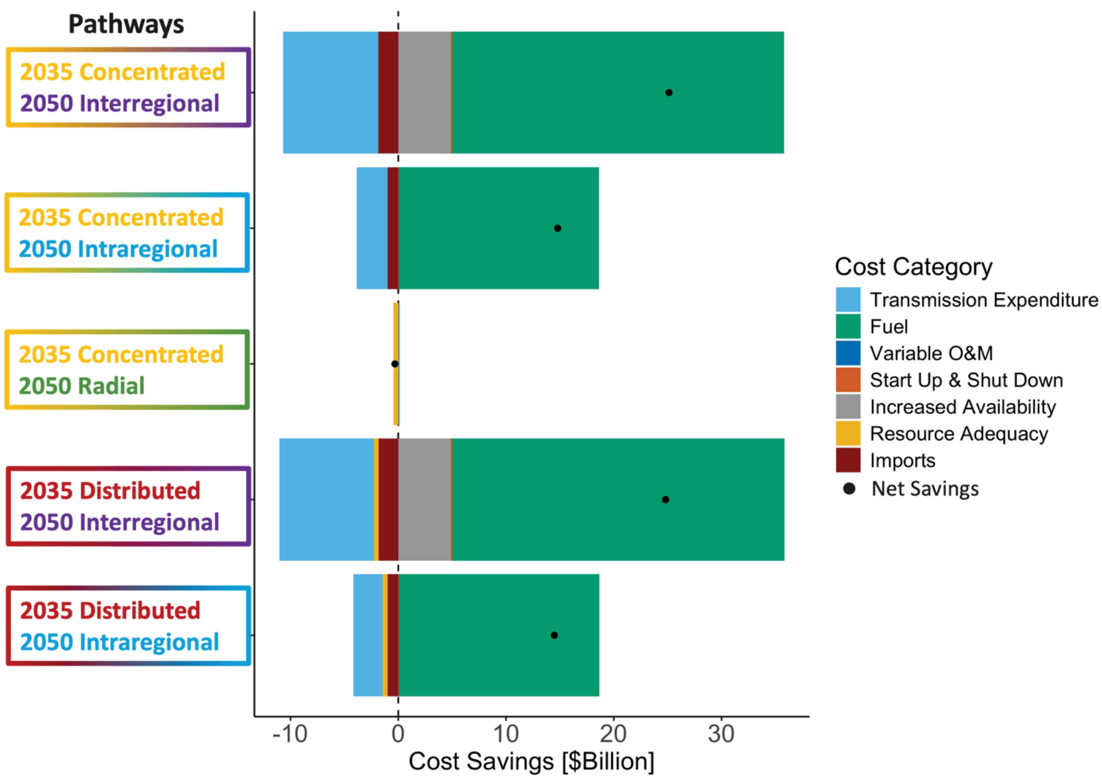

Figure ES. 3. System-wide lifecycle cost savings NPV of five pathways relative to the 2035 Distributed to 2050 Radial pathway

Black dot indicates the net savings across all cost categories. Reduced imports relative to the reference pathway are from Canada and Mexico. Reduced resource adequacy value is shown relative to the reference pathway, though all are adequate. Savings are primarily derived from less fuel use and increased availability under re-dispatch during a forced outage of export cables to the coast.

Alternate strategies in 2035 yield similar system net benefits but varying community benefit potential, without restricting long-term benefits.

Though higher ocean transmission costs are incurred through distributing power over more POIs (and thus more communities) in the 2035 Distributed Topology, the higher cost of reliability reinforcements in the 2035 Concentrated Topology bring the total costs into alignment. If net benefits can be preserved for coastal communities, there may be advantages to Distributed over Concentrated interconnections in 2035 to yield benefits to more coastal communities and increase energy resilience by spreading risk and harnessing greater geographic diversity of the OSW resource, without compromising benefits of 2050 futures.

Large geographic differences in benefits are observed between various 2050 futures, which are traced to differences of where congestion may be experienced. If congestion occurs along a transmission corridor without alternate paths for power flow, consumers in particular regions may bear unavoidable congestion costs. Further, if the pace of transmission development is not consistent across the West Coast, unintended cost penalties may be imposed. Transmission planners could account for the disaggregation of benefits, including outside of their region, to avoid such unintended cost impacts.

The benefits of OSW transmission depend on the fuel cost of dispatchable resources and the future buildout of transmission in the Western Interconnection. While coordinating OSW transmission within or between regions reduces production costs, this cost advantage is less pronounced in a future where dispatchable hydrogen combustion becomes cheaper by 2050. This suggests that dispatchable generation fills a role similar to coordinated electricity generation and transmission from variable energy sources. Greater use of the OSW transmission network is observed when onshore transmission is de-rated, suggesting that OSW transmission may provide additional value if future buildout of the onshore bulk transmission system is slowed due to permitting, wildfire, or other development risk.

Though the capacity contribution of West Coast OSW generation is shown to be robust, **the capacity value of offshore transmission networks is dependent on the level of onshore transmission and generation**. For the topologies studied in 2050, offshore transmission networks do not provide incremental capacity value on the West Coast. This is due to significant onshore transmission capacity which was modeled to yield 100% clean electricity by 2045 and meet growing energy demand through 2050.

Approximately 30 GW of OSW could be deployed into the most economically favorable areas around California and southern Oregon, after considering ocean co-uses and complex bathymetry. Associated turbine, cable, and substation infrastructure can be planned in this area. To exceed this amount of OSW would require deploying resources in alternative locations, including waters deeper than 1,300 meters and further from shore, or waters to the north with lesser quality wind resource. Both options would incur greater cost of energy. Figure ES. 4 depicts the geospatial analysis assumptions.

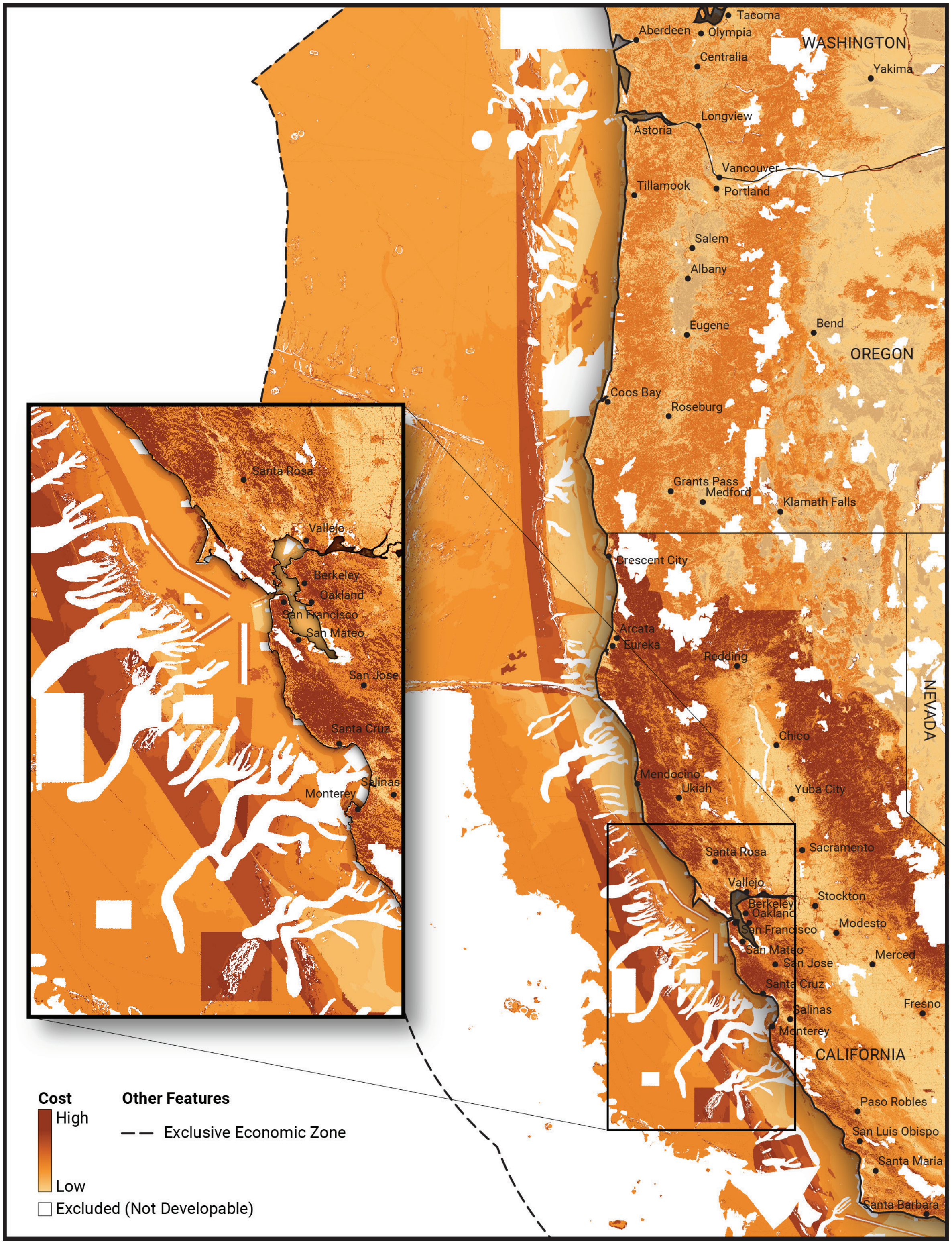

Figure ES. 4. Cost surface in offshore and land-based areas used for cable routing.

This work stands as a reference for further planning of transmission systems for incorporating OSW into the West Coast power system. Although this is not a siting study, challenges and opportunities for deploying (and interconnecting) 33 GW of OSW off the West Coast by 2050 were identified. Coordinated transmission planning, and offshore topologies involving High-Voltage Direct Current (HVDC) networking (onshore or offshore), are shown to be potentially beneficial to the future grid. In the near term, a variety of options for interconnection exist (including longer cables offshore or onshore and various POIs), and non-grid benefits may tip the scales on which interconnection plans are the most favorable, holistically, for the West Coast. Lastly, future planning could similarly consider pathways for system development such as shown in Figure ES. 5, defining near-term actions which support near-term net benefits and preserve the option for long-term net benefits for coastal communities and western states.

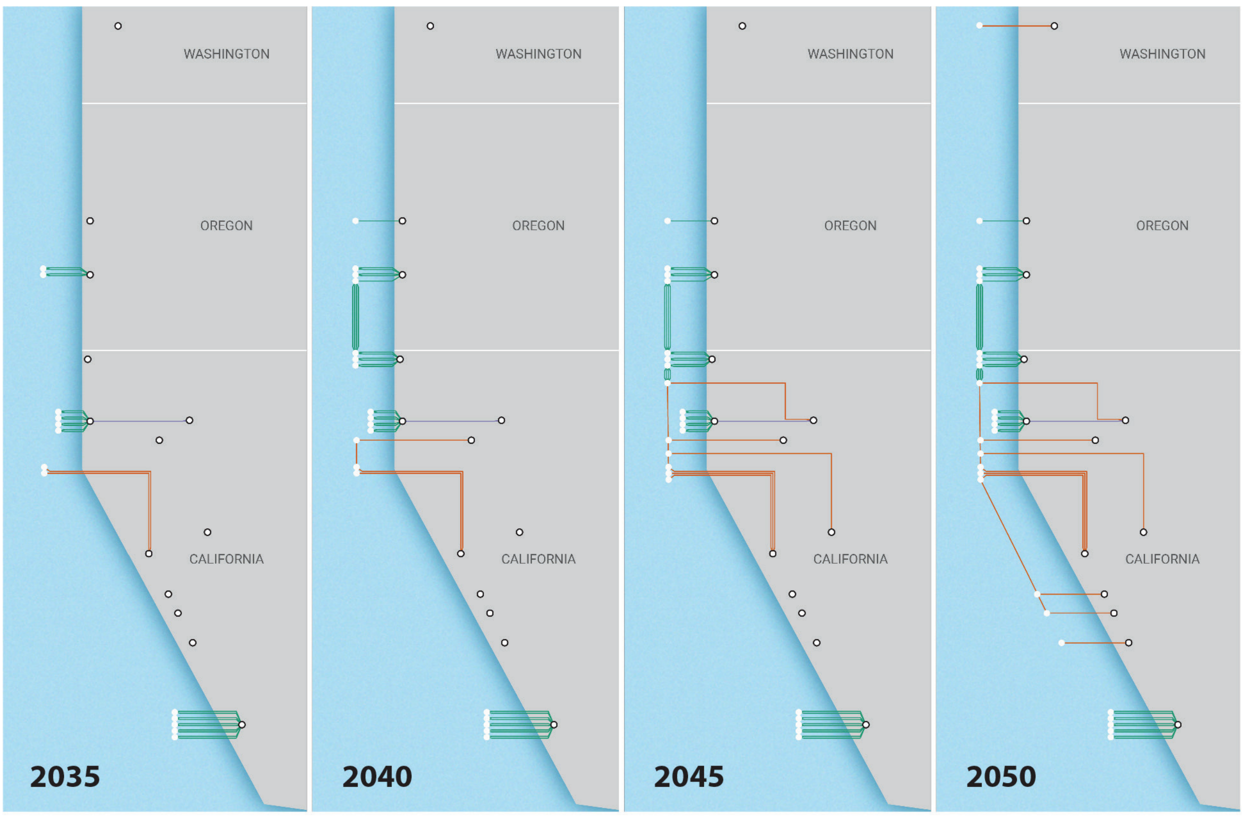

Figure ES. 5. Phased transition from 2035 Concentrated to 2050 Interregional Topology Sets. Orange lines are assumed to be HVDC; green lines are alternating current.

Contents

Figures

Tables

1.0 Introduction

Outlined against U.S. state and federal energy goals, West Coast offshore wind (OSW) transmission is poised to harness an untapped energy resource and lower the costs of electricity production in the Western Interconnection (WI). West Coast OSW power offers compelling attributes to the generation mix, namely robust capacity contributions that complement the existing generation fleet, and the injection of power into underdeveloped sections of the onshore grid (Douville and Bhatnagar 2021; Douville et al. 2024; Jorgenson et al. 2021).

However, the latter of these attributes underscores an acute challenge for West Coast OSW development. Precisely where the resource is strongest, limited onshore transmission exists to support the interconnection of large generation. Though system operators have been responsive to requests by OSW interconnection applicants or proactive state-led electric grid planning processes, broad planning across the West Coast has not been completed (CAISO 2024). Meanwhile, noting the benefits and the prevalence of the national OSW resource in deep waters requiring floating infrastructure, the Biden-Harris Administration established a national goal to develop 15 GW of floating OSW by 2035 and the U.S. Department of Energy (DOE) created the Floating Offshore Wind Shot. For these reasons and to evaluate various strategies to OSW transmission development across the U.S. West Coast from 2035 to 2050, the U.S. DOE Grid Deployment Office and Wind Energy Technologies Office launched the West Coast Offshore Wind Transmission Study (WOW-TS) in May 2023.

1.1 State of West Coast OSW

Over the next 10 years, competitive opportunities for floating offshore wind deployment are expected on the West Coast. On December 2022, the Bureau of Ocean Energy Management (BOEM) leased federal water for OSW plant development in Morro Bay and Humboldt, California to five developers for a total of $757 million dollars BOEM (2022). The two leases in Humboldt and three leases near Morro Bay hold the potential for approximately 3 gigawatts (GW) and 5 GW, respectively (see Section 3.1). The California Independent System Operator (CAISO) board of governors has also approved the construction of $4.59 billion of North Coast OSW transmission to enable OSW development as indicated in the CAISO 2023-2024 Transmission Plan (ISO Staff 2024). In the Northwest, an auction for 3.1 GW of Oregon lease areas was postponed in September 2024 (BOEM 2024b). Oregon is now composing an Offshore Wind Energy Roadmap (Oregon.gov 2024). Additional leasing activity will be required to support California's OSW procurement goal of 7.6 GW (Assembly Bill [AB] 1373) and California's and Oregon's offshore wind planning goals of 25 GW by 2045 (AB 525) and 3 GW by 2030 (House Bill 3375 2021), respectively.

1.2 Scope and Objectives

As floating OSW has emerged as a potential large-scale source of electricity on the West Coast, transmission system operators, transmission planners, national laboratories, consultants, and academics have conducted transmission studies to assess system impacts and plan for the integration of offshore wind. The West Coast Offshore Wind Literature Review and Gaps Analysis reviewed these studies. It concluded that West Coast OSW transmission offers a clean-slate opportunity to plan for community benefits and ocean co-use, minimum investment and production cost considering other potential sources of power generation, emerging resilience threats, and the pending growth and shift of electricity demand patterns (Douville et al. 2023). The primary objective of the West Coast OSW Transmission Study (WOW-TS) is to explore this opportunity and support recommendations for action.

The following guiding questions emerged from the gaps analysis and framed the study effort:

- What role could West Coast offshore wind play in the generation mix in 2035 and 2050? Within the context of other types of clean energy generation, what are the west coast-wide offshore wind installed capacity contributions toward meeting state and federal clean energy goals through 2050?
- Where might the generation and transmission infrastructure be developed? What deployment pathways emerge from nodal representations of offshore transmission and generation from 2035 to 2050?
- How does the Western Interconnection (WI) function in 2035 and 2050 with offshore wind contributions? What is the nodal composition of WI generation and transmission resources which meet adequacy, contingency, steady-state and transient stability requirements?
- How do these 2035 and 2050 WI resources perform under resilience events?
- What are the technoeconomic and socioeconomic benefit-costs tradeoffs of varying (i) points of interconnection and cable routing strategies and (ii) degrees of coordinated transmission (i.e., radial vs. "within region" vs. "between regions")?

WOW-TS informs these questions through the use of industry tools and state-of-the-science methods. It does not replace studies by utilities, developers, and regional transmission organizations in addressing these questions, as indicated in Table 1.

Table 1. Specification of WOW-TS scope

What the study is	What the study is not
WOW-TS presents a big-picture analysis of the potential siting challenges offshore for both turbines and cable routes.	The study is not a permitting or detailed siting study for any specific project. Real projects will need to do geophysical studies and surveys.
WOW-TS performs detailed power flow analysis for offshore wind injections at a suite of POIs that are identified as potentially favorable POIs to assess these questions.	The study should not be considered a prescription or specific suggestion for these POIs or topologies.
WOW-TS compares the benefits and costs of various topologies assuming market structures exist to trade power and ancillary services efficiently.	The study does not evaluate how and when market structure will change as today's market structure may not be able to take full advantage of some of the transmission topologies.

This study is not a detailed siting or permitting-style study, and the Points of Interconnection and topologies are developed to assess big-picture questions and should not be considered prescriptive or as specific suggestions.

1.3 Advisory Committee

The WOW-TS was guided through a general Advisory Committee of approximately 100 active members representing Tribal Nations, coastal communities, states, system operators, project developers, Original Equipment Manufacturers, federal agencies, environmentalists, and others. The general Advisory Committee was briefed throughout the project on a quarterly basis. In addition, the following five subgroups were formed and met on an ad-hoc basis during the study:

- System Operators—invited grid planners from the Load Serving Entities and Balancing Authorities with interest in OSW along the West Coast.
- Planning—open to all general Advisory Committee participants with an interest or expertise in the evolution of electricity demand and supply and supporting transmission.
- Environment and Siting—open to all general Advisory Committee participants with an interest or expertise in marine and coastal environmental and ocean co-use impacts of OSW generation and transmission development.
- Technology—open to all general Advisory Committee participants with an interest or expertise in floating OSW generation and transmission technology.
- Community Values—invited representatives from Tribal Nations, coastal communities, and state agencies with an interest or expertise in impacts (benefits and costs) of OSW generation and transmission development to coastal communities.

In addition to the Advisory Committee, the WOW-TS work was presented through the West Coast OSW Transmission Convening series of workshops and other forums through 2024.

1.4 Outline of this Report

The work of the WOW-TS is presented in the following seven main chapters and supporting appendices and conclusions are posed in chapter nine.

- Chapter Two describes the capacity expansion modeling which framed the generation targets in 2035 and 2050 for the detailed topology set definitions and modeling.
- Chapter Three describes the geospatial considerations which resulted in plausible definitions of OSW generation and transmission along the West Coast considering many co-uses of the ocean and environmental impacts.
- Chapter Four describes the topology sets in 2035 and 2050 which incorporate system operator plans, support state goals for energy deployment, and match the least-cost capacity expansion builds.
- Chapter Five describes the production cost and resource adequacy models and simulations which characterized each topology set and its impact in the three west coast states and overall production costs of the WI.
- Chapter Six describes the reliability and resilience analyses, which were coordinated with system operators and led to discrete system reinforcements for each topology set.
- Chapter Seven describes the economic analysis at system scale and disaggregated by region and generators, transmission owners, or load-serving entities.
- Chapter Eight describes the community value analysis leveraging detailed natural capital modeling of three ecosystem services prioritized by the Advisory Committee subgroup.

2.0 Power System Evolution for 2035 and 2050

This forward-looking study was designed to assess the potential impacts of offshore wind deployment in the Western United States. There is always uncertainty in how the power system may evolve over time. To study a possible power system evolution through the future years of 2035 and 2050, we used a generator, transmission, and storage build-out from the ReEDS capacity expansion model (CEM) (Ho et al. 2021). ReEDS simulates planning and operation decisions of the electric power system for the continental United States for decades into the future. It is formulated as linear optimization program that determines least-cost investment and operation of the power system, while adhering to key constraints, including physical, operational, reliability, and policy considerations. The primary goal of the capacity expansion analysis was to create a feasible future power system with a significant, though attainable, amount of offshore wind deployment in the West for the detailed power system and transmission studies covered in the remainder of the report.

2.1 Key Inputs and Assumptions

Floating offshore wind deployment has made strides but still requires considerable technology cost reductions(U.S. DOE n.d.). In order to see sustained development in the study years of 2035 and 2050, we developed a set of conditions for the capacity expansion analysis that represent favorable conditions for offshore wind growth. The future scenarios include the following key assumptions:

- **Annual Technology Baseline** 2023 Moderate cost projections for all generation and storage technologies, including offshore wind (NREL 2023).
- **National clean electricity policy** of 90% reduction in electricity sector carbon dioxide emissions (relative to 2005) achieved by 2035, 100% by 2045. This assumed reduction is overlaid on top of existing state renewable portfolio standards and clean energy standards in the Western states (LBNL 2024). These assumptions were advised by the Advisory Committee and consistent with the central decarbonization scenarios of the recent National Transmission Planning Study (U.S. DOE 2024).
- **Demand growth and electrification:** electricity demand is assumed to grow to nearly 1,300 TWh for the West in 2050 which corresponds to a compound annual growth rate of 2.2% between 2021 and 2050. This represents Evolved Energy Research’s Mid Case (Bistline et al. 2023), shown in Figure 1 for the West, as well as the three coastal states. Major data center demand growth is not incorporated into this projection.
- **Limited access for land-based renewable energy sources:** Limited siting assumptions allow less land-based wind and utility-scale photovoltaic resources (Zuckerman et al. 2023).
- **Low-carbon emissions technology restrictions:** We did not allow ReEDS to invest in currently nascent technologies such as nuclear small-modular reactors or carbon-dioxide removal technologies such as direct air capture or carbon capture and sequestration.
- **Other assumptions are consistent with Standard Scenarios 2023** (Gagnon et al. 2024).
- **Offshore wind target for the coastal states** which totals 15 GW by 2035 (13 GW in California, 2 GW in Oregon) and 33 GW by 2050 (25 GW in California, 6 GW in Oregon, and 2 GW in Washington). The origin of this target is discussed in Section 2.2.

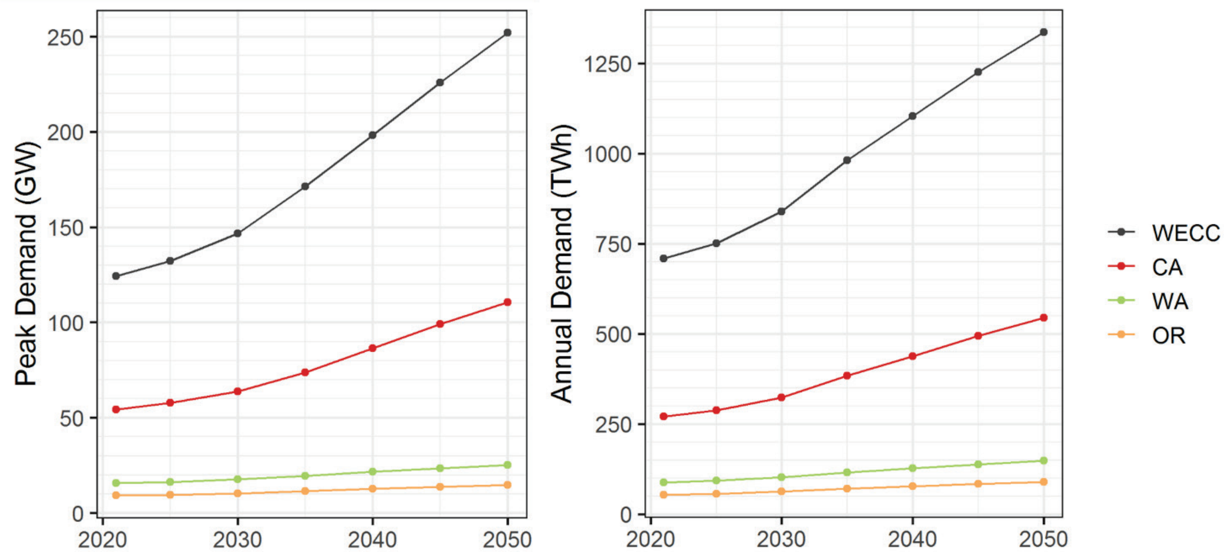

Figure 1. Assumed load growth for the footprint of the Western Interconnection (WI) and the West Coast states assumed through 2050.

2.2 Offshore Wind Deployment Trajectory

The capacity expansion modeling also included an explicit trajectory for offshore wind deployment in the West. This trajectory, shown in Figure 2 and highlighted in black, was informed by existing analysis, enacted policy, and stakeholder feedback. Figure 2 also shows enacted and previous analysis policy (on the west coast, and across the country) for comparison. It is a target for offshore wind capacity that the CEM must deploy, although the model could choose to build more if economical. We also completed dozens of exploratory runs with ReEDS to find reasonable bounds for offshore wind deployment in the West. Figure 3 shows the wide range of offshore wind deployment. The lowest amount of deployment (around 4.7 GW as influenced by California's state goals, shown in red) is achieved under "Base" conditions, with no additional carbon reduction trajectory beyond existing state goals. In a case with the 100% by 2045 carbon reduction trajectory and limited options for other low carbon technologies (restricted siting for land-based with and PV, along with no CCS and nuclear deployment), over 20 GW of offshore wind deployment is achieved (shown in yellow). Finally, with those same conditions and with an advanced reduction in the cost for floating offshore wind, around 33 GW of deployment is achieved by 2050, which aligns with the target imposed in this study.

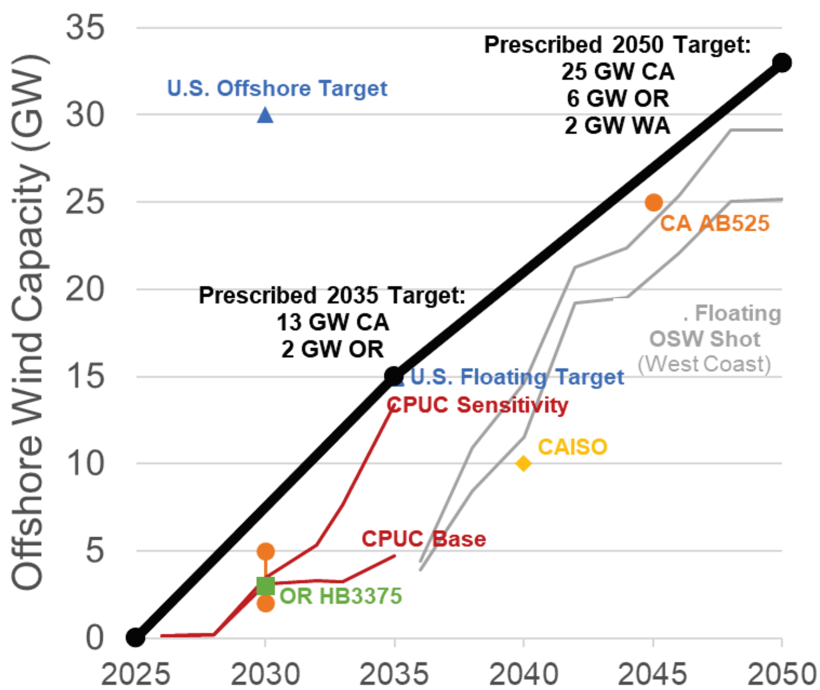

Figure 2. Enacted policy and analysis considering offshore wind estimates as of 2023.

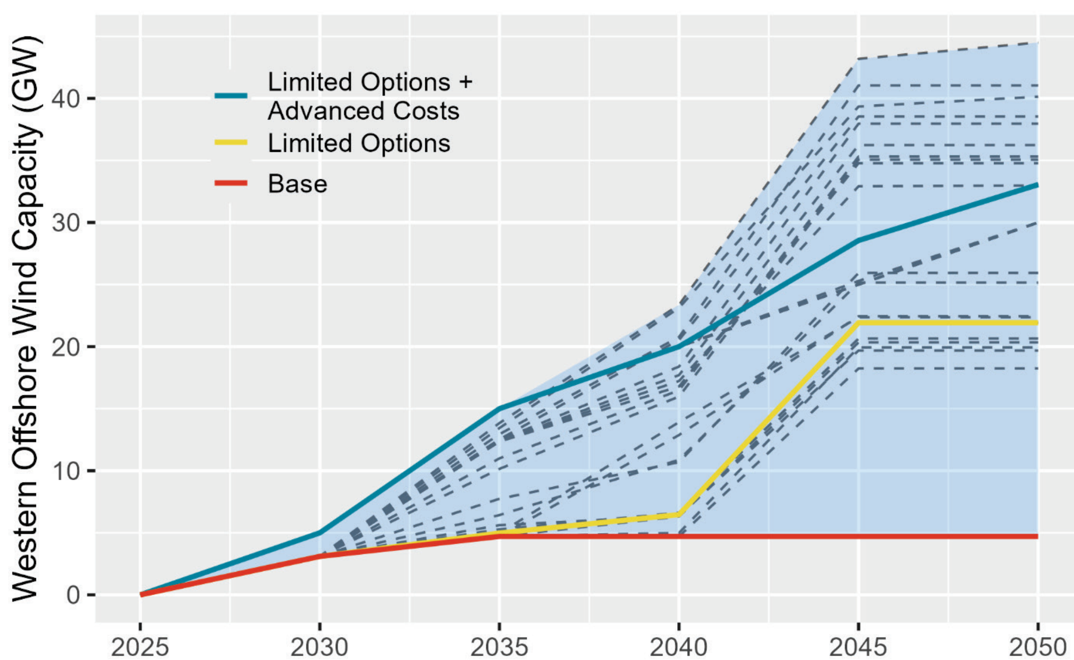

Figure 3. Exploratory CEM results illustrating the 33 GW target as a reasonable trajectory for this study. “Base” case represents default CEM settings. “Limited Options” restricts builds of carbon capture and sequestration technologies, nuclear capacity, and limits the siting options of land-based wind and solar. “Limited Options + Advanced Costs” represents the same technology restrictions plus uses an advanced reductions in the cost trajectory for floating offshore wind.

2.3 ReEDS Model

The ReEDS CEM simulates planning decisions for the continental United States and has been used for high-impact studies examining the potential future of the power grid (Brinkman et al. 2024; Gagnon et al. 2024; U.S. DOE 2024). ReEDS determines the optimal investment pathway for generation, storage and transmission to minimize system costs for decades into the future, while adhering to physical, operational, reliability, and policy constraints. A unique characteristic of ReEDS is the high spatial resolution for representation of variable and weather-dependent resources such as wind (land-based and offshore) and solar. Wind and solar resource availability and hourly profiles are determined by the Renewable Energy Potential (reV) model, using seven years of historical data and detailed characterizations of land use which determine where resources may be deployed (Maclaurin et al. 2021; Lopez et al. 2023). Wind and solar hourly resource data are at 2 km and 4 km resolution, respectively, but hourly generation profiles are produced for each development site (11.5 km x 11.5 km).

Though the spatial representation of renewable resources is highly detailed, there are other key limitations of ReEDS (and with many capacity expansion modeling tools more generally) that are worth noting. First, ReEDS performs a full system-wide optimization, where each region must meet their own planning reserve margin with allowable contributions from neighboring regions. In reality, many entities perform their own resource planning with or without consideration for neighboring regions, and there is very little large-scale, cross-region planning for generation and transmission (U.S. DOE 2024). Further, the transmission representation is simplified due to tractability. Power transfers are simplified with 134 regions represented as single nodes, using a simple transport model (Brown et al. 2023; Sun and Wesley Cole 2017). Within each region, transmission is not explicitly modeled, although the costs of transmission reinforcements and spur lines are accounted for in the total system costs.

For this study, we consider the evolution of the system until 2050 in five-year increments. We include no ability to build additional transmission between interconnections (i.e., between the Western and Eastern Interconnections, or between the West and Texas) since the focus of the downstream detailed models are for the Western Interconnection only. We do include planned transmission additions determined by WECC's Anchor Data Set (ADS 2032) to be consistent with the production cost modeling (Section 5.0). As discussed in the previous section, we also impose an offshore wind capacity target for the three coastal states as shown in Figure 4, imposed as a minimum bound. The ReEDS model could choose to build offshore wind beyond this target, but no less.

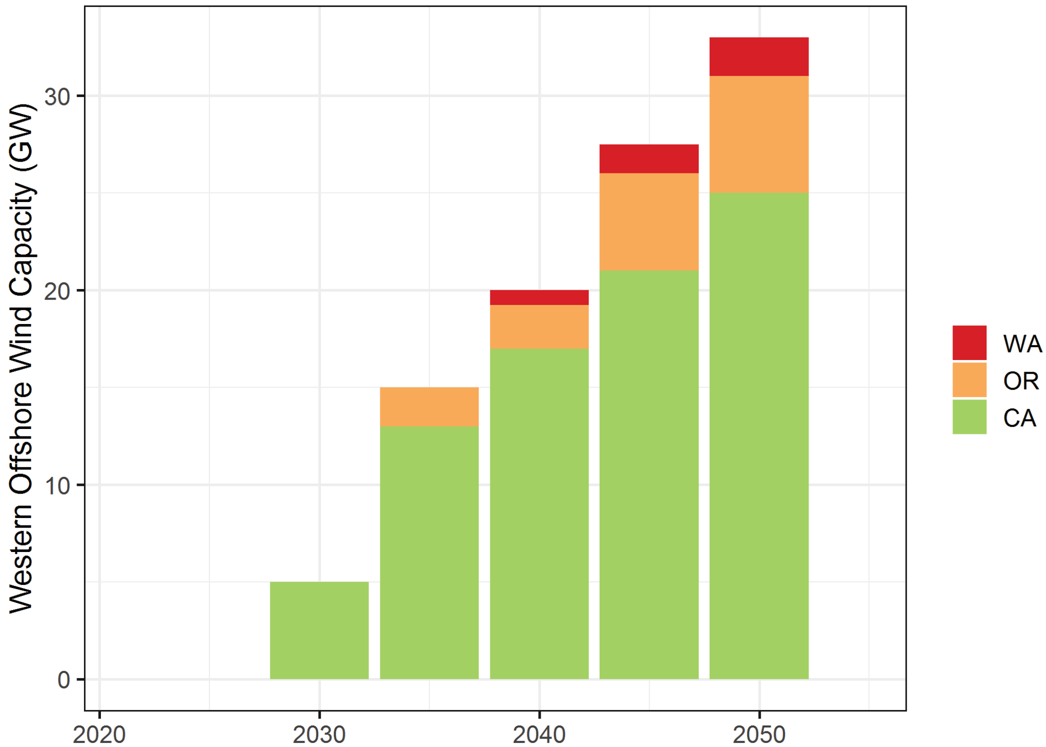

Figure 4. Offshore wind targets (by coastal state) used as an input to the CEM.

2.4 Capacity Expansion Results and Discussion

Figure 5 shows the results of ReEDS through 2050 for the inputs discussed in Section 2.1 for the United States portion of the Western Interconnection. Firstly, the results indicate an approximate doubling in installed generation capacity by 2050 on the power system due to assumed load increases from electrification, as well as lower average capacity factor for deployed resources such as wind, solar, and storage. Secondly, due to the requirement to decarbonize by 2045, the results show a transition from fossil-based resources (coal and natural gas) to a system primarily made of wind, solar, and storage. The 2050 system also has around 125 GW of hydrogen-fueled combustion turbines[1]. These combustion turbines, along with storage, serve as the main source of dispatchable firm capacity to help balance the increased amounts of wind and solar.

[1] In the configuration used for this study, ReEDS assumes that hydrogen is available to power the combustion turbines at a fuel cost of $20/MMBtu. It assumes the fuel is always available at that price and does not consider the origin of the fuel. This hydrogen would likely be, at least in part, created from electricity via electrolysis and would require additional generation capacity to meet the electrolyzer load, possibly increasing the need for generation resources such as offshore wind. However, this additional complexity increases model computation time and tractability. This simplification will be explored in future work.

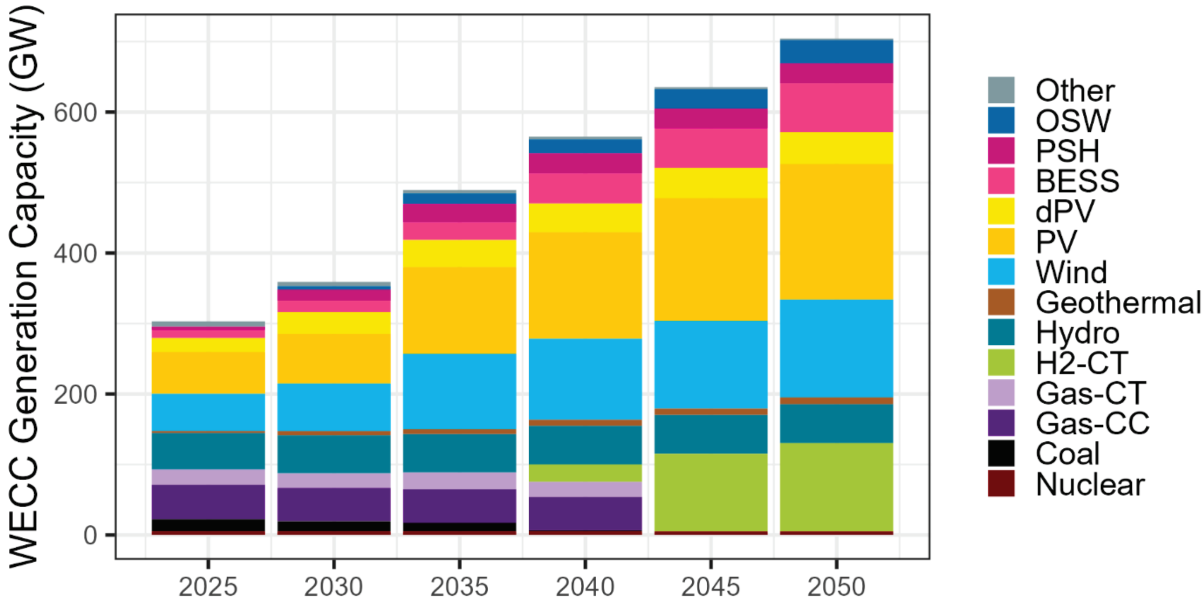

Figure 5. Power system expansion results for the U.S. WI footprint for this study. The Other category encompasses Concentrating Solar Power, Net Imports from Canada, Gas-Steam units, and Biopower. BESS is battery energy storage systems, and PSH is pumped storage hydropower. H2-CT represents hydrogen combustion turbine.

Figure 6 shows the installed capacity (by generation type) for the three coastal states. The figure indicates that a significant fraction of the West's hydrogen-fueled combustion turbines is assumed to be located in California, with some in the other coastal states as well. ReEDS built a total of 33 GW of floating offshore wind with the same state-wide breakdown as shown in Figure 4. See Section 5.0 for analysis of the potential operations of this generation.

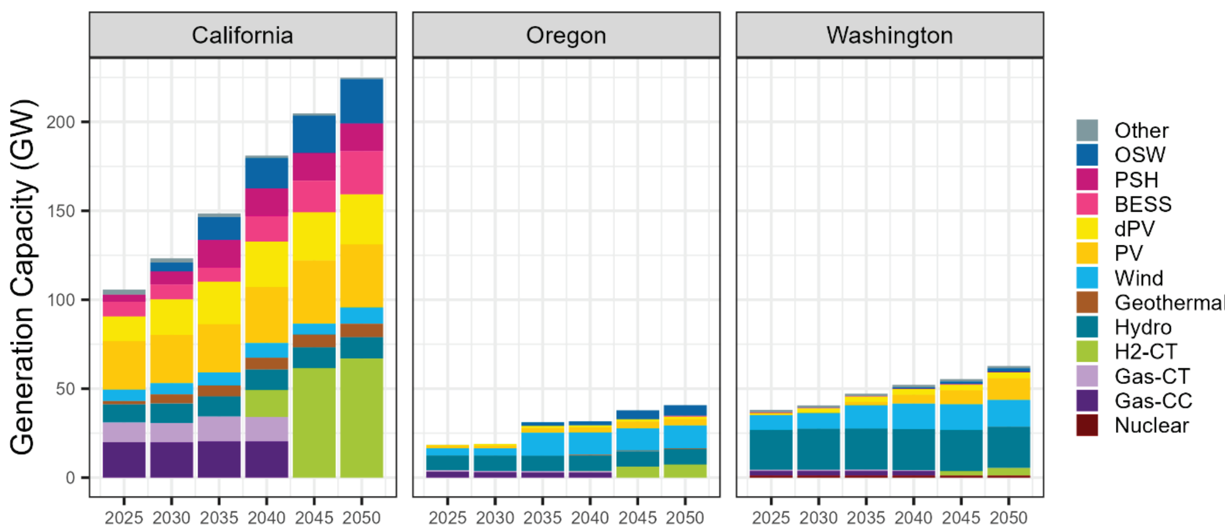

Figure 6. Total capacity builds out for the coastal states assumed by 2050 for this study. The Other category encompasses Concentrating Solar Power, Net Imports from Canada, Gas-Steam units, and Biopower. BESS is battery energy storage systems, and PSH is pumped storage hydropower. H2-CT represents hydrogen combustion turbine.

2.5 Summary and Key Findings

To conclude, the capacity expansion analysis provided the basis for the detailed downstream power system modeling for this study. The following observations constitute key findings:

- Initial analysis of potential offshore wind on the West coast showed that the key drivers for deployment include load growth, emissions reduction targets, and capital cost trajectory of floating offshore wind technology.
- Another important driver of offshore wind deployment is the availability and cost of competing low- or zero- carbon technologies, such as land-based wind, solar, carbon capture and sequestration, and geothermal.
- Given the uncertainty in the evolution of the power system and underlying technologies, we determined that using a target of 33 GW of Western offshore wind by 2050 to be a reasonable amount of deployment, while providing a basis to study the impacts to the power system.

3.0 Geospatial Analysis and Technology

This chapter discusses offshore wind and transmission geospatial analysis, hypothetical cable routes, and topologies designed for the subsequent grid modeling. It concludes with a discussion of the state of technology of floating offshore wind.

We collected a set of geospatial layers and used them to route hypothetical routes (see section 3.1) to pre-selected POIs (see Section 4.0) and selected from those connections based on the overall levelized cost of electricity to create the topologies (see Section 3.2). We iterated between early stages of this work and early stages of the production cost modeling work to ensure that the POIs were reasonable and that the connections between offshore and onshore were reasonable.

The goal of this analysis is to understand big-picture siting challenges and select a set of routes between POIs and potentially good offshore wind turbine locations. The work is not intended to be an analysis for permitting or detailed project siting. Potential projects will need to do project-specific geophysical studies and surveys.

3.1 Geospatial Analysis and Cable Routing

Wind plant siting followed the reference scenario siting assumptions from Lopez et al. (In Press), although used a 30 km distance to shore threshold to match the Atlantic Offshore Wind Transmission Study (AOSWTS) (Brinkman et al. 2024). Wind plants are modeled with 15 MW turbines (150 m hub-height, and 242 m rotor diameter) with a 5 MW/km^2 capacity density assumption (except when known to be otherwise in a lease area) using the Renewable Energy Potential (reV) model (Maclaurin et al. 2019). This resulted in a technical potential of 83.5 GW of floating OSW off the coasts of California, Oregon, and Washington. We calculated the site-based LCOE for each wind plant using 2024 ATB values (NREL 2024).

We followed a similar routine as the AOSWTS for siting cables, using the reV exchange tool (Rossol et al. 2024), with a few notable updates. First, with guidance from stakeholders through multiple Advisory Committee meetings, we identified additional layers to include in our cable siting considerations, while simplifying friction assumptions (see Table 2). Second, we updated costs for offshore cables using analysis for this study (see Appendix D). And third, we utilized an integrated land and sea cost surface that incorporated higher-fidelity land-based spur-line costs.

3.2 Transmission Siting Layers

Table 2 details the layers used in the cable routing. Areas where no cables are allowed to pass through are denoted as an exclusion. Where cables can pass through, a friction value is assigned by the algorithm described below, with de-prioritization weighted by friction level. There are likely additional siting considerations that we did not incorporate into this analysis, including additional Department of Defense considerations (see Appendix C).

Table 2. Offshore cable siting considerations.

Category	Name	Data Source	Description	Constraint Type
Physical	Seafloor Slope	British Oceanographic Data Centre (2024)	This dataset was calculated from the water depth layer. Steep areas are constrained due to difficulty laying cable.	10-15 degrees: medium friction >15 degrees: excluded
Physical	Water Depth	British Oceanographic Data Centre (2024)	Water depth used to inform cabling exclusion due to technology limitation. Also used to determine site specific costs	>4,000m: excluded
Physical	Seafloor Sediment	NOAA (n.d.-a)	Hard seafloor substrate types make dredging cables difficult or impossible	Bedrock/hard: excluded Mixed/gravel: medium friction
Physical	Canyons	Harris et al. (2014)	Placement of cables in canyons not possible due to high turbidity flows. Canyons can also be sensitive habitat	Excluded
Physical	Rocky Shorelines	NOAA (2017)	Rocky shorelines are very difficult to drill through for cable landings	High Friction
Physical	Artificial Reefs	Office for Coastal Management (2024)	Laying cable would damage reefs or vice versa	Excluded
Physical	Shipwrecks	NOAA (2016)	Laying cable would damage shipwrecks or vice versa	Excluded
Infrastructure	Oil and Gas Pipelines and Platforms	Homeland Infrastructure Foundation- Level Data (Geospatial Management Office n.d.)	Areas with existing infrastructure may require approval from owners	Medium Friction
Infrastructure	Submarine Cables	BOEM-NOAA Marine Cadastre (BOEM n.d.)	Requires additional coordination; installation could damage existing cables	Low Friction
Military	Danger Zones and Restricted Areas	BOEM-NOAA Marine Cadastre (BOEM n.d.)	Department of Defense restricted area	Excluded

Category	Name	Data Source	Description	Constraint Type
Military	Unexploded Ordinances	BOEM-NOAA Marine Cadastre (BOEM n.d.)	Risk during installation, possibility to damage cabling if exploded	Excluded
Military	Oregon Restricted Area	Provided by US Navy	Department of Navy restricted area off the coast of Oregon	Excluded
Military	Ship Shock Boxes	BOEM-NOAA Marine Cadastre (BOEM n.d.)	Approved use of explosives in these areas could damage cables	Excluded
Shipping / Navigation	USCG Anchorage Sites	Provided by USCG	High vessel activity in these anchorage sites	Excluded
Shipping / Navigation	Shipping Lanes	Provided by USCG	PAC-PARS draft. High vessel activity	Shipping Fairways /Traffic Lanes: Medium Friction Traffic Separation Schemes: Excluded
Shipping / Navigation	Crabber and Tug Lanes	Provided by USCG	High vessel activity	Medium Friction
Regulatory	Usual and Accustomed Tribal Fishing Areas	Hand digitized from (Schlosser 2012)	Tribal sovereign waters	Excluded
Regulatory	Ocean Disposal Areas	BOEM-NOAA Marine Cadastre (BOEM n.d.)	Use of these areas exclusive to ocean disposal	Excluded
Regulatory	Sand Borrow Areas	USACE (2024)	Frequent dredging to use sand could damage cables	Excluded
Regulatory	State Waters	NOAA (2023b)	Highly used areas	Low friction
Regulatory	BOEM Lease and Planning Areas	(BOEM 2024a)	Cabling always allowed within Lease and Planning areas to facilitate power evacuation	Force Included
Conservation	Marine Protected Areas	NOAA (2023a)	In no take, no impact, and no access, no access or infrastructure is allowed to minimize disturbance to sensitive or culturally important areas. In uniformed and zoned multiple use MPAs access and infrastructure are allowed but discouraged. Includes the newly designated Chumash	No take, no impact, and no access MPAs: excluded Uniformed and zoned multiple use MPAs: medium friction

Category	Name	Data Source	Description	Constraint Type
			Heritage National Marine Sanctuary	

3.2.1 Integrated Onshore and Offshore Siting/Cost Surface for Routing

A detailed description of the routing methodology is available in Lopez et al. (In Press), but at a high-level, the routing algorithm uses the site-specific costs modulated by friction (low friction increases costs by 33%, medium friction by 67%, and high friction doubles costs). These friction values are used to find the least cost path from the starting point to the ending point (see Figure 7). The friction-weighted costs are only used to identify routing pathways, and do not inform the actual costs. With the integrated land-sea routing surface (onshore siting layers informed by Lopez et al. (In Press)), this approach was used to route export cables connected to onshore spur-lines, offshore interlinks, and new onshore cable builds.

In addition to the friction and exclusions, we applied a 10% friction per 500 m of water depth, starting at 500 m to prevent ultradeep cable runs we saw in early iterations of the analysis. This is applied as friction and does not impact the costs reported in the study. This had the effect of disincentivizing cables from going to deeper waters. Because of this friction, the selected topologies did not include any ultradeep cable runs.

Once cable routes were established from each potential wind farm to each potential POI, we calculated the transmission costs by using the equations in Appendix D for the offshore portions of export cable systems. The onshore cable costs were informed by the WECC Transmission Cost Calculator (WECC 2019). Unless otherwise informed though Advisory Committee meetings, offshore HVAC cables were used if export cable routes were less than 80 km in length, and HVDC offshore cables were used otherwise.

We selected wind plants and associated cable paths using a system-wide cost optimization described in Section 4.0, which considers site-based LCOE for all potential wind plants, combined with all the least cost cable routes and cost information. While this methodology provided potential paths the cables could take and characterized relative differences in costs and lengths, the results are not meant to inform detailed siting decisions or permitting.

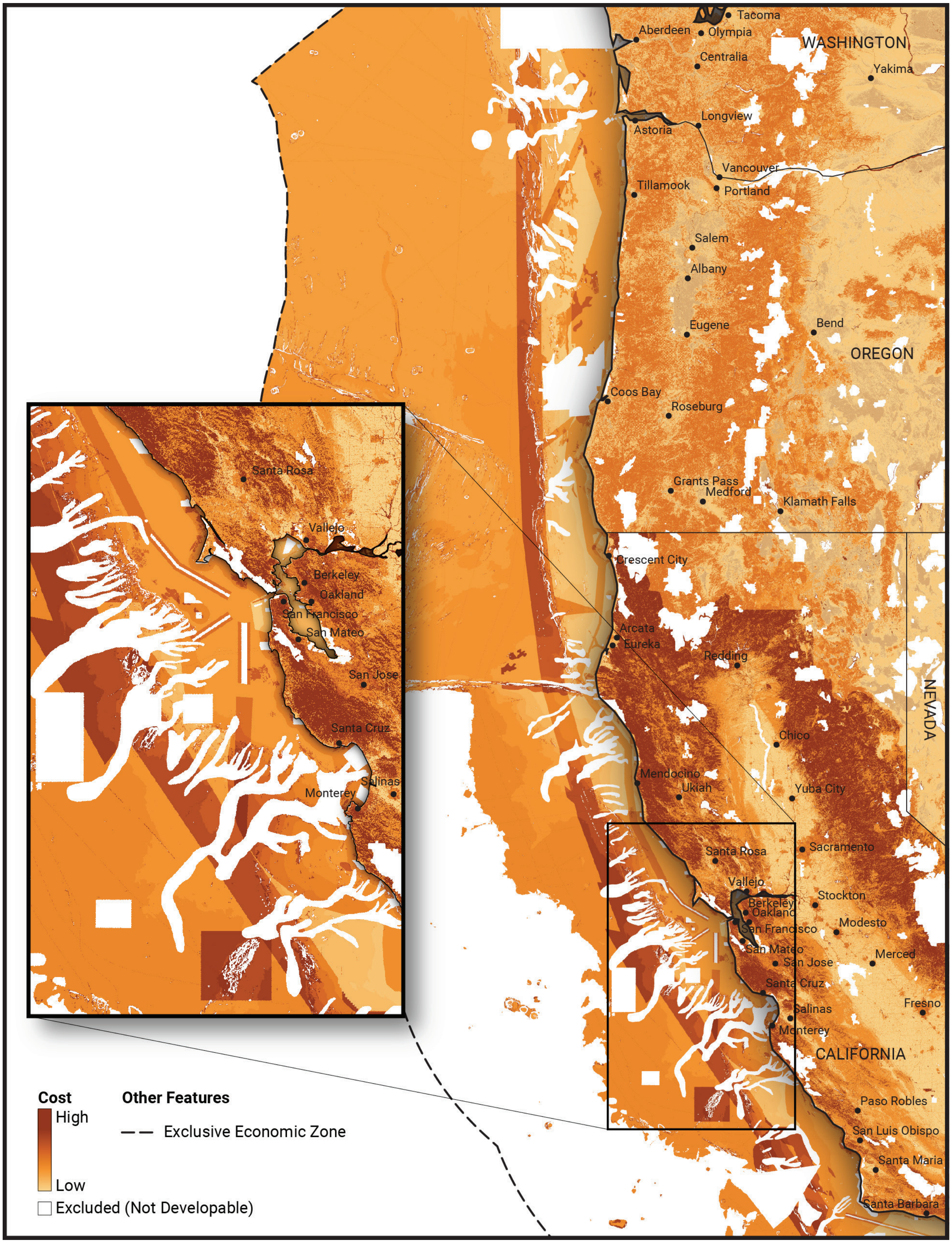

Figure 7. Cost surface in offshore and land-based areas used for cable routing.

3.3 Technology

3.3.1 Introduction

The development of commercial floating offshore wind projects is both a current challenge and opportunity worldwide. The west coast of the U.S. is in a good position to be a global leader on this front. Worldwide, there is roughly 200 MW of floating wind energy capacity installed. The U.S. would need to install significant commercial floating wind energy capacity offshore in its west coast in order to reach the levels of offshore wind studied here. The potential for wind energy farms offshore Washington State is currently being investigated.

The main challenges for floating offshore wind deployment on the West Coast include general lack of port and grid infrastructure (Shields et al. 2023a), inadequate supply chain (Shields et al. 2023b), lack of floating wind technology experience in deep (300-1300 m) and ultradeep (1300 m or deeper) water, and lack of established substation solutions for deep water. Few ports and points of interconnection, sometimes far away from the best wind resource areas, result in a higher levelized cost of energy (LCOE). The development of a domestic supply chain could be incentivized through benefits from the Inflation Reduction Act (IRA). Developing the domestic supply chain has the potential to improve job availability and career-specific education in port communities which tend to comprise underrepresented minority populations and face economic challenges (Gillingham and P. Huang 2021; Greenberg 2021; Prochaska et al. 2014; WECC 2019). Engineering challenges of floating wind turbines in very deep water include uncertainties in the best mooring system design and installation methods because it has not been done before in practice. Floating substation design and dynamic cabling (allowing for some movement of the export and array cables) are also in early stages of development.

Commercialization of floating offshore wind energy can take lessons from the historic evolution of the land-based wind industry. At the start of the land-based wind industry, turbine ratings were lower than today, but from 2004-2016, there was no significant upscaling of turbine ratings (1.7 to 2.1 MW). The cost reduction came in a large part from rapid industrialization of the turbine and assembly line components along with the domestic supply chain. After cost reductions had already been achieved through industrialization, then further increases in turbine rating were achieved (Wiser et al. 2023). Huge investments are required from turbine manufacturers to develop larger technology platforms and turbine prototypes. Building a new supply and assembly process to allow for larger turbines can take many years to develop, and the benefits to economies of scale must be compared to the cost reduction benefits of more rapid industrialization.

In this chapter, we outline the necessary infrastructure for floating offshore wind farms, including ports and vessels, export system, and points of interconnection. This is followed by a discussion of engineering challenges for floating wind farms. Tradeoffs between different floating substructure topologies are discussed, as well as dynamic cabling and floating substations. Mooring systems for ultradeep water are explored. Operations and maintenance steps for these floating components is explained. Appendix D describes the cost assumptions used in this study.

3.3.2 Infrastructure

3.3.2.1 Facilities, Ports, and Vessels

Significant investment is required for facilities and ports on the West Coast to be able to support the installation of floating offshore wind farms there (Shields et al. 2023b). Who provides this investment, whether it be the government, industry, or port authorities, is unclear and needs to be solved. Further, strong coordination between these entities and local communities is necessary to support planned offshore wind buildout. Understanding how port development can impact local communities and workforce is crucial to inform strategic investments to provide the most beneficial outcomes for port expansion on the West Coast.

In recent conversations with cable suppliers, domestic cable production facilities will need to be newly constructed and provide space for on-site activities such as the import of raw materials, processing those materials into subcomponents, applying nonconducting layers, and storing on-site turntables for loading onto cable-laying vessels (Shields et al. 2023b). Many cabling facilities require towers that can be more than 450 feet tall in order to hold the conductor vertical so materials such as insulation can be applied during the manufacturing process. Once assembled, the conductor needs to be stored before adding more insulation or jacketing to finish the production (Shields et al. 2023b). Quayside infrastructure is needed to load cables from storage turntables to vessels, including load and non-load bearing wharfs. Suitable infrastructure to support any necessary delivery methods of cable subcomponents will be required, such as areas to accept goods from train or truck (Shields et al. 2023b).

Some barriers to cable production are the associated costs and limited available space for building new manufacturing facilities. These facilities need to be located along the coast with large laydown areas. Further, uncertain timelines for permitting and construction, as well as lack of specialized workforce are also a problem to developing cable production facilities (Shields et al. 2023b).

In terms of cost and time, developing a port site could cost $1 billion and take roughly 10 years to complete (Shields et al. 2023a). In this case, port site is defined as a location within a port the includes a wharf to load/unload vessels as well as an area for storage of components and manufacturing activities. A recent study evaluating the impacts of developing a port network for floating offshore wind energy on the West Coast (Shields et al. 2023a) a found that the number of ports required on the West Coast to reach 55 GW of offshore wind energy by 2045 is 9 staging and integration sites (4-5 ports) and 17 operations and maintenance sites. This would require an investment of roughly $11 billion.

Manufacturing ports are required in addition to the staging, integration, operations and maintenance sites mentioned above. Manufacturing ports along the coast are required because offshore wind components are, in general, too large to be transported over land toward the coastline. An additional $11-19 billion would be needed to build these manufacturing sites and the consequent local supply chain developed would reduce lifetime vessel emissions by 40% since it would eliminate the need for transporting major offshore wind components across the Pacific Ocean (Shields et al. 2023a). It is unlikely that port sites will be constructed for single purposes such as staging mooring equipment or cables, because these can be co-located with either existing infrastructure or larger offshore wind port sites (Lim and Trowbridge 2023).

West Coast states would possibly need to collaborate to install and operate offshore wind at the levels in existing goals and in this study. This collaboration is necessary because no single state on the West Coast (California, Oregon, or Washington) has the port sites on its own that are required to meet these offshore wind targets. Such collaboration can involve the communities that are expected to be impacted by port and offshore wind development. Port communities tend to face challenging economic, health, environmental and educational burdens and could greatly benefit from more job and associated educational opportunities from port and offshore wind development. Effective communication between port authorities, local communities and tribes is essential to implement solutions in the best way (Shields et al. 2023a).

The U.S. shipbuilding capacity will need to be expanded to implement offshore wind energy projects, but the requirements for this fleet remain unclear. Shields et al. (2023a) identified three major actions that could help alleviate the problem of lack of vessels suitable for floating offshore wind activities. The first action would be to maintain communication between key groups such that new vessels are able to accommodate future wind turbines and their installation methods. The key groups here include manufacturers, project developers, port owners, vessel operators, and shipyards. The second action involves consideration of new funding mechanisms aimed at de-risking investments in new vessels. This would require collaboration between financial institutions, state and federal governments, and vessel operators. The third action to address the lack of floating offshore wind vessels would be to conduct a gaps analysis between the availability of shipyards planned to be built over the next decade with the long-term demand for floating wind vessels.

3.3.2.2 Electrical infrastructure

Electrical infrastructure includes export cables, offshore substation costs, and onshore costs of transmission. The export cable choice depends on how far the offshore wind farm is from shore, with HVAC being more economical for shorter distances (Appendix D). The cost of the cables depends on the total cable length and carrying capacity. Offshore substation costs differ between HVAC and HVDC, with the HVDC platforms typically larger than the HVAC platforms due to the need for AC/DC converters. Cable installation costs are dependent on the day rates of vessels, where the time required for each vessel varies from distance to shore. Onshore costs include a minimum cost of interconnection and major electrical components. Our costs are based on recent expert surveys. Although there are significant uncertainties with future inflation and supply chain price impacts, we have tried to incorporate this as much as possible in our input values and by communicating with recent industry values. The electrical infrastructure was modelled following the methods used in the AOSWTS (Brinkman et al. 2024). To represent costs of the export system, an updated cost curve was developed as a function of export cable length (Appendix D). The major cost components included here include the substation cost and cost of the cable. Floating wind farms require dynamic cabling for only a short distance away from the substation (see Figure 8 and sections 3.3.3 below). After recent talks with industry, we decided not to account for any significant cable cost difference between a system coming from a floating platform compared to one designed for a fixed bottom platform.

Following discussions with industry and previous studies, we chose to model 525 kV bipole HVDC technology for HVDC systems, and 420 kV HVAC for HVAC systems. These technologies are currently available for static submarine cables, but will need additional development for the dynamic portion of the cable system.

3.3.3 Engineering Challenges for Floating Wind Farms

State-of-the-art dynamic cables and floating substations

Floating substations and dynamic cables will be critical for many floating offshore wind projects. There are gaps in offshore substation technology standards, and a strong need to optimize the design process for integrated floating platform, high voltage equipment, and cable systems. The most novel components in cabling and substation systems are HVDC/HVAC dynamic cables and HVDC equipment. One of the biggest gaps in the design process is a lack of guidance for the economic benefit of reducing floating platform motions against the benefit of reinforcing the equipment for higher platform motions (DNV n.d.). More studies in this field will help identify further gaps and the need for new or revised standards to aid in the development of floating offshore substations and dynamic cabling.

Dynamic power cables

Dynamic cables are power cables that are suspended through the water column and are designed to move with floating platforms, instead of being secured to a structure or laid along the seabed. They are designed to have enough fatigue resistance to withstand a lifetime of movement. There is a strong demand for a more robust design of dynamic cables due to the frequent occurrence of power cable failures, which can contribute significantly to electrical losses. Most insurance claims are attributed to offshore cabling failure, with 53% of claims by value from 2014 – 2020 relating to cable damage (Allianz Commercial 2023), but from industry talks we expect this to be much higher, around 75%. Cable failure can potentially put a whole network of turbines out of commission and result in multi-million dollar losses. The readiness to replace or repair damaged cables and contain incurred losses is an important consideration for subsea cabling work insurers (Allianz Commercial 2023) and a broad range of stakeholders including wind farm developers and general shared ocean users such as fishermen and shippers.

High voltage cables that can withstand currents, waves, deep water, as well as being connected to a moving, floating substation are required for floating offshore wind farms. It is also imperative that no water penetrate the insulation of the cable. Static export cables typically have a lead sheath to protect their interior from water, but this lead sheath cannot bend easily with wave and current motion. Depending on seafloor characteristics, the static cable can be trenched, or have a concrete mattress on top of it to provide added weight and stabilization. Due to this high susceptibility of fatigue, a dynamic cable can be developed containing options such as copper, stainless steel, aluminum, a metallic foil or polymer sandwich (Huang et al. 2023). Other components such as buoyancy modules, touchdown protection, bend restrictors, bend stiffeners, and subsea connectors (Figure 9) can also be added depending on site-specific requirements.

Fatigue is a critical consideration and probabilistic reliability analysis has been conducted under realistic environmental loads (Okpokparoro and Sriramula 2023). Optical fibers may also be incorporated to identify if the cable is under extreme stress (Huang et al. 2023). Ultradeep cabling will require more protection at greater water depths, but installation in deep water remains to be the biggest hurdle. So far, export cables have been installed only for depths up to 1300 m, which is sufficient for development of the 5 topologies studied here, with up to 33 GW of OSW in the Pacific. A recent trial by Prysmian successfully tested a submarine cable at 2,150 m depth (Prysmian 2024). Other scenarios involving different offshore development off the West

Coast could need to transverse deep canyons and/or water depths between 3000 m and 4000 m.

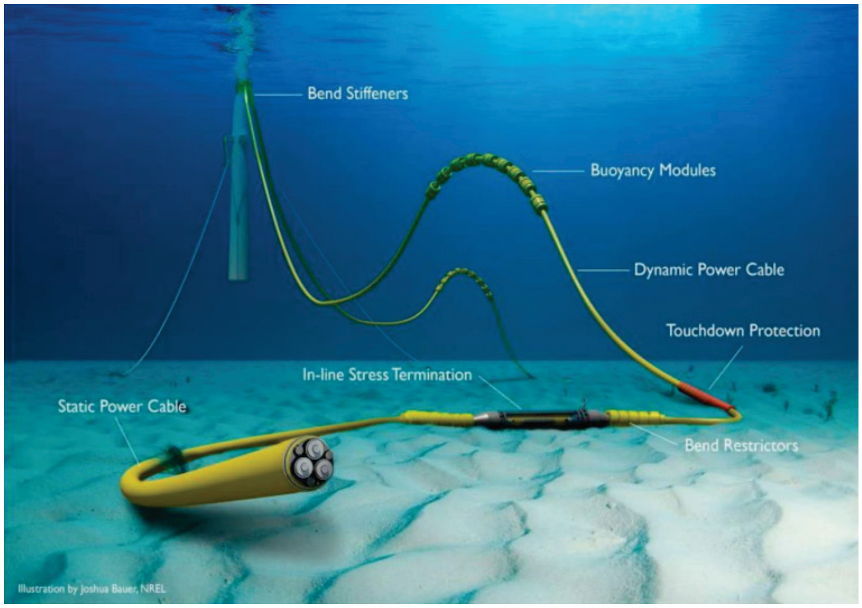

Figure 8. Components of a dynamic export cable with ancillary equipment. Figure by Joshua Bauer (NREL)

Floating substations

To date, the only floating offshore substation platform in the world was installed as part of a demonstration project in Japan in 2013, connected to three turbines. There are three main design concepts for floating substation platforms: semi-submersibles, tension leg platforms, barge and spars (DNV 2022), similar to those of floating wind turbines (Appendix E). The semi-submersible, barge and spar buoy are moored to the ocean floor with steel cables, chains, or fiber ropes that are connected to anchors. Different anchor types are used depending on the type of soil conditions and mooring system.

Technical challenges for floating substation platforms include developing dynamic cables that can connect from structures fixed to the seabed to the floating platform. Further, high voltage equipment must be capable of withstanding ocean-induced stresses. There are challenges for HVDC transmission equipment to be able to withstand the extreme dynamics of being placed on a floating platform. Fatigue endurance of more than 20 years of cyclic movements as well as the ability to withstand strong ocean storms are required of high voltage subsea cables. HVAC floating technologies are more developed, but it is expected that floating HVDC technologies will be ready when commercial-scale floating wind projects are deployed (DNV 2022).

3.3.4 Operations and Maintenance

Although the initial capital investment makes up the largest part of the cost of offshore wind, operations and maintenance costs are also significant. Operations and maintenance (O&M) costs are estimated to represent approximately 18% of the cost of a floating offshore wind plant over its lifetime(Stehly et al. 2023). The “operations” portion of O&M costs (OpEx) covers a wide range of recurring costs including facility leases, insurance, salaries for operations staff, and services such as weather forecasting and condition monitoring.

Maintenance at a floating offshore wind farm includes scheduled or preventative maintenance—tasks such as inspecting components and lubricating moving parts—as well as repairs or replacements when needed. Routine visits to an offshore wind farm are carried out in a similar fashion for fixed-bottom or floating wind turbines. Crew transfer vessels (CTVs) can be used for daily trips when the O&M port is within roughly 1.5 hours of travel. Larger wind farms or those located farther from port are likely to rely on service operations vessels (SOVs) that can remain at sea for 1–2 weeks before returning to port to resupply and exchange crew (American Clean Power 2023). The distinction between O&M for fixed-bottom and floating offshore wind farms is more relevant for major repairs such as replacement of large components. Repairs of fixed-bottom turbines must occur at site, but floating turbines can be towed to port, where maintenance can be carried out in a protected harbor. On-site maintenance may also be an option for floating wind turbines but might require the development of specialized vessels with advanced motion compensation to enable floating-to-floating transfer of large components. The tow-to-port strategy relies on less-costly towing vessels, enabling lower maintenance costs as long as the downtime associated with towing can be limited. Repairs to floating substations would likely be accomplished by heavy-lift vessel, and repairs to cables would happen on the deck of a cable-laying vessel (BVG Associates 2023).

3.4 Summary and Key Findings

One of the goals of the geospatial and technology analysis was to ensure the topologies studied were reasonable from a siting and technology standpoint. The work is not intended to be an analysis for permitting or detailed project siting. There were several key findings from these analyses. The following observations constitute key findings from the geospatial analysis (considering the topology sets described in Section 4.0):

- The topologies studied, with up to 33 GW of OSW, can be planned while only considering water depths less than 1,300 meters for cables, turbines, and substations.
- Approximately 30 GW of OSW could be deployed into the most economically favorable areas around California and southern Oregon, after considering ocean co-uses and complex bathymetry.
- To exceed this amount of OSW would require deploying resources in alternative locations, including waters deeper than 1,300 meters and further from shore, or waters to the north with lesser quality wind resource. Both options will incur greater cost of energy.

The technology analysis provides an overview of some of the relevant learnings for developing up to 33 GW of OSW in the Pacific region, including:

- Commercial floating wind is both a challenge and an opportunity. The industry is currently in early stages, but working towards solutions for deep water.
- One of the main challenges is that port and grid infrastructure required for this level of offshore wind deployment does not exist along the west coast today.
- Strong coordination between local communities and workforce is crucial to offshore wind development (both for infrastructure and plan installation/operations and maintenance)
- Cables that can move with floating substructures (dynamic cables) are required, and cable failure remains a high insurance risk, so these must be well developed.
- HVDC export systems are likely more cost effective at greater distances.

- Floating substation technology is an active area of research and development for deep water and for the voltages we studied.

4.0 Topology Sets

Following from the capacity expansion modeling of Section 2.0, in conjunction with the onshore production cost model builds, and drawing from a literature review of transmission plans for West Coast OSW to ensure consistency with leasing activity and active planning by system operators and target research gaps, five collections of OSW generation and transmission infrastructure along the West Coast, referred to as “topology sets,” were defined for detailed analysis on this study. This section details the process through which these topology sets were defined and provides detailed connectivity and siting information.

4.1 Incorporation of System Operator Plans

Pulling from the West Coast OSW Transmission Literature Review and Gaps Analysis (Douville et al. 2023) and follow-on engagement with Advisory Committee members, the study team incorporated elements of active plans for OSW Points of Interconnection (POIs) and supporting onshore transmission to enable OSW injections across the West Coast. The target POIs were also iterated with models and in consideration of OSW development to ensure a consistent and reasonable starting set. The list of POIs which were selected for use is shown in Table 3 below.

Table 3. Points of Interconnection assumed for OSW along the West Coast

Name	Approximate Location	State	Voltage Rating at POI (kV)
Satsop	Grays Harbor	WA	500
Wendson	Florence	OR	230
Fairview	Coquille	OR	500
Del Norte[2]	Crescent City	CA	500
Humboldt	Eureka	CA	500
Fern Road	Whitmore	CA	500
Cottonwood	Cottonwood	CA	230
Collinsville	Collinsville	CA	500
Elverta	Elverta	CA	230
Tesla	Tracy	CA	230
Bay Hub at Potrero[3]	San Francisco	CA	230
Moss Landing	Watsonville	CA	230
Diablo Canyon	Avila Beach	CA	500[4]

[2] Del Norte injections were counted toward the CEM targets to OR given that the onshore transmission from Crescent City, CA will directly link this power to OR bulk transmission grids.
[3] The Bay Hub involves landing export cables at the Potrero 230 kV substation in the San Francisco Bay and distributing the power injection across three or five additional 230 kV substations in the local area.
[4] Although only a single POI is indicated in the Morro Bay area at Diablo Canyon, this interconnection could represent injections at Diablo Canyon and/or injections nearby and tapping into the 500 kV network in this area.

4.2 Offshore Topology Sets

The Points of Interconnection (POIs) were developed from stakeholder discussions and informed by early iterations of the geospatial and dispatch analyses for this study. These are described in more detail in Sections 3.0 and 5.0, respectively. To select the offshore wind power plant locations and export cables for each 2050 topology for this project, we selected the 33 GW with the lowest total costs, considering:

- Electricity generation cost, which is a function of wind resource quality, costs, availability, and location (assumptions based on NREL's Annual Technology Baseline, 2024)
- Transmission costs, which are a function of the cable routes (described in Section 3.2.1) and the cost assumptions (described in Appendix D)

This optimization was similar to the method used for the AOSWTS, although the POIs were decided pre-optimization in this work. The aforementioned steps resulted in the offshore wind generation areas, export cables, and POIs for the five topology sets of OSW along the US West Coast (see Figure 9). The topology sets were inspired by the goal of analyzing the differences in 2035 between more distributed injections (*2035 Distributed*) and more concentrated (with fewer POIs, the *2035 Concentrated*). These two topologies do also inherently contain different geographic locations for offshore wind generation. In 2050, the analysis and differences between the topologies was focused on designing a topology that is entirely radial (*2050 Radial*), compared to one with onshore MT-HVDC interlinks within regions (*2050 Intraregional*), and compared to another with offshore MT-HVDC interlinks (*2050 Interregional*). All 2035 topologies can transition to all of the 2050 topologies studied; there are no inconsistencies.

For the offshore turbine locations off of the state of Washington, initial analysis led to a large geographic distribution for the 2 GW of injection, so a manual adjustment was made to cluster the wind. All transmission was designed to meet contingency limits of West Coast system operators.[5] Given the emergence of 2 GW HVDC subsea bi-poles in various markets, increased source limits were assumed for HVDC bi-pole reliability. Figure 10 through Figure 14 depict the geographic layout (left) and connectivity (right) of each topology.

[5] The limiting single source loss of 1150 MW and double source loss of 1400 MW was assumed after consultation with system operators. For contingencies of 2000 MVA HVDC bi-poles, reliability could be maintained through either (i) a combination of networked transmission and generation assets and emergency converter and conductor ratings or (ii) increased single-source contingency limits supported by planners.

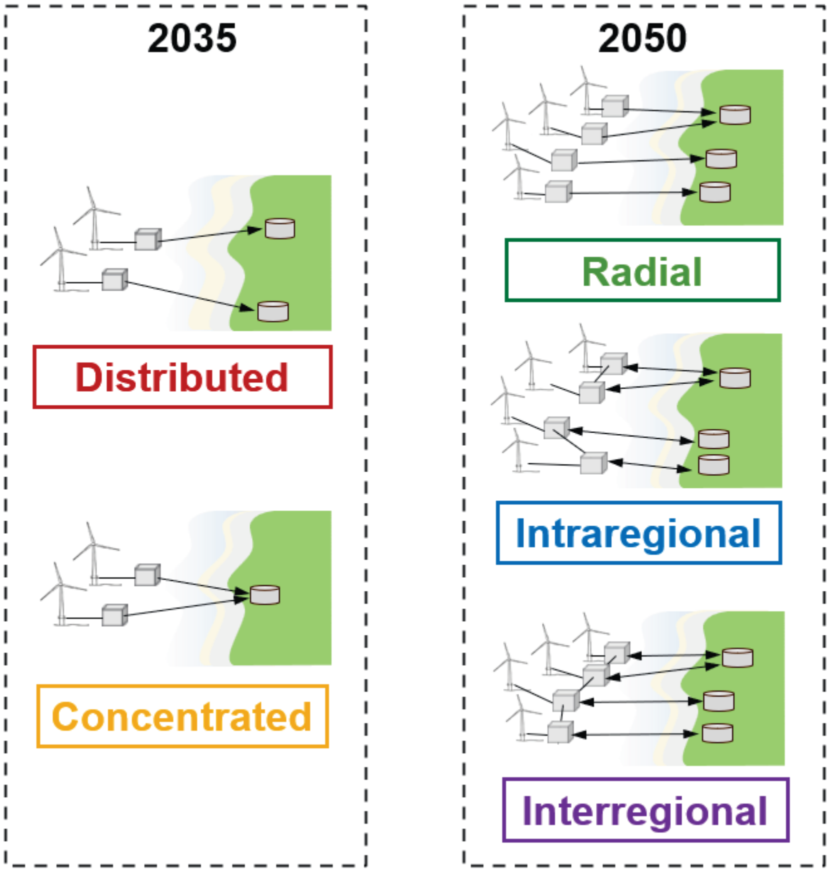

Figure 9. Conceptual diagram of topology sets and pathways from 2035 to 2050

The topologies studied include:

2035 Distributed (Figure 10)—15 GW of OSW generation which are interconnected radially through HVAC lines at nine points of interconnection. Though more POIs are considered than in the 2035 Concentrated Topology, the upgrades to accommodate each landing and power injection may be less costly overall. The Distributed Topology may provide a more resilient bulk system by harnessing greater geographic variability of the OSW resource and spreading power over more of the coastal grid, as compared to the Concentrated Topology.

2035 Concentrated (Figure 11) —15 gigawatts (GW) of OSW generation which are interconnected radially through High Voltage Alternating Current (HVAC) lines at five POIs, each with capacity for multiple GW of power flows. These interconnections drive significant onshore upgrades and landing point impacts, but in relatively few locations. The geographic locations of offshore wind generation are different compared to the 2035 Distributed Topology.

2050 Radial (Figure 12)—33 GW of OSW is connecting radially to the same 13 POIs used by the other 2050 topology sets, through a combination of HVAC and HVDC equipment. The most simplistic of the 2050 designs, this topology set was intended to provide a comparison to permit the isolation of the value of various OSW transmission concepts.

2050 Intraregional (Figure 13)—33 GW of OSW generation and transmission which provides connections *within* the combined Bonneville Power Administration (BPA) and PacifiCorp West (PACW) region, and California Independent System Operator (CAISO) region with HVAC and

High Voltage Direct Current (HVDC) transmission equipment. Nearly 16 GW are routed primarily through HVDC in a single north coast corridor. This strategy may be conducive to permitting risk at the expense of wildfire contingency risk. The HVDC is connected through a Multi-Terminal, Direct Current (MTDC) transmission network on land. This topology set includes all the offshore generation and transmission defined in both 2035 topology sets; this ensures that all deployment pathways (e.g., from 2035 topology to 2050 topology) on the West Coast are feasible and do not strand investments.

2050 Interregional (Figure 14)—33 GW of OSW generation and transmission which provides additional connectivity *between* BPA, PACW, and CAISO with HVAC and HVDC transmission concepts. The same POIs are used as in the Intraregional Topology and all the generation and transmission defined in both 2035 topology sets are included to allow for consideration of multiple deployment pathways on the West Coast. The HVDC lines are connected through a MTDC backbone in the ocean and lines to shore are routed in a distributed manner to the target POIs.

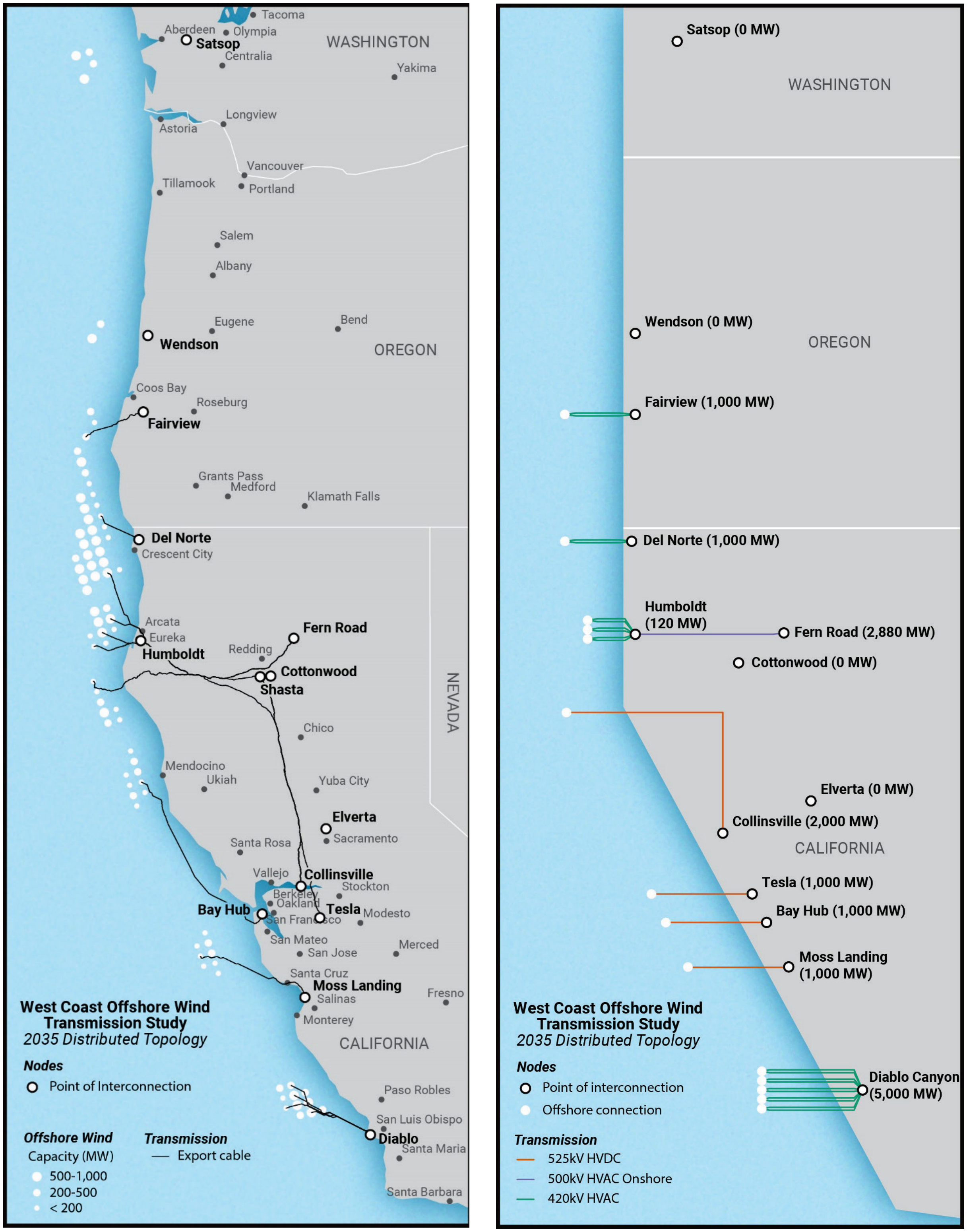

Figure 10. 2035 Distributed Topology: 15 GW, 9 POIs (left: geographic layout; right: connectivity)

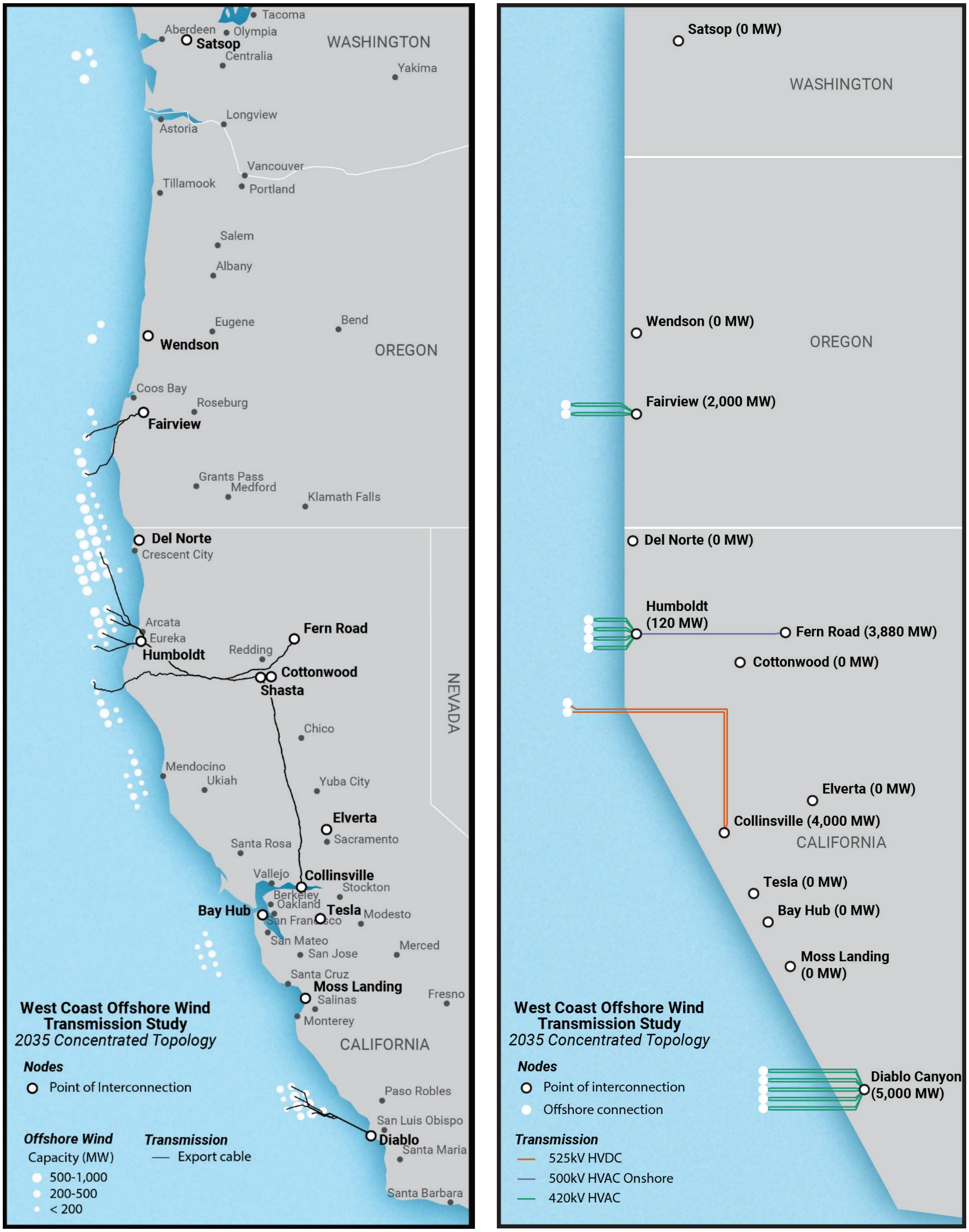

Figure 11. 2035 Concentrated Topology: 15 GW, 5 POIs (left: geographic; right: connectivity)

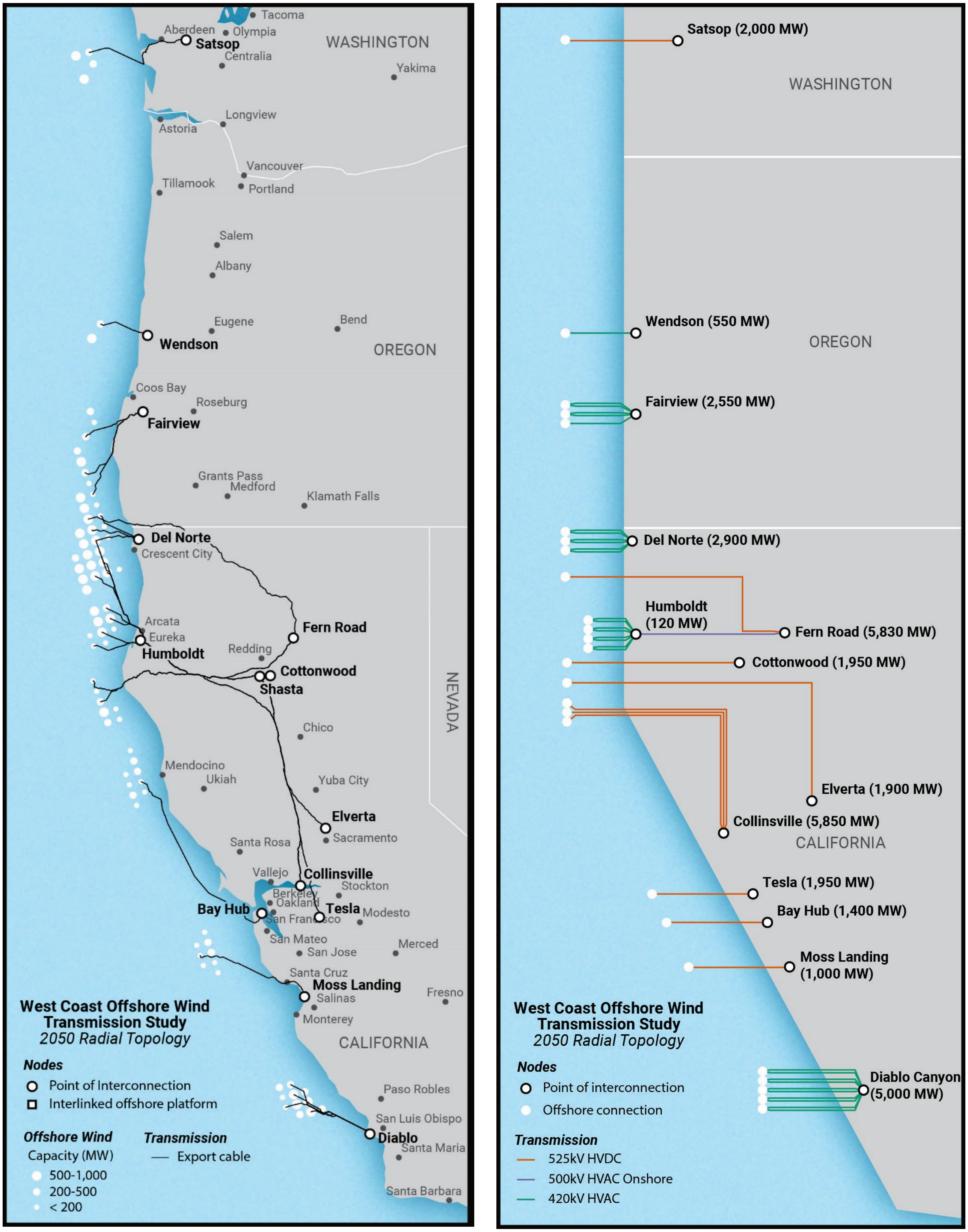

Figure 12. 2050 Radial Topology: 33 GW, 13 POIs (left: geographic; right: connectivity)

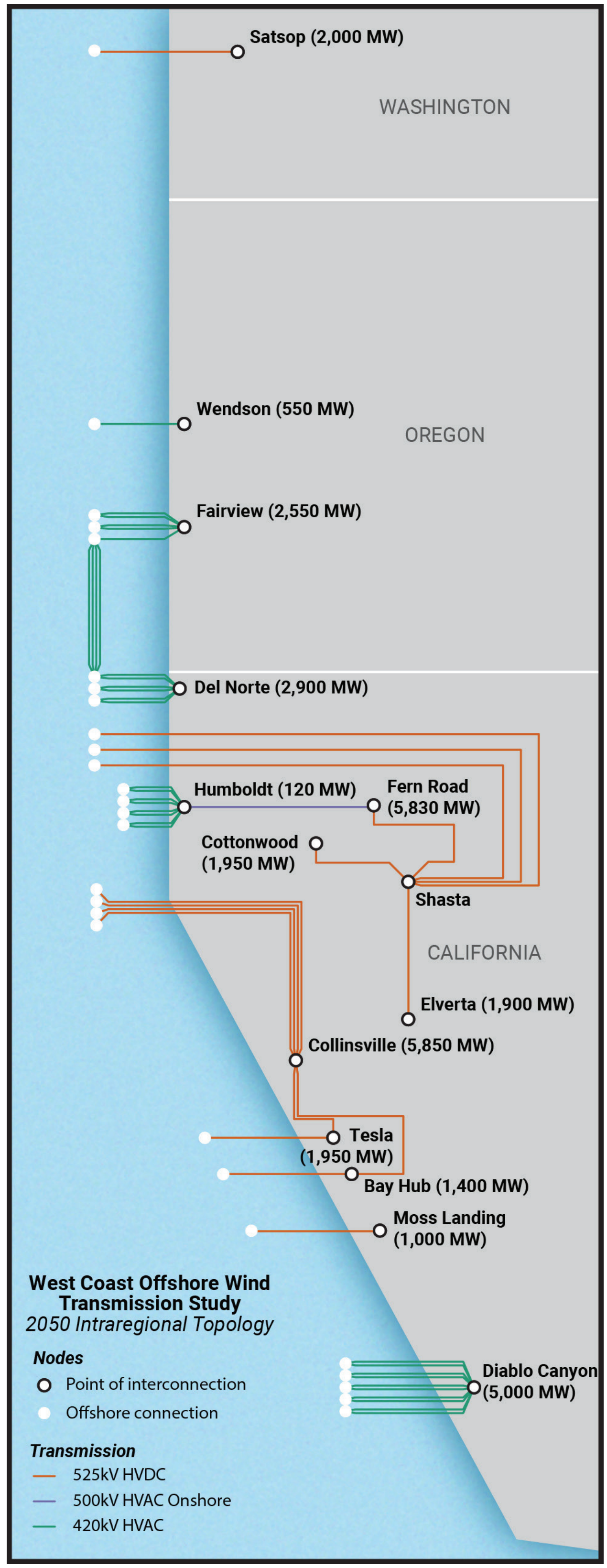

Figure 13. 2050 Intraregional Topology: 33 GW, 13 POIs (left: geographic; right: connectivity)

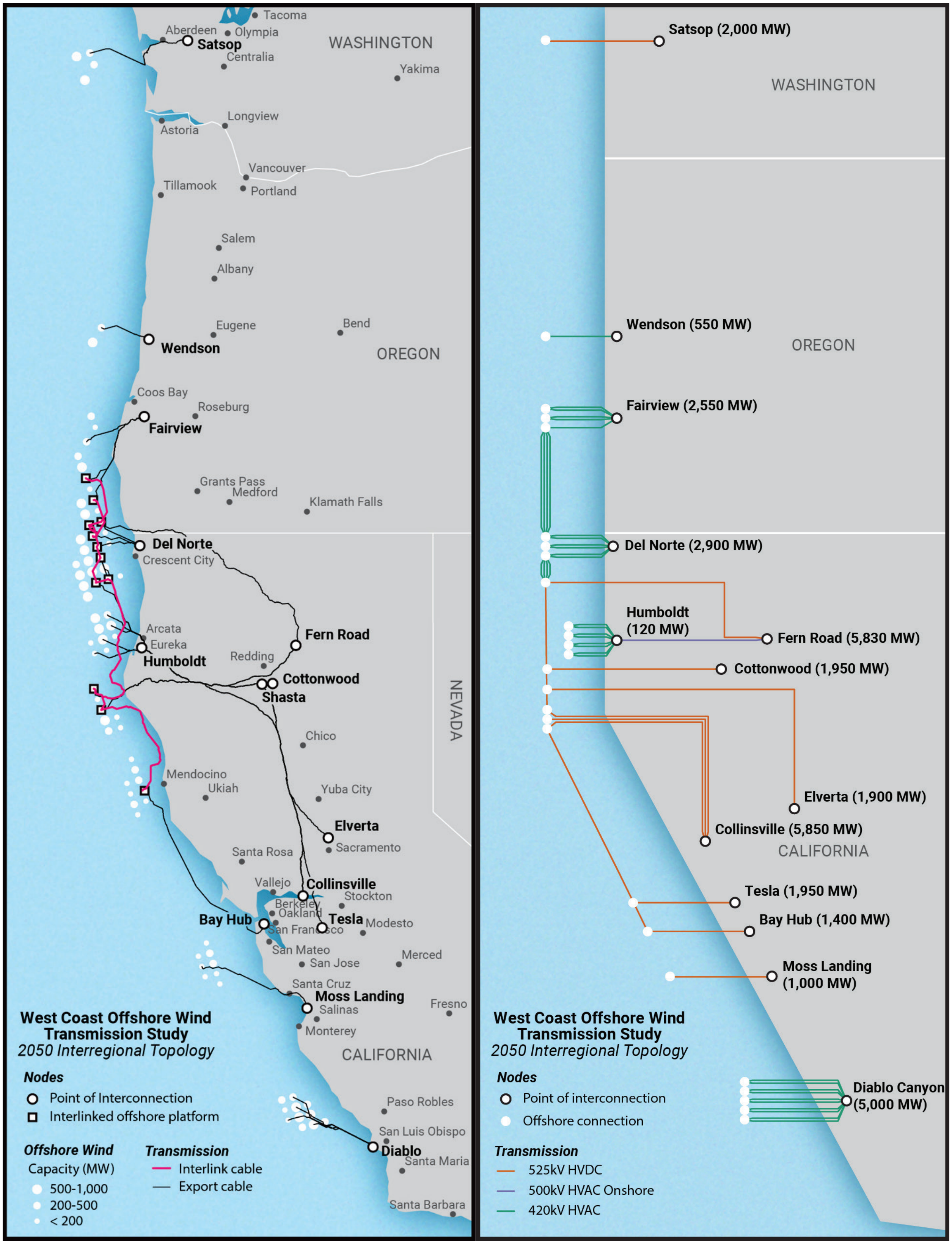

Figure 14. 2050 Interregional Topology: 33 GW, 13 POIs (left: geographic; right: connectivity)

In all the topologies, the cables and turbines can be sited without requiring siting in ultradeep waters (deeper than 1300 meters). In all of the 33 GW (2050) topology sets, the sea space off the California coast and southern Oregon is crowded. South of the wind energy areas off Eureka, California, 99% of the non-excluded sea space is developed by 2050 in these topologies. South of Coos Bay, Oregon, 85% is developed. North of Coos Bay is less crowded, as only 6% of the non-excluded space is developed by 2050. If more of the sea space off California is unusable compared to our assumptions, then more of the less-favorable resource north of Coos Bay (or ultradeep waters) would need to be developed to reach 33 GW.

4.3 Pathways from 2035 to 2050

Care was taken in the construction of the topology sets to include all 2035 details, in terms of wind power plant siting, transmission siting, and power injections at specific points of interconnection, in all of the 2050 sets. Such compatibility allowed for the evaluation of two 2035 interim builds towards 2050 future builds. Table 4 indicates the planned power injections across the five topology sets to secure deployment pathways and still total to the CEM targets by state, and Figure 15 indicates the six pathways which are available from this design of experiment. Section 9.0 contains maps of a phased transition between 2035 and 2050 for one pathway.

Table 4. Maximum power injections by POI in MW for each topology set

POI	2035 Distributed	2035 Concentrated	2050 Radial/Intraregional/Interregional
Satsop	0	0	2000
Wendson	0	0	550
Fairview	1000	2000	2550
Del Norte	1000	0	2900
Humboldt	120	120	120
Fern Rd	2880	3880	5830
Cottonwood	0	0	1950
Collinvsille	2000	4000	5850
Elverta	0	0	1900
Tesla	1000	0	1950
Bay Hub	1000	0	1400
Moss Landing	1000	0	1000
Diablo Canyon	5000	5000	5000
Total	15000	15000	33000
Total, CA	13000	13000	25000
Total, OR	2000	2000	6000
Total, WA	0	0	2000

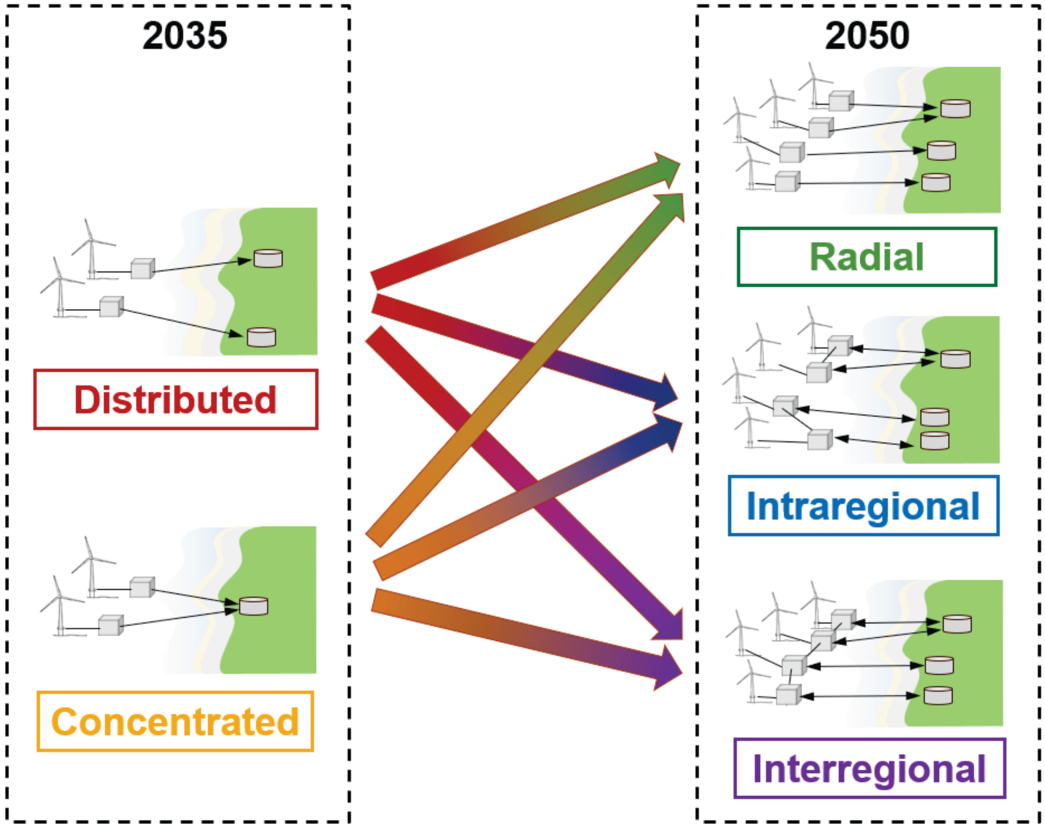

Figure 15. Six development pathways enabled through the topology set definitions

4.4 Summary and Key Findings

In this section, the design of experiment was presented. The topologies are intended as representative for study and analysis and not intended as recommendations or prescriptions. The following observations constitute key findings:

- Five topology sets, which included spatial definitions of OSW generation, transmission, and POIs, were defined. These definitions were a result of literature review and survey of transmission plans and the state of floating OSW transmission technology, capacity expansion modeling, production cost modeling, and state and federal planning activities. Ratings of transmission lines and POI substations were detailed in the topology sets and maps were constructed to indicate geospatial layouts and transmission connectivity.

- The topology sets were constructed such that various 2035 (15 GW of OSW) and 2050 (33 GW of OSW) futures could be directly compared, and all 2035 topology sets (including generation, transmission, and POIs) were compatible with 2050 topology sets.

- This resulted in six distinct pathways for development of OSW along the West Coast through 2050. Each pathway provides an option for a phased approach to development.

- Across the six pathways, flexibility is afforded to adjust to unforeseen advances or challenges to development as they arise. These topology sets and development pathways were then analyzed throughout the study.

5.0 Production Cost and Resource Adequacy Modeling

After topology sets had been defined as detailed in Section 4.0, they each were analyzed through production cost and resource adequacy models. Production cost models (PCMs) simulate the least-cost dispatch of individual generators to meet loads, subject to physical limits of the transmission system and reliability requirements to meet electricity demand and reserves at all hours of the year. Resource adequacy models consider the likelihood of energy supply given generation fleets, fuel variability, transmission capacities, and load growth and variability. Comparing the various topology sets in the PCMs and resource adequacy models allowed for relative economic analyses between scenarios in 2035 or 2050 and between pathways from 2035 to 2050 (Section 7.0).

5.1 Production Cost Model Methodology

PCMs of the five topology sets were constructed with high spatial resolution (~22,000 network nodes and ~23,000 transmission lines) in GridView, starting from WECC 2032 Anchor Data Set (ADS) inputs, as specified in Appendix A. These origins provide an industry-informed and updated projection of generation additions and retirements, transmission assets, and load growth within the Western Interconnection on a 10-year planning horizon. Ancillary service (AS) requirements are an additional input to the model, calculated from load and generator characteristics at hourly resolution.[6]

Simulations were conducted in GridView, a chronological unit commitment and economic dispatch modelling software (Hitachi Energy 2024). In every hour of the year, the model minimizes power system operating costs by selecting transmission capacity and generators to meet electricity demand and reserve requirements subject to a wide variety of operating constraints. These constraints consist of unit-specific constraints (e.g., generator capacity limits, minimum operating and maintenance times, rate of power increase or decrease limits or “ramp rates”) and system-wide constraints (e.g., transmission line capacity limits, operating reserves, emission limits, hurdle rates[7]). Operating costs largely consist of fuel costs, variable operating and maintenance costs, and unit start-up and shut-down costs. Outputs of these simulations, including overall operating costs by year, season, or month, utilization of generators and transmission paths, price variations of power supply, particulate and greenhouse gas emissions and curtailments, congestion, or unserved loads, can yield valuable insights into the benefits and costs associated with various system designs. Figure 16 summarizes the key modeling inputs and representative outputs of the PCM analysis (Oikonomou et al. 2024).

[6] Regulation up and down, load following up and down, and spinning reserves are the AS inputs to the PCM.

[7] Hurdle rates are economic constraints on generator dispatch, which are not a function of generation cost. These may be used to model policy tariffs dictating power transfers between regions or charges for the use of transmission lines. They also may be used to achieve reasonable interregional transfers.

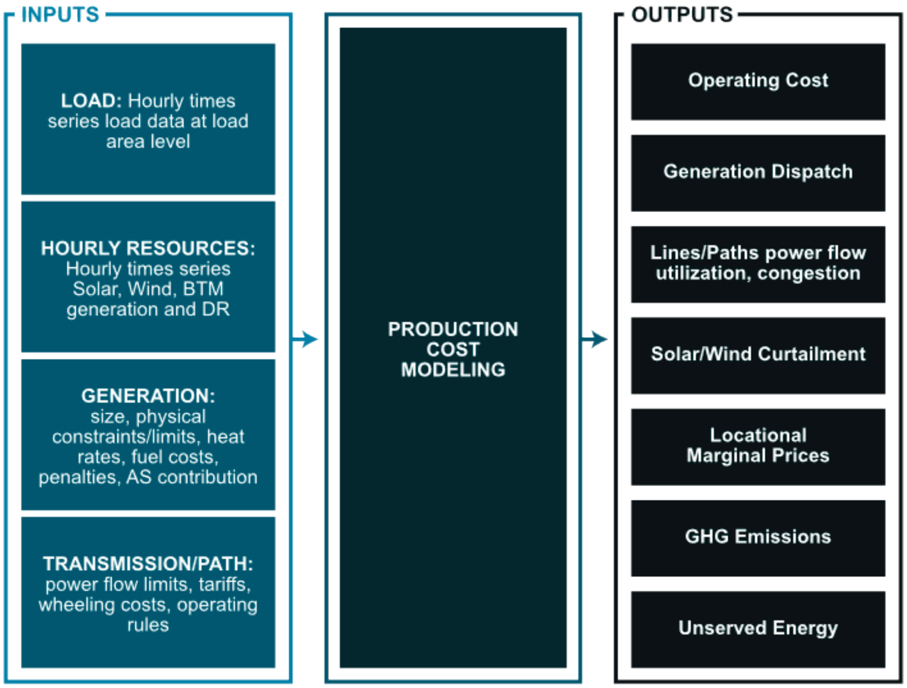

Figure 16. Modeling inputs and outputs of the PCM analysis (U.S. DOE 2024). BTM—Behind the Meter, DR—Demand Response, GHG—Greenhouse Gas

5.2 Construction of the 2035 and 2050 Models

In order to represent the years 2035 and 2050 in the PCM, the ADS 2032 data were incremented in several steps.

First, as the ADS 2032 was under development at the initiation of the study, the critical power flow model convergence from the ADS 2030 process was preserved by manually adjusting the ADS 2030 inputs to yield the ADS 2032 inputs. This process is explained in Appendix A. As a result of this step, 2009 weather was inherited from the ADS 2030 inputs. Weekly hydropower budgets were incorporated, as they are in ADS 2032, but based on the 2009 hydrology to be consistent with wind and solar profiles that are based on 2009 weather year.

Secondly, generation mixes were updated to meet the capacity expansion results from the CEM (Section 2.4). The resulting change with respect to the initial installed capacities in the ADS 2032 are illustrated in Figure 17 for the two study years. The added OSW is 15 GW in 2035 and 33 GW in 2050 based on the study design. Wind profiles for the new wind power plants and the ADS 2032 set were extracted from the Wind Toolkit for the 2009 weather year (Draxl et al. 2017). Similarly, solar profiles for all solar power plants in the nodal PCM were extracted from the National Solar Radiation Database for 2009 weather (Sengupta et al. 2018).

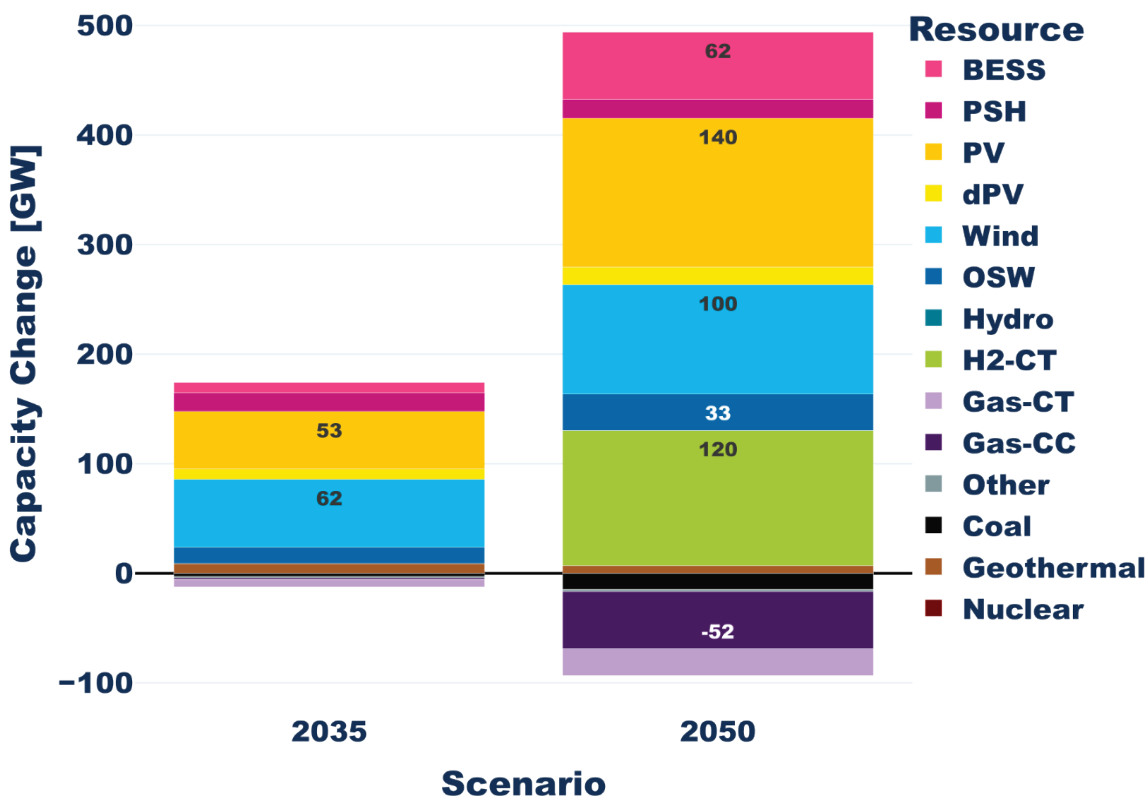

Figure 17. Generation capacity change from ADS 2032 in U.S. footprint of the WI.

Hourly load profiles for the year 2035 and 2050 were obtained from Haley et al. (2023) which projected a demand growth trajectory from bottom-up estimates of building and transportation electrification, population growth, weather shifts, and influence from the Inflation Reduction Act on technology adoption. These loads were provided at a state-level which were first disaggregated at the nodal level using load distribution factors from the 2030HS (Heavy Summer) Power Flow dataset and were then back aggregated to the 38 WECC balancing authorities. Demand projections corresponding to the three West Coast regions of particular interest to this study indicate the winter peaking of the Northwest (NW) and the summer peaking of California through 2050 (Figure 18 and Figure 19).

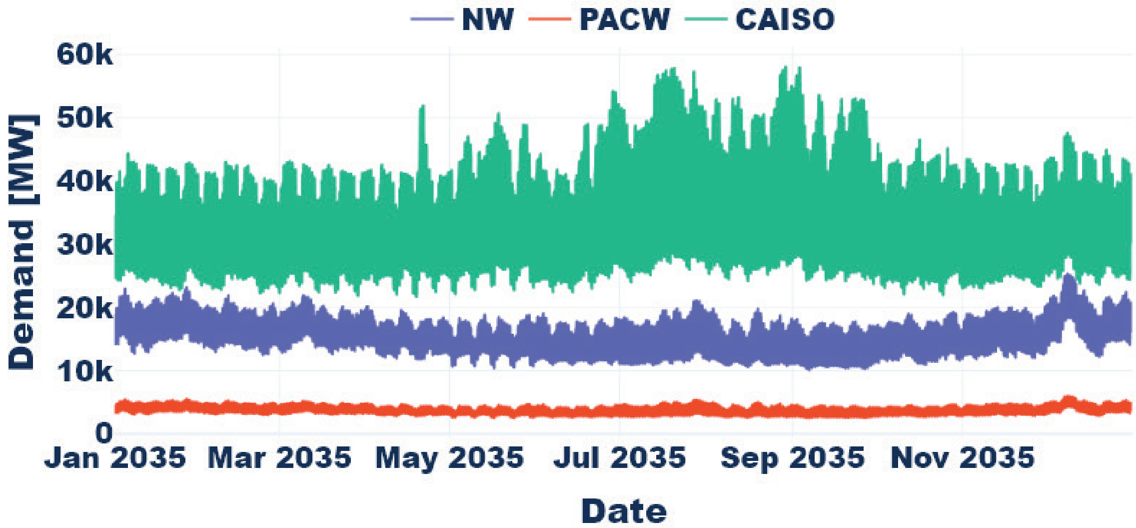

Figure 18. Projected 2035 Demand in NW, PACW, and CAISO regions

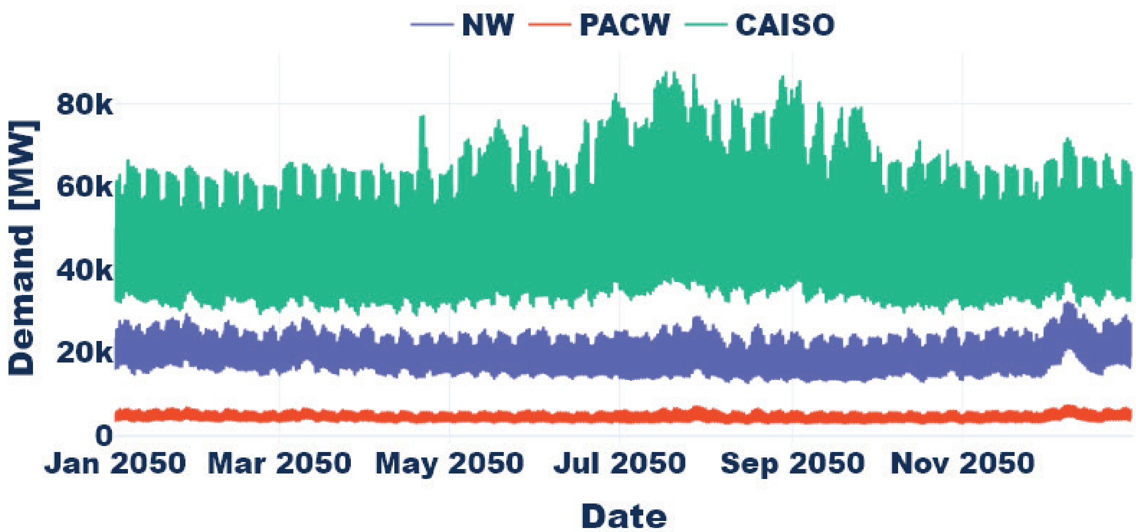

Figure 19. Projected 2050 Demand in NW, PACW, and CAISO regions

Finally, interregional transmission was expanded until average generator curtailment dropped below 20%. The total MVA of added transmission is reported in Figure 20, with maps illustrating how the new transmission intersects with the generation resources shown in Figure 21. The maps are primarily intended to give a sense of the onshore expansion. For that reason, there is only one for each expansion year, as only the offshore topology changes as part of the topology sets within a given year (i.e., 2035 Concentrated vs. 2035 Distributed).

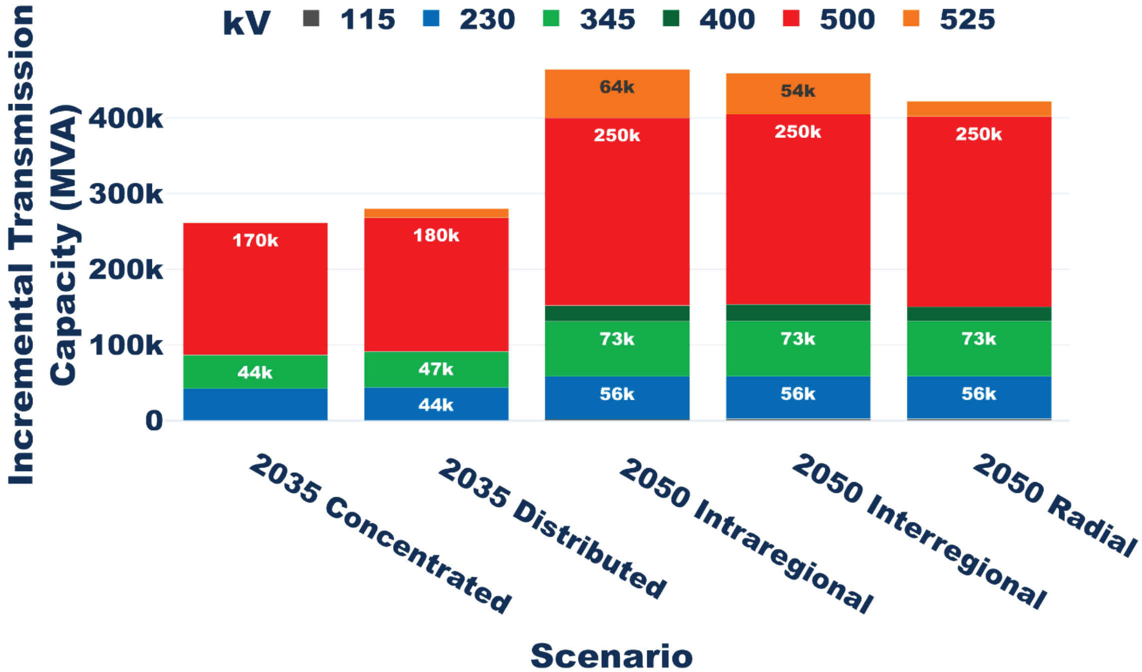

Figure 20. Total MVA of added transmission in the 5 scenarios from the ADS 2032 starting point.

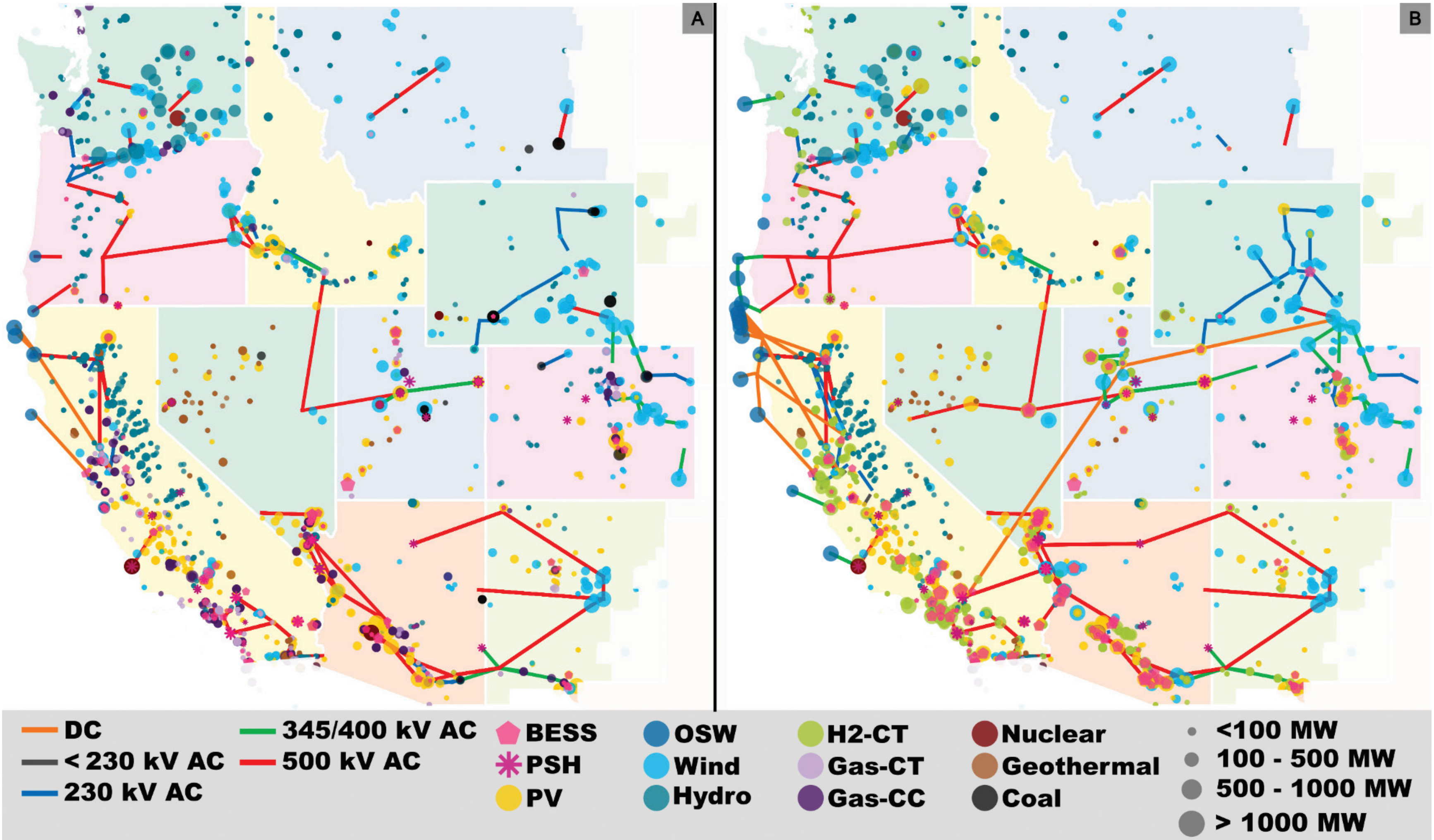

Figure 21. Nodal expansion maps for 2035 (panel A) and 2050 (panel B) relative to the ADS 2032 model. All onshore components remain identical between the topology sets within a given year.

5.3 Key Assumptions of the PCM

5.3.1 Fuel Price Variations

The WECC ADS models several different natural gas prices by region, to capture trading hub nature of gas more accurately. The same geographic distribution is used in the 2050 scenarios for the price of hydrogen. Figure 31 in Sensitivity #1: Hydrogen Price Variation shows the range of prices.

5.3.2 OSW Interconnections

As described in Section 4.0, OSW interconnections were of HVAC and HVDC types, and were either radial (connecting directly from an OSW plant to a POI) or networked (connecting multiple OSW plant and/or POIs) designs. Some radial interconnections were modeled as point injections directly to the POI, while all elements of the networked designs were represented explicitly in the PCM.

5.3.3 Market Concept

A PCM approach to modeling the Western Interconnection implies a single market type of operation in the study. Bi-lateral contracts for power supply and the transmission rights associated with them are therefore not directly captured. The concept of firm transmission rights is not captured. Finally, as each simulation consists of a single, 8760-hour run, any additional markets, such as the Energy Imbalance Market or the Western Resource Adequacy markets, are not captured.

At the same time, the PCM, unlike actual markets, operates on production cost rather than bids. The results of the simulations aim to represent the lowest cost dispatch of the system. The implicit assumption is that market structures strive towards this same lowest cost solution, and as a result will converge to a similar operating point.

The WECC ADS model contains several constraint types, namely, path limits, wheeling costs, and export/import charges, to indirectly represent the reliability and market forces that shape how the various entities operate. Since the developed topologies deviate markedly from the current system, most of these were deactivated in the PCM simulations. Only the path limits external to the U.S. (P3, P83, and P45[8]) were kept active given the geographic focus of this study on the U.S. footprint as discussed next.

5.3.4 Capturing Interregional Exchanges

The PCM analysis considers imports and exports between the load areas in the PCM[9]. For the purposes of the following analysis, an import/export is defined as any flow on a branch component (transmission line, transformer, converter, etc.), where the load areas on either end do not match. As an example, generation in PacifiCorp East (PACE) that is consumed in PacifiCorp West (PACW) will be captured by the model as exports from PACE and imports into PACW. This accounting is related to the already mentioned fact, that the market model captures neither bi-lateral contracts nor firm transmission rights.

---

[8] For a map indicating the location of these paths see Appendix A.
[9] For a map and list of the load areas in the PCM see Appendix A.

5.3.5 Geographic Extent of Analysis

The WECC ADS model covers the full extent of the Western Interconnection, which includes parts of Mexico and Canada. However, the ReEDS capacity expansion does not consider regions outside of the U.S. As a result, no expansion is performed outside of the U.S. and therefore, none of the Mexican or Canadian portions of the nodal PCM and power flow models are modified in any way. While they are still included in simulations, all reported results such as production cost, curtailment, etc. are limited to the U.S. footprint of the model. The cost of imports is calculated by multiplying the LMP on the US side of each link crossing the border by the flow in the direction of the US. In other words, the cost of purchasing the energy at the import node is assumed.

While the subsequent analysis focuses on the U.S. portion of the WI, particular attention is given to the regions along the coast, where OSW is integrated. Some regional aggregations are referred in the analysis, which are made up of several load areas in the PCM model, as described in Table 5.

Table 5. Load area aggregation for PCM analysis[10]

Aggregate Region Name	Composing Load Areas in PCM[11]
CAISO	CIPV, CIPB, CISC, CISD
NW	BPAT, PGE, SCL, PSEI, TPWR
PACE	PAID, PAUT, PAWY

5.4 Production Cost Model Results

In this section, base scenario results from the topologies introduced in Section 4 and four additional sensitivities are presented. Overall production cost findings for the WI are summarized in Table 6 below. Figure 22 illustrates the WI-wide production cost results by resource type and Figure 23 shows the OSW curtailment[12].

Table 6. Base production cost results, all topology sets

Topology Set	Description	Production Cost [$B]	Offshore Wind Curtailment [GWh]
2035 Distributed	15 GW (13 CA, 2 OR), 9 radial interconnections	4.545	2045 (3.8%)

[10] The PacifiCorp West BA is also isolated in the PCM and RA analyses and referred to as "PACW."
[11] Definitions of the load areas in the PCM can be found in Appendix A.
[12] Details about how the PCM determines curtailment are provided in Appendix A.

Topology Set	Description	Production Cost [$B]	Offshore Wind Curtailment [GWh]
2035 Concentrated	15 GW (13 CA, 2 OR), 5 radial interconnections	4.542	2530 (4.6%)
2050 Radial	33 GW (25 CA, 6 OR, 2 WA), 13 radial interconnections	23.917	9061 (7.7%)
2050 Intraregional	33 GW (25 CA, 6 OR, 2 WA), 13 networked interconnections within regions	23.284	8014 (6.8%)
2050 Interregional	33 GW (25 CA, 6 OR, 2 WA), 13 networked interconnections within and between regions	22.872	7377 (6.2 %)

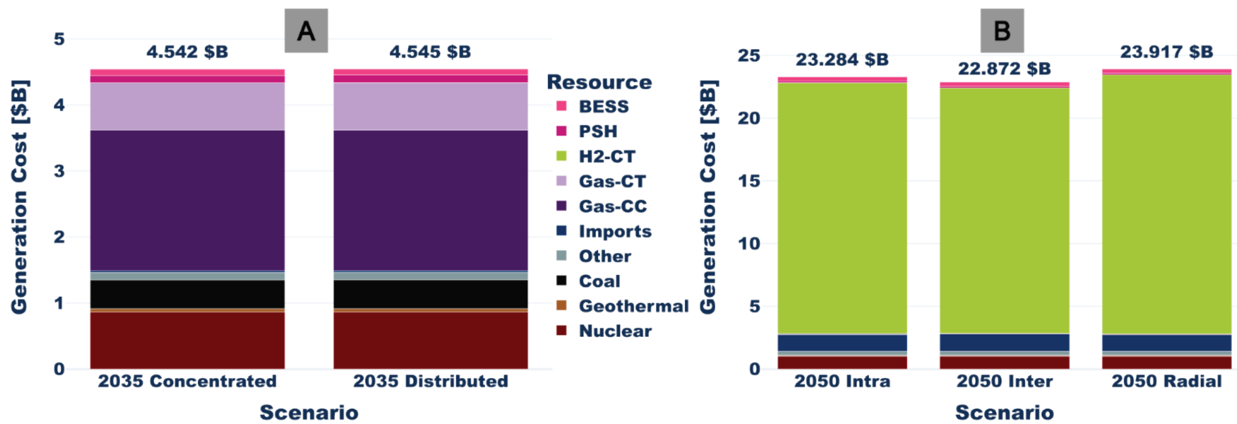

Figure 22. Production cost results with resource type indication in A) 2035 and B) 2050 topology sets

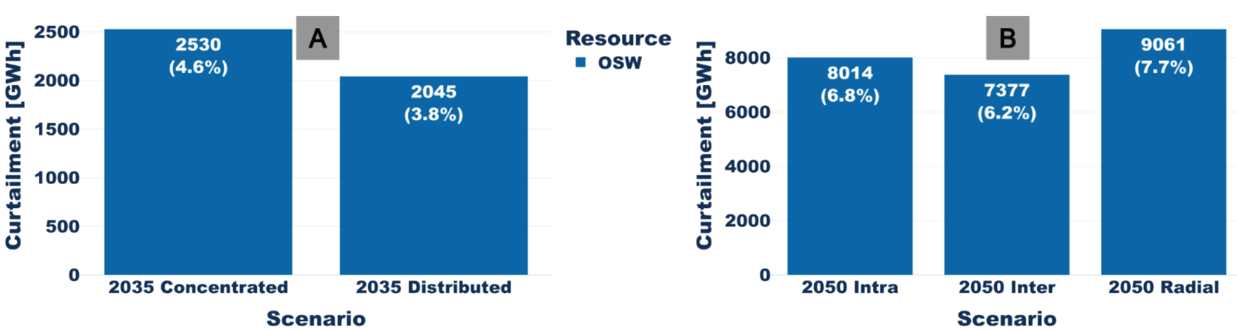

Figure 23. OSW curtailment in the base scenarios in A) 2035 and B) 2050 topology sets

5.4.1 2035 Topology Sets—Generation Dispatch and Key Transmission Paths

Total generation dispatch for both 2035 topologies is summarized in Figure 24 for the whole US portion of the WI, as well as for the coastal regions. Overall, the dispatch is very similar, with the exception of PACW, which has a POI at Del Norte in the Distributed Topology, leading to an increase in OSW dispatch in that region, and a corresponding reduction in imports.

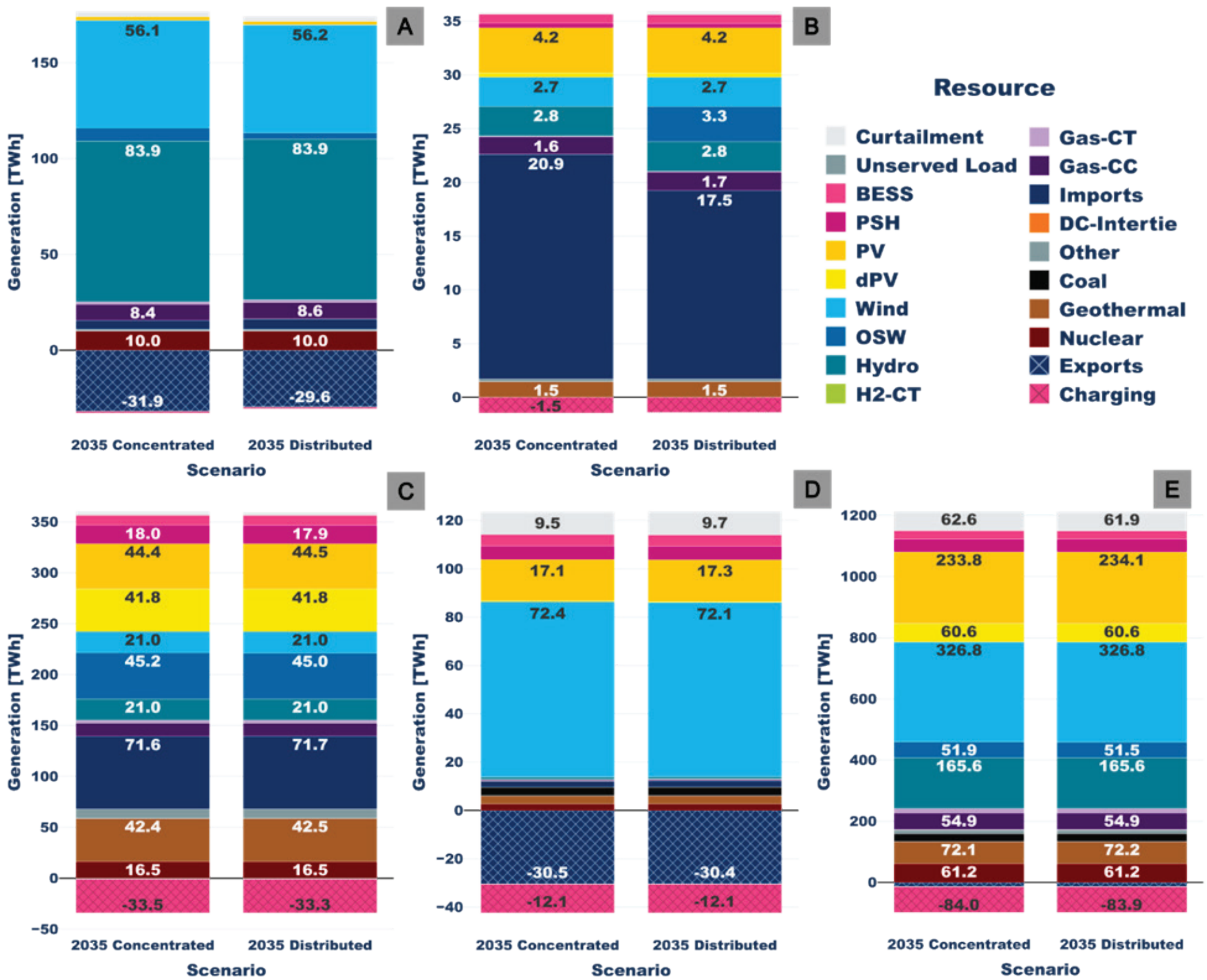

Figure 24. 2035 yearly generation in A) NW B) PACW C) CAISO D) PACE and E) US portion of the WI.

The impact of distributing the OSW POIs on PACW can be observed in some of the system flows. Figure 25 shows the flow on the California-Oregon Intertie (COI, path 66) as well as the link between the Round Mountain and Fern Road substations. In both cases, the Distributed Topology shows higher North-South (positive) flows compared to the concentrated one. This observation matches the reduced imports observed in PACW. The important takeaway, that becomes even more pronounced in 2050 and the sensitivities, is that any potential for low-cost imports into California are preferred by the model. Adding OSW to Del Norte and connecting it via the 500 kV to Captain Jack and thus the northern end of the COI, allows more energy to be exported south.

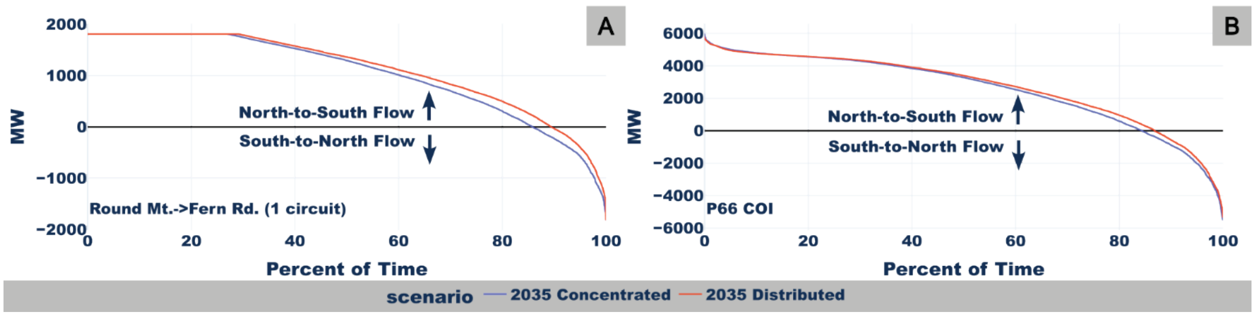

Figure 25. Load duration curve on (A) one of the circuits between Round Mt. and Fern Rd. and (B) Path 66 (COI). Both show slightly increased north-south flows in the Distributed Topology. Positive values are north-to-south flows, while negative values are south-to-north flows.

Finally, looking at the OSW generation dispatch in chronological time further illustrates how OSW replaces some of the PACW imports in the Distributed Topology. Figure 26 shows the dispatch of OSW and imports in PACW during the week containing the peak OSW production hour. The figure focuses on just the imports and OSW generation to highlight how the combination of these two resources in the Distributed Topology very closely matches the import only behavior in the Concentrated Topology.

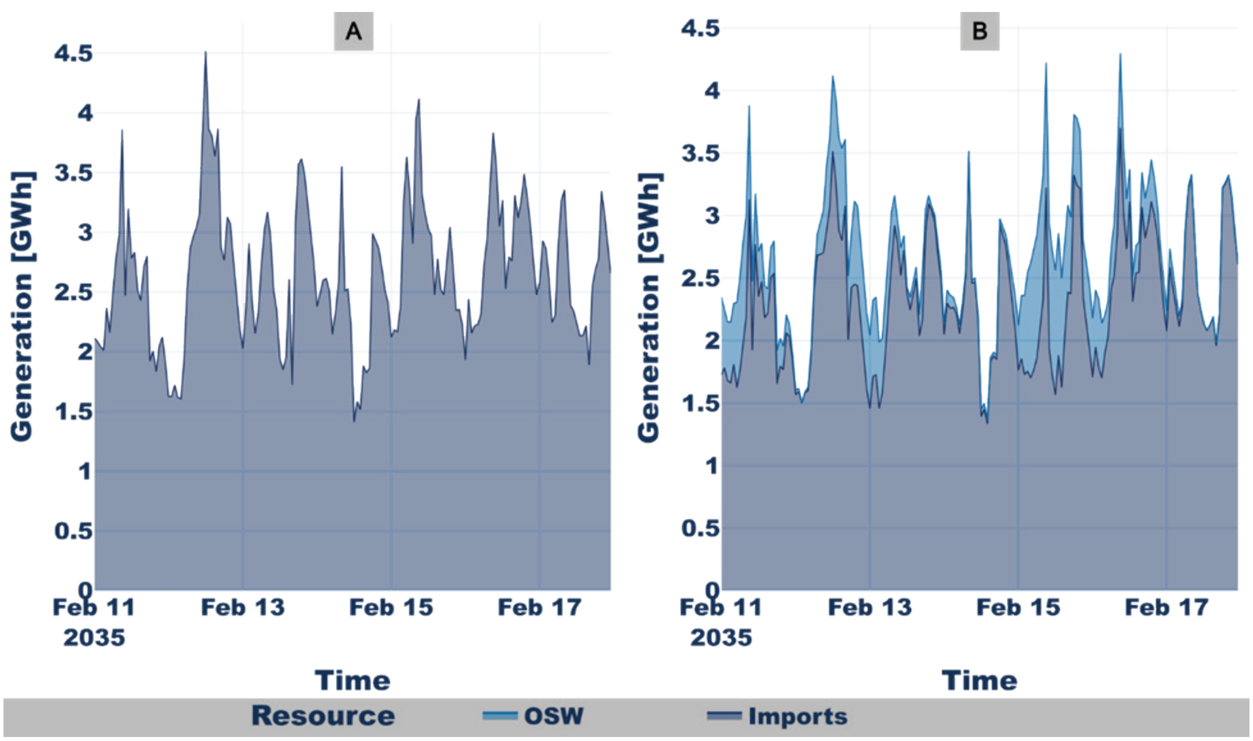

Figure 26. Import and OSW dispatch in PACW during the week with peak system OSW in all of the WI. (A) Concentrated (B) Distributed.

The results of the two topology sets for 2035 suggest that, at least at the granularity of the PCM, there are only small differences in terms of the system dispatch operations. The most significant difference is seen in PACW due to the addition of an OSW POI at Del Norte that offsets some of the imports into that region.

5.4.2 2050 Topology Sets—Generation Dispatch and Key Transmission Paths

Similar to the 2035 topologies, the generation dispatch for the 2050 topologies for the whole US portion of the WI, as well as the coastal regions is captured in Figure 27.

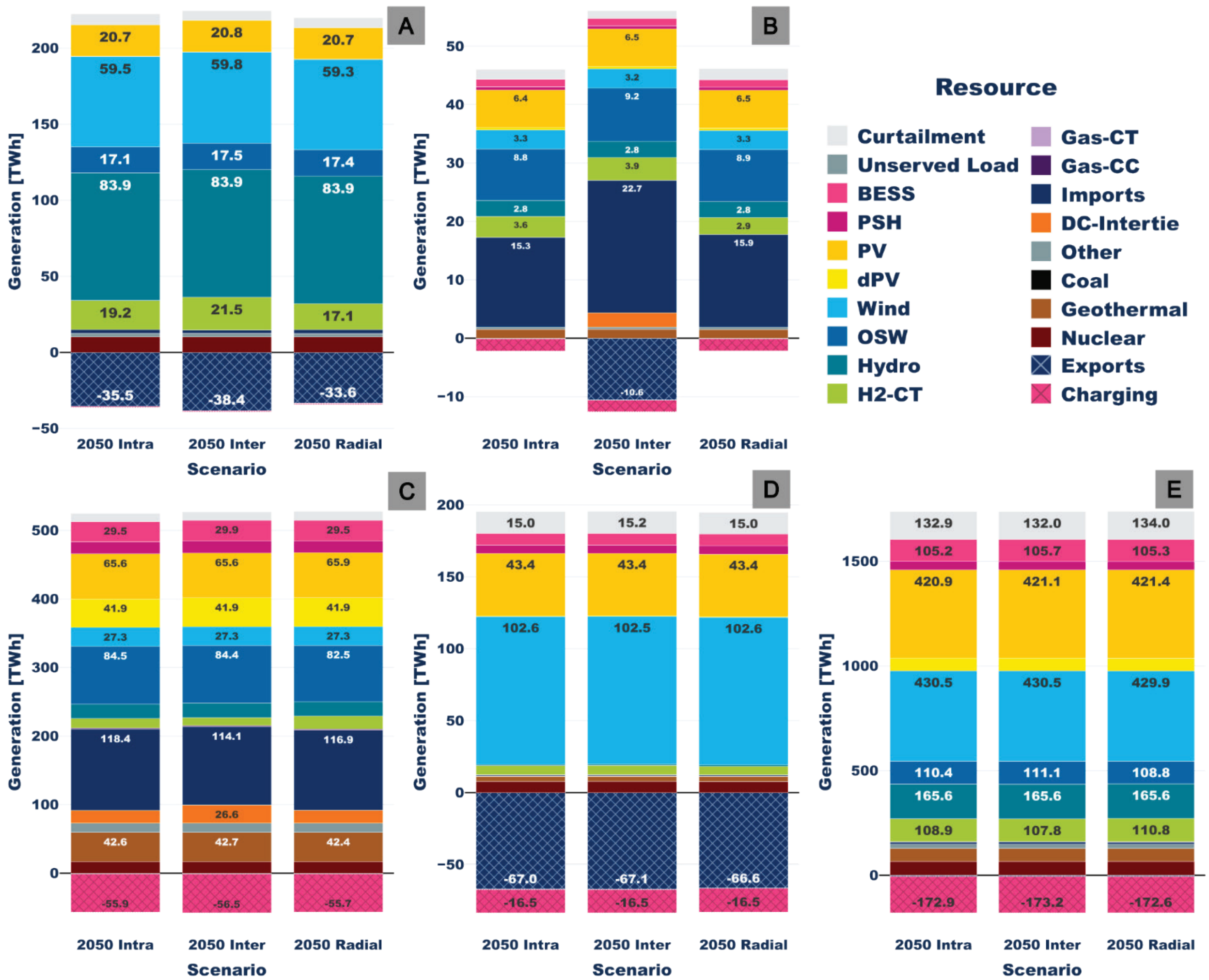

Figure 27. 2050 yearly generation in A) NW B) PACW C) CAISO D) PACE and E) US portion of the WI.

The system wide dispatch (panel E) shows a slight decrease in generation from variable renewable energy (VRE) resources[13] in the 2050 Radial Topology compared to the other two, offset by a slight increase in hydrogen generation. It is worth noting that a small change in hydrogen production is responsible for the majority of generation cost differential seen Figure 22.

Moving to the regional dispatch, the most notable difference is the increase in exports from PACW (panel B) in the Interregional Topology, due to the addition of the interregional OSW link. Figure 28 shows 2000 MW North-South flow nearly 50% of the year on the interregional link. At the same time, Figure 29 shows the COI to highlight that a) the flow in the Interregional

[13] VRE resources considered in this study are photovoltaic (PV), distributed photovoltaic (dPV), Wind, & OSW.

Topology is lightly reduced relative to the Intraregional Topology, as the interregional OSW link provides an alternative to the COI North-to-South corridor, and b) the Radial Topology is not able to utilize the COI to the same degree as the other two, partially due to the lack of flexibility in shifting injection afforded by the MTDC of the Interregional and Intraregional Topologies.

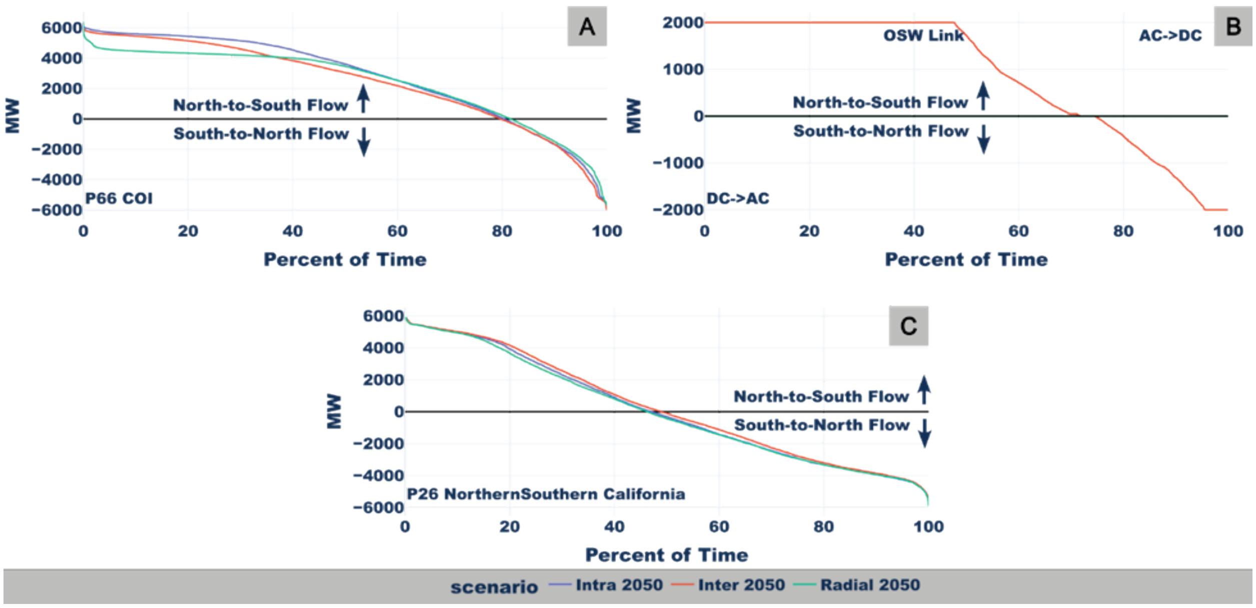

Figure 28. Load duration curves on the (A) COI, (B) interregional offshore link, which is only available in the Interregional Topology, and (C) Path 26 between northern and southern California.

The final flow duration curve in Figure 28 shows the flow on Path 26 connecting northern and southern California. While the differences are small, there is progressively more North-South flow moving from the 2050 Radial, to the Intraregional, and finally to the Interregional Topologies. The increased transfers are reflected in a reduction and flattening of the locational marginal price (LMP) differences moving from the Radial Topology to the other two, as seen in Figure 29. The LMPs also show how the additional flows from Oregon further flatten and reduce the LMPs across the Fern Road substation in the Interregional Topology.

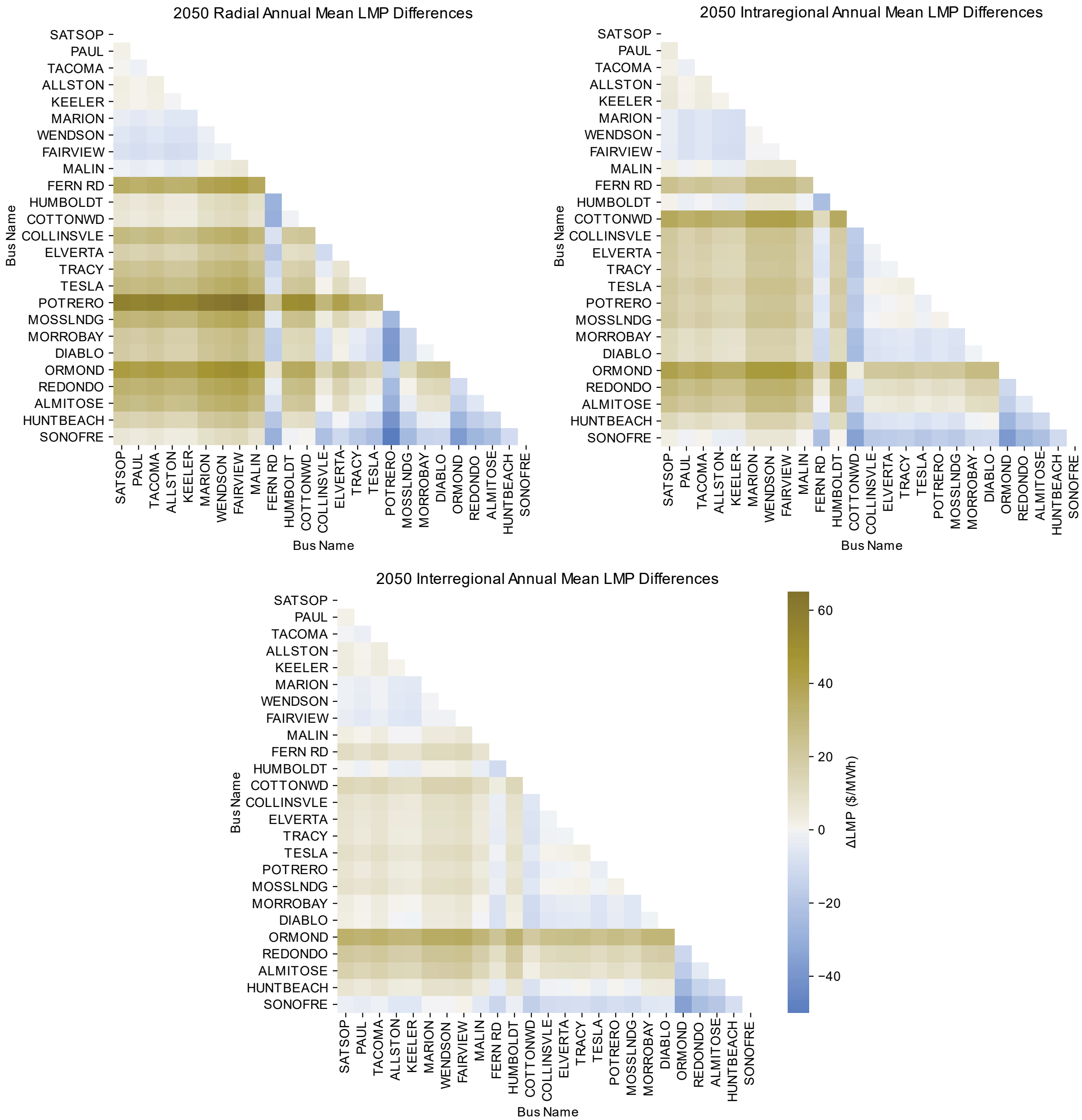

Figure 29. Annual Average LMP differences (LMPs from POI on horizonal axis subtracted from POI on vertical axis POI), 2050 Radial (left), 2050 Intraregional (middle), 2050 Interregional (right)

Finally, for the 2050 Interregional Topology, there is an increase of imports into CAISO that aligns with the increase in exports from PACW, as well as an increase in exports and hydrogen production in the NW (Figure 26). The link between hydrogen production in the NW and CAISO imports is due to the pricing differential of hydrogen and is further investigated in Sensitivity #4 and Figure 30.

Figure 30. Dispatch during peak hydrogen generation in the NW focusing on resources that differ between topologies.

The left-most column of Figure 30 shows the generation dispatch during the week with the peak hydrogen utilization in the NW in the Interregional Topology. Moving from NW south through PACW to CAISO, there is a shift from exporting to importing. The peaks in hydrogen generation in CAISO are aligned with reductions in exports from both NW and PACW indicating the preference for imports over the expensive hydrogen resource.

The center and right columns of Figure 30 show the difference between the dispatch in the Interregional Topology and the Radial and Intraregional ones, respectively. For all resources, except exports, positive values mean more of that resource in the Interregional Topology compared to the Radial or Intraregional Topologies. For exports, negative values indicate more exports in the Interregional Topology compared to the others. These show more hydrogen dispatch in the NW and PACW in the interregional case, and less hydrogen dispatch in CAISO.

This illustrates once again the geographic H2 fuel price arbitrage that the Interregional and the Intraregional Topologies can provide.

As a final observation, the difference in OSW generation between the interregional and radial topologies is generally positive in Figure 30, indicating that the OSW infrastructure does help transport some additional OSW resources. Notably, there is little difference between the interregional and Intraregional Topologies, indicating that in terms of OSW delivery, these topologies are comparable.

5.4.3 Production Cost Modeling Sensitivities

Four additional sensitivities were run to understand how dispatch and production cost results may change under different futures. First, a sensitivity on hydrogen price was motivated by the technological challenges with production, storage, and distribution at scale of green hydrogen for the hydrogen combustion turbine fleet of the 2050 models. Secondly, a contingency-secure dispatch was considered both as a restriction on the assumed transmission builds in the models and also to serve as a alternate dispatch check of the system reliability reinforcements from Section 6.0. Third, new interregional transmission was derated to understand how OSW transmission could be utilized differently. Finally, hydrogen combustion turbine capacities were derated to understand the utility of OSW transmission with less dispatchable, firm, clean generation available to the WI.

Sensitivity #1: Hydrogen Price Variation

The first sensitivity looks at how variations in the price of hydrogen impacts the study results. Hydrogen generation costs dominate the total production cost in the 2050 scenarios (see Figure 23). This sensitivity compares the base results, where hydrogen costs five times the geographically varied natural gas price, versus an overly optimistic scenario where hydrogen costs the same as natural gas, which is lower than the DOE Hydrogen Shot target of $1/kg[14]. Figure 31 shows the price variation of hydrogen in the low and high price assumptions.

[14] See https://www.energy.gov/eere/fuelcells/hydrogen-shot

Figure 31. Hydrogen price based on geographic distribution of natural gas prices in ADS and a heat rate of 8.64 MMBTU/MWh

Hydrogen represents the firm capacity, marginal dispatchable unit in the model. Since it is the marginal unit, variation in cost does not meaningfully change system operations, as the PCM always prefers other, cheaper resources over hydrogen. Figure 32 shows the dispatch difference between the base and reduced hydrogen cost runs, as well as the production cost. There is a small difference in total hydrogen production between the base and reduced hydrogen cost runs that is largely offset by the imports from Canada and Mexico. Recall that while no modifications have been made outside the U.S. footprint of the WI, but that the Canadian and Mexican load areas are still part of the simulation and the interaction with them is constrained by WECC path limits P3, P83, and P45. As hydrogen prices increase, it becomes less attractive to export from the U.S. and becomes more attractive to import. Meanwhile, the production cost differences, seen in panel C of Figure 32, are very significant, despite the small dispatch changes.

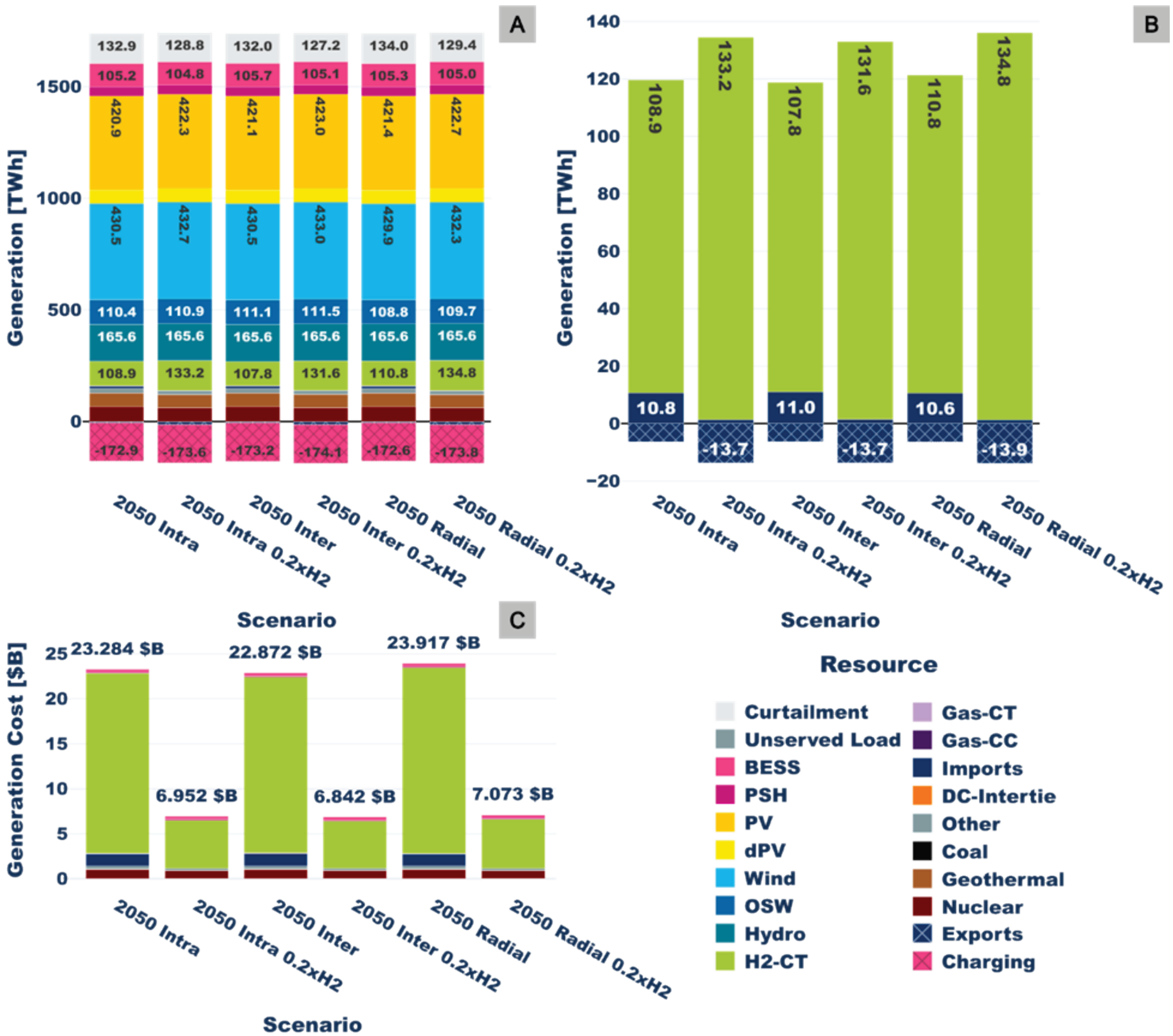

Figure 32. 2050 Generation Mix for base and reduced H2 Price Sensitivities. (A) Full mix showing little change in most resources. (B) Focus on Hydrogen and Imports/Exports to Mexico and Canada. (C) Significant change in production cost resulting from small generation difference.

The difference between hydrogen energy production between the Intraregional and Interregional Topologies with respect to the radial counterfactual is tabulated in Table 7 along with the difference in production cost. The negative values in the production difference (first two columns) indicate that there is less hydrogen production in both topologies compared to the radial. The negative production cost difference (last two columns) similarly indicate that the cost of hydrogen production is lower in the two topologies compared to the radial. While the production numbers in the reduced-price sensitivity are similar (84% and 107%) to those in base scenarios, the difference in cost is substantial. The cost benefit relative to the Radial Topology of both the intra- and interregional topologies in the reduced-price sensitivity is roughly 20% of the benefit in the base scenarios. This difference aligns closely with the 20% reduction in price since hydrogen is the main driver of production cost.

Table 7. Hydrogen production and production cost variation as a function of hydrogen price

Topology Set	H2 Production Difference w.r.t 2050 Radial [TWh]		Production Cost Difference w.r.t 2050 Radial [$B]	
	Base	Reduced Price Sensitivity (% w.r.t Base Price Result)	Base	Reduced Price Sensitivity (% w.r.t Base Price Result)
2050 Intraregional	-1.9	-1.6 (84%)	-0.633	-0.121 (19%)
2050 Interregional	-3.0	-3.2 (107%)	-1.045	-0.231 (22%)

Since the larger production cost savings accumulate year after year, the impact of a ~5x decrease in hydrogen price changes the cost benefit calculation of the infrastructure investments, which remain fixed in both scenarios (Section 7.0).

This sensitivity highlights the flexibility role of transmission. With a high hydrogen price, even small production savings, achieved through added flexibility from transmission, translate to significant lifetime savings. As the hydrogen price decreases, hydrogen becomes a more attractive source of flexibility, and the added benefit of transmission is less significant. This sensitivity offers two ends of a spectrum. In reality, the hydrogen price may fall below the base scenario level, but not as far as the modeled reduced-price sensitivity. This sensitivity suggests that the benefit of additional transmission around OSW should be assessed with consideration to the confidence in the forecasted hydrogen price prediction: the less bullish the prediction, the more valuable the OSW transmission expansion.

Sensitivity #2: Security-constrained Operations

The base operation scenarios assume normal, or system intact, operation. In practice, many of the decisions around system operations hinge on providing secure operation, meaning that the system is tolerant to a number of contingency scenarios. A robust set of contingency scenarios is assembled and analyzed in Section 6.3 resulting in a set of system upgrades to ensure reliable operations in Section 6.4.

In addition, the PCM can also incorporate security constraints to produce a preventative, and normal operations dispatch that remains reliable in the event that any of the modeled contingencies occur. The security-constrained operations sensitivity takes all the contingencies from Section 6.3 that can be modeled in the PCM[15] and that showed significant thermal violations[16] of the emergency limits in the power flow analysis and then adds them to the PCM.

[15] These are line outages, generation outages, and load outages. Contingencies such as shunt faults cannot be modeled in the linearized representation of the PCM.

[16] For the purposes of this sensitivity, only violations greater than or equal to 105% of the emergency rating are used.

Each modeled contingency consists of a set of altered elements, which undergo service status changes, and a set of monitored branches with emergency ratings that may not be violated, despite the status changes in the altered set. For each contingency, the set of monitored branches are all those that exceed their limit in the power flow analysis, prior to any system upgrades. Therefore, this approach yields an alternative dispatch with reliability similar to the base operation scenarios including the upgrades of Section 6.3 (corresponding to base operations of Section 5.4.2), while assuming that none of those system upgrades are implemented,[17] The contingencies and monitored branches from all 2050 scenarios are combined to create one unified set for the PCM sensitivity runs. The number of security constraints and monitored branches for each 2050 scenario is summarized in Table 8.

The purpose of the security-constrained sensitivity is twofold:

1) How do the reliability upgrades in Section 6.4 compare to higher operational cost due to system constraints?

2) How do different OSW integration topologies impact operations under a more constrained transmission scenario?

Table 8. Security constraints added to production cost models

Topology Set	No. of Contingencies	No. of Monitored Branches
2050 Intraregional	953	3427
2050 Interregional	953	3427
2050 Radial	953	3425[18]

To address the first question, the total production cost for the 2050 scenarios is presented alongside the base production cost in Figure 33. Additionally, the difference is plotted for each topology set. These costs exceed the annualized costs for the reliability upgrades in Section 6.4 suggesting that some reliability upgrades are certainly needed. In practice, neither option is an optimal path, which almost certainly involves a mixture of equipment upgrades and operational solutions (e.g., alternate generation dispatch). Nonetheless, the favorable comparison of the production cost savings with the annualized cost of upgrades, suggest that the cost presented for achieving reliable operations under the topology sets is likely a conservative estimate.

With security constraints, the cost savings of the non-radial topologies with respect to the radial counterfactual increases as shown in Table 9. With respect to the second question targeted by this sensitivity analysis, the results suggest that under increasing transmission constraints, the value of transmission flexibility increases, as realized by more connected OSW integration topologies.

[17] For all other PCM solutions, the reliability upgrades of Section 6.3 are assumed for reliability.
[18] The difference of two branches is the AC offshore link between Del Norte and Fairview that doesn’t exist in the Radial Topology.

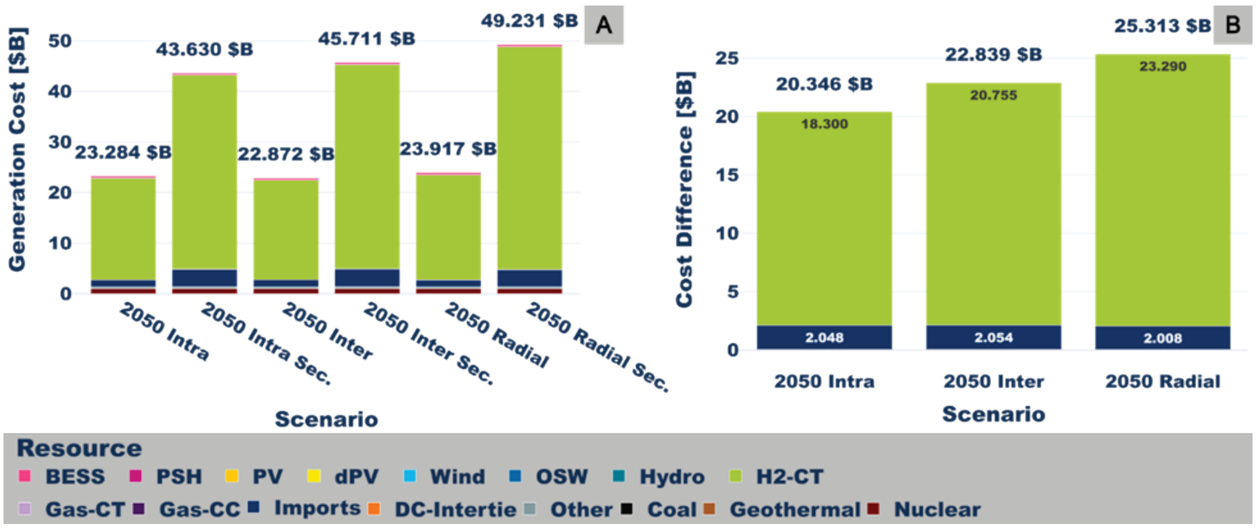

Figure 33. (A) Production cost with addition of security constraints (B) difference w.r.t system base runs.

Table 9. Cost savings with respect to Radial Topology of 2050 scenarios.

Topology Set	Base Operations	Security-constrained Operations
2050 Intraregional	2.6%	11.4%
2050 Interregional	4.4%	7.2%

With the security constraints enforced, the Intraregional Topology replaces the interregional one as the cheapest operationally. The full rationale for this switch will take additional analysis, however, looking at the converter station flows onshore provides some indication. Figure 34 shows the flows at the Tesla and Fern Road converter stations, that are respectively the southern and northern most converter stations in both MTDC topologies along the 500 kV AC backbone in northern California. The key observation, as to why Intraregional Topology might achieve cheaper operations under the security constraints, is that it maintains a much more symmetrical operation between these two ends (solid blue line crossing closer to 0.5 compared to solid red line), which corresponds to more transmission of cheaper generation southward.

The added constraints on the system require, in end effect, a reduction of flow in many lines. The added flexibility to shift power around via the MTDC helps alleviate that to a degree. In the Interregional Topology, this connection occurs offshore and therefore, flows from Tesla to Fern Rd., for example, accumulate with any other northbound flows to potentially trigger limits. The onshore construction in the intraregional scenario allows for some more separation between the OSW injections and the flexible operations offered by the MTDC backbone.

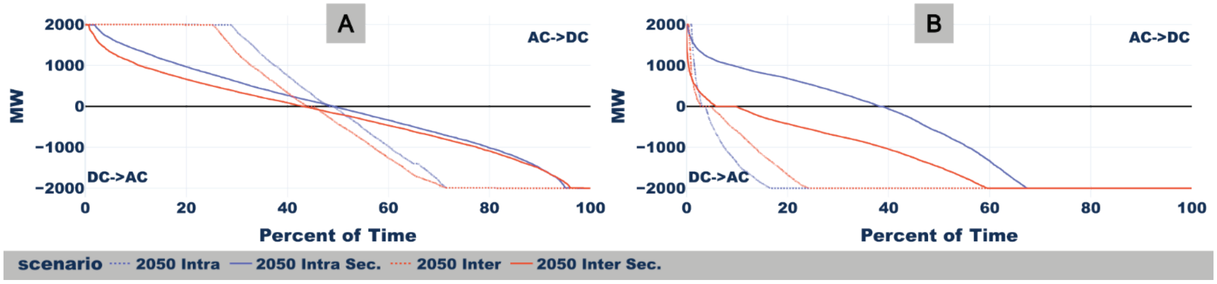

Figure 34. Flow duration plots in two onshore converter stations (A) Tesla (B) Fern Rd.

This raises an interesting question regarding the point on the cost spectrum between reliability upgrades and constrained dispatch discussed in addressing the first question in this sensitivity. Somewhere along that spectrum the value of the strong, onshore MTDC, with its tighter coupling to the AC backbone may surpass that of the offshore MTDC, that prevails in the base scenario. Further investigation is needed to determine where that point might be, the scope of secure operations that should be considered during dispatch, and the expected behavior of the MTDC in response.

Sensitivity #3: Interregional transmission de-rate

While this study focuses on the development of OSW and the transmission most directly considered to interconnect it, the system expansion includes very large additions of resources and transmission on land as shown in Figure 35. The motivation of this sensitivity is to consider how the system might behave if the onshore transmission expansion were not realized at the scale or pace that is assumed by the model. This is modeled by derating all *new* transmission *outside* of the coastal load areas under considerations. In total 145 branches are derated. The load areas they connect and the MVA capacity in the base scenarios is reported in

Table 10. Those capacities are then derated by 10%, 20%, and 30%.

Table 10. Derated transmission capacities by load area

Area 1	Area 2	Original MVA
AZPS	AZPS	4373
	CISC	4373
	PNM	4373
	TEPC	4373
	TH_PV	6992
	WALC	3902
BPAT	IPTV	2187

Area 1	Area 2	Original MVA
	NWMT	2187
CISC	NEVP	6928
	WALC	10392
EPE	EPE	1566
	PNM	4373
	TEPC	5939
	WALC	3066

Area 1	Area 2	Original MVA
IPMV	IPTV	3131
IPTV	IPTV	10125
LDWP	NEVP	3464
	PAUT	7828
NWMT	NWMT	4851
PAID	PAID	1055
PAUT	PAUT	20353
	WACM	896
PAWY	PAWY	20196
	WACM	4427
PNM	PNM	13856
	SRP	2187

Area 1	Area 2	Original MVA
PSCO	PSCO	24477
	WACM	4684
SPPC	SPPC	4373
SRP	SRP	598
	TEPC	5045
	TH_PV	3374
	WALC	2187
TEPC	TEPC	10247
TH_Mead	WALC	2187
TH_PV	TH_PV	3326
WACM	WACM	5561
WALC	WALC	500

Figure 35 shows the yearly generation dispatch for the transmission derated sensitivity on the interregional and radial topologies. In both cases, as the transmission is derated, onshore resources, that rely on that transmission to get to load, like land-based wind and solar, see their generation reduced. Hydrogen, which is the primary dispatchable resource in the 2050 systems makes up the difference, increasing production as the transmission capacity is derated. Importantly, since OSW is naturally connected along the coast, and that transmission is *not* derated as part of this sensitivity, the production from OSW does not meaningfully change. Since it is a zero marginal cost resource, the system is already taking as much OSW as possible during non-derated operations, the sensitivity therefore, cannot push OSW production meaningfully higher. Holding steady however, shows that the sensitivity does not reduce the base effectiveness of the OSW resource.

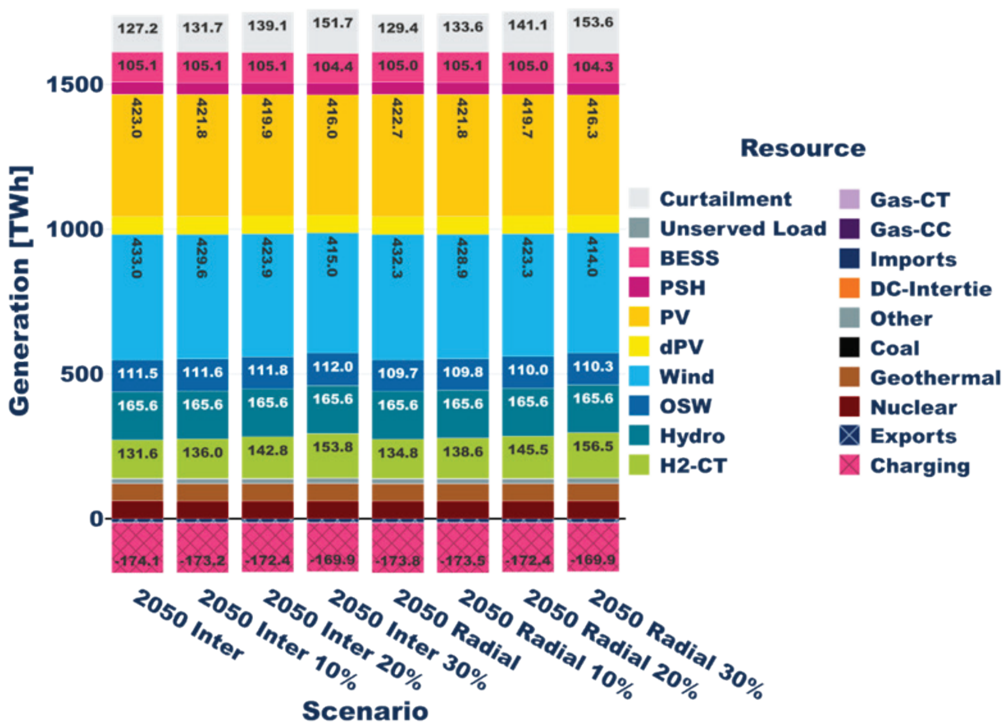

Figure 35. Energy production by resource with and without transmission derates. Onshore wind and solar that rely on onshore transmission are reduced in favor of hydrogen when the transmission is derated.

Given that the transmission paths in the system are derated, the hypothesis is that that the interregional link in the Interregional Topology will provide additional value. Figure 36 shows the flow on the offshore link. The northbound flow (DC to AC) increases as the new transmission is further derated, as expected. Unexpectedly however, southbound flows (AC to DC) *decrease* as the transmission is further derated.

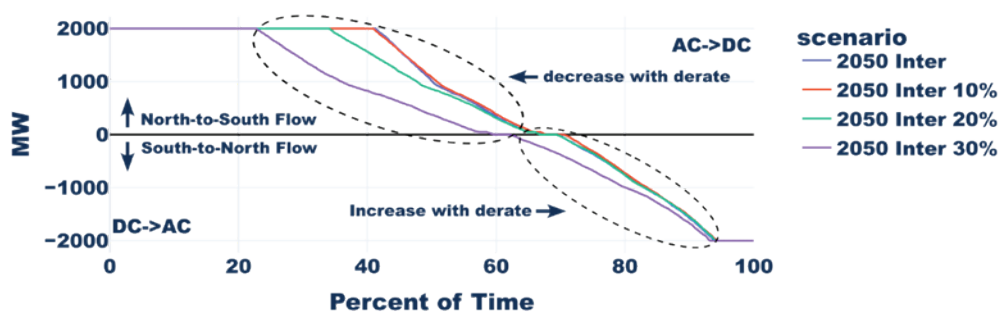

Figure 36. Flow on the interregional link with increasing transmission derating outside of the coastal region.

An explanation for the decrease in southbound flows is explained by Figure 37. A portion of the flows going south through the offshore interregional link, come from the onshore expansion to the east. As the connection from Owyhee to Whispering Pines is derated, less wind and solar can flow westward, reducing the flow to Dixonville and from there to the offshore system.

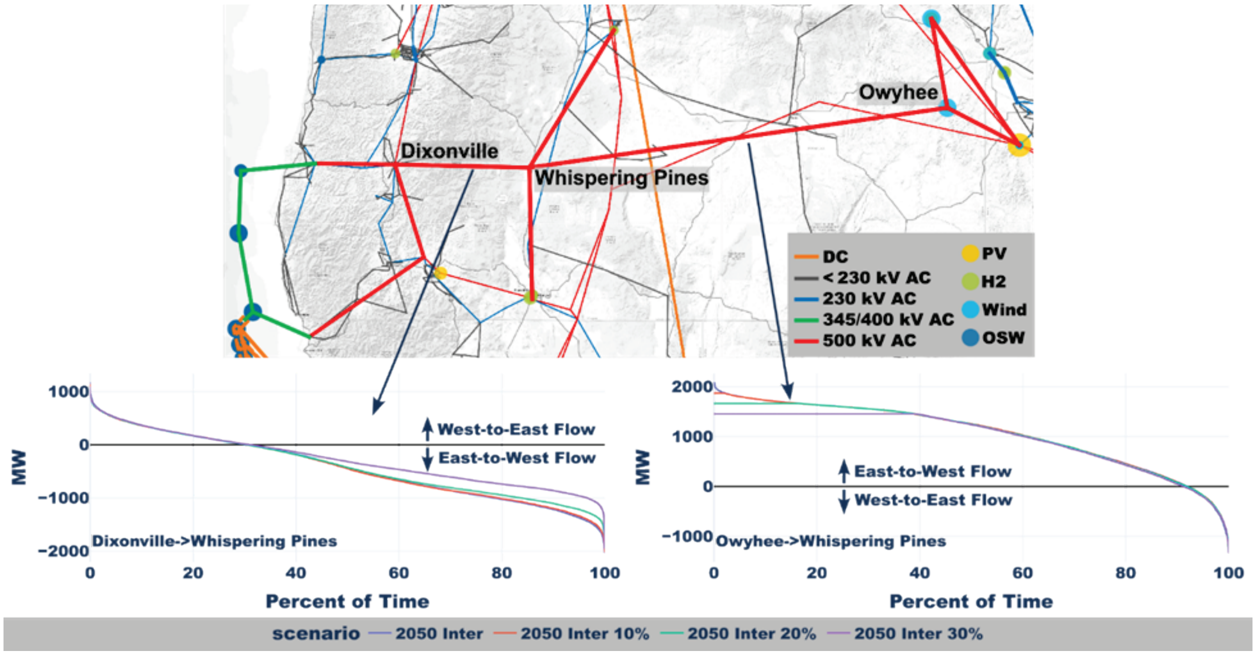

Figure 37. Flows in Oregon indicating reduced available capacity in the NW to send southward.

The value of transmission capacity with respect to the choice of transmission topology is considered in Table 11, which tabulates the change in production cost between the base scenario and the 30% transmission derated sensitivity. The change is greater in the Interregional Topology, underscoring that the additional transmission capacity helps the system better utilize resources overall, therefore, as transmission capacity increases (moving from the 30% derated sensitivity back to the base scenario) the benefits of the Interregional Topology accrue more quickly.

Table 11. Production cost change of 30% transmission derate compared to base scenario.

Topology Set	Production cost change between base and 30% derate
2050 Radial	10.0%
2050 Interregional	10.6%

Sensitivity #4: Hydrogen Combustion Turbine Capacity Derate

The production cost results reveal that usage of hydrogen combustion turbine (H2-CT) power generation is critical to the economic operations of the system. While it only accounts for 10% or less of total generation, the cost of the H2-CT generation makes up the bulk of total production cost. The sensitivity of system operations to the installed capacity of H2-CT generation is therefore of interest. In this sensitivity, the H2-CT total capacity is derated by 15% and 30%.

Figure 38 shows the yearly dispatch of the US portion of the WI focusing on the key generation technologies (all others are effectively flat). Counter to intuition, the generation from H2-CTs actually *increases* slightly, at the expense of onshore wind and solar (but not offshore wind).

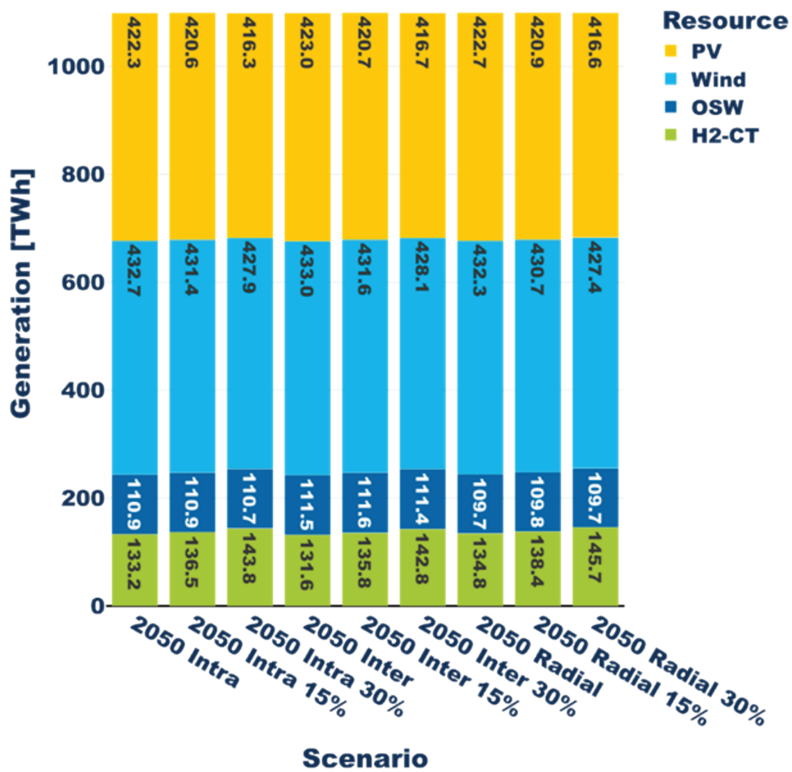

Figure 38. Generation dispatch on the US portion of the WI with hydrogen capacity derating.

Since H2-CTs are the marginal technology, as discussed in Sensitivity #1, this behavior suggests that the observed change is due to regional variations in the hydrogen price, leading to geographically dependent saturation of the H2-CT capacity. This intuition is strengthened when considering the dispatch in the CAISO and NW[19] footprint in Figure 39. Recall, from Figure 30, that H2-CTs are cheaper in the NW compared to CAISO. As the system wide capacity is derated, production shifts from NW to CAISO. The capacity factors in CAISO jump significantly as the H2-CT fleet there makes up for imports. In the NW, the dispatch change matches the derate and as a result the capacity factor does not change much.

[19] Recall from Table 5 that NW is defined as BPA, PGE, SCL, PSEI, and TPWR.

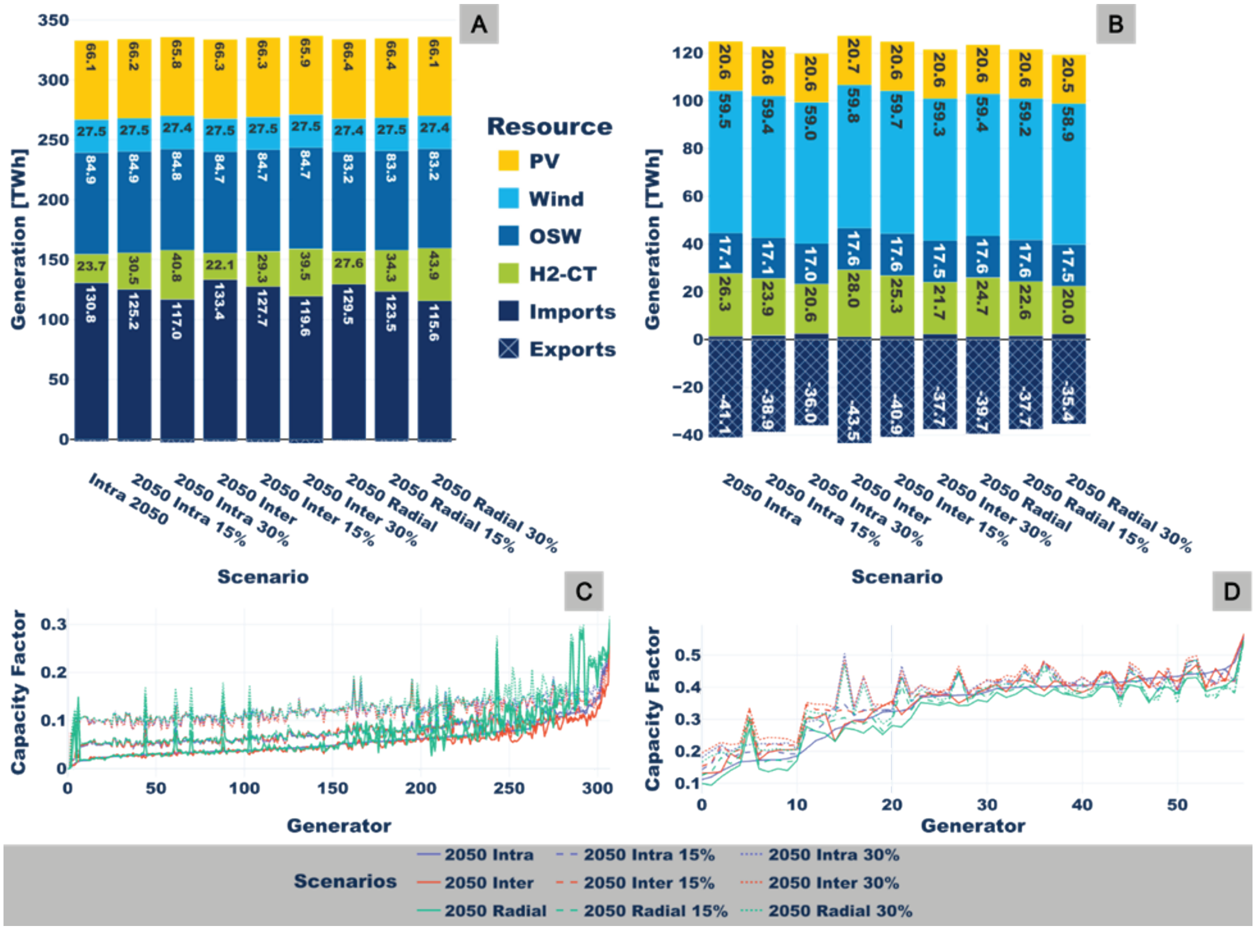

Figure 39. Dispatch in CAISO (A) and NW (B) considering progressively derated H2-CT capacity. The capacity factor in CAISO (C) increases significantly, while that in NW (D) is generally higher but does not change significantly with the derate.

Figure 39 presents analysis on an aggregate level, however, the geographic shift in H2-CT production is a function of price arbitrage, dependent on installed capacity and transmission congestion at given operating points in time. To further illustrate how the capacity derate shifts production geographically, Figure 40 shows the dispatch of H2-CTs in the NW and CAISO during a week where the H2-CT generation in the NW reaches its peak in the base scenario. The H2-CT generation peaks in the NW reduce as the capacity is derated, since the generation reaches its maximum output. To compensate, exports are reduced and imports increase. In CAISO, the peaks do not change dramatically since generation is not at maximum. As the total H2-CT capacity is derated, the volume of generation in CAISO is seen to increase, and it begins to export[20] at times that also correspond to imports in the NW.

[20] CAISO Imports are not show in this plot because their scale, even when reduced, obscures the trend seen for the hydrogen.

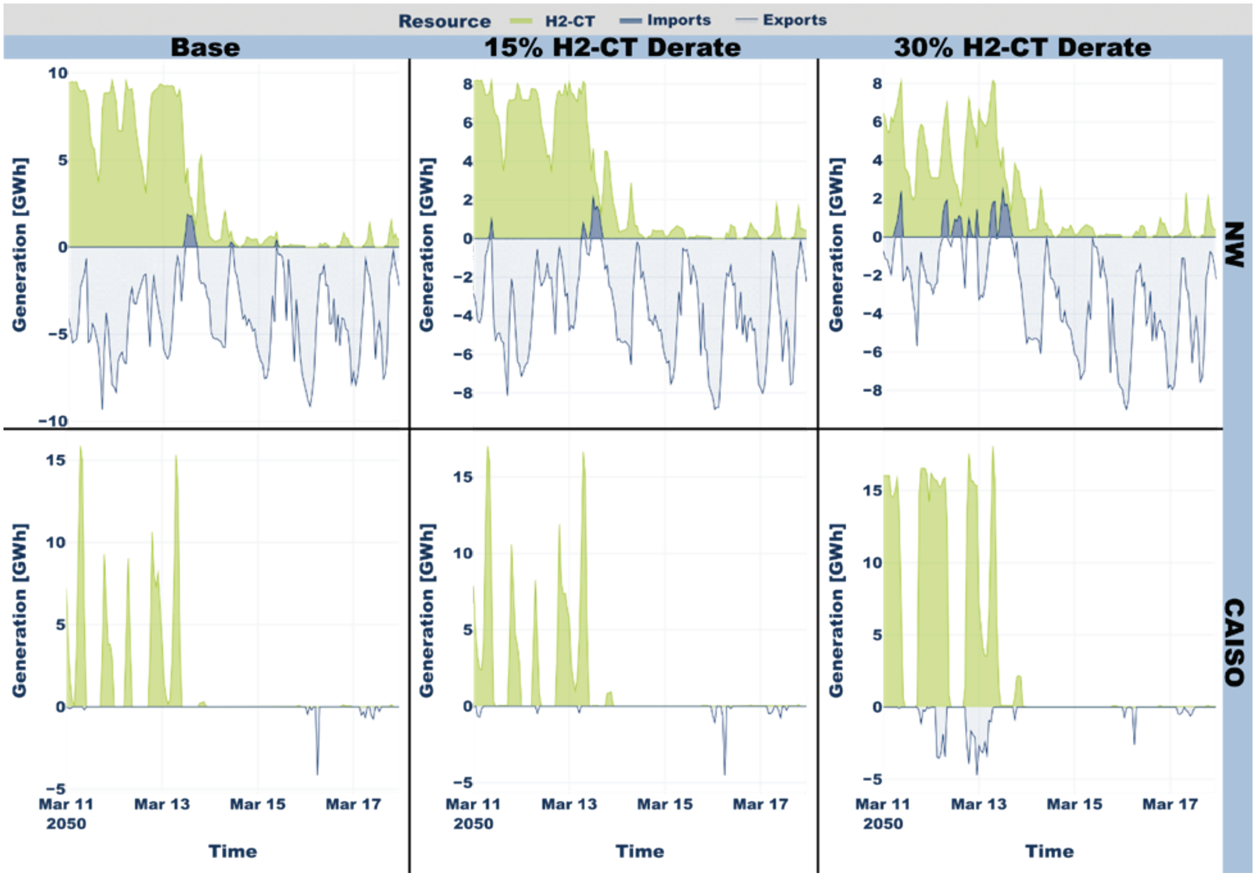

Figure 40. Relationship between H2-CT capacity, generation, imports and exports in the Interregional Topology for the NW and CAISO.

The final illustration of the geographic shift in hydrogen is provided in the flows on the interregional offshore link in the Interregional Topology, shown in Figure 41. As the hydrogen capacity decreases the north-to-south flows (AC-to-DC) reduce, consistent with the observed reduction in NW exports. At the same time, south-to-north flows (DC-to-AC) increase, consistent with the observation of increasing CAISO exports.

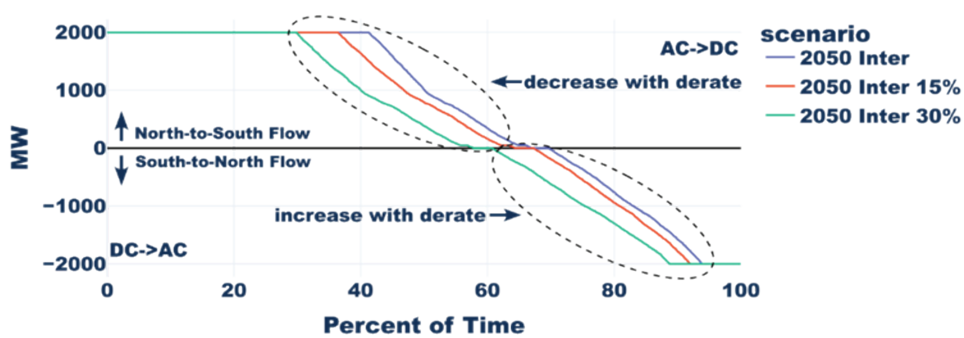

Figure 41. Flow duration curve for the offshore interregional link. Under progressively derated hydrogen production capacity flow. AC->DC is north-to-south.

The production cost change, with respect to the base scenario, as the H2-CT capacity is de-rated is reported in Table 12. It shows an increasing change from the radial, to the intraregional, to the Interregional Topology. Given the observation that the main impact of the sensitivity is to shift H2-CT production geographically, this can be seen as an added value of the OSW transmission infrastructure. In the Intraregional, and especially the interregional, the OSW transmission is able to move more low-cost H2-CT power into CA, thus allowing for better utilization of the cheaper resources.

Table 12. Production cost change of 30% hydrogen CT derate compared to base scenario.

Topology Set	Production cost change between base and 30% derate
2050 Radial	14.8%
2050 Intraregional	15.0%
2050 Interregional	15.6%

5.5 Resource Adequacy Methodology

Resource adequacy analysis was conducted by comparing weather-synchronized demand and supply under topology set transmission constraints for as many weather years as possible. Key steps were to (1) assemble many historical and future years of weather predictions at plant and BA resolution, (2) link that weather to land-based wind, OSW, and solar power time series, (3) assemble historical hydropower profiles, and (4) represent the offshore transmission of the topology sets along with the rest of the inland transmission in the WI.

5.5.1 Wind, Solar, and Hydropower Profiles

Hourly solar and wind profiles were developed in the same method as utilized for the National Transmission Planning Study (U.S. DOE 2024). Meteorological data were extracted from the Integrated Multisector Modeling (IM3) Thermodynamic Global Warming (TGW) dataset and then processed for conversion into renewable energy production through NREL's Renewable Energy Potential (reV) model (Maclaurin et al. 2021; U.S. DOE 2024). For wind capacity factors, hub height wind speeds were scaled by an NREL reference power curve[21]. Then, the simple wake loss model was applied to four-by-four uniform grid layouts (Freeman and Jorgenson 2014). Resulting capacity factors were scaled based on installed capacity by plant location to yield power time series net of wake losses. To account for additional losses, the study team also scaled the wind and solar data by 85% and 86%, respectively, prior to being imported into Gridpath. The wind and solar profiles, linked to TGW, could thus be synchronized with load projections for 43 historical and 80 future years.

For hydropower profiles, observed monthly and weekly volumes from 2001-2022 are sourced from EIA923 data (Turner et al. 2022). When convolved with the hydropower profiles, a total of 2706 weather-synchronized combinations are available to the toolkit. Additional details regarding the creation of weather-informed wind, solar, and hydropower profiles are available in Appendix A.

[21] Corresponding to a wind turbine with a rotor diameter of 113-meters and a hub height of 86 meters.

5.5.2 Demand Profiles

Demand profiles for the resource adequacy assessment combined historical and future weather variations with load projections accounting for population shifts and building and transportation electrification. Forty years (1980–2019) of hourly historical meteorology (e.g., temperature and humidity) at a 12-kilometer (km) spatial resolution were sourced from TGW. Then, the study team repeated the 40-year historical record twice into the future (2020–2059 and 2060–2099) with two levels of additional warming (Representative Concentration Pathways [RCPs] 4.5 and 8.5, with radiative forcing of 4.5 and 8.5 W/m^2, respectively) applied to the boundary conditions of the Weather Research and Forecasting (WRF) model used to dynamically downscale the meteorology.

Then, the Total ELectricity Loads (TELL) software package was referenced to develop machine learning (ML)-based models trained on historical weather and bottom-up demand electrification projections of demand in 2035 and 2050. These models enabled the approximation of many years of historical and future weather on anticipated demand patterns, including increased electrification of building and transportation loads, in the 2035 and 2050 study years. Under historical weather, peak and annual demand growth in the WI through 2050 was approximately 3.7% and 3.1%, respectively. Additional details regarding the creation of weather-informed demand profiles are available in Appendix A. The resulting 2050 demand less wind and solar production (also known as "net load") is indicated in Figure 42 for a single weather year and shown for all historical weather years in Figure 43. The dominance of CAISO loads drives net load peaks in the late summer months which are approximately 15% larger than winter peaks from the NW.

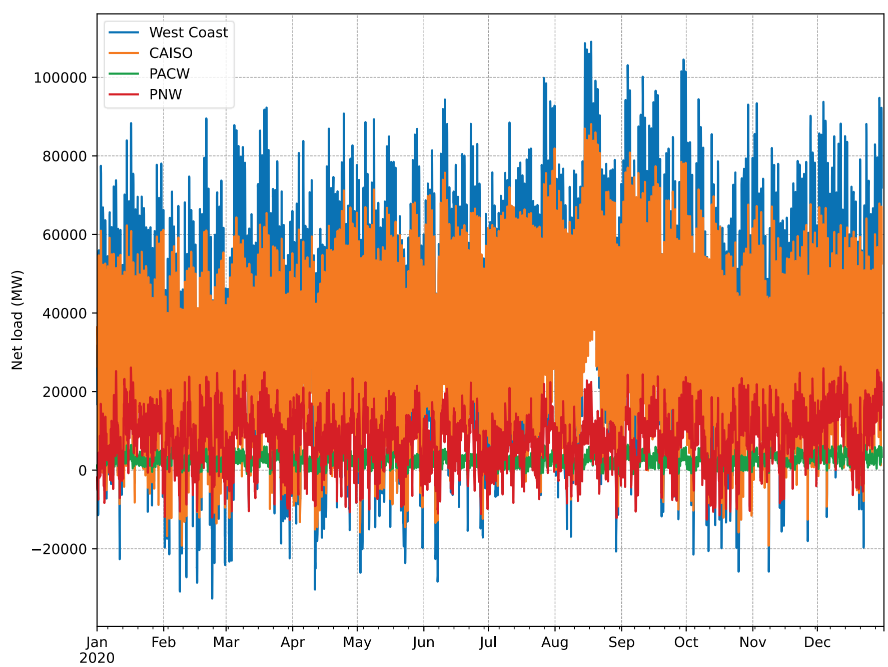

Figure 42. 2050 net load in the three West Coast regions of interest, 2020 weather year

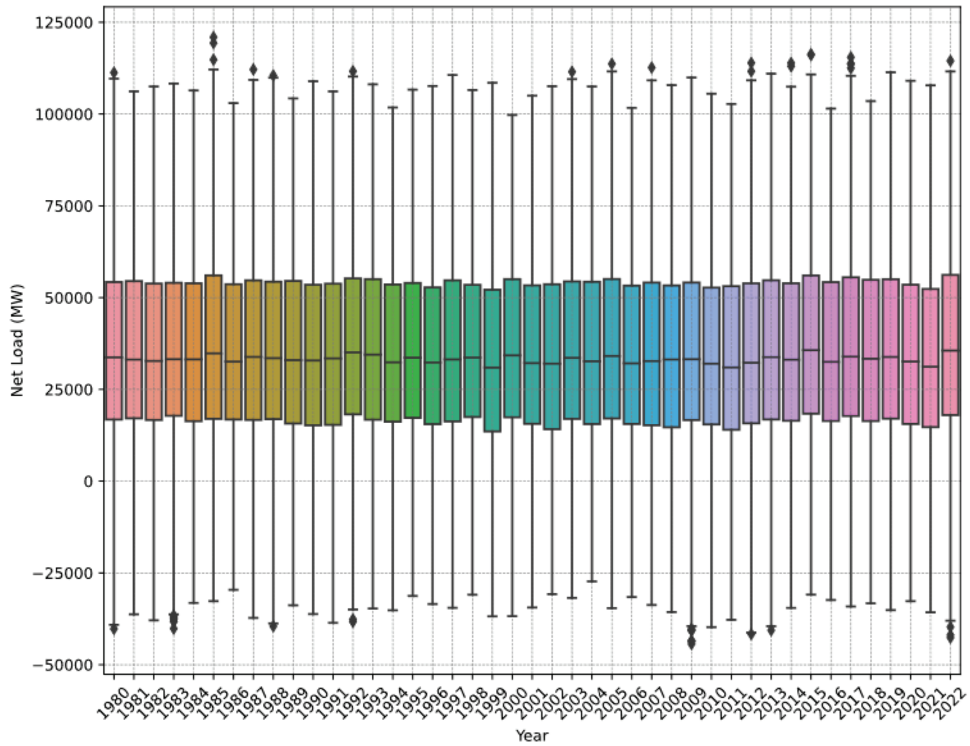

Figure 43. 2050 West Coast net loads for weather years 1980-2022

These data were loaded into Gridpath, a publicly available, open-source, power systems software. Gridpath resource adequacy toolkits were assembled for 2035 and 2050 in similar fashion to Hart and Mileva (2022). These toolkits featured a 38-zone topology compatible with WI Load Area and key path interfaces. Line ratings and path limits were synched with the production cost models and the topology set definitions. Forced outages rates (FORs) between 3% and 5.5% were assumed for thermal (fossil fuel, nuclear and geothermal) generation and energy storage but not for transmission. [22] Weather-dependent de-rates of generation and transmission were not assumed. Adequacy problems were broken into seven-day subproblems, during which hydropower and energy storage assets had perfect foresight.[23]

5.5.3 Extraction of Extreme Events

Before quantification of resource adequacy, a qualitative assessment of OSW supply during periods of extreme weather was undertaken. Multi-day periods of high and low temperatures, extending over significant distances, are an emerging concern of system operators in the west. These events, referred to as “heat waves” and “cold snaps,” pose an adequacy concern because they drive significant cooling or heating demand, respectively, and may see correlated reductions in land-based wind production.

[22] FORs of wind and solar generators were not assumed as these generators are distributed, even in the case of utility scale plants, and the loss of any single generator (typically less than 15 MW in nameplate rating) does not pose a significant impact on the balance of supply and demand across a transmission system. Historic hydropower profiles were used to reflect operations directly instead of modeling FORs.
[23] This degree of flexibility was demonstrated on the Federal Columbia River Power System during the January 2024 polar vortex event in the NW (Kieper et al. In Press).

Leveraging TGW simulations, hourly weather were projected by BA by Burleyson et al. (2023a) for each year from 1980-2019. Heat waves and cold snaps were then extracted by picking the hottest and coldest day of each year. Figure 44 illustrates the individual heat wave and cold snap events as well as the average temperature trend over the historical record. Both events are typically six days in duration, symmetrical around the extreme temperature maximum or minimum for heat waves and cold snaps, respectively. Trends are similar for all BAs in the WI.

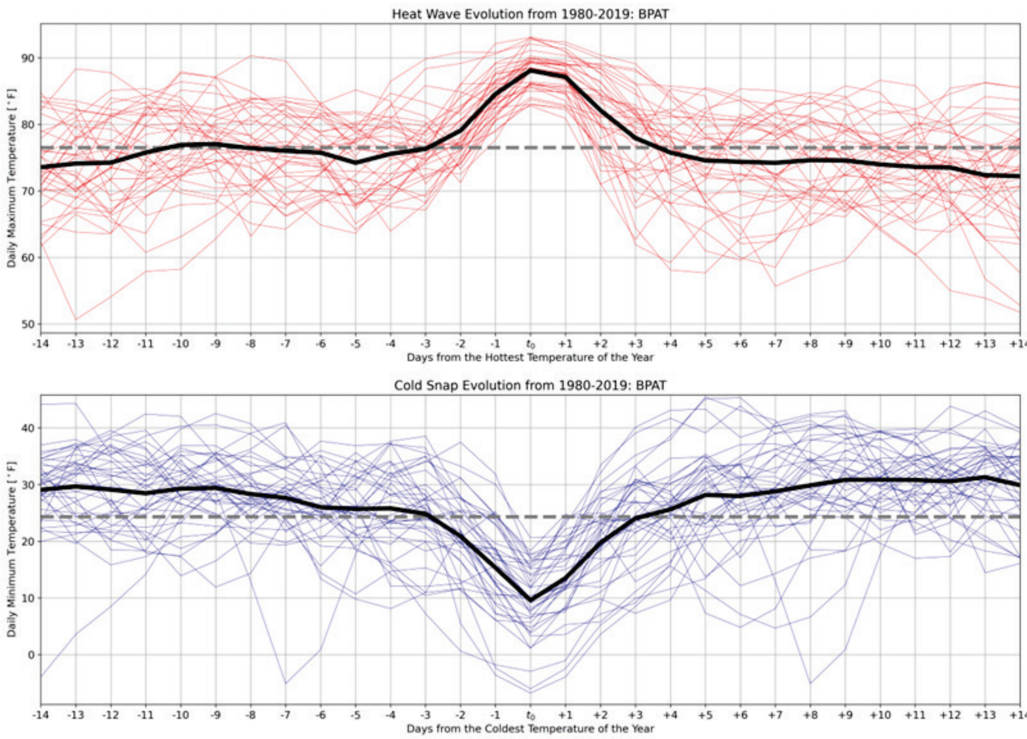

Figure 44. Temperature variations during heat waves and cold snaps in the BPAT BA, 1980-2019 (Burleyson et al. 2023a).

5.5.4 Metrics

The use the multiple metrics to describe resource adequacy was prioritized in this study. The following metrics were used to quantify resource adequacy trends (Hart and Mileva 2022):

Loss of Load Expectation (LOLE)—the expected number of periods of loss of load over a time duration, where periods are the time durations within which a loss of load event is tracked.[24]

Loss of Load Hours (LOLH)—the expected number of hours per year which encounter loss of load.

Expected Unserved Energy (EUE)—the average amount of energy not served within a given year.

[24] Commonly, LOLE periods are defined in terms of the number of days in which a loss of load event occurs. Planners often refer to a one-day-in-ten-years LOLE benchmark, or 0.1 days/year.

Effective Load Carrying Capability (ELCC)—a measure of the amount of load which can be supported by a resource or group of resources, typically expressed in terms of megawatts or a percentage of the perfect capacity relative to the rated resource capacity.

A multi-step method to calculate ELCC in the regions of interest to this study was developed and implemented. This method is detailed in Appendix A.

5.6 Resource Adequacy Results

In this section, OSW temporal characteristics relevant to extreme annual heat and cold events in the NW, PACW, and CAISO regions are shown. Then findings from the adequacy analysis across historical and future weather years are presented. Finally, ELCC valuations are tabulated.

5.6.1 OSW Gross Capacity Factors During Extreme Events

Trends of the gross capacity factors of OSW resources in the BA's of BPAT (as a proxy for the NW), PACW, and CAISO (including CISC, CISD, CIPV, CIPB) for heat waves and cold snaps revealed superior performance to existing land-based wind fleets ahead of the events. OSW production drops during the middle of the heat waves are seen in the mean power production curve for BPAT and PACW. However, this sensitivity is not observed in the CAISO regions, suggesting an anticorrelation which could be captured through interregional transmission design. These trends are shown for historical weather in Figure 45 below and were similar for future weather.

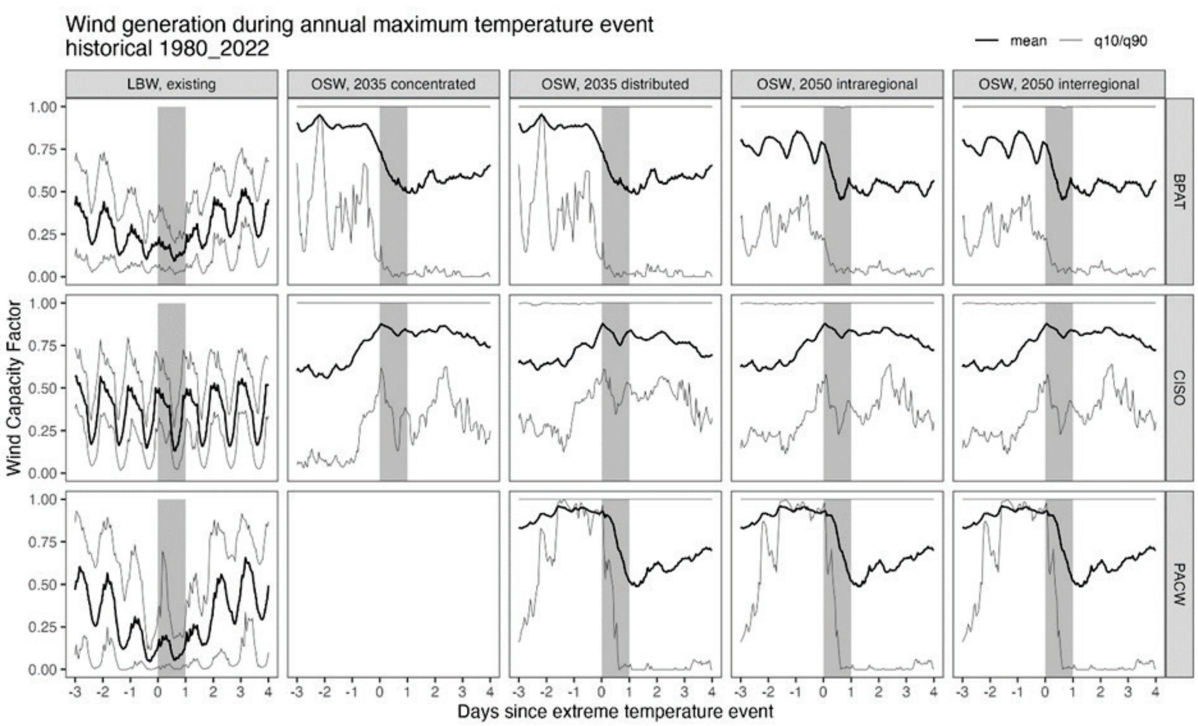

Figure 45. Average and 10th, and 90th deciles of gross capacity factor of land-based wind and OSW during 6-day heat waves, 1980-2022. 2035 Concentrated and Distributed Topologies include different generation locations, as detailed in Section 4.0.

With cold snaps, again the more robust capacity factors of OSW than land-based wind ahead of the event could enhance the system's ability to bolster storage and hydropower resources. In the middle of the cold period, the trends from heat waves are reversed and California OSW shows reductions while OSW interconnected to PACW and BPAT maintains high capacity factors on average.

These trends are shown for historical weather in Figure 46 below and were similar for future weather.

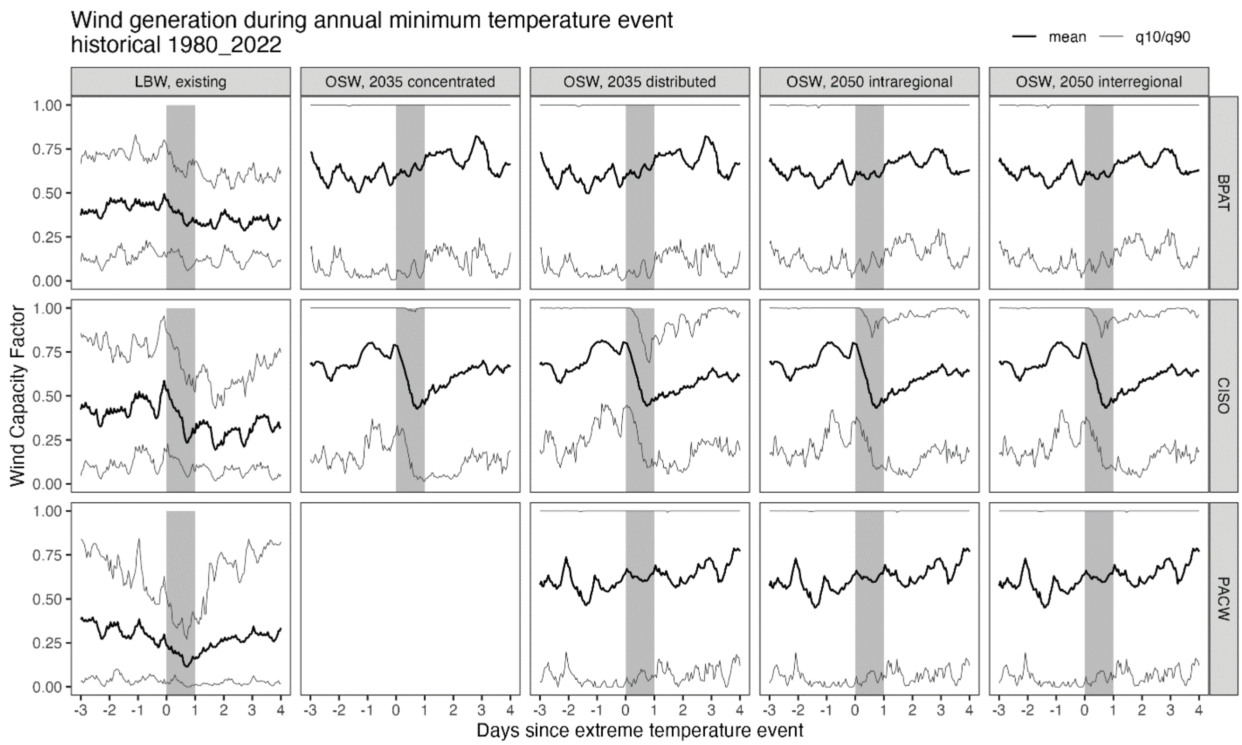

Figure 46. Average and 10th and 90th deciles of gross capacity factor of land-based wind and OSW during 6-day cold snaps, 1980-2022. 2035 Concentrated and Distributed Topologies include different generation locations, as detailed in Section 4.0.

5.6.2 Base Adequacy Sweeps

Adequacy of all topology sets, under all weather and hydropower years, met and exceeded the one-day-in-ten-years Loss of Load Expectancy (LOLE) standard. The potential for unserved energy was zero for all topology sets through historical and future weather under the RCP 4.5 warming. Only for the 2035 Concentrated Topology was unserved load concluded in the RCP 8.5 scenario. Loss of load hours across all weather years analyzed in the study were only observed in July evenings, as shown in Table 13.

Table 13. Loss of Load Hours for 2035 Concentrated Topology Set, RCP 8.5 climate scenario

		Month of year											
		1	2	3	4	5	6	7	8	9	10	11	12
Hour of day (MT)	1	0	0	0	0	0	0	0	0	0	0	0	0
	2	0	0	0	0	0	0	0	0	0	0	0	0
	3	0	0	0	0	0	0	0	0	0	0	0	0
	4	0	0	0	0	0	0	0	0	0	0	0	0
	5	0	0	0	0	0	0	0	0	0	0	0	0
	6	0	0	0	0	0	0	0	0	0	0	0	0
	7	0	0	0	0	0	0	0	0	0	0	0	0
	8	0	0	0	0	0	0	0	0	0	0	0	0
	9	0	0	0	0	0	0	0	0	0	0	0	0
	10	0	0	0	0	0	0	0	0	0	0	0	0
	11	0	0	0	0	0	0	0	0	0	0	0	0
	12	0	0	0	0	0	0	0	0	0	0	0	0
	13	0	0	0	0	0	0	0	0	0	0	0	0
	14	0	0	0	0	0	0	0	0	0	0	0	0
	15	0	0	0	0	0	0	0	0	0	0	0	0
	16	0	0	0	0	0	0	0	0	0	0	0	0
	17	0	0	0	0	0	0	0	0	0	0	0	0
	18	0	0	0	0	0	0	0	0	0	0	0	0
	19	0	0	0	0	0	0	0	0	0	0	0	0
	20	0	0	0	0	0	0	0.005	0	0	0	0	0
	21	0	0	0	0	0	0	0.002	0	0	0	0	0
	22	0	0	0	0	0	0	0	0	0	0	0	0
	23	0	0	0	0	0	0	0	0	0	0	0	0
	24	0	0	0	0	0	0	0	0	0	0	0	0

Over the 880 weather and hydro year combinations of the RCP 8.5 climate future, a total of 4.52 MWh of USE was observed in the WI, primarily at 8 pm MT. LOLE for this case was 0.005 days per year, below the 0.1 days per year benchmark.

5.6.3 Effective Load Carrying Capability

ELCC of OSW for each topology set was calculated using the method outlined in Appendix A, where the three POI-host regions (CAISO, PACW, and NW) were isolated to assess capacity contributions. Loads were incremented in each region independently to reach LOLE of 0.1, with and without OSW. As shown in Table 14, ELCC metrics revealed robust capacity value to CAISO of OSW in all 2035 topology sets, in line with OSW capacity credit conclusions and exceeding land-based wind values of approximately 15% as found by Jorgenson et al. (2021).

Of the 2035 topology sets, the 2035 Distributed provided slightly better ELCC than the 2035 Concentrated because more OSW Is interconnected directly into CIPB, where the loss of load is mostly experienced. The 2035 Concentrated case served this load with adequate transmission into CIPB, but it incurred transmission losses in doing so.

However, capacity credit eroded as more OSW is interconnected and summer evening net load peaks continued to be the hours which defined the adequacy value.

Table 14. ELCC findings of OSW for all topology sets

Topology Set	Installed Capacity (MW)	CAISO ELCC (MW)	PACW ELCC (MW)	NW ELCC (MW)	Total ELCC (%)
2035 Concentrated	15000	6102	0	0	41%
2035 Distributed	15000	6322	0	0	42%
2050 Radial	33000	11451	0	0	35%
2050 Intraregional	33000	11451	0	0	35%
2050 Interregional	33000	11453	0	0	35%

In 2050, all topology sets yielded similar ELCC, which is driven by summer evening net load peaks in California. These same net loads were dominant in 2035. For this reason, there was negligible ELCC naturally attributed to PACW or NW regions across all topologies. These findings indicate that markets would be needed to equitably attribute the ELCC value by region of OSW development. The findings also indicate that negligible ELCC is solely attributed to the transmission in these topology sets, due to the abundance of onshore transmission and generation. These values were monetized using an estimate of the marginal value of firm capacity in Section 7.1.3.

5.7 Summary and Key Findings

In this section, the production cost and resource adequacy modeling efforts are summarized.

5.7.1 Production Cost Modeling

Optimal dispatch simulations of all five topology sets were conducted. The following observations constitute key findings:

- The PCM simulations of the five topology sets revealed comparable system-wide benefits of the 2035 topology sets and significant cost advantages to the 2050 Interregional and Intraregional Topologies over the 2050 Radial Topology.
- OSW generation and curtailment was similar between the 2050 topologies.
- The main source of the benefits accruing through the 2050 topologies was the use of the transmission to share lower cost generation, particularly from hydrogen combustion turbines, across regions.

- Though dispatch was unchanged, this production cost advantage of coordinated OSW transmission was significantly reduced in the case of hydrogen prices equivalent to today's natural gas prices. While such low prices of green hydrogen are unlikely in 2050, this sensitivity suggests that the value of OSW transmission is linked to the technology maturation of clean, dispatchable generation in 2050. This analysis also shows that coordinated generation and transmission fills a similar role to dispatchable generation.

Three additional sensitivities shed the following insights on the base findings:

- Security-constrained operations indicated that redispatch around key contingencies resulted in significantly higher production costs than reliability reinforcement costs associated with each topology set.
- Security-constrained operations also promoted the 2050 Intraregional Topology as the least-cost future, suggesting that further analysis of system redispatch versus reliability upgrades may result in the overall production cost leader between 2050 Intraregional and 2050 Interregional Topologies.
- Interregional transmission de-rates and hydrogen combustion turbine de-rates bolstered the case for OSW transmission by avoiding some increased dispatch of higher cost hydrogen CTs in CA through use of the interregional OSW backbone.

5.7.2 Resource Adequacy

Resource adequacy assessments were completed for all topology sets leveraging 2706 weather-synchronized combinations of annual demand, wind and solar power production, and hydropower production. The following observations constitute key findings:

- Adequacy of all topologies across all weather year combinations exceeded the LOLE benchmark of one-day-in-ten-years.
- LOLH of 0.00738 hours per year and 4.52 MWh of unserved load were observed only in future weather (RCP 8.5 climate scenario) during July evenings, for the 2035 Concentrated Topology.
- In these models, average OSW capacity factors were shown to be better than existing land-based wind fleets through extreme heat wave and cold snap events which drive emerging RA concerns on the West Coast.
- A natural complementarity presented in which NW and PACW regions may see more persistent OSW generation through heat waves by importing OSW from CAISO.
- Conversely, CAISO may be assisted by more persistent OSW production from the NW and PACW regions during cold snaps.
- ELCC values were solely associated with net load peaks in late summer evenings, given the prevalence of California loads.
- Comparing ELCC metrics of the 2050 Intraregional and Interregional Topologies to the 2050 Radial counterfactual revealed that negligible ELCC could be isolated to OSW transmission, due to the abundance of modeled onshore transmission and generation.

6.0 Reliability and Resilience Analysis

Analysis of system reliability and resilience extended from the production cost modeling work. First, a smart sampling technique was deployed to select the key hours of power system dispatch, under which generation, transmission, and demand-side infrastructure were uniquely utilized. Next, for each of the prioritized representative hours, conversions from direct current (DC) production cost simulations to AC power systems simulations were completed. Then, detailed contingency analyses, coordinated with BPA, PacifiCorp, and CAISO planners, were conducted in steady-state and transient domains. Finally, an iterative power system process revealed reliability reinforcements for each topology set, which were included in downstream economic analyses. Qualitative assessments of performance under critical dynamic contingencies, including emerging resilience threats, were also conducted. This analysis seeks to evaluate, at a high level, system reliability and resilience of OSW topologies in 2035 and 2050. It is not a substitute for the comprehensive analyses conducted by system planners.

6.1 Representative Hours

An innovative smart sampling method aimed at selecting a specific subset of representative hours using one year of production cost modeling data was developed for this study (Chen et al. 2024). Utilizing a hierarchical design, the method groups the hours according to seasonal and diurnal variations of renewable energy sources. Then, a statistically representative subset of hours from each group was selected. The results of the validation tests indicate that the sampled subset shares the same statistical properties as the original one-year data.

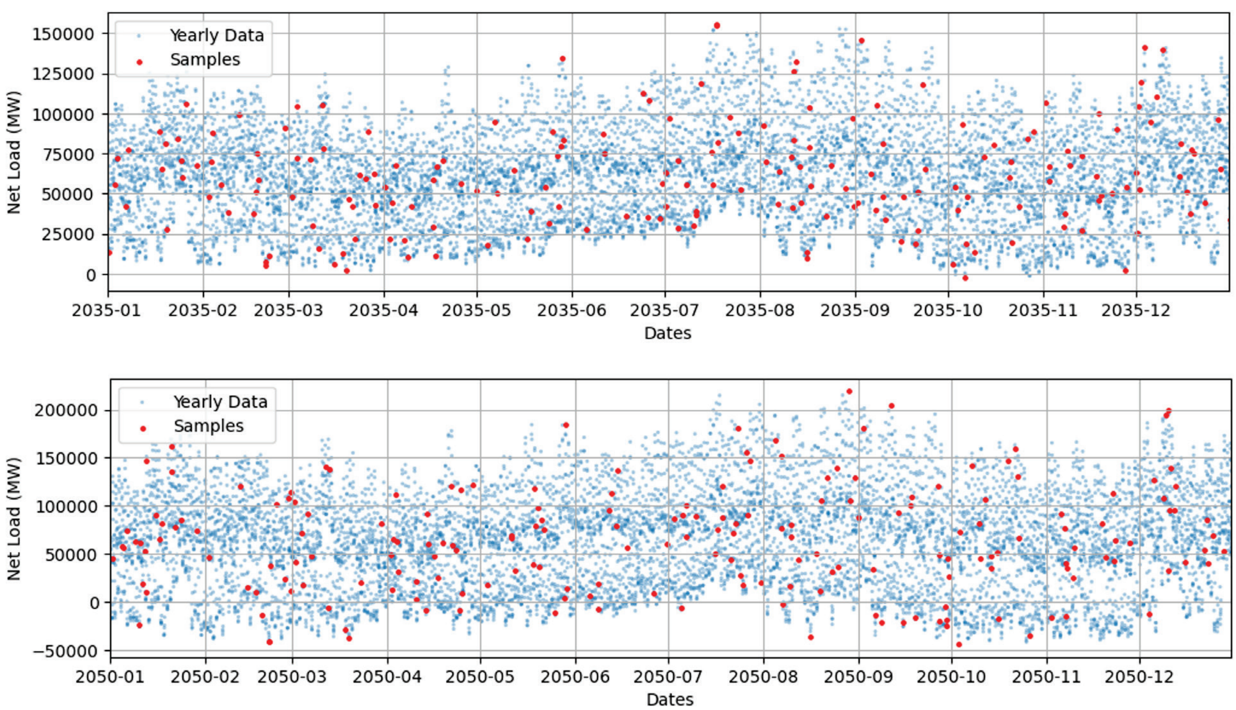

Figure 47. 2035 (top) and 2050 (bottom) net loads (load less wind and solar power generation) for all (in blue) and representative (in red) hours

Of these representative hours, 50 hours were prioritized for power flow analysis of every topology set. This representative set was composed of the top ten hours of solar generation, wind generation, solar and wind generation, load, and net load. Table 15 indicates the range of system load and solar and wind generation through the representative hours.

Table 15. Ranges of system load and wind and solar generation in 2035 and 2050 representative sets

Year	System Load (GW)	Solar Generation (GW)	Wind Generation (GW)
2035	100-196	0-92	10-47
2050	120-279	0-161	13-82

6.2 Creation of Converged Power Flow

Grid planners require datasets, tools, and models that enable the examination of solutions across thousands of chronological power flow cases to comprehend the operational impacts of increased penetration of VRE and evolving load patterns (Hitachi Energy 2024). Creating a single, operable AC power flow model requires a significant investment of time, as it encompasses production cost modeling, the convergence of the AC power flow, and reactive power planning(ISO New England Inc. 2019; Leite da Silva et al. 2012; WECC n.d.). In response to these challenges, PNNL created a chronological AC power flow automated generation (C-PAGE) tool (Vyakaranam et al. 2021) to integrate system dispatch time series from the production cost model into time-sequenced power flow runs for reliability analysis. The team utilized C-PAGE (Vyakaranam et al. 2021) to convert nodal production cost model outputs into AC power flow cases for the specific representative hours derived from the smart sampling method outlined in Section 6.1. Converged time-sequenced power flow solutions and corresponding dynamic models were converted from production cost model states at the selected representative hours using C-PAGE. Disaggregation from Balancing Authority and power plant levels to the power flow spatial resolution were necessary to support this step. Other adjustments to AC power flow loads and reactive power devices to compensate for transmission losses and maintain suitable voltage profiles, respectively, are also necessary. These steps are described in detail by Oikonomou et al. (2024).

6.3 Standard Contingency Analysis

Contingency sets were assembled through direct coordination through the Advisory Committee System Operator Subgroup, and direct correspondence with system planning staff at BPA, PacifiCorp, and CAISO.

6.3.1 Steady-State Analysis

Steady-state contingencies were assembled from the critical contingencies of BPA, PacifiCorp, and CAISO, including N-1 for all 230 kV and higher transmission lines in the CAISO system. Lines with voltages of 230 kV and higher were monitored across the BPA, PACW, and CAISO systems. Table 16 indicates the voltage and overload limits and number of contingencies analyzed for all topology sets.

Table 16. BPA, CAISO and PAC steady-state contingencies and ratings

System	Voltage Limits—Low (p.u.)	Voltage Limits—High (p.u.)	Overload Limits	Number of Contingencies
BPA	0.9	1.1	100% of Rate B	2100
PACW	0.9	1.1	100% of Rate B	103
CAISO	0.9	1.1	100% of Rate B	4032

As a result of the steady-state contingency analysis, the maps in Figure 48 and Figure 49 display the contingency locations that cause overloads in the selected representative hours. Additionally, the color and size of the circles indicate the cumulative number of overloads caused by each contingency across 50 selected operating conditions. Less overloads were seen in the 2035 Distributed Topology set than the 2035 Concentrated Topology set. In San Francisco, the direct injection of OSW and use of the Bay Hub in the 2035 Distributed Topology set mitigates N-1 overloads that are otherwise incurred through greater reliance on imports in the 2035 Concentrated Topology set.

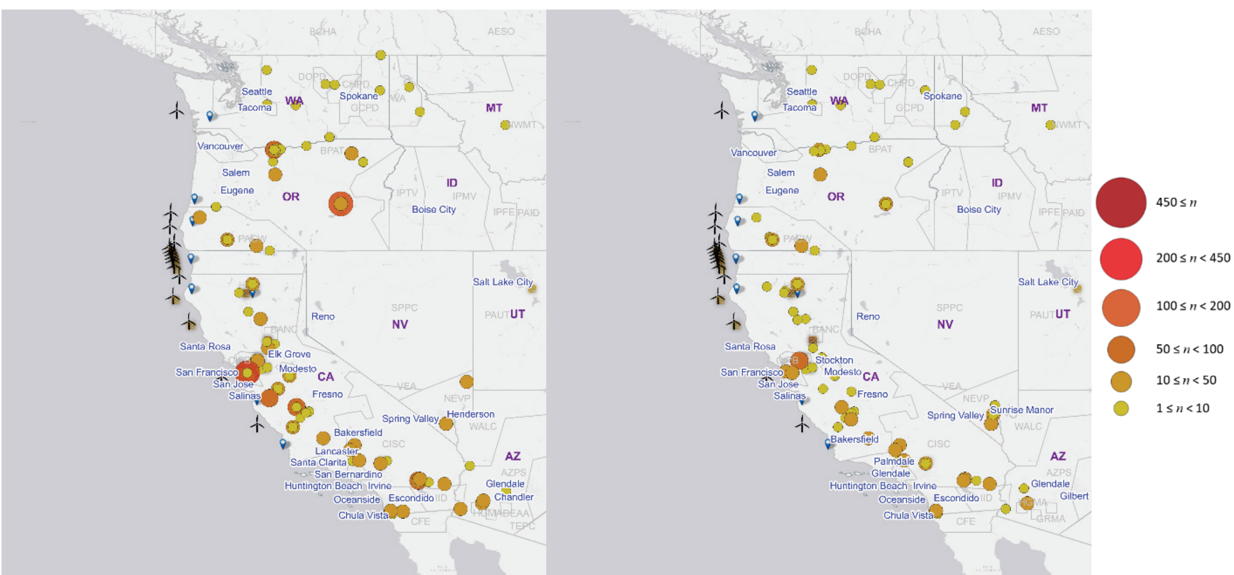

Figure 48. Overloads, *n*, caused by steady-state contingencies in BPA, CAISO and PACW region, 2035 Concentrated Topology (left) and 2035 Distributed Topology (right)

In the 2050 topologies, the Interregional Topology indicated fewer overloads as a result of the steady-state contingencies than the Intraregional Topology. However, the Interregional Topology has 758 unique overloading branches across all representative hours while the Intraregional Topology has only 659.

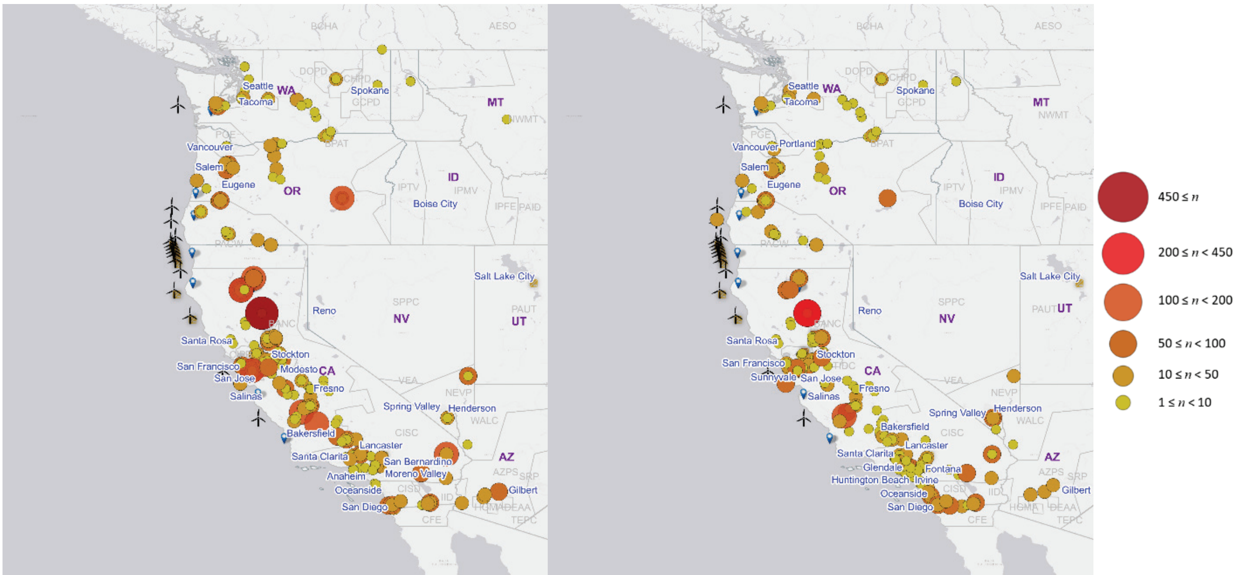

Figure 49. Overloads, *n*, caused by steady-state contingencies in BPA, CAISO and PAC region, 2050 Intraregional Topology (left) and 2050 Interregional Topology (right)

Following the contingency analyses of the 2050 Intraregional and Interregional Topologies, the ability of the MTDC networks to redispatch to limit overloads resulting from contingency events, without increasing OSW curtailment, was considered. The process of selecting redispatch operations was stated as an optimal power flow problem with the objective function of reducing converter control shifts while adhering to control limitations and operating conditions. Solutions returned the system to a dependable and secure state by reducing the target overload branches to below 100% of the secure rating under contingencies, accomplishing in as short amount of time with as little control adjustment as possible. Only overloads near the MTDC network were able to be influenced significantly by this redispatch. Several steady-state contingencies were resolvable through MTDC redispatch, and Figure 50 shows one sample overload for the 2050 Intraregional Topology.

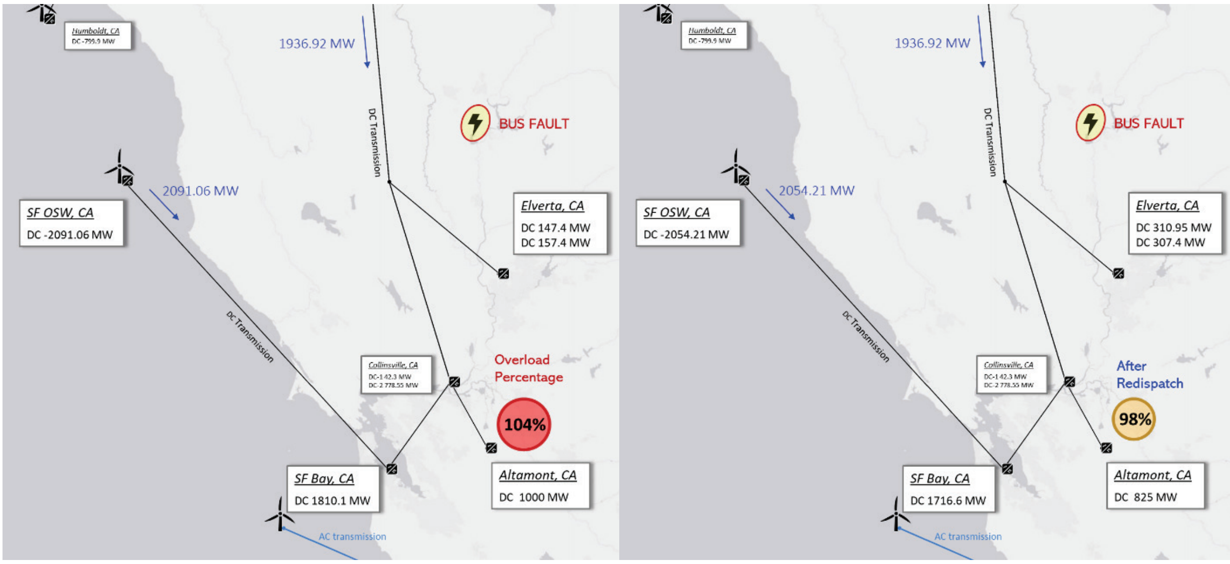

Figure 50. An example of MTDC redispatch to limit an overload near Altamount, CA, which was caused by a steady-state bus fault. Redispatch shown in blue font. Overload shown at left and elimination of overload shown after redispatch at right.

6.3.2 Dynamic Contingency Analyses

In a similar fashion, dynamic contingencies were conducted for all topology sets. Dynamic contingency analysis considers transient changes in system voltage and frequency during the response following a contingency before reaching a new equilibrium state. BPA and CAISO provided 219 and 215 contingencies, respectively, and they suggested analyses at summer peak and spring off-peak conditions, respectively. In addition, seven critical dynamic contingencies for the entire WI as defined by WECC were included and run at spring off-peak and summer peak. Some contingencies resulted in unstable dynamic response, and remedial action schemes or infrastructure enhancements may be required.[25] These contingencies are summarized in Table 17.

[25] Transmission enhancements or BESS may rectify dynamic response to these contingencies.

Table 17. BPA, CAISO and WECC dynamic contingencies and loading conditions assumed for analysis

			Contingencies with unstable dynamic response			
System	**System Load Condition**	**Number of Contingencies**	**2035 Distributed**	**2035 Concentrated**	**2050 Radial & Intraregional**	**2050 Interrregional**
BPA	Summer peak	219	8	8	6	6
CAISO	Spring off-peak	215	37	37	24	26
WECC	Summer peak	7	0	0	2	2
WECC	Spring off-peak	7	3	2	0	0

The WECC standard dynamic contingencies analyzed are as follows (Jensen et al. 2020):

- Chief Joseph brake insertion: A 1400 MW brake resistor is inserted at BPA's Chief Joseph Dam, a major Columbia River hydroelectric project (2620 MW).
- Double Palo Verde Outage: Two units of the Palo Verde nuclear plant fail. Total loss of generation is 2626 MW.
- Colorado River-Red Bluff 500kV Line Outage: The Colorado River-Red Bluff 500 kV line outage is part of Path 46, which is vital to the Arizona-California electrical grid.
- Gates – Midway and Two Diablo – Midway 500kV Line Outages: Major transmission line outages on California's Path 15, a group of lines between the northern and southern CA.
- Brownlee – Hells Canyon 230kV Line Outage: Outage of transmission line connecting the Brownlee Dam (585 MW) in Idaho to Hells Canyon.
- Daniel Park – Comanche 345kV Line Outage: The Comanche 345 kV line outage affected the transmission line to the Comanche Generating Station (766 MW).
- Pacific DC Intertie (PDCI) 500kV DC Intertie Block: The outage of PDCI removes a transmission capacity of 3100 MW between Pacific Northwest to Southern California.

Table 18 includes the results of the dynamic contingency analysis of the critical WECC contingencies. For unstable responses, remedial action schemes and potentially additional infrastructure may be necessary to achieve acceptable system response.[26]

[26] Transmission enhancements or BESS may rectify dynamic response to these contingencies.

Table 18. Results of WECC critical dynamic contingencies analysis of all topology sets

Contingency	Topology and System Load Condition				
	2035 Distributed & Concentrated Summer peak	2035 Distributed Spring off-speak	2035 Concentrated Spring off-peak	2050 Radial/Intraregional/ Interregional Summer peak	2050 Radial/Intraregional/ Interregional Spring off-peak
Ringdown	Stable	Stable	Stable	Stable	Stable
Palo Verde	Stable	Unstable[27]	Unstable[27]	Stable	Stable
Diablo-Midway	Stable	Stable	Stable	Unstable	Stable
Daniel Park Comanche	Stable	Unstable	Unstable	Stable	Stable
Colorado River – Red Bluff	Stable	Stable	Stable	Unstable	Stable
Brownlee-Hells Canyon	Stable	Stable	Stable	Stable	Stable
North Gila - Imperial Valley	Stable	Unstable[27]	Stable	Stable	Stable
PDCI Block	Stable	Stable	Stable	Stable	Stable

6.4 System Reliability Reinforcements

Following the contingency analyses, an iterative approach was employed to identify a minimum set of reinforcements given a fixed dispatch assumed from the production cost modeling. First, transmission lines that were experiencing overloads of 230 kV or above were extracted from all the data. Next, upgrades were designed to rectify these overloads if a line was overloaded for five or more representative hours. These upgrades were implemented in the power flow solution and the overloads were re-examined. The procedure was repeated with upgraded lines until minimal overloads were observed in five or more representative hours. Following the initial contingency, generation redispatch may have decreased overloads, but, as an assumption of this analysis, generators were not redispatched. A comparison of redispatch versus reliability reinforcements is made in Section 5.4.3.

System reinforcement costs of the 2050 Radial Topology were assumed to be equivalent to that of the 2050 Intraregional Topology for several reasons. Due to the dispatch optimization, the aggregate OSW power injections at the POIs for the 2050 Intraregional Topology consistently exceeded those of the Interregional Topology during the representative hours most influential to

[27] This instability was not observed in the CAISO Transmission Plan Analysis (CAISO, 2024), though under a different model than used in this study. Further review may be warranted to ensure that numerical or modeling issues are not driving instability.

the justification of system reinforcements. The 2050 Intraregional Topology also supplied OSW in similar fashion to that of the 2050 Radial Topology, without offshore connections. Finally, the onshore MTDC reduced OSW curtailments over the radial case (see Table 6). Thus the 2050 Intraregional Topology provided a conservative proxy for upgrades required by OSW in the 2050 Radial Topology.

However, though clear attribution of reinforcements to a particular set of expansion changes would assist downstream economic assessments, reinforcements resulting from this analysis could not be solely attributed to OSW. To enable relative comparison between OSW interconnection and transmission topologies, reinforcements were limited to transmission lines with segments located within CAISO, BPA, and PACW regions. Figure 51 and Figure 52 depict the minimum set of system reinforcements resulting from this iterative process for 2035 and 2050 topology sets, respectively.

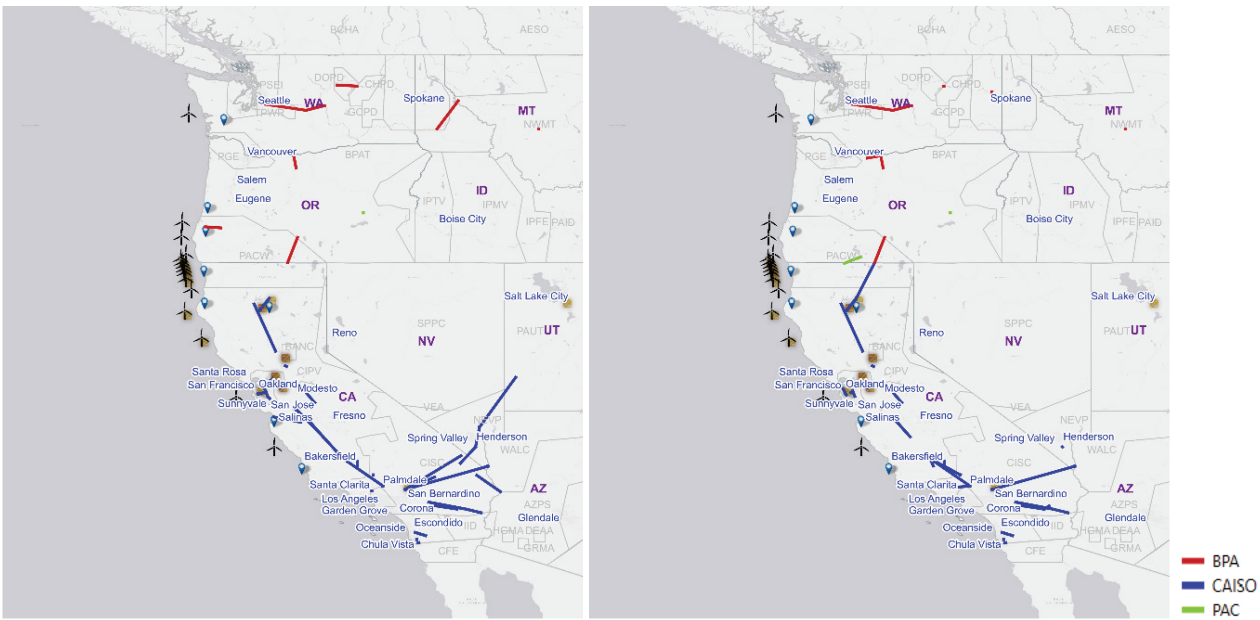

Figure 51. System Reliability Reinforcements for BPA, PAC, and CAISO Contingency Studies, 2035 Distributed Topology (left) and 2035 Concentrated Topology (right)

The purpose of these upgrades is to enhance the balance of power flows and reduce overload conditions arising from the contingencies prioritized by system operators. The primary areas targeted for improvement include the lines connecting the Humboldt substation to the Fern Road 500 kV substation, the substations at Gates and Midway, the Los Banos-Midway 500 kV line, which includes a loop into the Gates Substation, and the transmission upgrades in the Fern Road and Lugo areas.

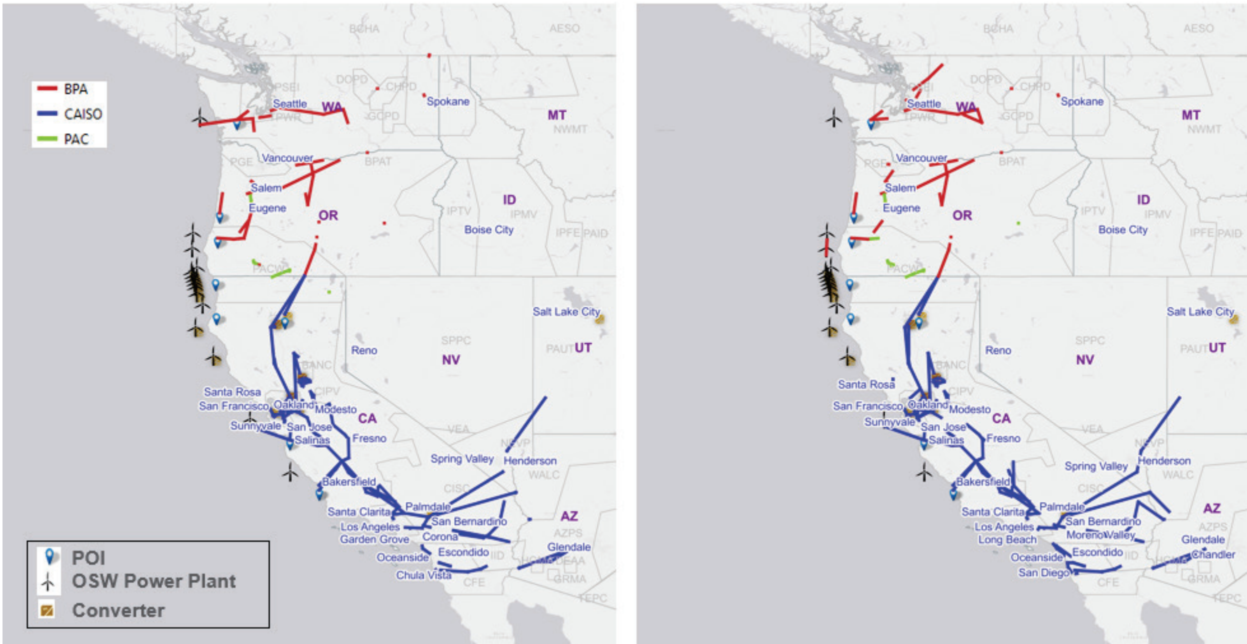

Figure 52. System Reliability Reinforcements for BPA, PAC, and CAISO Contingency Studies, 230 kV and higher line ratings, 2050 Intraregional Topology (left) and 2050 Interregional Topology (right)

Compared to the 2050 Intraregional Topology, the 2050 Interregional Topology required greater enhancements, particularly in the Moreno Valley, Bakersfield, Santa Rosa, and Oceanside areas. This is because, despite having the same total generation and load during these two scenarios at the same operating time, there is a notable difference in generation dispatch from individual fuel types and different areas, as illustrated in Figure 53 and Figure 54. This results in varying system responses to specific contingencies.

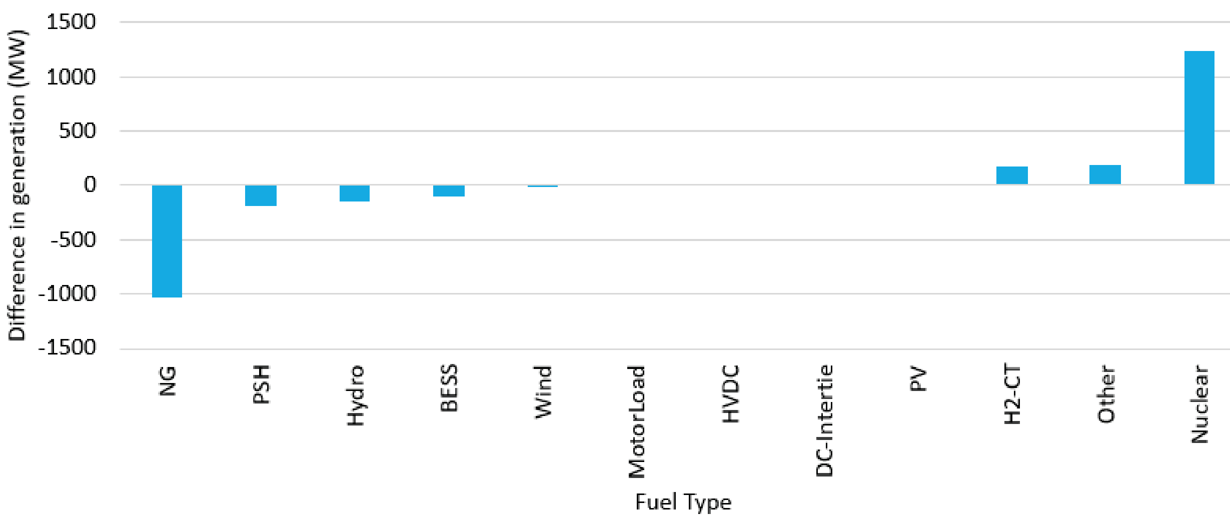

Figure 53. Difference in generation dispatch, 2050 Intraregional compared to 2050 Interregional Topology sets by fuel type (NG—natural gas)

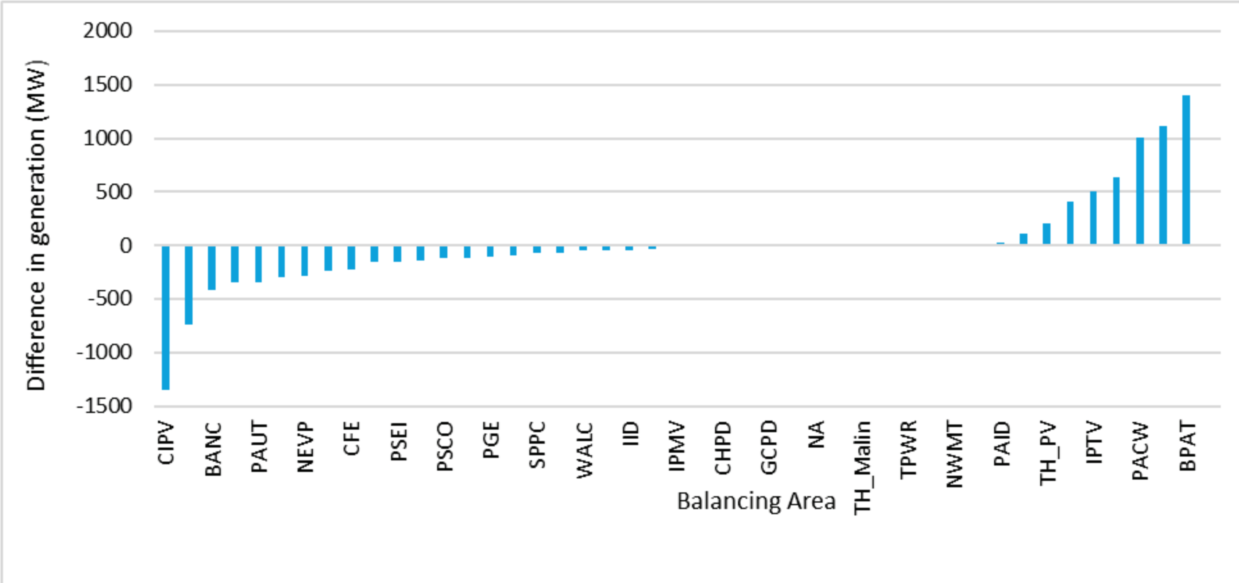

Figure 54. Difference in generation dispatch, 2050 Intraregional compared to 2050 Interregional Topology sets by BA (for BA definitions, see Appendix A)

A summary of the system reinforcements is shown in Table 19. Costs were estimated through the WECC Transmission Expansion Planning Policy Committee Cost Calculator of 2019 and adjusted for inflation to 2024 dollars[28]. These costs were then used in the economic analysis.[29]

Table 19. System reinforcements in coastal states required for reliability for all topology sets

	2035 Distributed	2035 Concentrated	2050 Radial & Intraregional	2050 Interregional
Miles of line upgrades	2295	3139	6351	6033
Number of transformer upgrades	13	24	47	43
Number of series capacitors	15	19	40	28
Number of substation upgrades	3	4	11	25
Total Cost (2024$ B)	10.8	14.4	26	26.7

[28] This tool was provided through the Advisory Committee by Jamie Austin, formerly of PacifiCorp and the WECC Production Cost Data Subcommittee. It is not currently available online.
[29] Cost estimates of these upgrades vary by source. Cost uncertainty may impact economic findings.

6.5 System Strength Analysis

An important screening tool that has been used in this project to evaluate the overall reliability of the planned 2035 topology sets relies on grid strength matrix. The purpose of this analysis is to assess offshore wind Points of Interconnection (POIs) based on system strength. The findings aim to assist system planners by identifying cases where further reliability assessments may be needed to integrate offshore wind energy at weaker POIs. Grid strength refers to the system's capacity to maintain stable voltage amidst varying grid conditions and disturbances. Strong grids provide a robust voltage reference, helping grid-connected devices stay synchronized. Conversely, weak grids present challenges, particularly for connecting inverter-based resources (IBRs) such as wind and solar PV, due to their asynchronous behavior, which can cause inverters to disconnect when their support is crucial for grid stability. Grid following IBRs require sufficient grid strength, relative to the resource's size, for synchronizing power electronics. Although these issues don't inherently threaten reliability, current control and protection systems must adapt to accommodate the evolving characteristics of the generation fleet.

Appendix B contains the full results for the topologies and system conditions studied, which include N-0, N-1, and N-2 for high and low wind conditions. Figure 55 shows an example of a map of grid strength before and after considering short-circuit contributions from IBRs. In the Distributed Topology, one POI (Fern Rd.) has weak grid conditions during high offshore wind dispatch scenarios. Note, grid strength is influenced by assumed OSW interconnections, which are higher at Fern Rd. than Humboldt, for example. Weak grid conditions do not indicate that injections are infeasible. Instead, they indicate that additional studies (and possibly equipment) are needed to ensure stable and reliable operation of any IBR that injects into weak grid.

Figure 55. Grid strength visualization for the 2035 Distributed Topology for high offshore wind penetration scenario (left) without contribution of IBRs (right) considering short-circuit contribution of large IBRs (>100 MW)

6.6 Resilience Analyses

In addition to contingency analysis reflected by current transmission planning procedures, new threats to the electricity system are emerging in the West. For example, several load-serving entities have needed to proactively de-energize transmission lines to limit the potential for starting or worsening wildfire conditions. Large transmission lines have also been de-energized in response to wildfire front propagation or smoke-induced arcing. The Bootleg fire of 2020 is one such event, during which CA lost 5500 MW of imports during a heat wave.

Seismic events also stand as a significant resilience threat and carry the additional natural hazard of tsunami waves to coastal infrastructure. Seismic resilience methods and findings are provided in Appendix B.

6.6.1 Methods

PNNL's Electrical Grid Resilience and Assessment System (EGRASS) was augmented with Wildfire Risk Estimation for Energy Systems (WiRES) framework developed at PNNL, which has capabilities to generate grid contingencies resulting from wildfires (Datta et al. 2024; Chalishazar et al. 2023). A wildfire risk map was developed based on 55 years of historical data (1950-2005), which is used as the basis for failure probability of electrical grid asset classes across the WI. Fire perimeters from National Interagency Fire Center (NIFC) from 2020 to present were used, including only fires greater than 100,000 Acres within the WI. Fire dataset from 2020 to present includes 120 wildfires with an average and maximum duration of 161 days and 306 days (respectively) and average size of 280,000 acres. This data was integrated into the WiRES framework, which uses a 50 km x 50 km grid overlay across the region to evaluate the risk of transmission line outages due to wildfires. The WiRES framework's performance-based risk evaluation method allows for the translation of wildfire ignition probabilities into risks of electrical grid outages. This enables power system planners to make informed infrastructure decisions that consider the spatial dispersion of wildfire risk and prioritize resilience investments accordingly.

Failure probabilities were assessed for the transmission lines, substations and towers of each topology set subject to each extreme event. Monte Carlo draws against these probabilities defined the likely failures of lines, substations, or towers. The Dynamic Contingency Analysis Tool (DCAT) evaluated each contingency independently and combined all likely failures of any associated circuits in dynamic contingency simulations.

6.6.2 Wildfire

Wildfire resilience was considered as a result of steady state and dynamic contingency set definitions. Steady state definitions were manually defined as a function of the co-location of a significant number of lines to the Shasta North and South busses in Northern California, a region prone to wildfire. The dynamic contingency results from a synthetic composition of wildfire propagation as inspired by the Bootleg fire event.

6.6.2.1 Steady-State

In the 2050 Intraregional Topology set, these lines are grouped together, meaning that 14 GW of power flows through a wildfire-prone corridor. In the 2050 Interregional Topology set, only 6 GW flow through this same corridor. The resulting steady-state contingencies simply consider all these lines failing as a result of the same wildfire event. These lines correspond to the 525 kV HVDC bipoles highlighted in Figure 56.

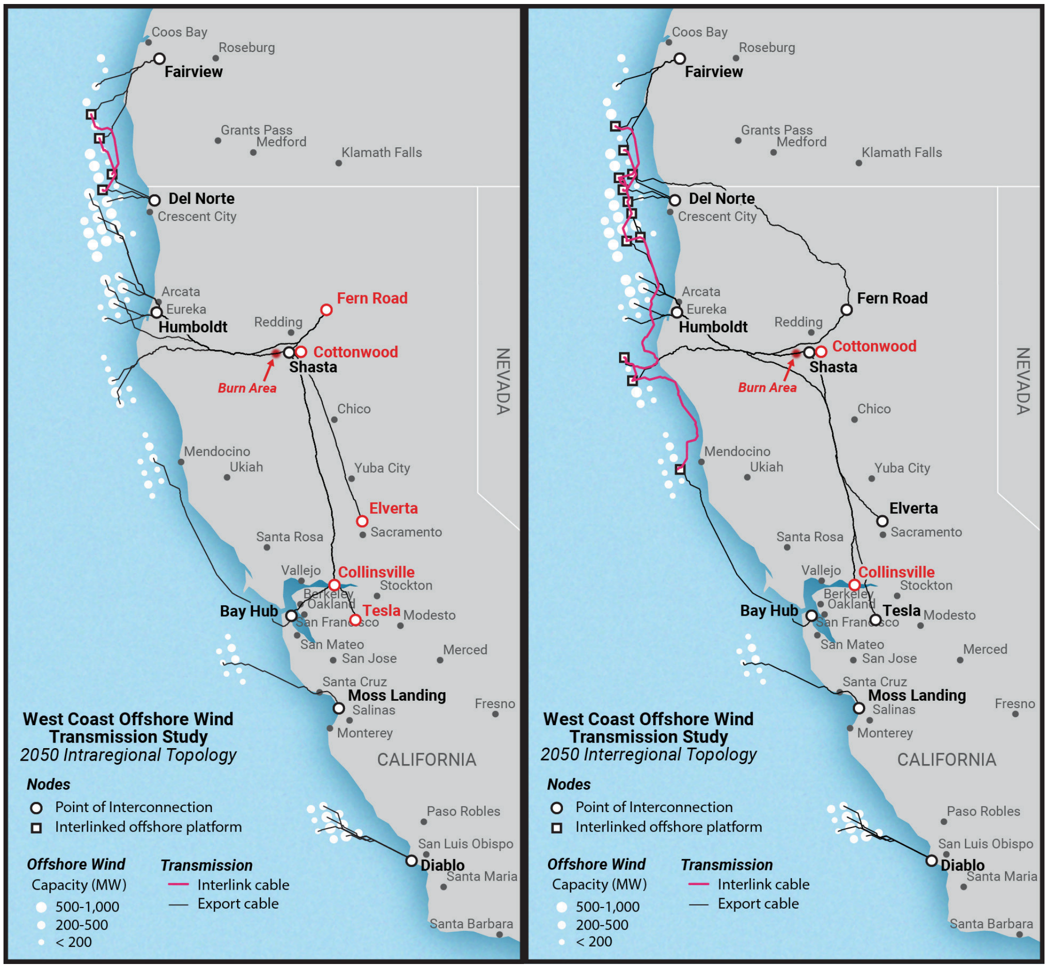

Figure 56. Lines of the 2050 Intraregional (left) and 2050 Interregional (right) Topologies that are failed in the steady-state wildfire contingency analysis.

Resulting overvoltage violations, overloads, and unsolved power flow cases indicate the significant system vulnerability to wildfire incurred by the land-based MTDC of the 2050 Intraregional topology set as seen in Table 20.

Table 20. System voltage and load violations due to steady-state wildfire contingency in proximity of Shasta bus.

Topology Set	Overvoltage Events	Overload Events	Unsolved Cases
2050 Intraregional	49	4	6
2050 Interregional	30	2	4

6.6.2.2 Dynamic

The Bootleg fire started from lightning strike on July 6th, 2021 and would eventually grow larger than 400,000 acres and merge with the Antelope Fire and the Cougar Peak Fire. On Friday afternoon, July 9th, 2021, the HVAC overhead transmission lines of the California-Oregon Intertie (COI) began to trip due to heavy wildfire smoke and particulate matter, which caused arcing from the lines to the ground. Eventually the entire interertie was taken offline and the Pacific DC intertie also was significantly de-rated. In total, CA lost 5500 MW of imports during a significant heat wave (Roth 2021).

To simulate the Bootleg, Antelope, and Cooger Peak Fire impacts on the transmission system, wildfire fronts were geolocated. A buffer was extended beyond the active front to indicate the likelihood of severe smoke and particulate matter which may trip lines in a similar way to COI lines in July 2021.

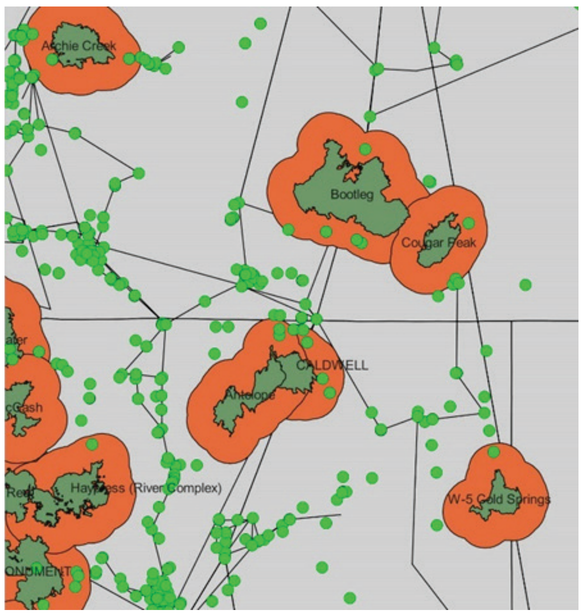

Figure 57. Bootleg, Cougar Peak, and Antelope wildfire fronts (in green) with offsets (in orange) to indicate assumed tripping of transmission lines due to heavy smoke and particular matter.

As the wildfire front progressed dynamically in time, additional substations and transmission lines were pulled out of service. Because the simulations were conducted in the electromagnetic transient domain and computational efficiency was prioritized, synthetic events were relatively short in duration. The Bootleg wildfire simulations lasted 22 seconds in total. Numerous transmission outages were encountered in sequence, including the loss of a 500 kV line (with roughly 2000 MVA capacity) at 18 seconds, and the system response was observed. Figure 58, Figure 59, Figure 60, and Figure 61 indicate the response for 2035 and 2050 topology sets. All system responses were stable, with 2035 Distributed and 2050 Intraregional exhibiting the largest frequency deviations from 60 Hz.

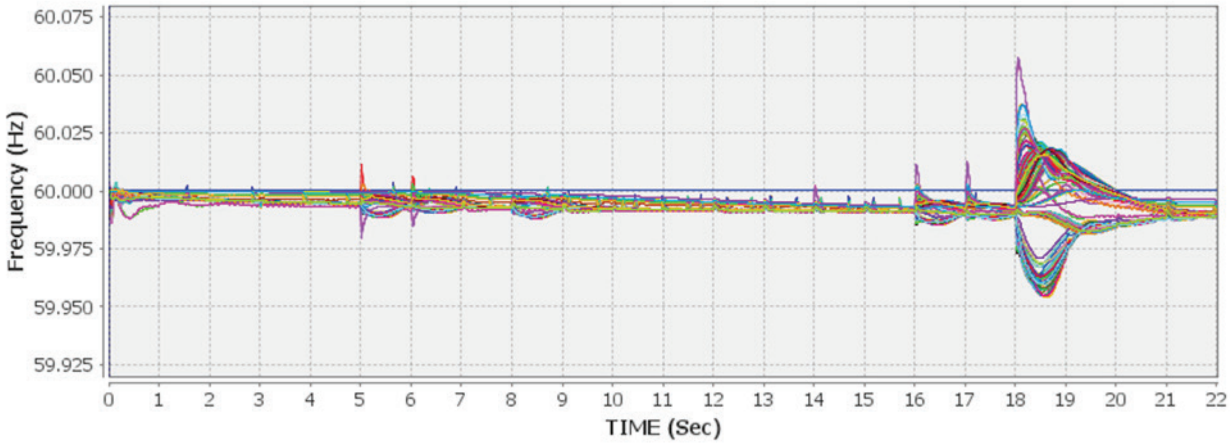

Figure 58. System response to Bootleg synthetic wildfire simulation, 2035 Concentrated Topology set. Different colors represent frequencies encountered at various busses on the system.

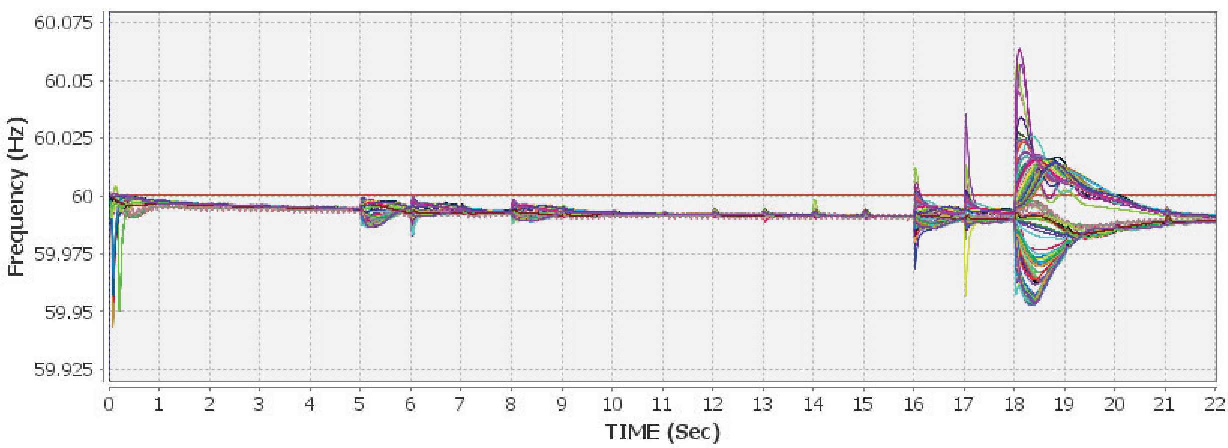

Figure 59. System response to Bootleg synthetic wildfire simulation, 2035 Distributed Topology set. Different colors represent frequencies encountered at various busses on the system.

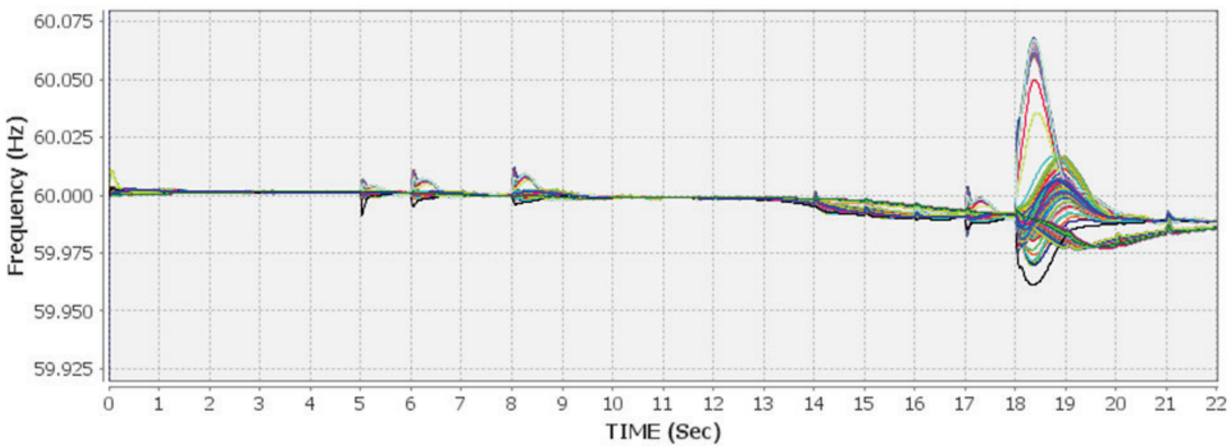

Figure 60. System response to Bootleg synthetic wildfire simulation, 2050 Intraregional Topology set. Different colors represent frequencies encountered at various busses on the system.

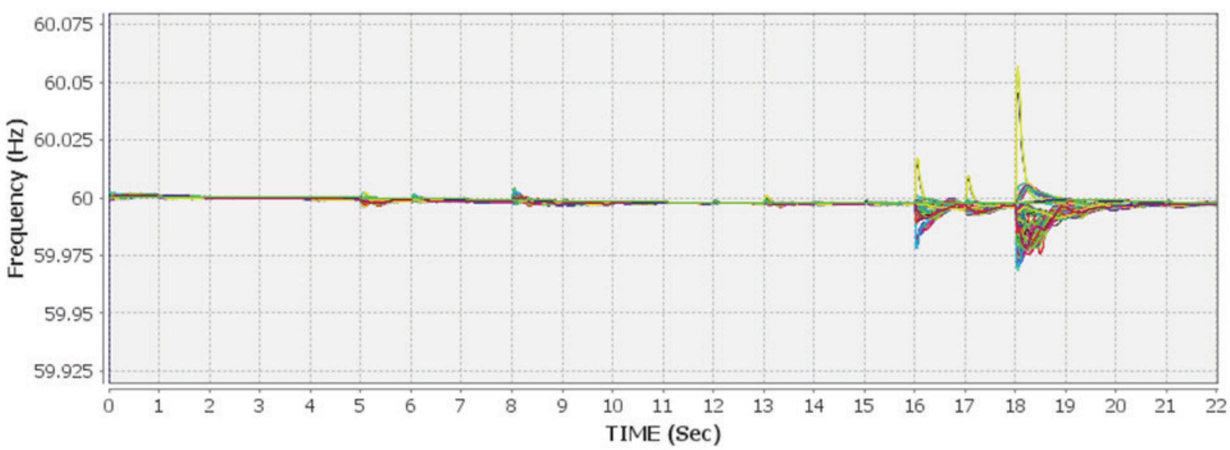

Figure 61. System response to Bootleg synthetic wildfire simulation, 2050 Interregional Topology set. Different colors represent frequencies encountered at various busses on the system.

6.7 Summary and Key Findings

To ensure reliability and resilience across all topology sets, system reliability analyses were coordinated with the system operators on the West Coast who are actively planning or fielding interconnection requests for OSW generation. Topology sets were shown to support reliable operations, costs of necessary system reinforcements were identified, and responses to potential resilience threats were characterized. The following observations constitute key findings:

- Upgrades for all topology sets ranged between 2295 and 6033 miles of conductors, 13-43 transformers, 15-28 series capacitors, and 3-25 substations.
- Upgrade costs were lowest for the 2035 Distributed Topology and highest for the 2050 Interregional Topology at $10.8B (2024$) and $26.7B (2024$), respectively.

- In 2035, distributing interconnections reduced system reinforcements by 25% or $3.6B (2024$) over the concentrated interconnections.
- Redispatch through MTDC networks in the 2050 topology sets was explored and found to offer minimal changes to the reinforcements.
- Though system response over all topology sets was stable for most dynamic contingencies, unstable responses were observed for as many as 8, 37, and 3 of the dynamic contingencies defined by BPA, CAISO, and WECC, respectively. Additional remedial action schemes or transmission infrastructure may be required to stabilize the responses to these contingencies. Such efforts were deemed out of scope for the study and are important considerations for future work.
- In the 2035 Concentrated Topologies, all POIs have moderate to strong grid conditions.
- In the 2035 Distributed Topology, the Fern Road POI has weak grid conditions during high offshore wind dispatch scenarios.
- Accounting for the contribution of the existing IBRs toward short-circuit current was shown to substantiate an improvement in grid strength at Fern Road and other POIs. Without this consideration of IBR contribution, grid strengthening support may be required to mitigate the risk of weak grid conditions.
- Wildfire events were simulated, and synthetic dynamic contingencies were defined based on the Bootleg, Antelope, and Cougar Creek fires of 2021. System frequency time histories indicated stable response to these events for all topology sets.

7.0 Economic Analysis

The planning and operational analyses demonstrate there are multiple feasible pathways to achieve offshore wind integration along the west coast while maintaining system reliability. The economic analysis aims to better understand the value of transmission to enable cost-effective offshore wind integration. Specifically, the analysis is designed to:

1. quantify the economic benefits of different offshore transmission development pathways,
2. identify the sources of cost savings and how those savings change over time, and
3. evaluate how transmission benefits are distributed among regions and types of network users for different transmission pathways.

7.1 System-Wide Analysis

7.1.1 Methods

The analytical approach developed to identify and evaluate transmission benefits is designed to enable comparisons across different transmission investment pathways and identify tradeoffs in near-term and long-term strategies for designing the offshore network. To enable comparisons across pathways, the 2035 Distributed to 2050 Radial pathway serves as the reference pathways against which other investment options are compared.

The analysis considers a broad range of economic impacts including changes in capital and operating costs associated with each pathway and potential benefits of sharing generation across interregional transmission to meet resource adequacy requirements. We do not consider broader macroeconomic impacts such as jobs, environmental impacts, or impacts to other ocean co-users. Chapter 8.0 presents an approach to broader community impacts associated with each transmission topology. To approximate how the system may change between the 2035 and 2050 model years, we assume linear growth in system costs between the two years. For present value calculations, we extend the study horizon to 2065, assuming constant system costs fixed at 2050 levels to capture at least 15 years of operating life for investments that occur at the end of the planning period.

To test the robustness of the results against future uncertainties, the analysis also considers a sensitivity regarding the cost of hydrogen. This is analyzed only with the production cost model and does not include potential impacts on the resource adequacy value of the network. In addition, we analyzed a further sensitivity related to uncertainty in the cost of transmission investments. We evaluate a low- and high-transmission scenario to quantify the impact of a 10% decrease or increase, respectively, in the capital cost of the network.

7.1.2 Transmission Investment Costs

For each pathway, we consider the portfolio of onshore and offshore transmission facilities developed for offshore wind integration as well as transmission needs for anticipated load growth and the addition of other generation resources. Table 21 shows the costs of the five transmission topologies. The export system costs are the result of the costs referenced in Appendix D, applied to the topology data from section 4.2. The onshore reliability upgrades are based on the WECC Transmission Cost Calculator, applied to the upgrades noted in section 6.4.[29] It is important to note that the onshore upgrades include reliability upgrades for offshore wind as well as those for demand and other resources added to the system that would be needed irrespective of any offshore wind deployment.

Table 21. Transmission cost summary (2024$)

Topology Set	Offshore transmission[30]	Onshore upgrades[31]
2035 Distributed	$25.7 billion	$11.4 billion
2035 Concentrated	$22.4 billion	$14.4 billion
2050 Radial	$51.0 billion	$26.0 billion
2050 Intraregional	$53.1 billion	$26.0 billion
2050 Interregional	$56.9 billion	$26.7 billion

In the near-term, the 2035 topologies illustrate tradeoffs in onshore and offshore transmission investment needs due to different offshore wind farm locations and strategies to deliver offshore wind generation to shore. The additional costs of the export cables associated with the 2035 Distributed are balanced by the lower costs for onshore reliability upgrades compared to the 2035 Concentrated. By contrast, the costs for export cables are lower in the 2035 Concentrated Topology because the total length of the export cables is shorter but this topology incurs higher onshore reliability upgrade costs. In the long-term, onshore transmission costs are similar across each transmission topology but offshore costs increase as more interlinks are added. The Intraregional and Interregional are approximately $2 billion and $6 billion higher, respectively, compared to a Radial Topology.

Figure 62 compares the present value of annualized transmission expenditures across the six 2035–2050 pathways to identify tradeoffs in different transmission philosophies for near-term and long-term network expansion.

[30] Offshore transmission costs include export system costs to the POI, and any onshore portions of multi-terminal HVDC networks (e.g., in the 2050 Intraregional).

[31] Prior to the contingency analysis and identification of system reinforcements for reliability, some onshore system upgrades were assumed for the 2035 Concentrated Topology set to support the significant power flows through the coastal POIs. The costs of these onshore system upgrades were added to the system reliability reinforcement costs for the economic comparisons.

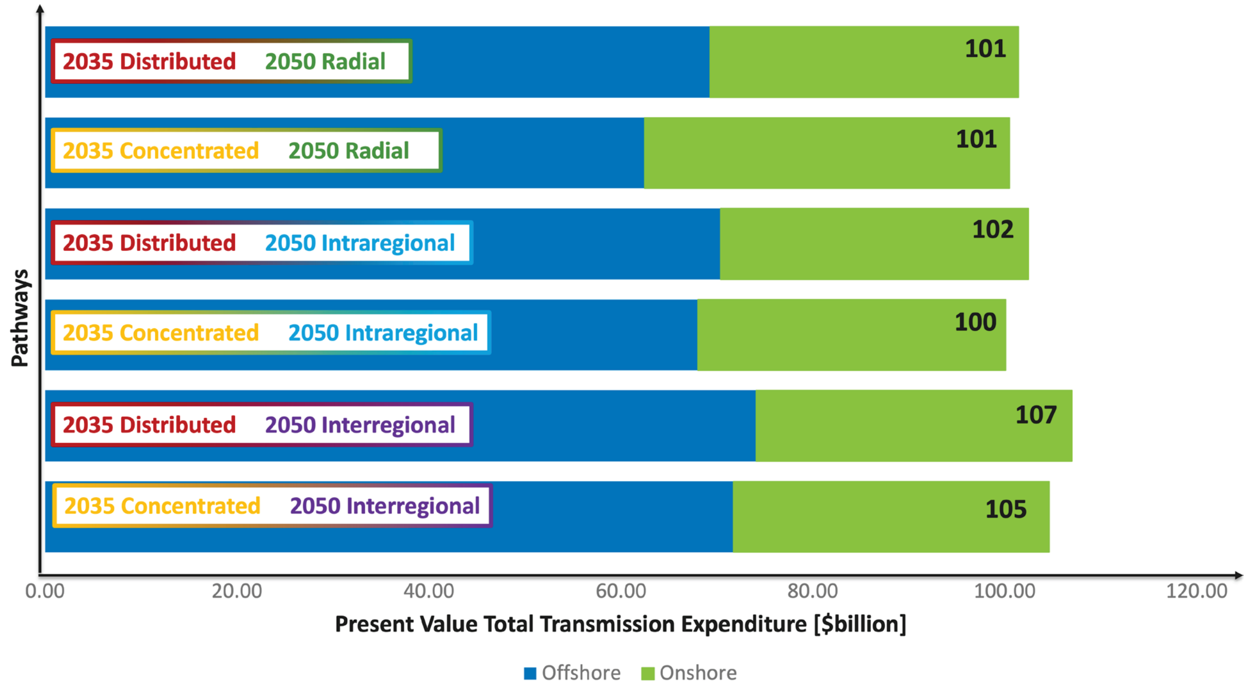

Figure 62. Present value total transmission expenditures for each network pathway (2024$)

Across each possible pathway, the annualized costs are within 10% of each other. The pathways that build from a Concentrated philosophy in 2035 tend to have slightly lower total costs compared to those that start with a Distributed Topology. Regardless of 2035 starting point, pathways to the Interregional Topology in 2050 have the highest annualized costs.

7.1.3 System-Wide Economic Benefits

The economic benefits of offshore transmission are based on changes in system costs compared to the 2035 Distributed to 2050 Radial Topology. These costs include capital and operating costs for new transmission, production costs, and costs to meet resource adequacy requirements. Figure 63 shows the total cost savings for each pathway compared to the 2035 Distributed to 2050 Radial pathway.

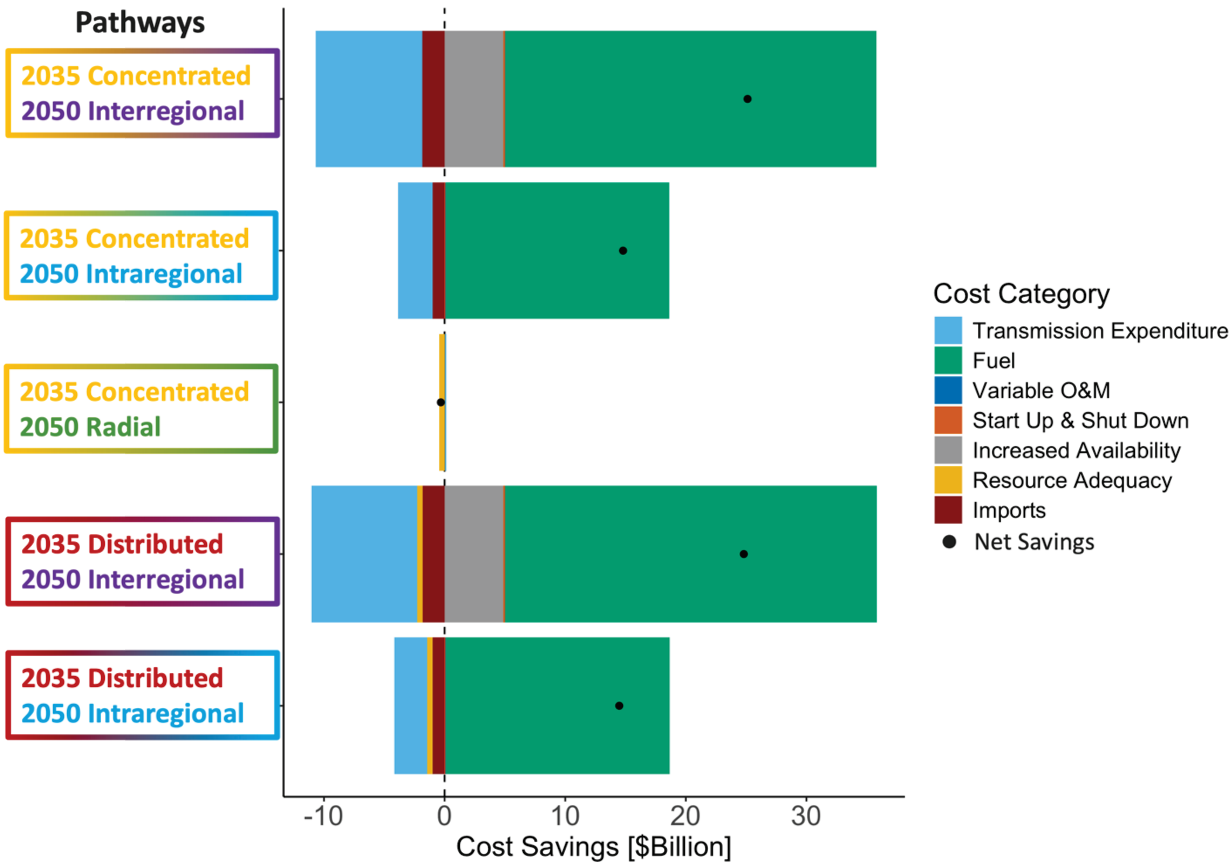

Figure 63. Total cost savings and transmission expenditures based on annualized expenses for 2035 – 2065 planning horizon (2024$)

Black dot indicates the net savings across all cost categories.

Despite higher costs for onshore and offshore transmission, pathways with more offshore links between POIs and across regions show the largest net savings compared to the 2035 Distributed to 2050 Radial pathway. Total savings reach $14 billion and $25 billion for Intraregional and Interregional development pathways, respectively. Avoided fuel costs are the largest source of savings, accounting for more than 85% of avoided costs in all Intraregional and Interregional pathways. The Interregional Topology provides an additional value through increased availability of offshore wind generation during export cable outages.[32] The Interregional network allows wind generation that would otherwise be curtailed to be rerouted through the offshore network during cable outages and displace higher cost generation sources. The cost of electricity imports from Mexico and Canada increase in all Intraregional and Interregional pathways, but this additional cost is outweighed by reductions in operating costs.

Resource adequacy value is derived from the ability of transmission to deliver equivalent firm capacity, potentially reducing the need for generation capacity investments to meet the same level of reliability. Along the west coast, offshore transmission links between and within regions did not impact the network's equivalent firm capacity. However, the number and configuration of POIs in the 2035 topologies did impact the resource adequacy value of the network. The 2035 Concentrated Topology with fewer POIs had lower resource adequacy value compared to the

[32] See Appendix A for more information on modeling of transmission outages.

2035 Distributed Topology that includes more POIs, indicating more generation resources would be required to maintain the same level of reliability. Based on the analysis presented in Section 5.6, the 2035 Concentrated Topology reduces the equivalent firm capacity of the network by 260 MW. This capacity translates to $53 million (2024$) in annualized additional generation investments costs.[33] We do not comprehensively evaluate the impact of each transmission pathway on system resilience.

Figure 64 shows the change in total cost savings over time for each pathway. In the near-term, there is very little change in system costs in the initial 2035 operating year as the 2035 Distributed and 2035 Concentrated have similar investment and operating costs. As the transmission topology designs diverge in 2050, the net savings for the Intraregional and Interregional Topologies increase over time, driven by increasing savings in fuel costs compared to the Radial Topology.

This study evaluates the potential economic impacts across a range of cost categories. It does not evaluate how the potential system savings can be achieved with existing market mechanisms.

[33] To monetize the megawatt values of equivalent firm capacity that transmission can provide, we calculated the annualized cost of new entry for marginal generation capacity at that location, estimated to be $202 per kW in the west in 2035. The cost of new entry at different locations is the shadow price of the capacity constraint from the capacity expansion model, ReEDS. The resource adequacy value is equal to the change in equivalent firm capacity times the annualized cost of new entry.

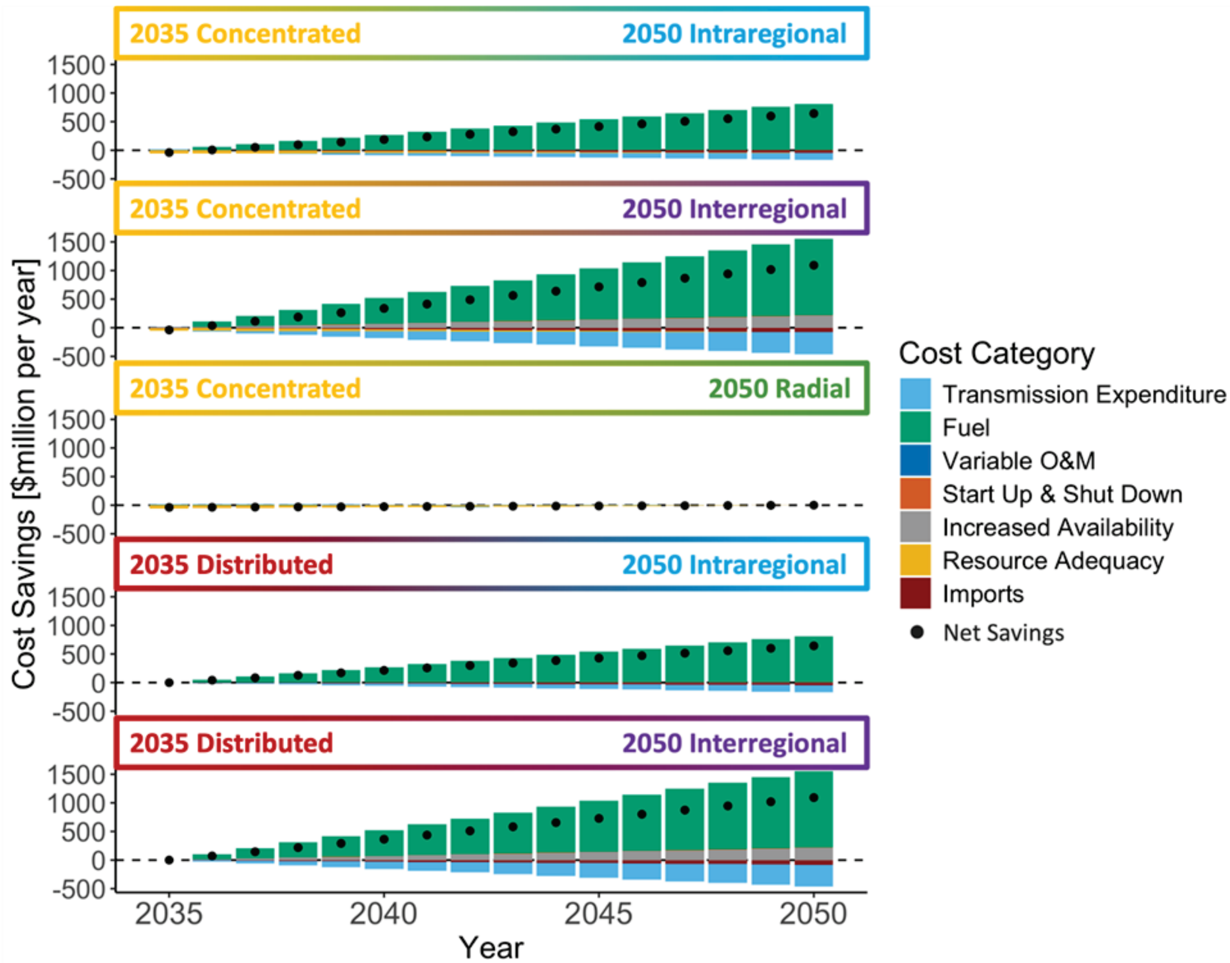

Figure 64. Annual cost savings compared to Distributed to 2050 Radial pathway (2024$)

7.1.4 Sensitivities

To understand the drivers of transmission value and robustness of the results, this study also considers sensitivities on the price of hydrogen and transmission cost. Figure 65 compares the total cost savings for each sensitivity compared to the base 2035 Distributed to 2050 Radial pathway.

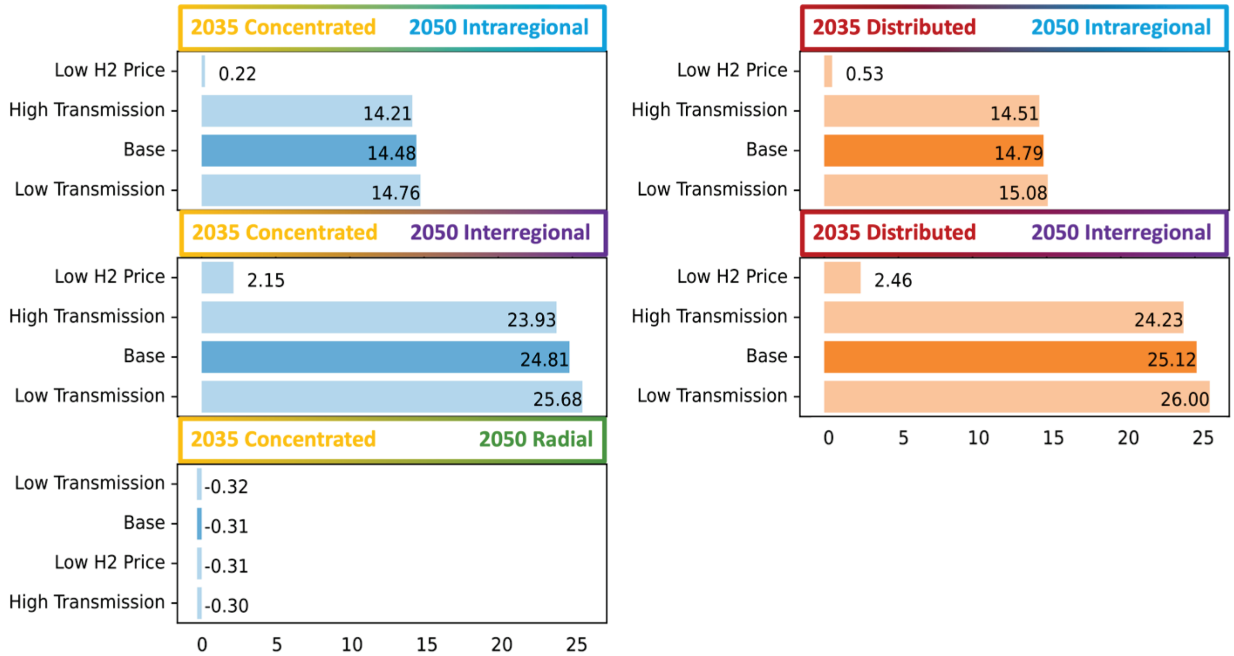

Figure 65. Sensitivity analysis of total cost savings and transmission expenditures based on annualized expenses for 2035 – 2065 planning horizon for each transmission pathway compared to the 2035 Distributed to 2050 Radial pathway in $Billion (2024$)

Under the Low H2 Price sensitivity, the value of alternative transmission pathways decreases to less than $3 billion compared to the 2035 Distributed to 2050 Radial pathway. This indicates that the ability to displace higher marginal cost H2 production with offshore wind generation and regional power trade is a primary driver of transmission value for the alternative transmission pathways.

By contrast, the value of transmission is less sensitive to the assumed cost of transmission. A 10% increase (High Transmission) or decrease (Low Transmission) in the cost of transmission results in a change in system value of less than 5% across all pathways.

7.2 Disaggregation of Benefits

7.2.1 By Geography

While the systemwide value of each transmission pathway may reveal common trends, the value to individual regions may vary. This is because the value to each region is driven by interregional trade in addition to changes in regional costs. To evaluate regional benefits, we use the adjusted production cost metric. This metric captures changes in total production costs in each region adjusted for the costs of meeting regional electricity load and revenues from exporting power to other regions.[34] Table 22 shows the total savings for each planning region and pathway compared to the 2035 Distributed to 2050 Radial pathway.

[34] The costs of meeting electricity load and export revenues are calculated based on hourly load and generator weighted locational marginal prices, respectively. See Brinkman et al. (2024) for details.

Table 22. Regional benefit [2024$ billion] for each pathway compared to the 2035 Distributed to 2050 Radial pathway

	BS	CA	PNW	RM	SW
2035 Concentrated 2050 Radial	10	-490	90	60	-5
2035 Concentrated 2050 Intraregional	-290	17,070	-18,240	110	1,040
2035 Concentrated 2050 Interregional	-160	28,830	-1,540	230	1,220
2035 Distributed 2050 Intraregional	-300	17,560	-18,340	60	1,050
2035 Distributed 2050 Interregional	-170	29,320	-1,630	170	1,230

BS - Basin; CA – California; PNW – Pacific Northwest; RM – Rocky Mountain; SW – Southwest

Compared to the 2050 Radial Topology, the Intraregional and Interregional 2050 Topologies enable greater energy trading among regions by adding more network reinforcements to facilitate power flows within a region (Intraregional) or network links among regions (Interregional). Among planning regions, the highest benefit accrues in California and, to a lesser extent, the Southwest. In these regions, low-cost offshore wind generation and imports from neighboring regions can displace higher-cost generation. As a result, the hourly locational marginal prices (LMPs) decrease across these regions leading to lower costs to meet electricity needs for load and storage charging.

By contrast, increased interregional trade results in higher LMPs for net exporting regions such as the Pacific Northwest. The increased costs to meet energy needs at higher marginal prices exceeds additional export revenue the region receives for both the Intraregional and Interregional Topologies. This impact is particularly pronounced in pathways to the Intraregional Topology. While the Intraregional Topology is focused on greater interconnections within the California footprint, these reinforcements enable more interregional power flows as California is able to make greater use of imports from the Pacific Northwest to meet electricity demand across its footprint. However, absent reinforcements across the California-Oregon border, the increased trade results in increased congestion across the intertie linking California with the Pacific Northwest resulting in significant increases in LMPs for demands in the Pacific Northwest. By contrast, in the Interregional Topology, greater interlinks across the California-Oregon seam relieves this congestion resulting in a smaller increase in LMPs across the Pacific Northwest. This congestion effect is indicated in Figure 66. While not explored in this study, alternative strategies such as new conductors or power flow controllers could be considered to minimize congestion across the intertie. This finding suggests the need for careful engineering assessments of how within-region reinforcements, such as those explored in the Intraregional Topology, may impact other regions.

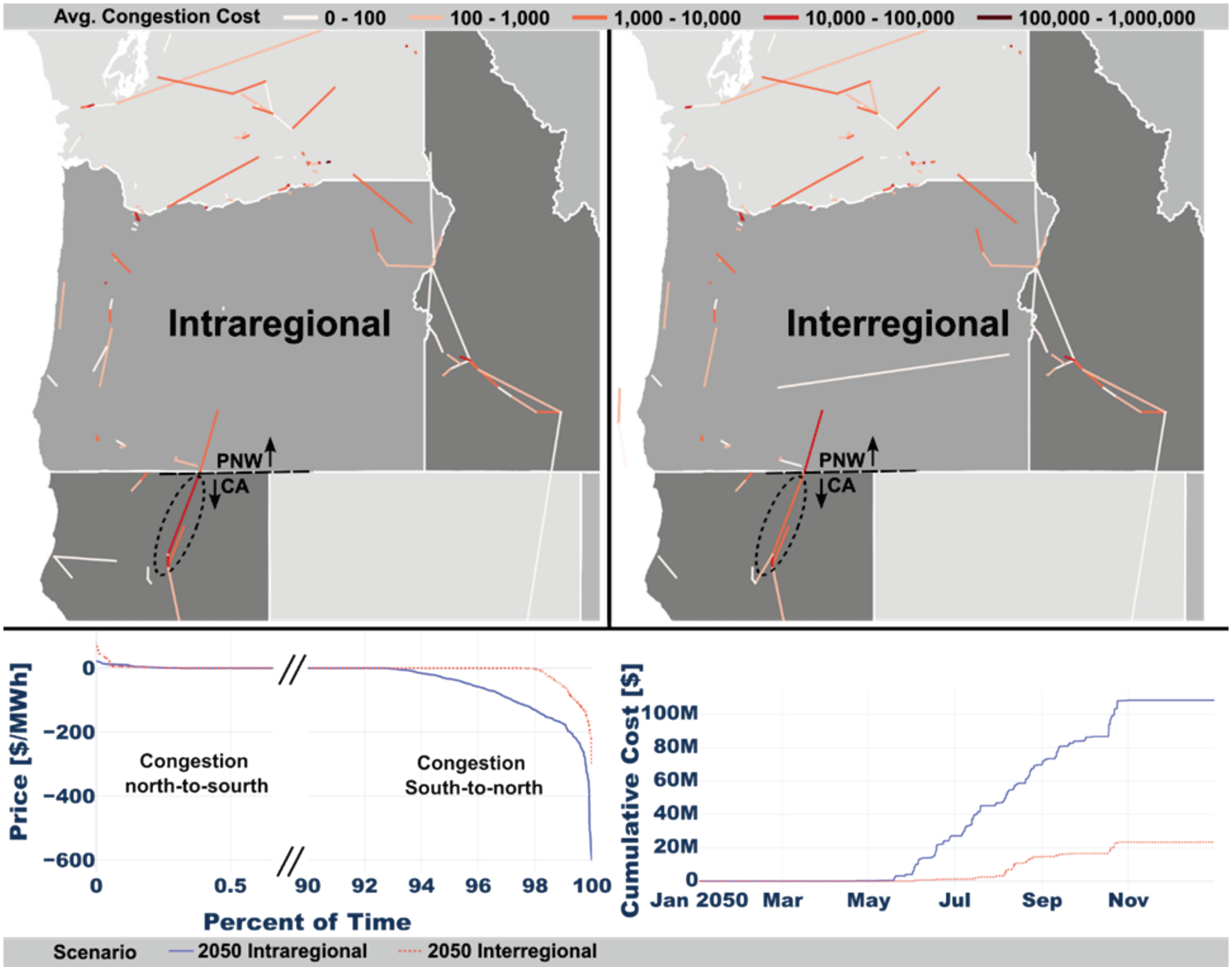

Figure 66. Map of congested lines in the 2050 Intraregional and Interregional Topology sets (top), and congestion price (bottom left) and congestion cost (bottom right) statistics.

The negative congestion prices indicate congestion on northbound flows (import to PNW), with higher overall congestion costs. The higher, south-to-north congestion cost just south of the PNW-CA border helps explain the rise in import costs in the Intraregional Topology compared to the Interregional one and, as a consequence, the regional benefit difference.

Finally, we note that the outcome is highly sensitive to the anticipated changes in LMPs. Under sensitivity analysis where the LMPs for the Intraregional and Interregional Topologies change by 5% or do not change compared to the 2050 Radial Topology, the Pacific Northwest could experience zero or even positive benefits. Follow on work could explore the impact of regional trade on nodal LMPs further.

7.2.2 Network-User

The system-wide benefits provide an estimate of how the transmission pathways can provide benefits through cost reduction to the grid. However, the grid is comprised of network users who will tend to prioritize their individual benefits when making decisions. A single decision maker, such as a single vertically integrated utility subject to a state regulator, would choose the transmission expansion plan that maximizes the total benefit of load minus the cost of generation and transmission (Hogan 2018). Single decision makers are becoming less prevalent as wholesale power markets are expanding to new areas and seeing wider adoption.

Privately owned plants now provide more electricity generation, and transmission rights have been sold to private owners. Modeling the grid as a single entity may not provide complete information. Perfectly competitive markets can achieve the same optimal outcome as the single decision maker when certain market conditions hold, but these conditions are generally not present in electricity markets (Joskow and Tirole 2005; Mas-Colell et al. 1995). Vertical integration between generators, utilities, and regional ISOs, and the nature of transmission investment (high initial cost and long operational lifetime with low cost) can create suboptimal decisions where some agents can free-ride. This can lead to transmission investment that is lower than optimal when the overall benefits are sufficient to justify the costs, but the benefits to the agents that would fund the transmission investment are not greater than their costs (Doorman and Frøystad 2013; Hogan 2018; Kristiansen et al. 2018; Schaber et al. 2012).

This network-user disaggregation models three agents: generators, transmission owners, and load-serving entities. Generators and load-serving entities are analogous to standard market participants, producers, and consumers. Transmission owners are analogous to the transportation or shipping industry. Appendix F includes more detail on the methodology and formulas used to compute these benefits. This analysis uses results from the production cost modeling to estimate the disaggregated benefits. Of note, this does not include a formal model of end-consumer or transmission payments. Consumer payments and rates are usually determined through the ratemaking process with oversight from PUCs. This process is not modeled here, but load-serving entity benefits can broadly be interpreted as being passed on to end-consumers through this process. The transmission owner benefits can be thought of as the right to the revenue received from purchasing power at low LMP locations and selling it at high LMP locations. Transmission revenues are not extended to practical payment formats used, such as postage stamp, pancake, license plate etc. (NCEP 2004).

7.2.2.1 Results

The network-user disaggregated benefits include only the annual operating benefits, and do not include capital costs or other benefits such as resource adequacy. Figure 67 shows the disaggregated benefits for the 2035 scenarios. Overall, the differences between the 2035 scenarios is smaller than for the 2050 scenarios. As shown in the system-wide benefits section, the difference in total benefits between the scenarios is small with the Distributed having $2.73 million higher costs per year. When the benefits are disaggregated, the generators gain $157 million more in annual benefits and transmission owners and load-serving entities experience a $88 million and $71 million per year reduction in benefits in the distributed scenario. However, these changes are relatively small for the 2035 scenarios, approximately a 1-percent change compared to the overall benefits for each network user.

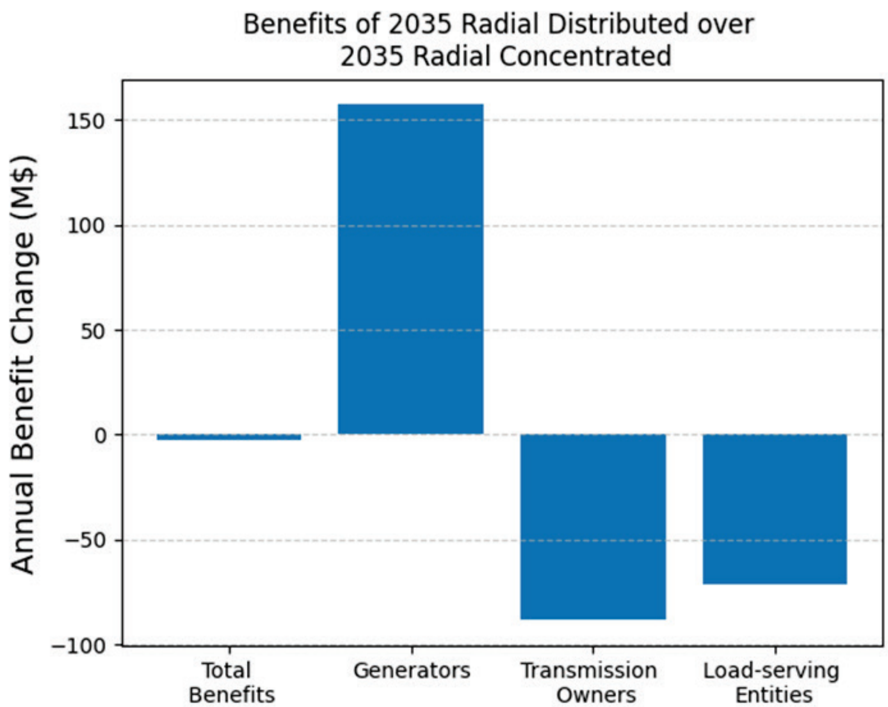

Figure 67. Benefits of the 2035 Distributed scenario compared to the 2035 Concentrated scenario.

Figure 68 shows the results of the network user disaggregation for the 2050 topologies. The Interregional Topology has benefits to load-serving entities of $4.1 billion per year and negative benefits to generators and transmission owners of $600 million and $2.4 billion per year. This indicates that the interregional transmission topology has reduced congestion costs and overall lower LMPs for generators and loads. The lower prices translate to a small reduction in benefits to the generators. The combination of the reduction in LMPs and congestion in the system translates to lower load payments. The Intraregional Topology has load-serving entity benefits of $128 million per year, transmission owner benefits of $812 million per year and a reduction in benefits to generators of $310 million per year. This shows that in the intraregional scenario, generator costs are reduced, but generator revenue is reduced to a larger extent. The system has increased overall congestion. The load-serving entities experience a relatively small benefit as the reduction in the cost to purchase generation is mostly offset by the increase in transmission payments.

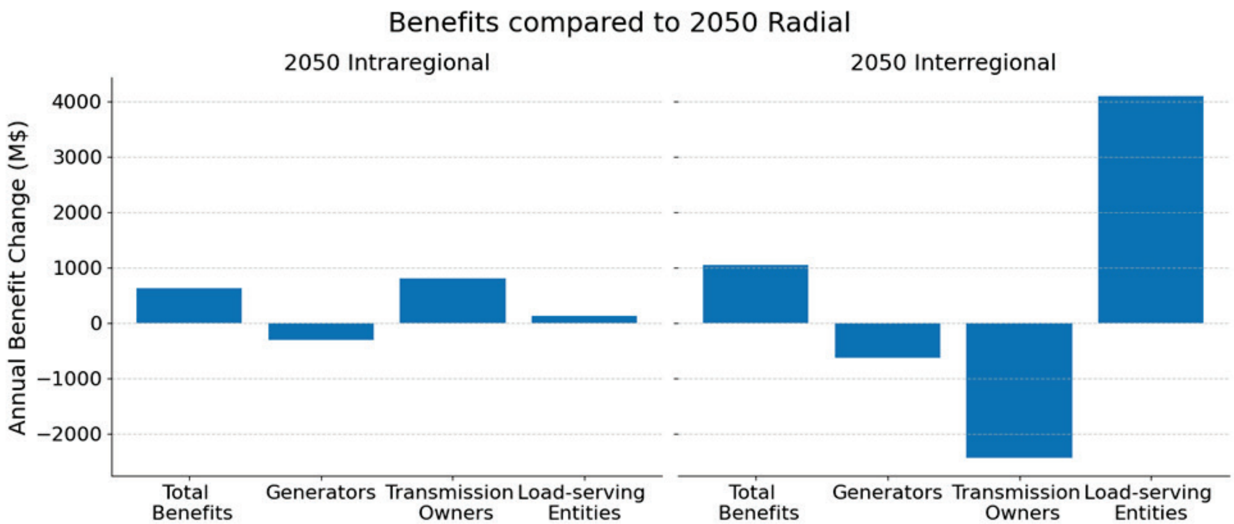

Figure 68. Benefits of the 2050 Intraregional and Interregional Topologies compared to the 2050 Radial Scenario

Regions benefit from increasing power exports through the increase in net export revenue, or from increasing imports through reducing production costs. In general, this means that regions with increased exports will see the benefits accrue to generators, and regions with increased imports will gain benefits to load-serving entities. The load-serving entity benefits are the greatest in California, where importing more low-cost offshore wind allows them to reduce generation by higher-cost alternatives. Generator benefits for the 2050 Intra and Interregional scenarios are the largest in the Northwest, while generators in California have reduced benefits as the lower usage of high-cost generation reduces generator revenue.

7.3 Summary and Key Findings

The technoeconomic work analyzes the benefits and costs of the different strategies for offshore wind transmission development. The following observations constitute key findings:

- The additional export system costs in the 2035 Distributed Topology are offset by lower onshore upgrade costs compared to the 2035 Concentrated Topology. Overall, both the total benefits and costs of those topologies are similar. Either topology makes a reasonable starting point for a pathway to 33 GW from an economic perspective.
- The topologies which include interlinking (offshore or onshore) have the most net benefit to the system. The topology with interregional interlinks offshore in 2050 (the Interregional) has more benefits (approximately $25 billion in total net benefits) compared to the Intraregional Topology (approximately $15 billion net benefits) over the planning horizon.
- The result is very sensitive to hydrogen fuel prices. If hydrogen prices are similar to natural gas, the system benefits are approximately $2 billion, or 10 times less than the base assumption ($20 per mmbtu).
- The distribution of benefits (both geographic and network-user) is uncertain, but careful design may be necessary to create a topology that benefits multiple regions from an economic perspective. Reliability and community values can also be considered.

8.0 Community Values Assessment

8.1 Background

Transmission development for OSW has the potential for community benefits, such as increases in energy access and resilience for coastal populations at the end of aging transmission and distribution lines (Douville and Bhatnagar 2021). However, development associated with transmission of floating OSW, such as cables, substations, and landing infrastructure, may also affect the health of ecosystems that West Coast communities depend upon for their livelihoods, economies, and human wellbeing (Maxwell et al. 2022; Watson et al. 2024). A Community Values Assessment is ongoing and aims to explore the potential trade-offs between benefits and negative impacts to communities.

The benefits that healthy coastal and marine ecosystems provide to people are typically referred to as “ecosystem services” and the natural assets (e.g., lands and seascapes) that provide these services are “natural capital” (Arkema et al. 2024; Guerry et al. 2011; Kareiva et al. 2011). Along the West Coast of the United States, the California Current Ecosystem provides numerous ecosystem services, including food and livelihoods from fisheries, resilience from coastal hazards, opportunities for aesthetic enjoyment, mental and physical health benefits from time spent in nature, and cultural and spiritual values. Ocean winds, waves, and tides can also provide renewable energy resources (Lester et al. 2013; Lester et al. 2010). Because of the importance of coastal and ocean ecosystems for economic development and human wellbeing, government agencies, non-governmental organizations, companies, and community-based organizations are increasingly considering the benefits of nature in numerous sectors including disaster risk reduction, sustainable development, agriculture, aquaculture, and renewable energy (Guerry et al. 2015; Mandle et al. 2019; Picchi et al. 2019). Yet, relationships between transmission development and ecosystem services are not well-studied.

8.2 Approach

We are applying an ecosystem services approach to explore the benefits and costs of alternative options for transmission development to West Coast communities. An ecosystem services approach typically involves three main elements: 1) engagement, 2) scenario design, and 3) social-ecological modeling (Rosenthal et al. 2014; Ruckelshaus et al. 2015). An ecosystem services approach also involves iteration among these three elements, with the engagement not only informing the scenarios and the modeling, but the results of the modeling also helping to improve the scenario design (Arkema et al. 2015; Arkema et al. 2013).

Our approach to assessing the benefits and costs of OSW transmission development for West Coast communities similarly involves three main components: 1) engagement with the Community Values Subgroup, 2) scenario and topology design and translation to the social-ecological models, and 3) social-ecological modeling of the values of three ecosystem services under each topology at various spatial scales. Here we share the outcomes of the subgroup engagement and briefly explain how we are incorporating these findings into the social-ecological modeling of ecosystem services to explore trade-offs among topologies. Future work could incorporate the findings of the Community Values Assessment into the transmission scenarios, and even tailor interventions to specific communities after broader Tribal and stakeholder engagement. Using socio-ecological modeling of ecosystem services to improve transmission strategies provides an opportunity for innovation going forward.

8.3 Community Values Subgroup

We convened a Community Values Subgroup to provide input on the WOW-TS data, Community Values analysis, and results. Self-selected from the broader WOW-TS Advisory Committee, the Community Values Subgroup included 27 interested members or representatives of Tribal Communities, federal, state, and local governments, community-based organizations, non-governmental organizations, utilities, and the private sector that play a role in the management and stewardship of coastal and marine ecosystems, OSW development, and/or transmission. We worked with the Subgroup to identify which benefits of coastal and ocean ecosystems to include in the study. The Subgroup also provided input on the data, results, and metrics for quantifying benefits and costs of transmission options for communities.

We met with the Subgroup four times between April 2024 and October 2024, in addition to holding one-on-one meetings with members individually. Over the course of our work with the Subgroup, we heard several main themes. The Subgroup emphasized the importance of participatory processes that center community values in all aspects of OSW development. Much of their feedback involved the notion that potential benefits of transmission for floating OSW (e.g., energy access/resilience) must be balanced and considered along-side potential burdens (e.g., impacts to fisheries) so that any communities experiencing negative effects are at least receiving energy benefits. The Subgroup also emphasized the importance of considering all aspects of OSW infrastructure (i.e., turbines, cables, landing infrastructure, port development) together so that benefits and costs could be assessed more holistically (Table 23); however, not all OSW infrastructure components are within the scope of this transmission study. The Subgroup encouraged us to quantify Community Values using diverse metrices for ecosystem services that will resonate with different groups (e.g., monetary, demographic, infrastructure); see Table 23.

In addition, the Subgroup helped select which ecosystem services to analyze. We have found from our past work, that assessing three to five ecosystem services provides a holistic view of changes in the benefits of ocean and coastal ecosystems that communities care about. This number of services also leads to an accessible and transparent set of results, without generating so much information that it becomes difficult for researchers, decision-makers, and the public to comprehend and use the outputs (Rosenthal et al. 2014; Ruckelshaus et al. 2015; Arkema et al. 2015).

We initially discussed five potential ecosystem services with the Subgroup (i.e., energy resilience, fisheries, coastal risk and resilience, viewsheds, recreation). Given the scope and timeline of the study, and based on previous research, we identified a set of criteria for selecting which three ecosystem services we would quantify. The criteria included model and data availability, the potential for differences among topologies in the ecosystem service, and interest expressed by the Subgroup. The Subgroup helped us narrow the services from five to three by sharing their priorities for assessing 1) energy resilience, 2) fisheries, and 3) coastal risk and resilience. The Subgroup also expressed interest in quantifying viewshed changes due to OSW turbines at sea and port; however, the influence of OSW infrastructure that are not directly related to transmission are not within the scope this study.

Table 23. Feedback from the Community Values Subgroup during the first meeting in April 2024.

Central Themes the Subgroup Emphasized
Participatory processes.
Improving energy access and resilience.
Understanding and balancing benefits and burdens in multiple dimensions/ecosystem services on communities from OSW.
Consider all dimensions of OSW infrastructure together so that benefits and burdens can be assessed more holistically.

Unique considerations by infrastructure type	Example issues the Subgroup raised related to transmission
Underwater cables	Risks to food supply from the operation and maintenance of these cables.
Landing points	Effects on beach going and ecosystems that provide coastal resilience for communities.

8.4 Ongoing Efforts in the Social Ecological Modeling of Ecosystem Services

We are currently conducting social-ecological modeling of three ecosystem services under the 2035 and 2050 scenarios and topologies.

- **Energy Resilience:** Many coastal communities on the West Coast receive electricity via low capacity transmission infrastructure through corridors that shut down power flow when there are wildfire risks. These power outages can have greater impacts on vulnerable communities and populations that have limited access to backup power sources, exacerbating health risks and disrupting essential services such as food storage, heating or cooling, and communication (Do et al. 2023). For West Coast communities, floating OSW has the potential to increase energy resilience and minimize power outages, if paired with technology that can convert the incoming high voltage electricity to low voltages accessible at distribution scales.

- **Fisheries:** West Coast commercial fisheries harvest nearly $1 billion worth of seafood every year (NOAA n.d.-b). These fisheries provide seafood to national and international markets, support local and regional economies, and preserve cultural heritage. We are considering three fishery complexes for the Community Values Assessment: bottom trawl groundfish, pot and trap Dungeness crab, and pole and line highly migratory species (HMS). These fisheries were chosen with input from the Community Values Subgroup and fishery researchers.

- **Coastal risk and resilience:** Increases in coastal development, sea-level rise, and the intensity and frequency of storms are leading to more people and infrastructure at risk from coastal flood and erosion. Shoreline ecosystems, such as wetlands and dunes, can help buffer communities from exposure to hazards by attenuating waves and securing sediments (Bridges et al. 2020). Understanding where coastlines are most exposed to flooding and erosion and where ecosystems help reduce exposure can inform OSW transmission development to protect ecosystems that increase the resilience of energy infrastructure and coastal populations (Arkema et al. 2024; Arkema et al. 2013).

Considering multiple ecosystems services is important for arriving at a more holistic assessment of the benefits and costs of floating OSW transmission for communities. Examining these factors in isolation would provide a fragmented picture of potential influence of transmission alternatives on community values. Instead, by assessing trade-offs among three ecosystem services, we aim to advance understanding of the potential for energy resilience for West Coast communities and critical interventions to foster equitable distribution of benefits and burdens.

9.0 Conclusions

Following a literature review and gaps analysis which accounted for transmission plans by system operators, state energy legislation, federal leasing activity, past research, and state and Biden Administration OSW goals, plausible West Coast OSW generation and transmission topologies corresponding to 2035 and 2050 futures were composed in this study. These designs incorporated West Coast POI capacities, the state of floating OSW technology, and ocean co-use, and they supported the evaluation of six potential pathways for development. Production cost, power system reliability and resiliency, community values, and economic analyses of the topologies yielded the following key findings:

- West Coast OSW transmission was shown to deliver valuable contributions to a reliable, resilient, and cost-effective power supply with lower emissions across the Western Interconnection in 2035 and 2050.
- After considering ocean co-uses and bathymetry, approximately 30 GW of OSW could be hosted in the available sea space off California and southern Oregon within 1,300 meter water depths. This level of OSW generation and transmission can be planned while only considering water depths less than 1,300 meters for cables, turbines, and substations.
- Coordinated OSW transmission holds strong economic value. Six development pathways were evaluated. Significant benefits-cost advantages of pathways leading to the 2050 Interregional and Intraregional Topologies over the 2050 Radial Topology were revealed. Production cost benefits exceeded the costs of offshore transmission development and the costs of onshore system reinforcements to maintain reliability. The main source of the benefits accruing through the 2050 topologies was the use of the transmission to share lower-cost generation across regions. The best net benefit pathway observed was the 2035 Distributed Topology to 2050 Interregional Topology, which delivered $25B (2024$) in net present value over the 2050 Radial Topology.
- Near term, 2035 Concentrated and Distributed topologies show similar system-wide benefits through alternate cost structures. With more POIs, the distributed approach requires higher ocean-side costs, while the larger power injections of the Concentrated Topology necessitate more significant onshore reliability reinforcements. The Distributed Topology may provide a more resilient bulk system by harnessing greater geographic variability of the OSW resource over the Concentrated Topology. If net benefits can be preserved for coastal communities, there may also be advantages to distributed interconnections in 2035 to yield greater coastal community benefits without degrading 2050 future benefits.
- Large geographic differences in benefits were observed between 2050 topologies, which were traced to differences of where congestion was experienced. If the pace of transmission development is not consistent across the West Coast, unintended cost penalties may be imposed. Transmission planners could account for this disaggregation of benefits in the planning process, including outside of their region.
- Though dispatch was unchanged, the production cost advantage of coordinated OSW transmission was significantly reduced as dispatchable hydrogen turbine power became cheaper in 2050, suggesting that coordinated variable generation and transmission fills a similar role to dispatchable generation.
- Greater use of the OSW transmission network was observed when onshore transmission was de-rated, suggesting that OSW transmission may provide additional value if future buildout of the onshore bulk transmission system is slowed due to permitting, wildfire, or other development risk.

- Though the capacity contribution of West Coast OSW was shown to be robust, the capacity value isolated to offshore transmission was dependent on the amount of onshore transmission and generation. Given the 2050 topologies of this study, offshore transmission networks were not shown to provide capacity value on the West Coast. This is due to significant onshore transmission and distributed generation capacity to yield 100% clean electricity by 2045 and to meet growing energy demand through 2050.
- Significant costs of new transmission infrastructure, including conductors, substations, capacitors, and transformers, needed to ensure reliability, were estimated in all topology sets. These costs were shown to be cheaper than the increased production cost associated with redispatching generation and transmission around contingencies.
- Commercial floating wind transmission is both a challenge and an opportunity. The industry is currently in early stages, but offshore wind has the potential to help nearby states achieve renewable energy goals. Key technology hurdles related to export cables, floating substations, floating HVDC equipment, and operations and maintenance exist.

Drawing from these findings, the study team considered the phasing of the least-cost pathways examined in this work, one of which is presented in Figure 69. Starting from the 2035 Concentrated Topology Set, additional generation and transmission assets are included in 2040 and 2045 until the 2050 Interregional Topology Set is reached. More favorable projects as a function of wind resource and transmission cost are developed earlier in this phasing and interlinks are made as soon as possible. MTDC networks do not present until 2040.

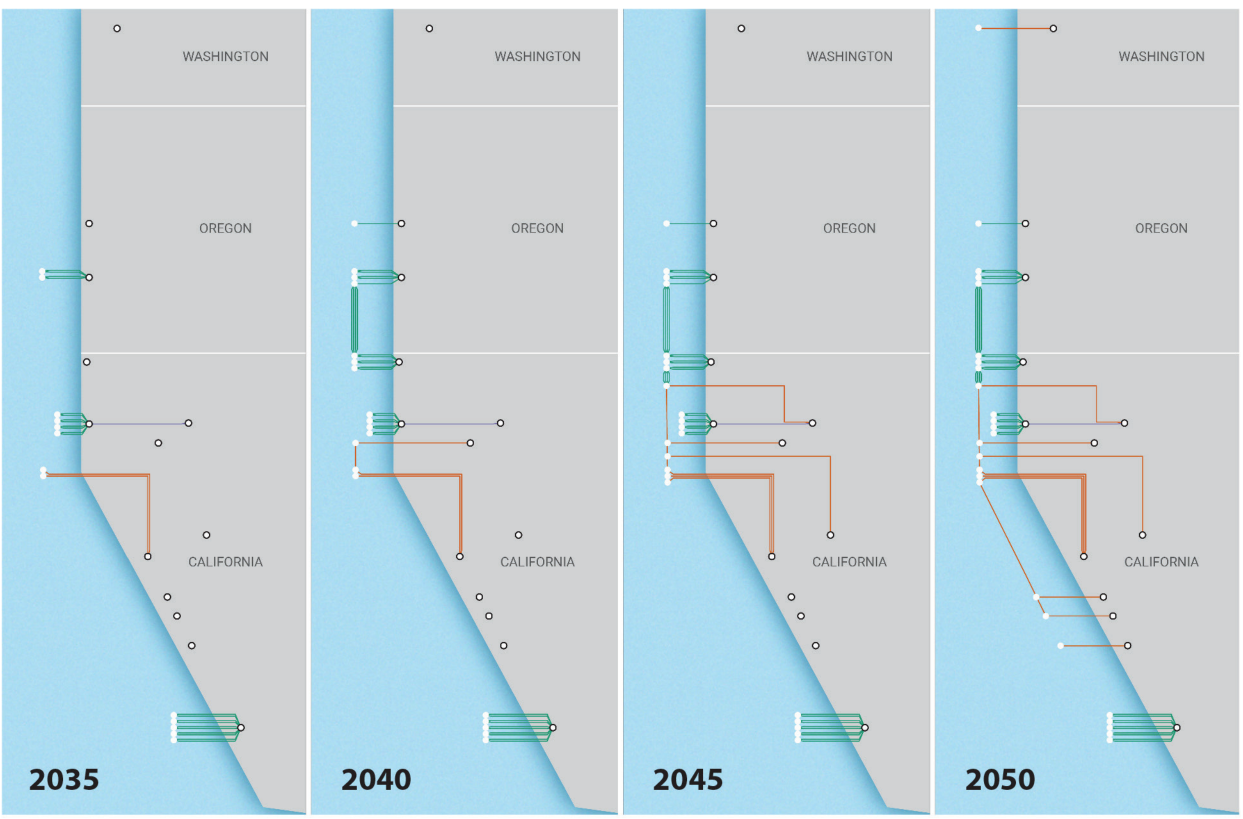

Figure 69. Phased transition from 2035 Concentrated to 2050 Interregional Topology Sets. Orange lines are assumed to be HVDC; green lines are alternating current.

Future work lies in resolving optimum investments for reliability through a combination of system reinforcements and alternate dispatch of the power system to address critical contingencies. Additionally, ongoing community values analyses could be incorporated in the further refinement of all topology sets. Though hydrogen combustion turbines provided a critical dispatchable generation source in 2050, endogenous hydrogen production was not considered in the capacity expansion analysis of this work. Doing so would drive greater renewable energy deployments which should be considered in the context of OSW transmission. Similarly, more detailed consideration of data center load growth and multi-sector emissions reduction could be incorporated in future work. Lastly, the interregional backbone build assumed in this study was sized for the purpose of delivering OSW energy. If the alternative to onshore transmission in the West is compelling to system planners, additional work could consider larger offshore transmission designs from a multi-value perspective, within the context of future load growth, diversified clean energy supply, and emerging resilience threats.

10.0 References

Allianz Commercial. 2023. *A turning point for offshore wind: Global opportunities and risk trends.* https://www.allianz.com/content/dam/onemarketing/azcom/Allianz_com/press/document/Allianz-Commercial_A-turning-point-for-offshore-wind.pdf.

American Clean Power. 2023. *Offshore Wind Vessel Needs.* American Clean Power. https://cleanpower.org/wp-content/uploads/2021/09/OffshoreWind_Vessel_Needs_230104.pdf.

Arkema, K. K., G. Guannel, G. Verutes, S. A. Wood, A. Guerry, M. Ruckelshaus, P. Kareiva, M. Lacayo, and J. M. Silver. 2013. "Coastal habitats shield people and property from sea-level rise and storms." *Nature Climate Change* 3 (10): 913-918. https://doi.org/10.1038/nclimate1944.

Arkema, K. K., Gregory M. Verutes, Spencer A. Wood, Chantalle Clarke-Samuels, Samir Rosado, Maritza Canto, Amy Rosenthal, and et al. 2015. "Embedding Ecosystem Services in Coastal Planning Leads to Better Outcomes for People and Nature." In *Proceedings of the National Academy of Sciences* 112 (24): 7390–95. https://doi.org/https://doi.org/10.1073/pnas.1406483112.

Arkema, K. K., S. K. Cunningham, J. M. S. Delevaux, B. G. Celina, S. Klain, J. B. Lamb, L. K. Nelson, S. Scyphers, H. Stewart, and A. Sutton-Grier. 2024. "Beneficiaries, Equity, and Trade-Offs in Estuarine and Coastal Ecosystem Services." In *Treatise on Estuarine and Coastal Science (Second Edition)*, 208-237. https://doi.org/10.1016/b978-0-323-90798-9.00106-2.

ATSDR. 2022. "CDC SVI Documentation 2020." Agency for Toxic Substances and Disease Registry. https://www.atsdr.cdc.gov/placeandhealth/svi/documentation/SVI_documentation_2020.html.

Beiter, P., W. Musial, P. Duffy, A. Cooperman, M. Shields, D. Heimiller, and M. Optis. 2020a. *The Cost of Floating Offshore Wind Energy in California Between 2019 and 2032 (Technical Report NREL/TP-5000-77384).* National Renewable Energy Laboratory (NREL). https://doi.org/10.2172/1710181.

Bistline, J., G. Blanford, M. Brown, D. Burtraw, M. Domeshek, J. Farbes, A. Fawcett, A. Hamilton, J. Jenkins, R. Jones, B. King, H. Kolus, J. Larsen, A. Levin, M. Mahajan, C. Marcy, E. Mayfield, J. McFarland, H. McJeon, R. Orvis, N. Patankar, K. Rennert, C. Roney, N. Roy, G. Schivley, D. Steinberg, N. Victor, S. Wenzel, J. Weyant, R. Wiser, M. Yuan, and A. Zhao. 2023. "Emissions and energy impacts of the Inflation Reduction Act." *Science* 380 (6652): 1324-1327. https://doi.org/10.1126/science.adg3781. PMCID: PMC10336889.

BOEM, 2022, "Biden-Harris Administration Announces Winners of California Offshore Wind Energy Auction," https://www.doi.gov/pressreleases/biden-harris-administration-announces-winners-california-offshore-wind-energy-auction.

BOEM. 2024a. *Renewable Energy GIS Data [Renewable Energy Leases and Planning Areas].* Bureau of Ocean Energy Management, . https://www.boem.gov/renewable-energy/mapping-and-data/renewable-energy-gis-data.

BOEM. 2024b. "BOEM Postpones Oregon Offshore Wind Energy Auction." U.S. Department of the Interior. https://www.boem.gov/newsroom/press-releases/boem-postpones-oregon-offshore-wind-energy-auction.

BOEM. n.d. "Marine Cadastre: Your trusted source for ocean geospatial data." https://hub.marinecadastre.gov/.

Bridges, T. S., J. K. King, J. D. Simm, M. W. Beck, G. Collins, Q. Lodder, and K. Mohan. 2020. *International Guidelines on Natural and Nature-Based Features for Flood Risk Management Executive Summary*.

Brinkman, G., Mike Bannister, Sophie Bredenkamp, Lanaia Carveth, Dave Corbus, Rebecca Green, Luke Lavin, Anthony Lopez, Melinda Marquis, Joseph Mowers, Matthew Mowers, Leonardo Rese, Billy Roberts, Amy Rose, Shahil Shah, Pranav Sharma, Hongfei Sun, Bin Wang, Bharat Vyakaranam, Zhenyu (Henry) Huang, Kevin Harris, Chuan Qin, Nader Samaan, Marcelo Elizondo, Tony Nguyen, Quan Nguyen, Krishan P Guddanti, Patrick Royer, Fernando Bereta dos Reis, Shahnawaz Siddiqui, Sameer Nekkalapu, and Michael Abdelmalak. 2024. *Atlantic Offshore Wind Transmission Study.* Golden, CO: N. R. E. Laboratory. https://www.nrel.gov/docs/fy24osti/88003.pdf.

British Oceanographic Data Centre. 2024. “Gridded Bathymetry Data.” General Bathymetric Chart of the Oceans. https://www.gebco.net/data_and_products/gridded_bathymetry_data/.

Brown, P., Clayton Barrows, Jarrad Wright, Gregory Brinkman, Sourabh Dalvi, Jiazi Zhang, and T. Mai. 2023. “A general method for estimating zonal transmission interface limits from nodal network data.” *Electrical Engineering and Systems Science, Systems and Control*. https://doi.org/https://doi.org/10.48550/arXiv.2308.03612.

Burleyson, C., Travis Thurber, and C. Vernon. 2023a. “Projections of Hourly Meteorology by Balancing Authority Based on the IM3/HyperFACETS Thermodynamic Global Warming (TGW) Simulations.” https://doi.org/https://doi.org/10.57931/1960530.

Burleyson, C., Travis Thurber, and Chris Vernon. 2023b. “Projections of Hourly Meteorology by County Based on the IM3/HyperFACETS Thermodynamic Global Warming (TGW) Simulations.” https://data.msdlive.org/records/g4kct-fhy96.

BVG Associates. 2023. Guide to a Floating Offshore Wind Farm. https://guidetofloatingoffshorewind.com/wp-content/uploads/2023/10/BVGA-16444-Floating-Guide-r2.pdf.

CAISO. 2017. *Transmission Economic Assessment Methodology (TEAM).* California ISO. https://www.caiso.com/Documents/TransmissionEconomicAssessmentMethodology-Nov2_2017.pdf.

CAISO. 2024. *Transmission Plan.* https://www.caiso.com/documents/iso-board-approved-2023-2024-transmission-plan.pdf.

Chalishazar, V. H., J. Westman, J. Deines, S. Datta, J. Tagestad, A. Coleman, E. Barrett, M. Hoffman, A. Somani, and J. G. Schaad. 2023. “Wildfire Risk Evaluation Framework for Grid Operations and Planning.” 2023 IEEE Power & Energy Society General Meeting (PESGM). https://doi.org/10.1109/pesgm52003.2023.10252841.

Chen, T.-C., M. Ramesh, C. Qin, B. Vyakaranam, Z. Hou, T. C. Douville, and N. A. Samaan. 2024. “Smart Sampling of Representative Hourly Power Generation Scenario With High Renewable Penetration.” *IEEE Access* 12: 115319-115328. https://doi.org/10.1109/access.2024.3445409.

Ciara, E., T. Garcia, C. Ortega, and L. Richmond. 2020. “Social Impacts to Other Communities that Experienced Offshore Wind.” In *California North Coast Offshore Wind Studies*, edited by Z. A. M. Severy, G. Chapman, M. Cheli, T. Garcia, C. Ortega, N. Salas, A. Younes, J. Zoellick, & A. Jacobson. Humboldt, CA: Schatz Energy Research Center.

Connolly, P., and M. Hall. 2019. “Comparison of pilot-scale floating offshore wind farms with shared moorings.” *Ocean Engineering* 171: 172–180. https://doi.org/10.1016/j.oceaneng.2018.08.040.

Corewind. 2021. *D4.2: Floating wind O&M strategies assessment.* C. Ramboll, Equinor, Esteyco, Fihac.

Crowle, A. P., and P. R. Thies. 2022. “Floating offshore wind turbines port requirements for construction.” *Journal of Engineering for the Maritime Environment* 236 (4): 1047-1056.

Datta, S., V. H. Chalishazar, J. Westman, T. Saltiel, J. Deines, S. A. Siddiqui, K. A. Tamaddun, S. E. Barrows, A. R. Fernandez, A. Coleman, J. Tagestad, and A. Somani. 2024. "Enhancing Grid Resilience during Wildfires in Socioeconomic Vulnerable Regions using Powered and Non-Powered Hydro Dams." 2024 IEEE Power & Energy Society General Meeting (PESGM). https://doi.org/10.1109/pesgm51994.2024.10688862.

DNV. 2022. *Maine OSW DNV Offshore Wind Transmission Technical Review Final Report (Report to the Maine Governor's Energy Office and Maine Offshore Wind Roadmap).* https://www.maine.gov/energy/sites/maine.gov.energy/files/inline-files/Maine%20OSW%20DNV%20Offshore%20Wind%20Transmission%20Technical%20Review%20Final%20Report.pdf.

DNV. n.d. "Floating Substations Joint Industry Project - Phase 1." https://www.maine.gov/energy/sites/maine.gov.energy/files/inline-files/Maine%20OSW%20DNV%20Offshore%20Wind%20Transmission%20Technical%20Review%20Final%20Report.pdf.

Do, V., H. McBrien, N. M. Flores, A. J. Northrop, J. Schlegelmilch, M. V. Kiang, and J. A. Casey. 2023. "Spatiotemporal distribution of power outages with climate events and social vulnerability in the USA." *Nat Commun* 14 (1): 2470. https://doi.org/10.1038/s41467-023-38084-6. PMCID: PMC10147900.

Doorman, G. L., and D. M. Frøystad. 2013. "The economic impacts of a submarine HVDC interconnection between Norway and Great Britain." *Energy Policy* 60: 334-344. https://doi.org/10.1016/j.enpol.2013.05.041.

Douville, T., M. Severy, J. Eisdorfer, L. He, and B. Pamintuan. 2023. *West Coast Offshore Wind Transmission Literature Review and Gaps Analysis.* U.S. Department of Energy, Office of Energy Efficiency & Renewable Energy. https://www.pnnl.gov/sites/default/files/media/file/West_Coast_OSW_Tx_Literature_Review__PNNL_WETO_021623_0.pdf.

Douville, T. C., and D. Bhatnagar. 2021. "Exploring the Grid Value of Offshore Wind Energy in Oregon." *Energies* 14 (15). https://doi.org/10.3390/en14154435.

Douville, T. C., S. Zhou, J. Zhu, and M. Severy. 2024. "Capacity contributions of Southern Oregon offshore wind to the Pacific Northwest and California." *The Electricity Journal* 37 (4-5). https://doi.org/10.1016/j.tej.2024.107407.

Draxl, C., Walt Musical, George Scott, and Caleb Phillips. 2017. *WIND Toolkit Offshore Summary Dataset.* Golden, CO: N. R. E. Laboratory. https://doi.org/10.7799/1375460.

Freeman, J., and J. Jorgenson. 2014. *Reference Manual for the System Advisor Model's Wind Power Performance Model.* National Renewable Energy Laboratory NREL/TP-6A20-60570. https://www.nrel.gov/docs/fy14osti/60570.pdf.

Gagnon, P., An Pham, Wesley Cole, and et al. 2024. *2023 Standard Scenarios Report: A U.S. Electricity Sector Outlook.* NREL/TP-6A40-87724. Golden, CO: N. R. E. Laboratory.

Geospatial Management Office. n.d. "HIFLD Open." https://hifld-geoplatform.hub.arcgis.com/pages/hifld-open.

Gillingham, K., and P. Huang. 2021. *Racial Disparities in the Health Effects from Air Pollution: Evidence from Ports (Working Paper 29108).* National Bureau of Economic Research. https://doi.org/10.3386/w29108.

Goldschmidt, M., and M. Muskulus. 2015. "Coupled Mooring Systems for Floating Wind Farms." *Energy Procedia* 80: 255–262. https://doi.org/10.1016/j.egypro.2015.11.429.

Green, R., Suzanne MacDonald, Rebecca Fuchs, and Matthew Hall. 2023. *Social Acceptance of a Reduced-Footprint Synthetic Mooring System for Floating Offshore Wind Turbines in the Gulf of Maine.* Golden, CO: N. R. E. L. (NREL). https://doi.org/10.2172/1974199.

Greenberg, M. R. 2021. "Ports and Environmental Justice in the United States: An Exploratory Statistical Analysis." *Risk Anal* 41 (11): 2112–2126. https://doi.org/10.1111/risa.13697.

Guerry, A., Mark Plummer, Mary Ruceklshaus, and C. Harvey. 2011. "Ecosystem Service Assessment for Marine Conservation." In *Natural Capital: Theory and Practice of Mapping Ecosystem Services*. Oxford University Press.

Guerry, A. D., Stephen Polasky, Jane Lubchenco, Rebecca Chaplin-Kramer, and Daily Gretchen. 2015. "Natural Capital and Ecosystem Services Informing Decisions: From Promise to Practice." In *Proceedings of the National Academy of Sciences* 112 (24): 7348–55.

Haley, B., R. A. Jones, J. H. Williams, G. Kwok, J. Farbes, D. Bentz, G. Schivley, and J. Jenkins. 2023. "Annual Decarbonization Perspective: Carbon Neutral Pathways for the United States 2023." *Evolved Energy Research, 2023*.

Hall, M., E. Lozon, S. Housner, and S. Sirnivas. 2022. "Design and analysis of a ten-turbine floating wind farm with shared mooring lines." *Journal of Physics: Conference Series* 2362 (1). https://doi.org/10.1088/1742-6596/2362/1/012016.

Harris, P. T., M. Macmillan-Lawler, J. Rupp, and E. K. Baker. 2014. "Geomorphology of the oceans." *Marine Geology* 352: 4-24. https://doi.org/10.1016/j.margeo.2014.01.011.

Hart, E., and A. Mileva. 2022. *Advancing resource adequacy analysis with the GridPath RA Toolkit: A case study of the Western US.* GridLab. https://gridlab.org/%20publications/.

Hitachi Energy. 2024. "GridView." Hitachi Energy. Accessed June 14, 2024. https://www.hitachienergy.com/products-and-solutions/energy-portfolio-management/enterprise/gridview.

Ho, J., Jonathon Becker, Maxwell Brown, Patrick Brown, Ilya Chernyakhovskiy, Stuart Cohen, Wesley Cole, Kelly Eurek, Will Frazier, Pieter Gagnon, Nathaniel Gates, Daniel Greer, Paige Jadun, Saroj Khanal, Scott Machen, Madeline Macmillan, Trieu Mai, Matthew Mowers, Caitlin Murphy, Amy Rose, Anna Schleifer, Brian Sergi, Daniel Steinberg, Yinong Sun, and E. Zhou. 2021. *Regional Energy Deployment System (ReEDS) Model Documentation: Version 2020.* NREL/TP-6A20-78195. Golden, CO: N. R. E. Laboratory. https://www.nrel.gov/docs/fy21osti/78195.pdf.

Hogan, W. W. 2018. "A Primer on Transmission Benefits and Cost Allocation." *Economics of Energy & Environmental Policy* 7 (1): 25-46. https://doi.org/https://www.jstor.org/stable/27030612.

81st Oregon Legislative Assembly. 2021. *House Bill 3375*. HB 3375-A.

Huang, C., Lily Busse, and Robert Baker. 2023. *Offshore Wind Transmission Technologies Assessment: Overview of Existing and Emerging Transmission Technologies.* Prepared for: California Energy Commission Guidehouse. https://efiling.energy.ca.gov/GetDocument.aspx?tn=250520.

ISO New England Inc. 2019. *Transmission Planning Technical Guide, Rev 5.0.* https://www.iso-ne.com/static-assets/documents/2019/10/transmission_plannings_techincal_guide_rev5.pdf.

ISO Staff. 2024. "Offshore wind big part of ISO's 2023-2024 Transmission Plan." California ISO. https://www.caiso.com/about/news/offshore-wind-big-part-of-isos-2023-2024-transmission-plan.

Jensen, J., K. Bolton, and D. Simons. 2020. *Changes to System Inertia with High Renewable Implementation Assessment.* WECC. https://www.wecc.org/sites/default/files/documents/meeting/2024/2019%20System%20Inertia%20with%20High%20Renewable%20Assessment%20Report.pdf.

Jones, A. D., D. Rastogi, P. Vahmani, A. M. Stansfield, K. A. Reed, T. Thurber, P. A. Ullrich, and J. S. Rice. 2023. "Continental United States climate projections based on thermodynamic modification of historical weather." *Sci Data* 10 (1): 664. https://doi.org/10.1038/s41597-023-02485-5. PMCID: PMC10539322.

Jorgenson, J., S. Awara, G. Stephen, and T. Mai. 2021. “A systematic evaluation of wind's capacity credit in the Western United States.” *Wind Energy* 24 (10): 1107-1121. https://doi.org/10.1002/we.2620.

Joskow, P., and J. Tirole. 2005. “Merchant Transmission Investment*.” *Journal of Industrial Economics* 53 (2): 233-264. https://doi.org/10.1111/j.0022-1821.2005.00253.x.

Kareiva, P., Heather Tallis, Taylor Ricketts, Gretchen Daily, and Stephen Polasky. 2011. *Natural Capital: Theory and Practice of Mapping Ecosystem Services*. Oxford University Press.

Kieper, T., S. Datta, A. Campbell, and A. Somani. In Press. “The contribution of hydropower and long-duration energy storage to grid resilience during extreme weather and electricity market scarcity events.” IEEE PES General Meeting, 2025.

Kristiansen, M., F. D. Muñoz, S. Oren, and M. Korpås. 2018. “A Mechanism for Allocating Benefits and Costs from Transmission Interconnections under Cooperation: A Case Study of the North Sea Offshore Grid.” *The Energy Journal* 39 (6): 209-234. https://doi.org/10.5547/01956574.39.6.mkri.

LBNL. 2024. “Renewables Portfolio Standards Resources.” Lawrence Berkeley National Laboratory. https://emp.lbl.gov/projects/renewables-portfolio/.

Leite da Silva, A. M., L. A. d. F. Manso, W. d. S. Sales, S. A. Flavio, G. J. Anders, and L. C. de Resende. 2012. “Chronological Power Flow for Planning Transmission Systems Considering Intermittent Sources.” *IEEE Transactions on Power Systems* 27 (4): 2314-2322. https://doi.org/10.1109/tpwrs.2012.2203830.

Leonard, J. L., and P. Watson. 2011. Description of the input-output model for Pacific Coast fisheries. NOAA Technical Memorandum NMFS-NWFSC-111. National Oceanic and Atmospheric Administration. https://repository.library.noaa.gov/view/noaa/8718.

Lester, S. E., K. L. McLeod, H. Tallis, M. Ruckelshaus, B. S. Halpern, P. S. Levin, F. P. Chavez, C. Pomeroy, B. J. McCay, C. Costello, S. D. Gaines, A. J. Mace, J. A. Barth, D. L. Fluharty, and J. K. Parrish. 2010. “Science in support of ecosystem-based management for the US West Coast and beyond.” *Biological Conservation* 143 (3): 576-587. https://doi.org/10.1016/j.biocon.2009.11.021.

Lester, S. E., C. Costello, B. S. Halpern, S. D. Gaines, C. White, and J. A. Barth. 2013. “Evaluating tradeoffs among ecosystem services to inform marine spatial planning.” *Marine Policy* 38: 80-89. https://doi.org/10.1016/j.marpol.2012.05.022.

Lim, J., and M. Trowbridge. 2023. *California Floating Offshore Wind Regional Ports Feasibility Analysis.* U.S. Department of Interior, Bureau of Ocean Energy Management Report No.: OCS Study BOEM 2023-038; Contract No.: 140M0121D008. Oakland, CA: Moffat & Nichol. https://www.boem.gov/sites/default/files/documents/regions/pacific-ocs-region/BOEM-2023-038.pdf.

Lopez, A., P. Pinchuk, M. Gleason, W. Cole, T. Mai, T. Williams, O. Roberts, M. Rivers, M. Bannister, S.-M. Thomson, G. Zuckerman, and B. Sergi. 2023. *Solar Photovoltaics and Land-Based Wind Technical Potential and Supply Curves for the Contiguous United States: 2023 Edition.* National Renewable Energy Laboratory NREL/TP-6A20-87843.

Lopez, A., G. R. Zuckerman, P. Pinchuk, M. Gleason, M. Rivers, S.-M. Thomson, D. Heimiller, O. Roberts, T. Williams, W. Cole, and T. Mai. In Press. *Renewable Energy Technical Potential and Supply Curves for the Contiguous United States: 2024 Edition.* Golden, CO: National Energy Renewable Energy Laboratory.

Maclaurin, G., Nick Grue, Anthony Lopez, Donna Heimiller, Michael Rossol, Grant Buster, and Travis Williams. 2019. *The Renewable Energy Potential (reV) Model: A Geospatial Platform for Technical Potential and Supply Curve Modeling.* NREL/TP-6A20-73067. Golden, CO: N. R. E. Laboratory. https://www.nrel.gov/docs/fy19osti/73067.pdf.

Maclaurin, G., Nick Grue, Anthony Lopez, Donna Heimiller, Michael Rossol, Grant Buster, and T. Williams. 2021. *The Renewable Energy Potential (reV) Model: A Geospatial Platform* *for Technical Potential and Supply Curve Modeling.* NREL/TP-6A20-73067. Golden, CO: N. R. E. Laboratory. https://www.nrel.gov/docs/fy19osti/73067.pdf.

Mandle, L., Zhiyun Ouyang, James Salzman, and Gretchen C Daily. 2019. *Green Growth That Works: Natural Capital Policy and Finance Mechanisms Around the World.* Washington, D.C.: I. Press.

Mankiw, G. N. 2024. *Principles of Microeconomics. 10th Edition*. https://faculty.cengage.com/titles/9780357722862.

Mas-Colell, A., Michael D. Whinston, and Jerry R. Green. 1995. *Microeconomic Theory*. https://global.oup.com/academic/product/microeconomic-theory-9780195073409?cc=us&lang=en&.

Maxwell, S. M., F. Kershaw, C. C. Locke, M. G. Conners, C. Dawson, S. Aylesworth, R. Loomis, and A. F. Johnson. 2022. "Potential impacts of floating wind turbine technology for marine species and habitats." *J Environ Manage* 307: 114577. https://doi.org/10.1016/j.jenvman.2022.114577.

McGrath, C. R., C. D. Burleyson, Z. Khan, A. Rahman, T. Thurber, C. R. Vernon, N. Voisin, and J. S. Rice. 2022. "tell: a Python package to model future total electricity loads in the United States." *Journal of Open Source Software* 7 (79). https://doi.org/10.21105/joss.04472.

National Marine Fisheries Service. 2021. *Fisheries of the United States, 2019 Report.* U.S. Department of Commerce, NOAA.

NCEP. 2004. *Electricity Transmission: A Primer.* N. C. o. E. Policy. https://www.energy.gov/oe/articles/electricity-transmission-primer.

NERC. n.d. *Generator Frequency and Voltage Protective Relay Settings.* Standard PRC-024-1. Atlanta, Georgia: North American Electric Reliability Corporation.

NOAA. 2016. *Wrecks and Obstructions Database. NOAA Office of Coast Survey.* National Oceanic and Atmospheric Administration. https://www.nauticalcharts.noaa.gov/data/wrecks-and-obstructions.html.

NOAA. 2017. *National Shoreline Environmental Sensitivity Index (ESI) Data [National Shoreline].* NOAA Office of Response and Restoration. https://response.restoration.noaa.gov/sites/default/files/esimaps/gisdata/NationalESI_Shoreline.zip.

NOAA. 2023a. "The MPA Inventory." NOAA National Marine Protected Areas Center. https://marineprotectedareas.noaa.gov/dataanalysis/mpainventory/.

NOAA. 2023b. "U.S. Marine Waters Boundaries [Coastal Waters (State and Territorial)]." NOAA ArcGIS Hub. National Oceanic and Atmospheric Administration. https://noaa.hub.arcgis.com/datasets/noaa::us-marine-waters-boundaries/about?layer=0.

NOAA. n.d.-a. US West Coast Seafloor Induration (Version 4.0) [Map service]. NOAA Northwest Fisheries Science Center. https://www.webapps.nwfsc.noaa.gov/server7/rest/services/FRAM/USWestCoast_SeafloorInduration_v4_0/MapServer.

NOAA. n.d.-b. "West Coast." National Oceanic and Atmospheric Administration. https://www.fisheries.noaa.gov/region/west-coast.

NREL. 2023. *2023 Annual Technology Baseline.* National Renewable Energy Laboratory. https://atb.nrel.gov/electricity/2023/index.

NREL. 2024. "2024 Annual Technology Baseline." National Renewable Energy Laboratory. https://atb.nrel.gov/.

Office for Coastal Management. 2024. "Artificial Reefs from 2010-06-15 to 2010-08-15." NOAA National Centers for Environmental Information. https://www.fisheries.noaa.gov/inport/item/54191.

Oikonomou, K., Bharat Vyakaranam, Tony B Nguyen, Kevin Harris, Eran Schweitzer, Nader Samaan, Chuan Qin, Fernando Bereta dos Reis, Michael M Abdelmalak, Michael Kintner-Meyer, and Jeff Dagle. 2024. *Western Interconnection Baseline Study.* PNNL-36452. https://www.pnnl.gov/main/publications/external/technical_reports/PNNL-36452.pdf.

Ojo, A., M. Collu, and A. Coraddu. 2022. "Multidisciplinary design analysis and optimization of floating offshore wind turbine substructures: A review." *Ocean Engineering* 266. https://doi.org/10.1016/j.oceaneng.2022.112727.

Okpokparoro, S., and S. Sriramula. 2023. "Reliability analysis of floating wind turbine dynamic cables under realistic environmental loads." *Ocean Engineering* 278. https://doi.org/10.1016/j.oceaneng.2023.114594.

Oregon.gov. 2024. "Oregon Offshore Wind Energy Roadmap." Oregon Coastal Management Program, Department of Land Conservation and Development. https://www.oregon.gov/lcd/ocmp/pages/offshore-wind-roadmap.aspx.

Pandian, S. 2024. "K-Fold Cross Validation Technique and its Essentials." Analytics Vidhya. https://www.analyticsvidhya.com/blog/2022/02/k-fold-cross-validation-technique-and-its-essentials/.

Park, H.-S., Byung Ho Choi, Jung Joong Kim, and T.-H. Lee. 2016. "Seismic performance evaluation of high voltage transmission towers in South Korea." *KSCE Journal of Civil Engineering* 20: 2499–2505. https://doi.org/https://doi.org/10.1007/s12205-015-0723-3

Picchi, P., M. van Lierop, D. Geneletti, and S. Stremke. 2019. "Advancing the relationship between renewable energy and ecosystem services for landscape planning and design: A literature review." *Ecosystem Services* 35: 241-259. https://doi.org/10.1016/j.ecoser.2018.12.010.

Prochaska, J. D., A. B. Nolen, H. Kelley, K. Sexton, S. H. Linder, and J. Sullivan. 2014. "Social Determinants of Health in Environmental Justice Communities: Examining Cumulative Risk in Terms of Environmental Exposures and Social Determinants of Health." *Hum Ecol Risk Assess* 20 (4): 980-994. https://doi.org/10.1080/10807039.2013.805957. PMCID: PMC3995452.

Prysmian. 2024. "Record breaking submarine cable installation at 2,150 m water depth: Prysmian successfully completes the sea trial tests for a 500 kv HVDC submarine cable in ultra-deep waters." https://www.prysmian.com/en/media/press-releases/record-breaking-submarine-cable-installation-at-2-150-m-water-depth.

Robertson, A., and J. Jonkman. n.d. Loads Analysis of Several Offshore Floating Wind Turbine Concepts.

Rosenthal, A., G. Verutes, E. McKenzie, K. K. Arkema, N. Bhagabati, L. L. Bremer, N. Olwero, and A. L. Vogl. 2014. "Process matters: a framework for conducting decision-relevant assessments of ecosystem services." *International Journal of Biodiversity Science, Ecosystem Services & Management* 11 (3): 190-204. https://doi.org/10.1080/21513732.2014.966149.

Rossol, M., Paul Pinchuk, Grant Buster, Robert Spencer, Brandon N. Benton, Travis Williams, and Mike Gleason. 2024. NREL/reVX: Layered HDF5 updates. Zenodo. https://doi.org/https://doi.org/10.5281/zenodo.13830866.

Roth, S. 2021. "How an Oregon wildfire almost derailed California's power grid." Los Angeles Times. https://www.latimes.com/business/story/2021-07-12/california-flex-alert-power-grid-heat-wildfire.

Ruckelshaus, M., E. McKenzie, H. Tallis, A. Guerry, G. Daily, P. Kareiva, S. Polasky, T. Ricketts, N. Bhagabati, S. A. Wood, and J. Bernhardt. 2015. "Notes from the field: Lessons learned from using ecosystem service approaches to inform real-world decisions." *Ecological Economics* 115: 11-21. https://doi.org/10.1016/j.ecolecon.2013.07.009.

Samaan, N. A., J. E. Dagle, Y. V. Makarov, R. Diao, M. R. Vallem, T. B. Nguyen, L. E. Miller, B. Vyakaranam, S. Wang, F. K. Tuffner, and M. A. Pai. 2015. *Dynamic Contingency Analysis Tool - Phase 1.* PNNL-24843. Richland, WA: Pacific Northwest National Laboratory. https://www.energy.gov/sites/default/files/2024-10/NationalTransmissionPlanningStudy-Chapter4.pdf.

Samhouri, J. F., B. E. Feist, M. Jacox, O. R. Liu, K. Richerson, E. Steiner, J. Wallace, K. Andrews, L. Barnett, A. Beaudreau, H.,, L. Bellquist, M. P. Buil, M. A. Haltuch, A. Harley, C. J. Harvey, I. C. Kaplan, K. Norman, A. Phillips, L. K. Rasmuson, E. J. Ward, C. Whitmire, and R. L. Selden. 2024. “Stay or go? Geographic variation in risks due to climate change for fishing fleets that adapt in-place or adapt on-the-move.” *Plos Climate*. https://doi.org/https://journals.plos.org/climate/article?id=10.1371/journal.pclm.0000285

Schaber, K., F. Steinke, and T. Hamacher. 2012. “Transmission grid extensions for the integration of variable renewable energies in Europe: Who benefits where?” *Energy Policy* 43: 123-135. https://doi.org/10.1016/j.enpol.2011.12.040.

Schlosser, W. E. 2012. *Usual and Accustomed Fishing Areas: Pacific Ocean Fishing Areas, Extent Determination.* http://resource-analysis.com/wp-content/uploads/2018/10/Usual-and-Accustomed-Fishing-Areas_20121022.pdf.

Sengupta, M., Y. Xie, A. Lopez, A. Habte, G. Maclaurin, and J. Shelby. 2018. “The National Solar Radiation Data Base (NSRDB).” *Renewable and Sustainable Energy Reviews* 89: 51-60. https://doi.org/10.1016/j.rser.2018.03.003.

Sharma, P., L. Rese, B. Wang, B. Vyakaranam, and S. Shah. 2023. “Grid Strength Analysis for Integrating 30 GW of Offshore Wind Generation by 2030 in the U.S. Eastern Interconnection: Preprint. .” 22nd Wind and Solar Integration Worksho, Copenhagen, Denmark. https://www.nrel.gov/docs/fy24osti/87392.pdf.

Shields, M., Jeremy Stefek, Frank Oteri, Matilda Kreider, Elizabeth Gill, Sabrina Maniak, Ross Gould, Courtney Malvik, Sam Tirone, and Eric Hines. 2023a. *A Suppy Chain Road Map for Offshore Wind Energy in the United States.* National Renewable Energy Laboratory. Technical Report NREL/TP-5000-84710. https://doi.org/10.2172/2005543. https://www.nrel.gov/docs/fy23osti/84710.pdf.

Shields, M., J. Stefek, F. Oteri, M. Kreider, E. Gill, S. Maniak, R. Gould, C. Malvik, S. Tirone, and E. Hines. 2023b. *The Impacts of Developing a Port Network for Floating Offshore Wind Energy on the West Coast of the United States.* https://www.nrel.gov/docs/fy23osti/84710.pdf.

Stehly, T., P. Duffy, and D. M. Hernando. 2023. *2022 Cost of Wind Energy Review.* National Renewable Energy Laboratory. https://www.nrel.gov/docs/fy24osti/88335.pdf.

Sun, Y., and Wesley Cole. 2017. *Transmission Flow Methodologies: Approximate DC Flow vs Pipe Flow along AC Lines.* NREL/PR-6A20-68929. Golden, CO: N. R. E. Laboratory.

Turner, S. W. D., N. Voisin, and K. Nelson. 2022. “Revised monthly energy generation estimates for 1,500 hydroelectric power plants in the United States.” *Sci Data* 9 (1): 675. https://doi.org/10.1038/s41597-022-01748-x. PMCID: PMC9636176.

Tyler, G., D. Bidwell, T. Smythe, and S. Trandafir. 2021. “Preferences for community benefits for offshore wind development projects: A case study of the Outer Banks of North Carolina, U.S.” *Journal of Environmental Policy & Planning* 24 (1): 39-55. https://doi.org/10.1080/1523908x.2021.1940896.

U.S. DOE. 2024. *The National Transmission Planning Study.* Washington, D.C.: U. S. D. o. E. Grid Deployment Office. https://www.energy.gov/gdo/national-transmission-planning-study.

U.S. DOE. n.d. “Floating Offshore Wind Shot.” U.S. Department of Energy, Wind Energy Technologies Office. Accessed May 2024. https://www.energy.gov/eere/wind/floating-offshore-wind-shot.

USACE. 2024. Deprecated USACE Placement Areas. USACE Geospatial Open Data. https://geospatial-usace.opendata.arcgis.com/maps/aed16678ea814ddc8fdb5d96f723d90b/about.

USGS. 2016. "M 7.1 Scenario Earthquake - Great Valley 3." https://earthquake.usgs.gov/scenarios/eventpage/nclegacygreatvalley3mysteriousridgem7p1_se/shakemap/intensity?source=us&code=nclegacygreatvalley3mysteriousridgem7p1_se.

USGS. 2022. "Earthquake Scenarios." https://www.usgs.gov/tools/earthquake-scenarios.

Varian, H. R. 1992. *Microeconomic analysis.* New York: Norton.

Vyakaranam, B., Q. H. Nguyen, T. B. Nguyen, N. A. Samaan, and R. Huang. 2021. "Automated Tool to Create Chronological AC Power Flow Cases for Large Interconnected Systems." *IEEE Open Access Journal of Power and Energy* 8: 166-174. https://doi.org/10.1109/oajpe.2021.3075659.

Wang, Y. H., B. I. Ruttenberg, R. K. Walter, F. Pendleton, J. F. Samhouri, O. R. Liu, and C. White. 2024. "High resolution assessment of commercial fisheries activity along the US West Coast using Vessel Monitoring System data with a case study using California groundfish fisheries." *PLoS One* 19 (6): e0298868. https://doi.org/10.1371/journal.pone.0298868. PMCID: PMC11156284.

Watson, S. C. L., P. J. Somerfield, A. J. Lemasson, A. M. Knights, A. Edwards-Jones, J. Nunes, C. Pascoe, C. L. McNeill, M. Schratzberger, M. S. A. Thompson, E. Couce, C. L. Szostek, H. Baxter, and N. J. Beaumont. 2024. "The global impact of offshore wind farms on ecosystem services." *Ocean & Coastal Management* 249. https://doi.org/10.1016/j.ocecoaman.2024.107023.

WECC. 2019. "WECC Transmission Capital Cost Calculator." Accessed May 2024. https://www.wecc.org/Administrative/TEPPC_TransCapCostCalculator_E3_2019_Update.xlsx.

WECC. 2020a. *2030 ADS PCM Release Notes.*

WECC. 2021. *Data Development and Validation Manual (DDVM), Version 3.1.* Production Cost Data Subcommittee (PCDS).

WECC. 2024. *2024 Path Rating Catalog--Public Version.* Studies Subcommittee. https://www.wecc.org/sites/default/files/documents/meeting/2024/2024%20Path%20Rating%20Catalog%20Public_v2.pdf.

WECC. n.d. "Production Cost Data Subcommittee." https://www.wecc.org/committees/pcds.

Wiser, R., M. Bolinger, B. Hoen, D. Millstein, J. Rand, G. Barbose, N. Darghouth, W. Gorman, S. Jeong, E. O'Shaughnessy, and B. Paulos. 2023. *Land-Based Wind Market Report: 2023 Edition.*

Zuckerman, G., Anthony Lopez, Travis Williams, Rebecca Green, and G. Buster. 2023. *Impacts of Siting Considerations on Offshore Wind Technical Potential in the United States.* NREL/TP-6A20-85088. Golden, CO: N. R. E. Laboratory.

Appendix A – Production Cost and Resource Adequacy Model Details

In this section additional detail is provided with regards to the Capacity Expansion Modeling (CEM), Production Cost Modeling (PCM), and Resource Adequacy (RA) models.

A.1 Detailed CEM Results

This section contains the numeric values of total generation and storage technology installed by the CEM for each solve year for each of the three coastal states (California in Table A.1, Oregon in Table A.2, and Washington in Table A.3). Although this study focuses only on 2035 and 2050, the rest of the years are shown for full context of the assumed power system evolution.

Table A.1. The installed capacity of generation and storage technologies by type, for each CEM solve year in the state of California. Units are GW.

Technology Type	2025	2030	2035	2040	2045	2050
Gas-CC	20.0	19.9	20.4	20.4	0	0
Gas-CT	11.0	10.9	13.9	13.6	0	0
H2-CT	0	0	0	15.2	61.5	67.0
Hydro	10.2	10.9	11.3	11.6	11.8	12.0
Geothermal	2.0	5.1	6.2	6.7	7.2	7.6
Wind	6.4	6.3	7.3	8.2	6.1	9.1
PV	27.1	27.1	27.1	31.4	35.6	35.5
dPV	13.9	19.9	23.9	25.6	27.0	28.1
BESS	8.3	8.3	7.9	14.3	17.8	24.3
PSH	3.9	7.5	15.6	15.6	15.6	15.6
OSW	0	5.0	13.0	17.0	21.0	25.0
Other	2.8	2.4	1.9	1.4	1.2	0.8

Table A.2. The installed capacity of generation and storage technologies by type, for each CEM solve year in the state of Oregon. Units are GW.

Technology Type	2025	2030	2035	2040	2045	2050
Gas-CC	3.4	3.0	2.9	2.9	0	0
Gas-CT	0.7	0.7	0.7	0.6	0	0
H2-CT	0	0	0	0.2	6.2	7.4
Hydro	8.4	8.7	8.7	8.7	8.7	8.7
Geothermal	0	0	0	0.4	0.4	0.4
Wind	4.0	4.0	12.8	12.5	12.4	12.9
PV	1.6	1.6	2.8.	2.8	3.8	3.5
dPV	0.3	0.7	1.1	1.2	1.3	1.4
BESS	0	0	0	0	0	0.4
OSW	0	0	2	2.3	5.0	6.0
Other	0.1	0.1	0.1	0.1	0.1	0.1

Table A.3. The installed capacity of generation and storage technologies by type, for each CEM solve year in the state of Washington. Units are GW.

Technology Type	2025	2030	2035	2040	2045	2050
Nuclear	1.2	1.2	1.2	1.2	1.2	1.2
Gas-CC	2.6	2.6	2.6	2.6	0	0
Gas-CT	0.6	0.6	0.7	0.3	0	0
H2-CT	0	0	0	0	2.5	4.3
Hydro	22.5	23.1	23.1	23.2	23.2	23.2
Wind	8.3	8.8	13.1	14.4	14.4	15.0
PV	0.4	0.4	1.9	5.0	7.9	12.2

Technology Type	2025	2030	2035	2040	2045	2050
dPV	0.8	2.2	3.0	3.1	3.2	3.2
PSH	0.3	0.3	0.3	0.3	0.3	0.3
OSW	0	0	0	0.8	1.5	2
Other	1.4	1.4	1.3	1.4	1.4	1.4

A.2 ADS Load Areas and Paths

Much of the analysis using the PCM model references load areas and various WECC paths. Figure A.1 reproduces the load areas in the WECC ADS for reference. Figure A.2 is a reproduction of the path overview from the WECC path catalogue indicating a few of the paths referred to in this report.

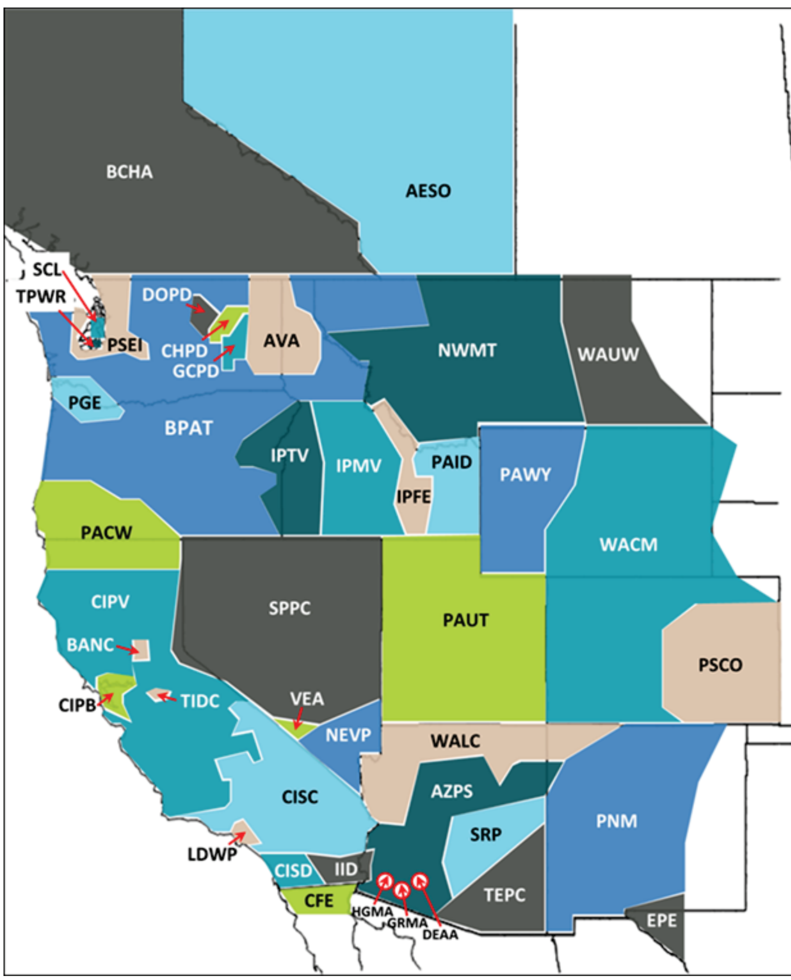

TEPPC Area	Area Description
AESO	Alberta Electric System Operator
AVA	Avista
AZPS	Arizona Public Service
BANC	Sacramento Municipal District
BCHA	British Columbia Hydro
BPAT	Bonneville Power Administration
CFE	Comision Federal de Electricidad
CHPD	Chelan Co PUD
CIPB	Pacific Gas & Electric Bay Area
CIPV	Pacific Gas & Electric Valley Area
CISC	Southern California Edison
CISD	San Diego Gas & Electric
DOPD	Douglas Co PUD
EPE	El Paso Electric
GCPD	Grant Co PUD
IID	Imperial Irrigation District
IPFE	Far East (Idaho Power)
IPMV	Magic Valley (Idaho Power)
IPTV	Treasure Valley (Idaho Power)
LDWP	Los Angeles Dept of Water & Power
NEVP	Nevada Power
NWMT	Northwestern Montana
PACW	PacifiCorp West
PAID	PacifiCorp East – Idaho
PAUT	PacifiCorp East – Utah
PAWY	PacifiCorp East - Wyoming
PGE	Portland Gen Electric
PNM	Public Service New Mexico
PSCO	Public Service Colorado (Xcel)
PSEI	Puget Sound Energy
SCL	Seattle City Light
SPPC	Sierra Pacific Power
SRP	Salt River Project
TEPC	Tucson Electric Power
TIDC	Turlock Irrigation District
TPWR	Tacoma Power
VEA	Valley Electric Association
WACM	Western Area Power Admin Colorado/Missouri
WALC	Western Area Power Admin Lower Colorado
WAUW	Western Area Power Admin Upper Missouri
N/A	DECA, LLC - Arlington Valley (DEAA)
N/A	Gila River Maricopa Arizona (GRMA)
N/A	Harquahala L.L.C. (HGMA)

Figure A.1. Load Areas in the WECC ADS 2032 (WECC 2021)

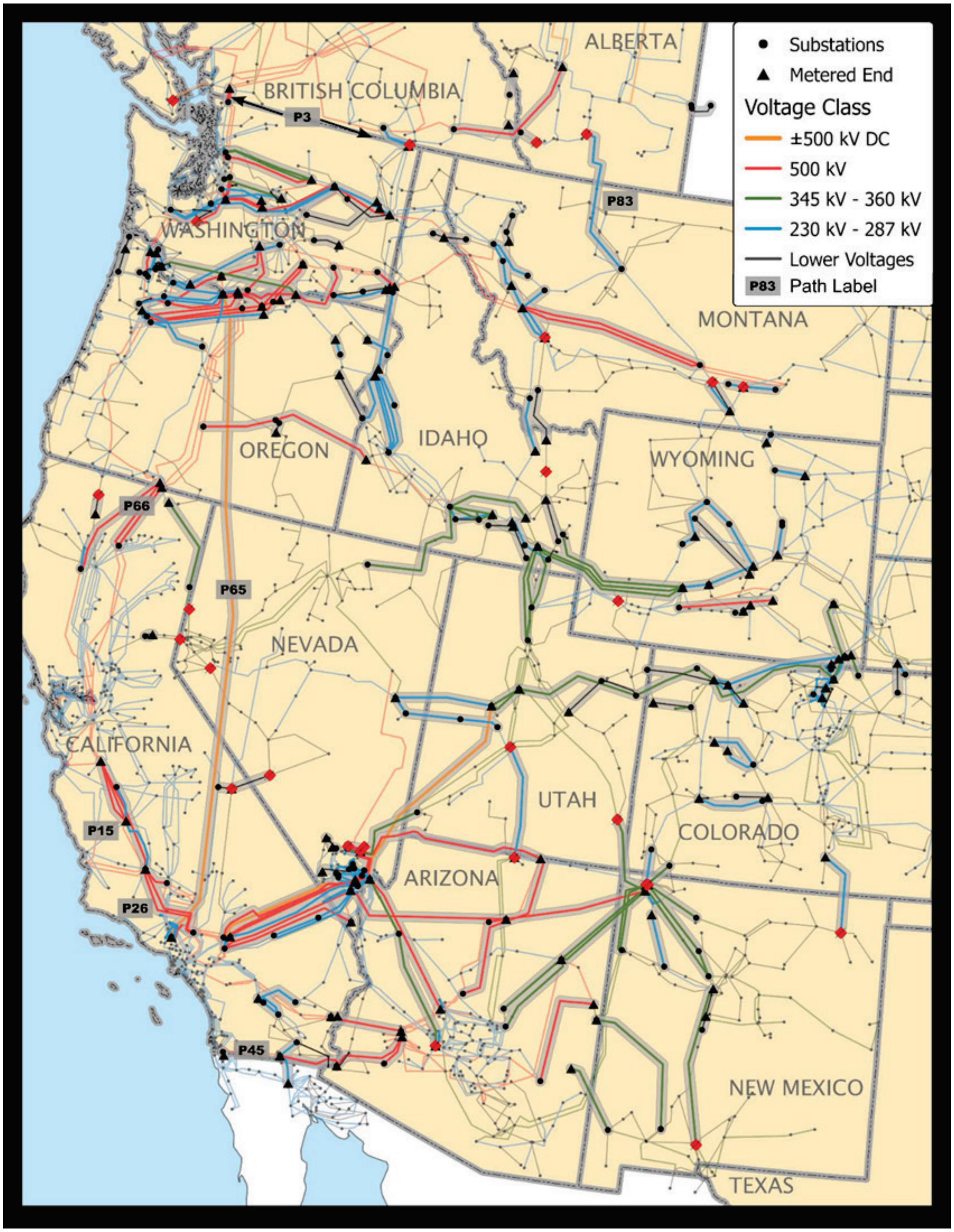

Figure A.2. WECC paths with selected labels indicated in grey boxes (WECC 2024)

A.3 Manual Build to ADS 2032

To maintain strong links to a proven WECC 2030 ADS power flow model, the WECC 2032 ADS changes were incorporated manually for this study into the WECC 2030 Anchor Data Set(WECC 2020a). The WECC 2030 ADS incorporates electrical load and supply projections from all planning regions in the Western Interconnection to the year 2030. It aims to project the Western Interconnection's infrastructure for the year 2030, based on the best available knowledge at the time of the case's release as well as existing state and federal laws. The transmission network of the ADS 2030 was derived from work by the WECC Reliability Assessment Committee and represents the best available projection of anticipated new generation, generation retirements, transmission assets, and load growth in the 10-year planning horizon within the WECC grid planning community.

To reflect ADS 2032 generation and transmission changes, WECC stakeholder generation and transmission projections submitted under the WECC ADS 2032 case were included in the Production Cost Model. In addition, similar to the assumption in the NTP study (U.S. DOE 2024), several transmission projects that were sufficiently far along in the development pipeline were added in the system model. The result is an initial case that is used as the starting point for the subsequent 2035 and 2050 scenario development work. Finally, a few other transmission projects (shown below in Table A.4) were manually added to the 2035 or the 2050 topologies as part of the expansion work. Table A.4 lists these transmission projects and indicates at which stage (initial, 2035, or 2050) they were incorporated. Though these projects are fairly mature, these projects remain in development at the time of study and may not reach completion.

Table A.4. Major transmission projects incorporated in PCM

Project	Where Modeled
Boardman to Hemmingway	Initial Dataset
Ten West Link	Initial Dataset
Gateway West	Initial Dataset
Gateway South	Initial Dataset
SWIP North	2035 & 2050 Topologies
Transwest AC & DC	Initial Dataset
Cross-tie	2035 & 2050 Topologies
Greenlink Nevada West	Initial Dataset
Greenlink Nevada North	2050 Topologies
Colorado Power Path	Initial Dataset
Southline	2035 & 2050 Topologies

Generation increments from the ADS 2030 to ADS 2032 totaling 29.4 GW were included (12.2 GW solar, 5.8 GW Wind, 10.1 GW storage, 1.2 GW natural gas). New buses (175) and high voltage transmission lines (177) were also added. Finally, a weekly hydropower budget was incorporated, consistent with the 2009 monthly hydrology of ADS 2030.

A.4 Additional Generation and Interregional Transmission Expansion

After the ADS 2032 starting point, additional generation and transmission projects were modeled to meet capacities resulting from the CEM (Section 2.4). For generation, zonal capacity expansion differences were disaggregated to nodal resolution to yield additional modifications.[35] These nodal capacity differences were computed by first subtracting the CEM zonal capacity by technology type and zone from the corresponding 2032 ADS capacity, after it had been aggregated and mapped to the CEM zones. Then, a semi-manual, geographic process was used to associate generation capacity additions with new or existing substations across the WI.

Interregional transmission projects listed in Table A.1 were assumed in the CEM. Following the zonal-to-nodal disaggregation of the generation as described above, additional interregional transmission was required to limit curtailment and congestion to acceptable levels. Additional transmission was built within and between CAISO, Northern Grid, and WestConnect regions through an iterative process. Starting from the ADS 2032 transmission and the projects listed in Table A.1, the generation capacities accounting for the CEM builds, and demand projections detailed in Section 5.2, successive production cost simulations were executed, and transmission congestion and generation curtailment were tallied. Transmission enhancements were implemented in the model to relieve congestion and curtailment and the model was rerun. This process was repeated to incrementally increase transmission capacities until congestion was resolved and curtailment of generation fell to acceptable levels, generally defined as less than 20% at a load area level per industry best practice.

A.5 Generation Curtailment

As VRE (Solar PV, Land based Wind, and Offshore wind) make up a larger portion of the generation mix, the number of hours where the available energy exceeds demand increase. Figure A.3 shows the distribution of the ratio of available VRE and hydro energy compared to load. In 2035, just a little less than 25% of the hours could theoretically have VRE and hydro meet all load (ratio of 1), whereas in 2050 this number is greater than 25%.

[35] The CEM discretizes the WI into 35 zones. The PCM resolves dispatch at much finer, nodal resolution, including more than 30,000 buses in the WI. Aggregation of the nodal PCM is required to compare it to the CEM. Disaggregation of the zonal CEM is required to compare it to the PCM.

Figure A.3 Distribution of the hourly ratio of available VRE and hydro generation compared to load. 25% of the values lie below the bottom edge of the box, and 25% of the values lie above its top edge. The middle line is located at the median. A ratio greater than 1 indicates overgeneration, even if no other resources would operate. Histograms may be read on the vertical axis.

A result of the increasing ratio from Figure A.3 is that curtailment will necessarily increase. VRE resources are modeled with a negative dispatch cost to create a disincentive for the PCM to reduce their output, as well as to capture the impacts of incentives like the production tax credit. In the simulations for this study all *existing* VRE have a dispatch cost of -25 $/MWh, while all *new* VRE, including OSW, have a cost of -15 $/MWh. The reason for the difference in cost is to give slight preferential treatment to existing resources, where it is assumed some power purchase agreement is in place. Besides this single price difference, the price of congestion will drive the model to decide, which specific units to curtail. It should be noted, however, that given the many VRE units, the solution is not unique and there is a degree of numerical arbitrariness to the unit specific curtailment decisions.

The amount of curtailment in the PCM was one of the critical monitored metrics during the development of the nodal models and transmission expansion work. The objective was to achieve sufficiently low curtailment[36]. Additionally, the change of curtailment from iteration to iteration serves as an indication for the impact of the transmission expansion process. The process ends when the changes in curtailment become minimal[37]. Figure A.4 shows the total yearly curtailment in all five base topologies. The increase in total curtailment matches the upward ratio shift from Figure A.3.

[36] For this study sufficiently low curtailment means below 20% of the generated power output is curtailed.
[37] Minimal is not defined by an exact number or threshold. However, changes in curtailment between iterations converged to less than 1% or even 0.5%.

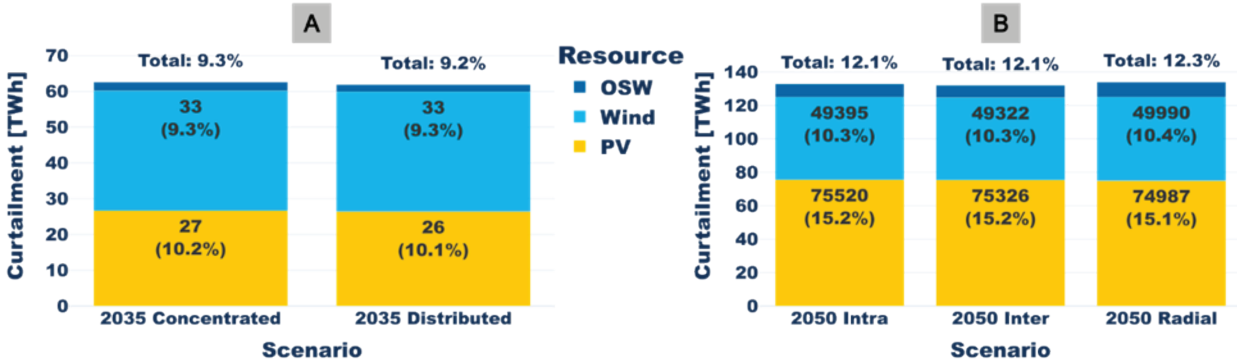

Figure A.4.Total curtailment in the base scenarios (A) 2035 (B) 2050.

While Figure A.4 captures aggregate behavior, Figure A.5 shows that underneath lies a much more dynamic trend. During the spring runoff, with lower loads and high hydro output, curtailment is particularly high[38]. The ability to seasonally shift the VRE generation from spring to summer could drastically alter the utilization of the installed capacity, however such long-term storage was not incorporated in this study due to lack of currently available modeling capabilities.

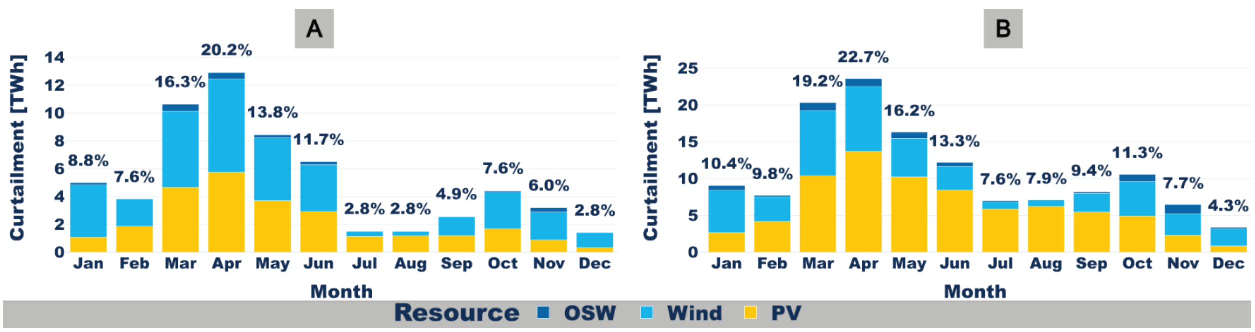

Figure A.5. Monthly curtailment in the (A) Distributed 2035 scenario and (B) Interregional 2050 scenario.

A.6 Net Exports/Imports

Just as the curtailment varies over the months of the year, so do the exports between regions[39]. Changes in exports over time, as well as between regions, provide some more context on how, and to what extent, the different topology design decisions impact operations.

In the NW, Figure A.6 shows an increase in net exports or reduction in net imports (negative exports) from 2035 to 2050. This can be seen by looking at the bottom of the boxes in the figure, which represent the 25th percentile (25% of the values lie below this number, and 75% above). While in 2035 this is negative (net importing) for seven months out of the year, in 2050 that is reduced to just three. In 2050, the Interregional Topology shows consistently higher exports, however, the difference with respect to the other topologies is starkest during the summer months. Recall from Figure 18 in Section 5.2, that the NW is winter peaking, while

[38] Hydro is modeled as more negative than all other resources to avoid spillage. Some of the plants have flexibility, which is modeled through their pondage and weekly budgets.
[39] In this section exports are indicated as positive and imports as negative.

CAISO is summer peaking. Additional export demand, the tail of the hydro runoff season with more generation available in the NW, and the increased transfer capability of the Interregional Topology, all combine to shift exports in the summer months further compared to the other topologies.

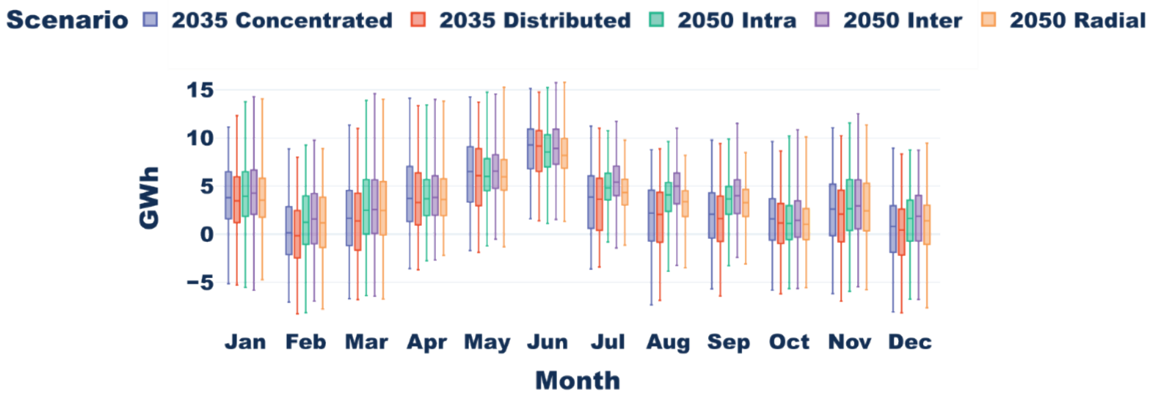

Figure A.6. Net exports from the NW.

In PACW, the impact of the added POI at Del Norte in the distributed 2035 topology is evident through lower imports (lower magnitude, negative exports) throughout the year, as seen in Figure A.7. During the winter months, the interquartile range[40] in the 2050 topologies is considerably smaller compared to the spring and summer months. This stands in interesting contrast to the NW flows that show an opposite pattern.

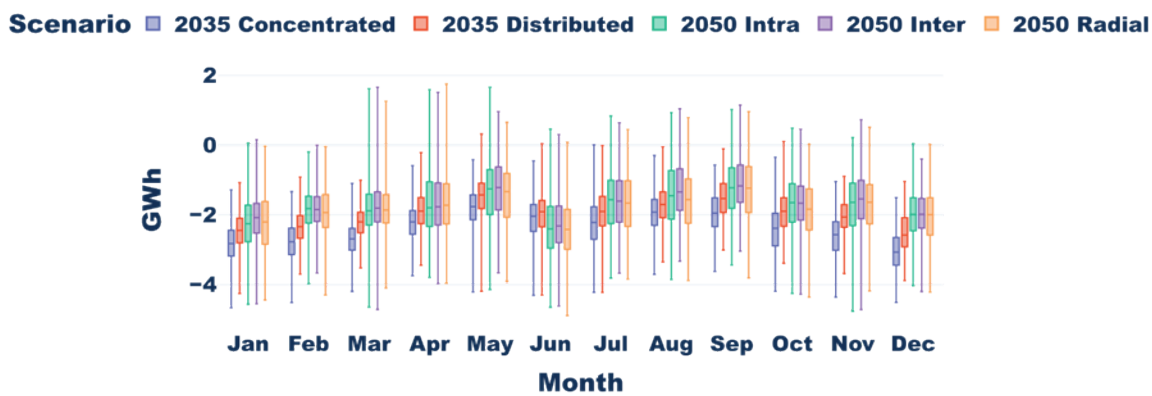

Figure A.7. Net exports from PACW.

Median imports (negative exports) in CAISO increase across the year but at different rates. For example, January is around a 60% increase, compared to around 100% increase in June and July, and slightly more in August. Complementary to the trend observed in the NW, imports to CAISO in the summer months are more significantly higher in the Interregional Topology during the summer months compared with the rest of the year.

[40] The range between the 25th and 75th percentile that is marked by the box in the box plot.

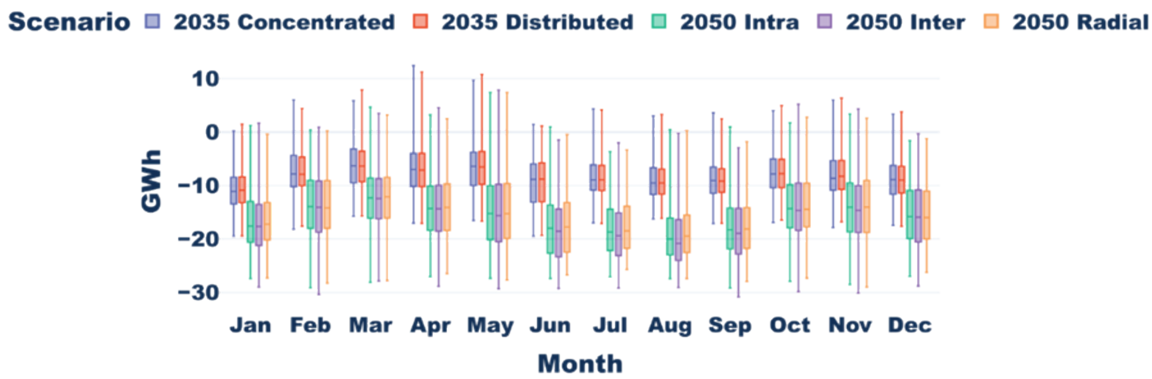

Figure A.8.Net exports from CAISO.

A.7 Avoided Loss Methodology

A unique feature of the offshore backbone design of the 2050 Interregional Topology is that in the event of a failure in one of the export cables, the generation could be diverted to one of the other offshore links and thus generation loss avoided. Since the PCM provides an optimal dispatch, avoiding such generation loss is translated to an economic benefit. The following describes the methodology used to calculate this benefit.

Avoided loss is the minimum of the amount exported on the cable and the spare capacity throughout the backbone. Flows can reverse direction (i.e. flow from shore to offshore) however, these are set to zero in the final avoided loss calculation, as it does not make sense to consider a *negative* avoided loss. Note that the value of power "wheeling" through the offshore system is implicitly captured in the high export on the cable through which it returns to shore.

To derive a dollar value for the avoided losses, the LMPs at the export cable's onshore POI is used. Here, negative LMPs pose a challenge since they would imply a *cost* imposed for *not losing* generation. Since this is not a reasonable assumption, the average LMP over the year is used, multiplied by the total avoided loss on the export cable, multiplied by an assumed forced-outage rate (FOR) to get the estimated avoided loss cost.

The average LMPs are used, rather than removing hours with negative LMPs, because the application of the FOR assumes statistics over all time. The FOR would need to be adjusted if LMPs at negative hours would be removed, and a methodology for adjusting the FOR is not readily apparent.

A.8 Supply and Demand Profiles for Resource Adequacy

The Gridpath resource adequacy toolkits developed for this study leveraged many years of coincident wind, solar, and demand profiles and observed hydropower profiles. This section provides additional detail regarding how these profiles were developed.

A.8.1 Variable Electricity Supply Profile Development

Hourly solar and wind profiles were developed in the same method as utilized for the National Transmission Planning Study (U.S. DOE 2024). The study team borrowed a suite of models and techniques developed in former work, including the IM3 project funded by the U.S. Department of Energy (DOE) Office of Science and PNNL's Grid Operations, Decarbonization, Environmental and Energy Equity Platform (GODEEEP) internal investment. From these models, hourly wind and solar generation were produced at every Thermodynamic Global Warming (TGW) grid cell. Then, at every 1/8th degree grid cell, relevant meteorological data were extracted and preprocessed for use with the National Renewable Energy Laboratory (NREL) Renewable Energy Potential (reV) model (Maclaurin et al. 2021; U.S. DOE 2024). reV is an interface to the System Advisor Model (SAM)—a collection of models for renewable energy. The study team used generic configuration options, such as a commonly used turbine hub height and panel array type, to describe the hypothetical power plant in each grid cell. The study team scaled the wind and solar data to remove alternating current (AC)/direct current (DC) losses prior to being imported into Gridpath. The wind and solar profiles, linked to TGW, could thus be synchronized with load projections for 43 historical and 80 future years.

For hydropower profiles, observed monthly and weekly volumes from 2001-2022 are sourced from EIA923 data (Turner et al. 2022). When convolved with the hydropower profiles, a total of 2706 weather-synchronized combinations are available in the toolkit.

A.8.2 Demand Profile Development

The original load data used in WOW-TS was a pair of bottom-up load electrification projections for 2035 and 2050. The demand data corresponded to the low demand net-zero scenario of the Annual Decarbonization Perspective 2023 (Haley et al. 2023). Electricity demand was approximated based on DOE's Annual Energy Outlook 2023, but assuming economy-wide net-zero greenhouse gas emissions through electrification of demand and implementation of carbon capture and storage strategies. The effects of conservation, energy efficiency and Inflation Reduction Act tax credits on technology development were also included in the demand projections.

The load data in 2035 and 2050 contains seven different weather years which represent the observed weather variability from 2007-2013. While there is a significant amount of weather variability in these years, the project wanted to extend the sampling to capture a broader range of weather-induced load variability. To do this we chose to leverage the extensively documented open-source Total ELectricity Loads (TELL; https://immm-sfa.github.io/tell/) model originally developed by the DOE Office of Science project Integrated Multisector Multiscale Modeling (IM3; https://im3.pnnl.gov/). TELL takes as input hourly time series of meteorology by BA and simulates the hourly evolution of the electricity demand within the BA in response to the variations in weather (McGrath et al. 2022). The input variables for TELL are hourly time series of temperature, humidity, shortwave radiation, longwave radiation, and wind speed for each BA. The model also considers the time of day (in Coordinated Universal Time [UTC]), the day of the week, and whether the day was a federal holiday.

TELL was originally trained on historical weather and observed total loads from 2016 to 2018. The historical total loads were from the Energy Information Administration (EIA) 930 dataset, which contains hourly total (net) load observations by BA going back to 2015. For this project, we retrained the TELL model on the seven years (2007-2013) of bottom-up load projects in both 2035 and 2050. A separate set of models was trained for the 2035 and 2050 load projections. Once the model was retrained and validated this allowed us to use TELL to pass a much larger sample of weather variability through the model to expand the historical weather years from seven years to forty years and thus capture a much broader range of weather variability and climate change.

Demand profiles were developed using similar meteorological forcing as utilized in the National Transmission Planning Study (U.S. DOE 2024). Forty years (1980–2019) of hourly historical meteorology (e.g., temperature, humidity, etc.) at a 12-kilometer (km) spatial resolution were sourced from the Thermodynamic Global Warming (TGW; (Jones et al. 2023)) dataset. The TGW dataset then repeats the 40-year historical record twice into the future (from 2020–2059 and from 2060–2099) with various levels of additional warming applied to the boundary conditions of the Weather Research and Forecasting (WRF) model used to dynamically downscale the meteorology. The additional warming comes from the average climate model warming levels for two radiative forcing scenarios (Representative Concentration Pathways [RCPs] 4.5 and 8.5, with global radiative forcing of 4.5 and 8.5 W/m^2, respectively). For the 12-km historical and future meteorology data (Jones et al. 2023), the study team postprocessed the data by first spatially aggregating them to the county scale (Burleyson et al. 2023b) and then weighting the county data by population to create hourly time series of the meteorology for each BA (Burleyson et al. 2023a).

A.8.3 Neural Network Model for Weather-Based Load Prediction

TELL uses multi-layered neural networks to project electricity loads for each BA based on population-weighted weather (McGrath et al. 2022). Figure A.9 below presents a schematic depicting how the historical and future loads were generated. For each BA, TELL uses a multi-layered perceptron (MLP) neural network to map the input features (i.e., date and weather-related variables) to the output (i.e., the demand forecast at each hour). This can be expressed as:

$$y_b(t) = f_{NN,b}\left(\boldsymbol{w_b}(t), \boldsymbol{c}(\boldsymbol{t})\right) \tag{1}$$

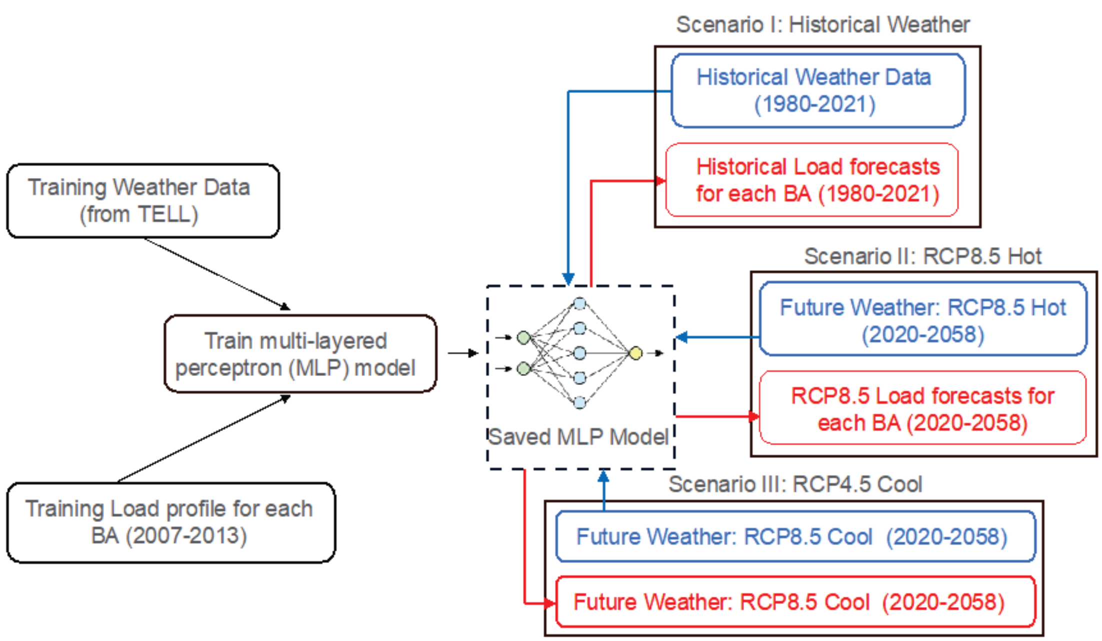

Figure A.9. Schematic depicting the workflow used to generate the historical demand, as well as the projected demand under the RCP4.5 and RCP8.5 radiative forcing scenarios.

In equation 1, $y(t)$ refers to the demand at each hour over the prediction horizon; $\boldsymbol{w}(t)$ denotes the meteorological variables at the corresponding hours, which include dry-bulb temperature, specific humidity, and long- and short-wave radiation specific to the BA; and $\boldsymbol{c}(t)$ denotes the calendar-related variables, including hour of the day, month, year, day of week (implemented as one-hot encoding) and whether a given day is a holiday (implemented as a binary variable). $f_{NN,b}$ denotes the MLP neural network function that maps the inputs to the corresponding demand at a given time. Here, b denotes the specific BA for which the demand projections were made. We used an MLP model with one hidden layer as $f_{NN,b}$ – note that we use a separate MLP model for each BA. The key hyperparameter for each model (specific to each BA) was the size (i.e., number of nodes) of the hidden layer. We used the hyperparameters optimized as part of the TELL development as the hyperparameters of $f_{NN,b}$.

To train and evaluate the models, we used the historical TGW meteorology data from January 1, 2007 to December 31, 2013. Note that for each of the years for which the models were trained (including leap years) the number of data points was 8760 (corresponding to 8760 hours in a year). In the case of leap years, the day omitted was December 31. We used hourly data from January 1, 2007 to December 30, 2012 to train and validate the new TELL MLP models, and used data from January 1, 2013 to December 31 2023 to evaluate our models. To validate our ML models, we used k-fold cross-validation and computed the mean cross-validation error (Pandian 2024). The fraction of missing timesteps (i.e., hours) for which data was missing (in the meteorological data) was small (<0.0001%). For the small number of cases for which data was missing, linear interpolation was used to perform missing value imputation. After training and validation, the models were evaluated on the ground truth data from January 1 to Dec 31, 2013. We used several metrics to evaluate the performance of the ML models. The key two metrics used for evaluation are:

$$MAPE = \left(\frac{1}{T}\right)\sum_{t}^{T}\frac{\left|y_{\{gt\}}(t) - y_{\{pred\}}(t)\right|}{y_{\{gt\}}(t)} \tag{2}$$

$$Peak\ MAPE\ [top\ N\%]\ = \left(\frac{1}{D_N}\right)\sum_{d}^{D_N}\frac{\left|y_{\{gt,peak\}}(d) - y_{\{pred,peak\}}(d)\right|}{y_{\{gt,peak\}}(d)} \tag{3}$$

In equations 2 and 3, T represents the total number of hours in the evaluation period (in our case T=8760); D_N corresponds to the number of days corresponding to the top N% daily peak demand; $y_{\{gt\}}$ and $y_{\{pred\}}$ represent the ground truth (i.e. the actual demand for 2013) and the ML projections respectively. Note that both $y_{\{gt\}}$ and $y_{\{pred\}}$ are computed at one-hour resolution. Here, mean average percentage error (MAPE) is used to quantify the discrepancies between the ML projections and the ground truth for every hour, whereas $Peak\ MAPE\ [top\ N\%]$ is used to quantify the discrepancies between the ML projections and the ground truth when considering the top N% daily peak demand. Figure A.10 presents the MAPE and peak MAPE (top 10%, $N = 10$) for all balancing authorities considered in this analysis. The figure shows that the MAPE values cross-validation and the evaluation <6% for all BAs and <4% for the majority of the BAs. The figure also indicates that peak MAPE values for the top 10% daily peaks show a similar trend. The results indicate that the MLP models across all BAs can capture the hourly demand for days with "typical" demand profiles, as well as for days with comparatively higher peak demands.

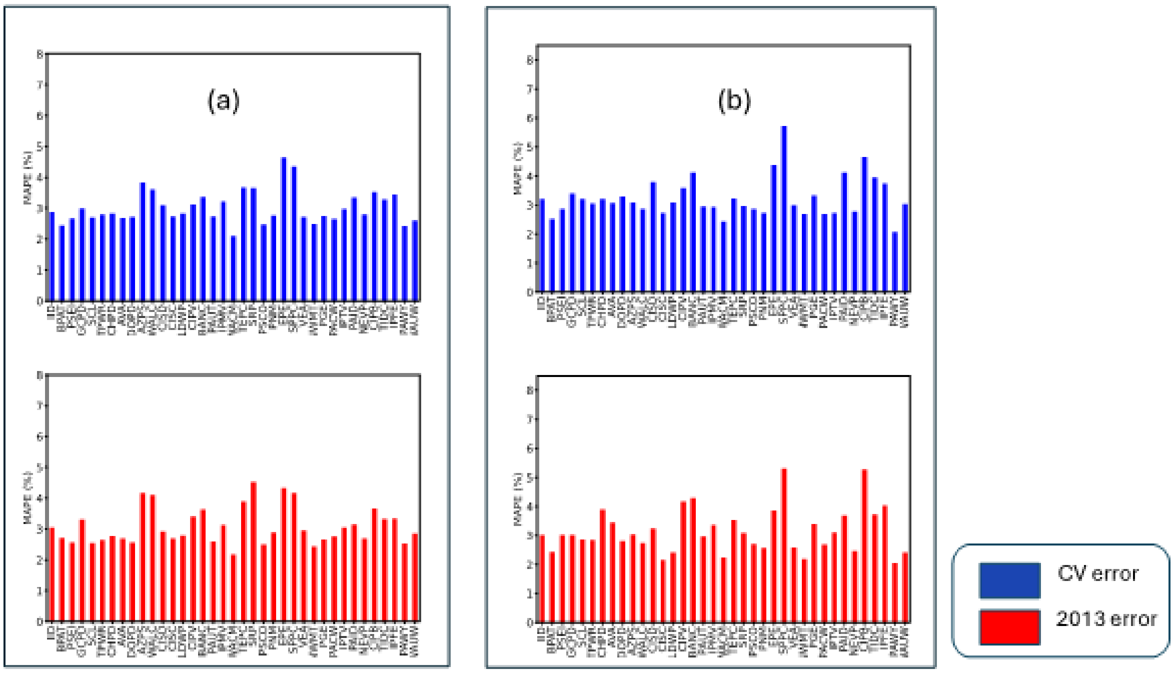

Figure A.10. a) Mean MAPE across all BAs for cross-validation (CV) and for evaluation (i.e. during the evaluation period of 2013); (b) mean peak MAPE (top 10% peaks) across all BAs for CV and evaluation.

A.9 Method for ELCC Calculation

To calculate the ELCC specifically in the regions of interest along the West Coast, a new multi-step method was introduced to GridpathRA and executed for each topology set.

With OSW included, all historical weather years, and seven representative hydro years (2001, 2002, 2004, 2005, 2007, 2009, 2011)[41]:

1. Seed the problem by running 150% load scaling for the combination of CAISO (CIPV, CIPB, CISC, CISD, VEA), PACW, and NW (BPAT, SCL, PSEI, TPWR, PGE) regions, and isolate weeks experiencing unserved energy (USE). Complete remaining steps on these problems only.
2. Disallow USE everywhere but CAISO. Increment CAISO load until LOLE of 0.1 is reached. Lock loads and USE in CAISO.
3. Retain loads and USE from prior step. Allow USE in NW and increment NW load until LOLE equals 0.1 in NW.

[41] Representative hydropower profiles were selected to reduce the computational burden of running all weather years for each hydropower year. However, one dry year, one wet year, and five moderate years were chosen to approximately match the statistical variation of wet and dry years in the historical record (2001-2022).

4. Retain loads and USE from prior step. Allow USE in PACW and increment PACW load until LOLE equals 0.1 in PACW.

Steps 1-4 were then repeated without OSW. The load increments between the balanced final runs define the perfect capacity supported by the OSW additions, from which the ELCC statistics could be computed.

Appendix B – Reliability and Resilience Analysis

In this appendix, detailed depictions of system upgrades due to contingencies of BPA, PACW, and CAISO are shown, new geographical image system-enabled plotting capabilities are demonstrated, a process for dynamic model preparation is documented, and finally the database module for the contingency analyses is introduced.

B.1 System Reliability Reinforcements by Region

In this section, Figures B.1 to B.6 depict the upgrades identified as a function of steady-state contingencies of BPA, PACW, and CAISO for the 2035 and 2050 topology.

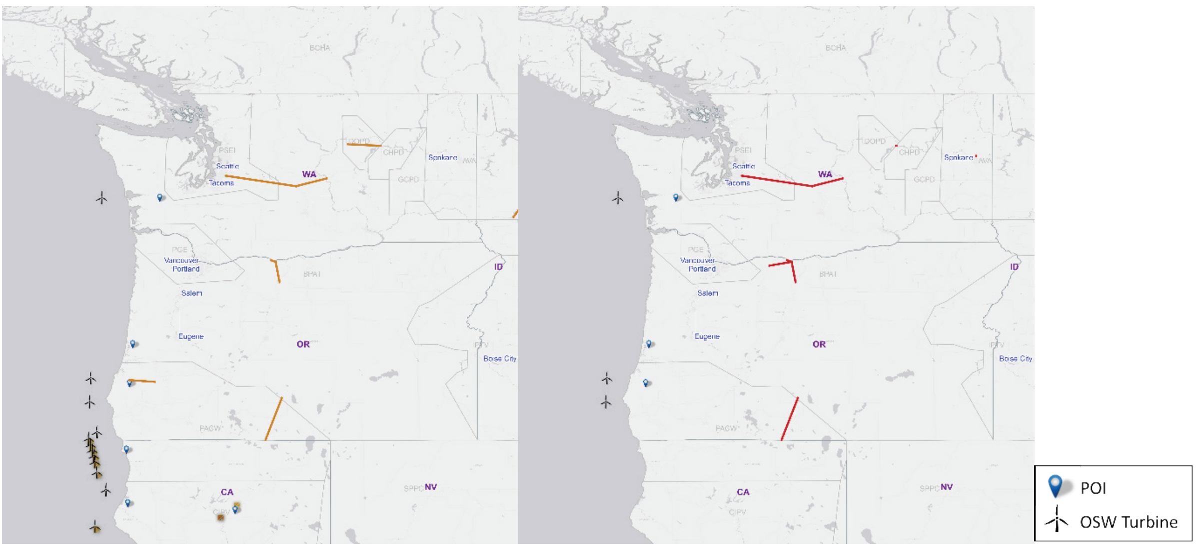

Figure B.1. System Reliability Reinforcements for BPA Contingencies, 2035 Distributed Topology (left) and 2035 Concentrated Topology (right). Turbine icons on land indicate a direct injection in the power flow model at the POI.

Figure B.2. System Reliability Reinforcements for PACW Contingencies, 2035 Distributed Topology

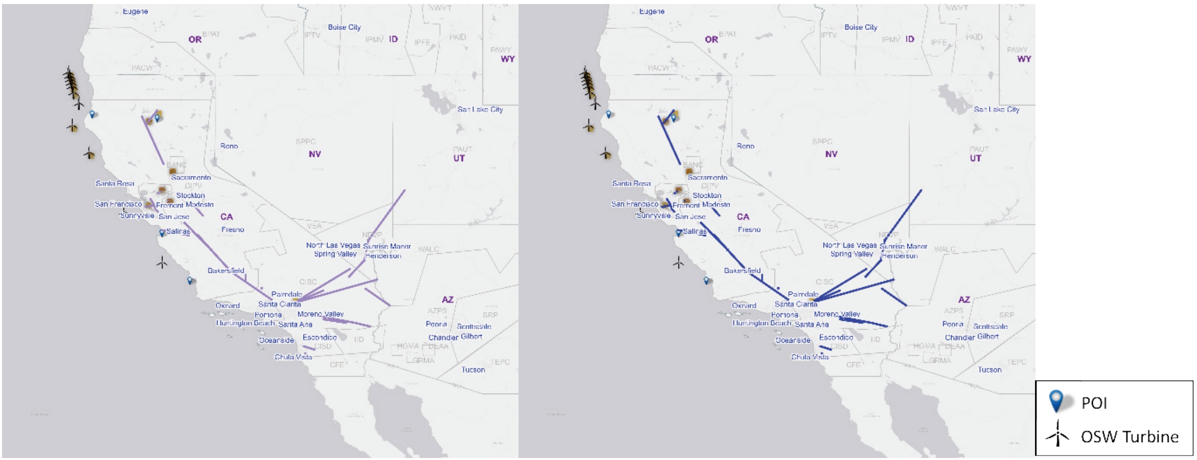

Figure B.3. System Reliability Reinforcements for CAISO Contingencies, 2035 Distributed Topology (left) and 2035 Concentrated Topology (right).

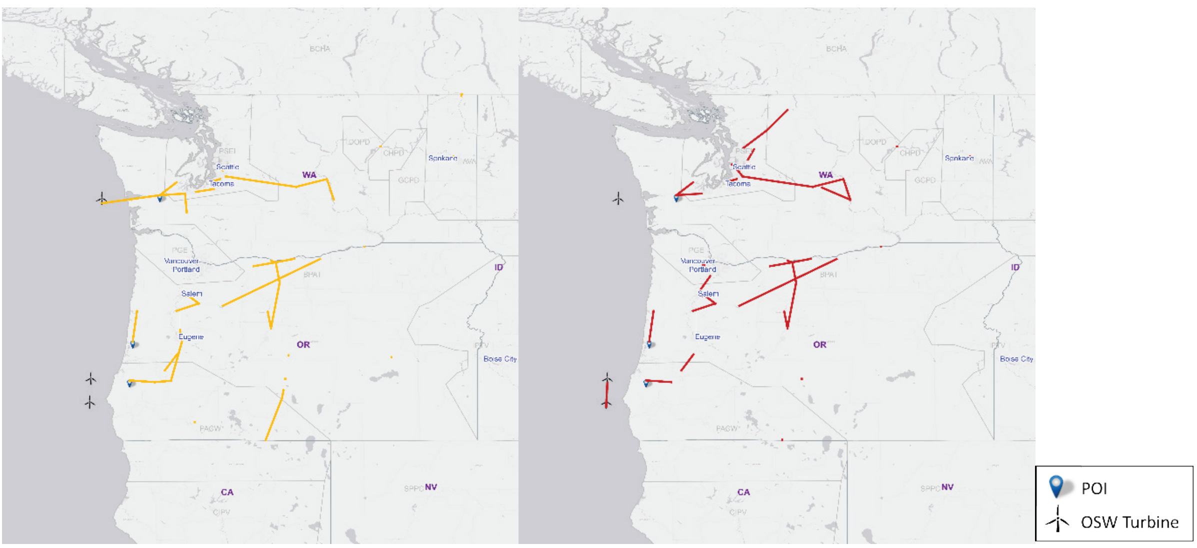

Figure B.4. System Reliability Reinforcements for BPA Contingencies, 2050 Intraregional Topology (left) and 2050 Interregional Topology (right)

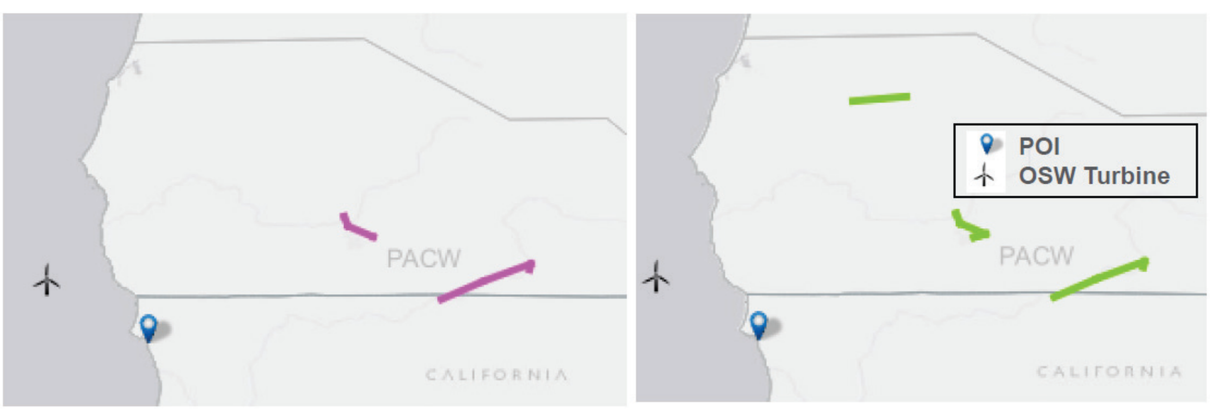

Figure B.5. System Reliability Reinforcements for PACW Contingencies, 2050 Intraregional Topology (left) and 2050 Interregional Topology (right)

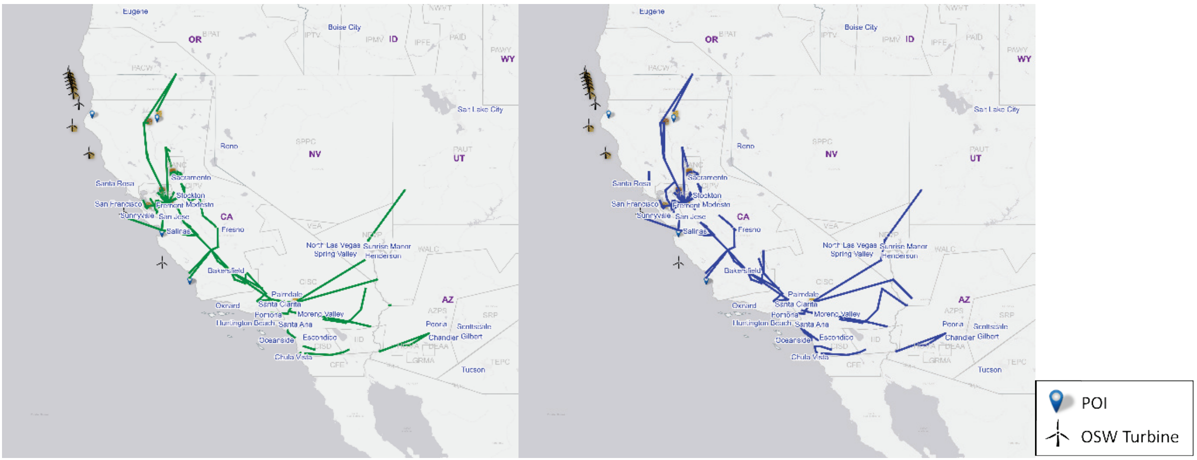

Figure B.6. System Reliability Reinforcements for CAISO Contingencies, 2050 Intraregional Topology (left) and 2050 Interregional Topology (right)

B.2 System Strength Analysis

An important screening tool that has been used in this project to evaluate the overall reliability of the planned 2035 topology sets relies on grid strength matrix. The purpose of this analysis is to assess OSW POIs based on system strength. The findings aim to assist system planners by identifying cases where further reliability assessments may be needed to integrate offshore wind energy at weaker POIs. Grid strength refers to the system's capacity to maintain stable voltage amidst varying grid conditions and disturbances. Strong grids provide a robust voltage reference, helping grid-connected devices stay synchronized. Conversely, weak grids present challenges, particularly for connecting inverter-based resources (IBRs), due to their asynchronous behavior, which can cause inverters to disconnect when their support is crucial for grid stability. IBRs require sufficient grid strength, relative to the resource's size, for synchronizing power electronics. Although these issues don't inherently threaten reliability, current control and protection systems must adapt to accommodate the evolving characteristics of the generation fleet.

B.2.1 Approach

In this study, grid strength at the POIs of offshore wind power plants is measured using the short-circuit ratio (SCR). The SCR metric represents the ratio between the short-circuit apparent power (SCMVA) from a three-phase-to-ground fault at a specific location in the power system and the rating of the IBR connected at that location.

$$SCR_{POI} = \frac{SCMVA_{POI}}{P_{nom,IBR}} \tag{4}$$

where:

SCR_{POI} is the short-circuit ratio at the POI

$SCMVA_{POI}$ is the short-circuit power (MVA) level at the POI without the fault current contribution of the IBR connected to the studied POI

$P_{nom,IBR}$ is the nominal active power rating of the IBR connected at the studied POI.

While the short-circuit ratio (SCR) metric is commonly used to evaluate the connection of a single inverter-based resource (IBR) to the bulk power system, in this study, it serves as an effective screening tool within the broader context of long-term planning for offshore wind energy integration. The SCR metric helps planners assess the suitability of Points of Interconnection (POIs) for new offshore wind plants by identifying potential system strength limitations early in the planning process.

In this study, the SCR at each POI, denoted as SCR_{POI} is calculated for all offshore wind plant POIs under consideration for 2035 topology sets (2035 Distributed and 2035 Concentrated). To obtain a conservative estimate, SCR_{POI} is determined by calculating the minimum short-circuit current levels at the POI busbars while excluding any contributions from neighboring offshore wind plants. This approach provides a conservative assessment of system strength at each POI and highlights areas that may require further analysis or reinforcement.

The short-circuit current calculations were performed following the International Electrotechnical Commission (IEC) 60909-0:2016 standard, that provides a consistent and internationally recognized framework for determining short-circuit currents, ensuring accuracy and comparability in assessing system strength across different locations.

A low short-circuit ratio (SCR) area, or “weak system,” indicates that voltage (both magnitude and phase angle) is highly sensitive to changes in power injection, which can lead to instability and difficulty in maintaining a reliable power flow. In such weak systems, even minor variations in power injected by generation sources can cause significant fluctuations in voltage. However, weak grid conditions do not indicate that injections are infeasible. It’s an indication that additional studies (and possibly additional equipment) are needed to ensure stable and reliable operation of any IBR that injects into weak grid.

Conversely, high SCR areas, often referred to as “stiff” systems, exhibit low sensitivity to changes in power injection. These systems are robust, maintaining stable voltage with minimal impact from power fluctuations, thus providing a stable environment for IBRs. Table B.1 summarizes the SCR threshold criteria.

Table B.1. Threshold value for grid strength evaluation for POIs

Grid strength classification	SCR Value
Weak	SCR ≤ 3
Moderate	$3 <$ SCR ≤ 5
Strong	SCR > 5

For this study, ASSET (Sharma et al. 2023) tool that has been utilized to automate the grid strength evaluation process and also identify critical network contingencies for each of the POIs. This tool has been developed for the AOSWTS study.

B.2.2 Grid strength studies

For grid strength studies, 2 topology sets namely 2035 Concentrated and 2035 Distributed were considered[42]. Further, for each of these topologies, two scenarios were considered accounting for low and high penetration of offshore wind resources. Further, SCR was also calculated for critical N-1 and N-2 network contingencies corresponding to each of the POIs. Here, critical contingencies could be different from those identified in section 6.3. For each POI bus, the critical N-1/N-2 contingencies aimed to identify the top two lines or transformers whose disconnections would cause the largest reductions in system strength without leading to an islanding condition at the POI.

Table B.2. SCR for 2035 concentrated Radial Topology for two dispatch scenarios with low and high offshore wind penetration for summer peak load condition

POI Details		Low offshore wind scenario		High offshore wind scenario	
POI Name	**OSW Capacity (MW)**	**Power injection (MW)**	**SCR**	**Power injection (MW)**	**SCR**
Fairview	2000	168	5.15	1786	4.88
Humboldt	120	4	15.14	120	15.07
Fern Rd	3880	81	3.21	3860	3.04
Collinsville	4000	180	9.94	3740	8.91
Diablo Canyon	5000	105	4.72	4990	4.45

As shown in, the POIs were moderate-to-strong for both high and low offshore wind generation scenarios. As evident from the results, grid strength was higher during the low offshore wind production case, as more synchronous machines were dispatched to supply the load, and these machines had higher short-circuited current capabilities. However, for N-1/N-2 contingencies for the same scenarios, the short circuit ratio dropped below three, which led to weak grid conditions. An important point to note here is that the contributions of IBRs in providing short circuit current capabilities initially were not considered, consistent with common practice. However, the WI has a large amount of these IBRs, and their contribution in short-circuit currents can further improve overall grid strength.

[42] Grid strength studies for the 2050 topologies are omitted from this study, as the overall grid topologies and generator models will be significantly different from present grid conditions, as a result the grid strength analysis may not correctly capture the short-circuit MVA available at POIs.

Figure B.7. Grid strength visualization for 2035 Concentrated Topology for (left) low offshore wind power and (right) high offshore wind power injection.

Table B.3. SCR during N-1/N-2 network contingencies for 2035 concentrated Radial Topology for two dispatch scenarios with low and high offshore wind penetration

POI details		Low offshore wind scenario		High offshore wind scenario	
POI name	**OSW capacity (MW)**	**SCR (N-1)**	**SCR (N-2)**	**SCR (N-1)**	**SCR (N-2)**
Fairview	2000	3.18	3.05	3.02	2.89
Humboldt	120	9.75	7.96	9.72	7.95
Fern Rd	3880	2.24	2.23	1.90	1.88
Collinvsille	4000	8.15	7.83	7.24	6.9
Diablo Canyon	5000	4.13	3.51	3.87	3.16

Similarly, POIs in 2035 Distributed Radial Topology were also analyzed. Few of the POIs observed improvement in grid strength in this new topology, however the trend from low wind scenario to high wind scenario remained the same. It is important to note that one of the POIs (Fern Rd) experienced weak grid conditions even during normal operating conditions.

Table B.4. SCR for 2035 Distributed Radial Topology for two dispatch scenarios with low and high offshore wind penetration for summer peak load condition

POI Details		Low offshore wind scenario		High offshore wind scenario	
POI name	**OSW capacity (MW)**	**Power Injection (MW)**	**SCR**	**Power injection (MW)**	**SCR**
Fairview	1000	174	6.07	920	5.92
Del Norte	1000	98	4.875	800	4.33
Humboldt	120	4.3	6.49	120	6.4
Fern Rd	2880	103.68	3.21	2800	2.94
Collinsville	2000	231	13.46	1920	12.8
Tesla	1000	78	8.83	940	8.24
Bay Hub	1000	25	14.04	940	13.97
Moss Landing	1000	204	4.74	940	4.59
Diablo Canyon	5000	30	4.71	4990	4.42

Further, for the same dispatch scenario we have assumed, all large IBR generation sources (>100 MW capacity) could provide fault ride-through capability and short-circuit MVA up to their MVA rating (i.e., impedance = 1). With that assumption, we observed significant improvement in grid strength for all POIs.

Table B.5. SCR for 2035 Distributed Radial Topology for high offshore wind injection case with and without the contribution of the IBRs in short-circuit current.

POI Details		Without contribution of IBRs		With short-circuit contribution of large IBRs	
POI name	**OSW capacity (MW)**	**Power injection (MW)**	**SCR**	**Power injection (MW)**	**SCR**
Fairview	1000	920	5.92	920	7.29
Del Norte	1000	800	4.33	800	5.84
Humboldt	120	120	6.4	120	7.62
Fern Rd	2880	2800	2.94	2800	4.18
Collinsville	2000	1920	12.8	1920	13.5
Tesla	1000	940	8.24	940	9.76
Bay Hub	1000	940	13.97	940	14.41
Moss Landing	1000	940	4.59	940	6.19
Diablo Canyon	5000	4990	4.42	4990	6.24

B.3 Seismic Resilience

In a similar way to wildfire, simulations for earthquakes were conducted to develop grid contingencies. Probabilistic Shakemap scenarios developed by the United States Geological Survey were used to represent earthquake events (USGS 2022). The resulting peak ground acceleration from the hypothetical scenarios at a given location was associated with the probability of failure of the transmission tower, as highlighted in Figure B.8. These fragility curves were not developed specifically for the West Coast context but were adopted from Park et al. (2016). The effect of earthquake across the entire area was deemed to be instantaneous. Dynamic simulations followed the system response to earthquake onset.

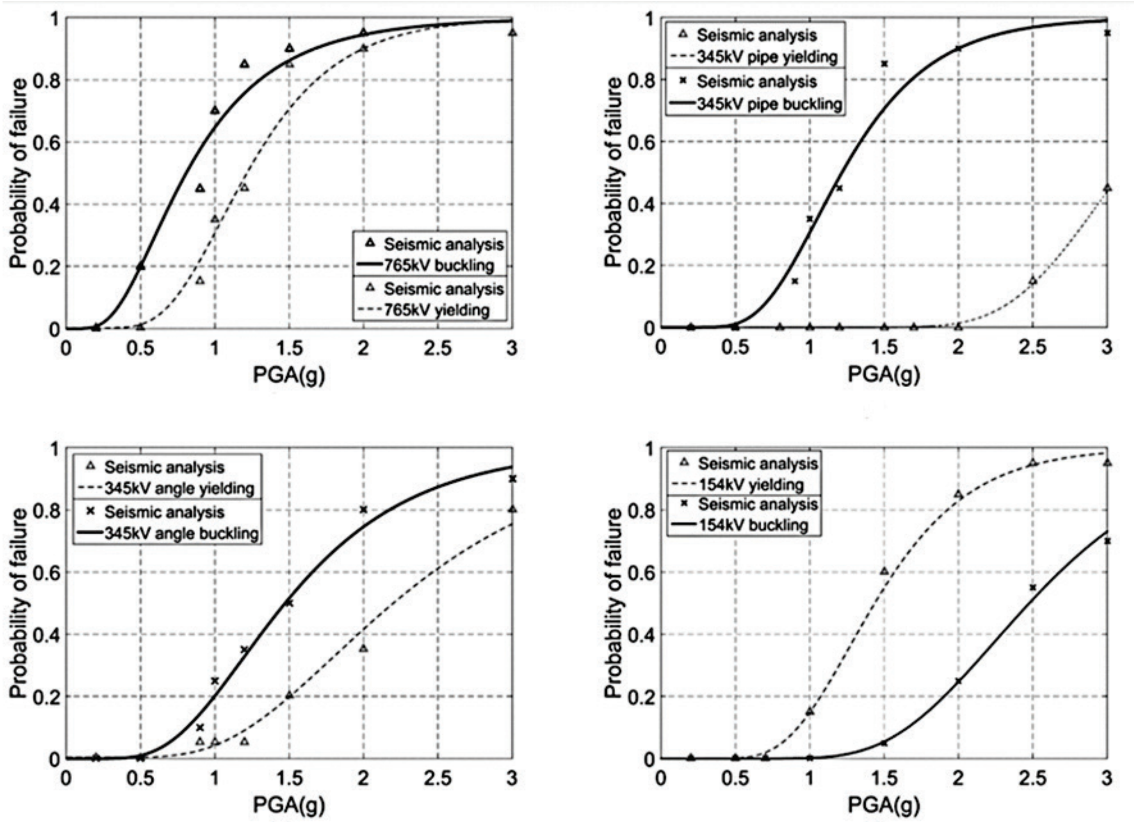

Figure B.8. Seismic Fragility Curves for a) Pipe-type 765 kV, b) Pipe-type 345 kV, c) Angle-type 345 kV, d) Angle type 154 kV Transmission Tower for Yielding and Buckling (Park et al. 2016)

To characterize the earthquake risk, a synthetic magnitude 7.1 time series was constructed based on the USGS Great Valley 3 Scenario and analyzed through EGRASS and DCAT (USGS 2016). The scenario is depicted in Figure B.9.

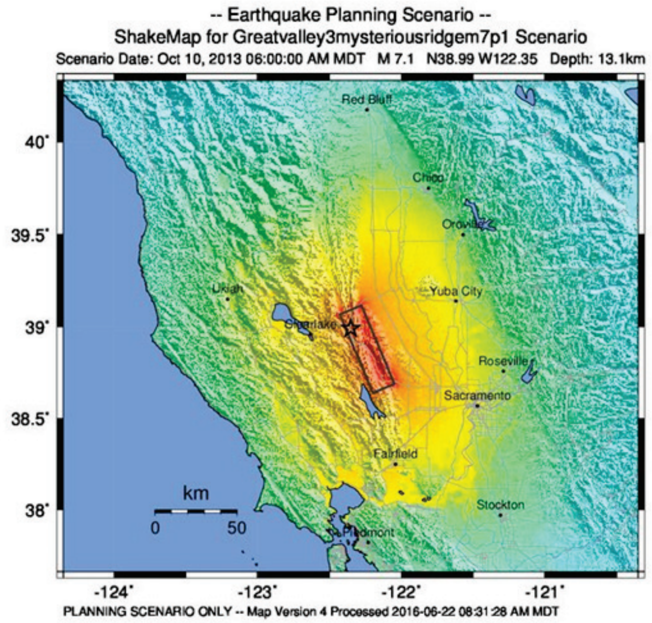

PERCEIVED SHAKING	Not felt	Weak	Light	Moderate	Strong	Very strong	Severe	Violent	Extreme
POTENTIAL DAMAGE	none	none	none	Very light	Light	Moderate	Mod./Heavy	Heavy	Very Heavy
PEAK ACC.(%g)	<0.1	0.5	2.4	6.7	13	24	44	83	>156
PEAK VEL.(cm/s)	<0.07	0.4	1.9	5.8	11	22	43	83	>160
INSTRUMENTAL INTENSITY	I	II-III	IV	V	VI	VII	VIII	IX	X+

Scale based upon Wald, et al.; 1999

Figure B.9. USGS Shakemap for Great Valley 3 Magnitude 7.1 earthquake scenario (USGS 2016)

Unlike wildfire, system response to the event was unstable due to the significant failure of onshore transmission towers and thus conductors, as shown for the 2035 Concentrated Topology set, as indicated in Figure B.10. Though OSW generation and transmission assets were not failed directly under the dynamic contingency, they were unable to mitigate system frequency departures resulting from the failure of the much larger onshore system.

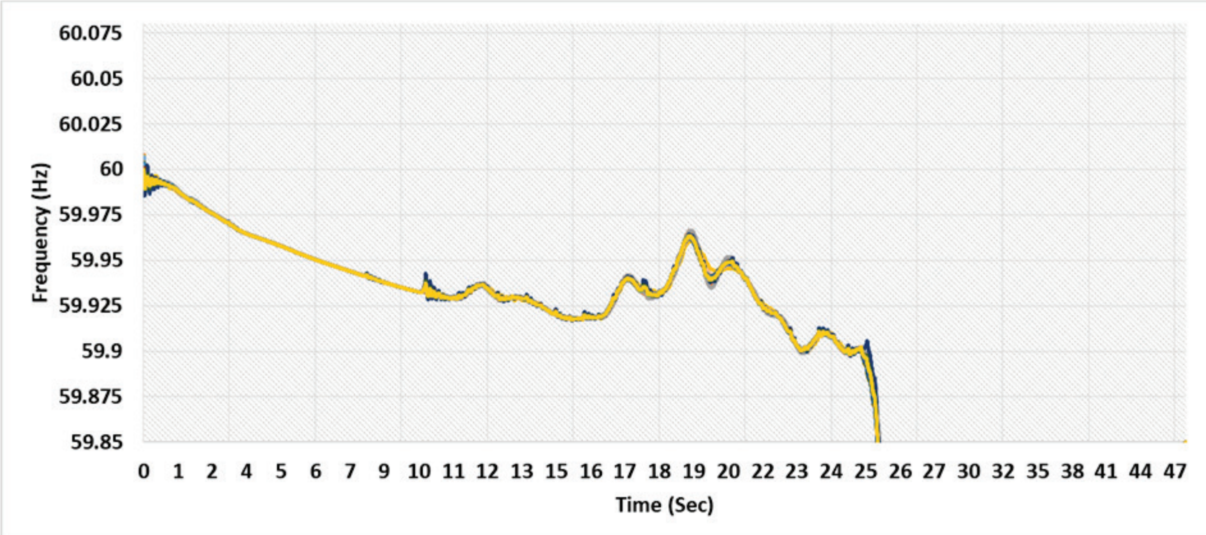

Figure B.10. System response to synthetic earthquake simulation, 2035 Concentrated Topology set. Different colors represent frequencies encountered at various busses on the system.

B.4 GIS Power System Plotting Tools

Several tools were developed to visualize the large set of operating conditions analyzed and system dynamic contingency responses analyzed on WOW-TS and to communicate the results to collaborators, system operators, and other Advisory Committee members. On the study, the state of the WECC bulk transmission system was analyzed across an entire year on an hour-by-hour basis for multiple future scenarios. The future scenarios captured various stages of planned integration of offshore wind generation through PCM followed by AC power flow analysis for each hour of the year. This effort produced the hourly variation in regional loads and generation mixes, with anticipated effects on transmission system congestion and bus voltage levels. The goal of visualizing these types of steady state results was to connect potential voltage and congestion issues to the hourly generation mixes and load levels. Figure B.11 shows an example visualization of power flow results for a specific hour from the 2035 Concentrated Topology set using the visualization process developed in the tool.

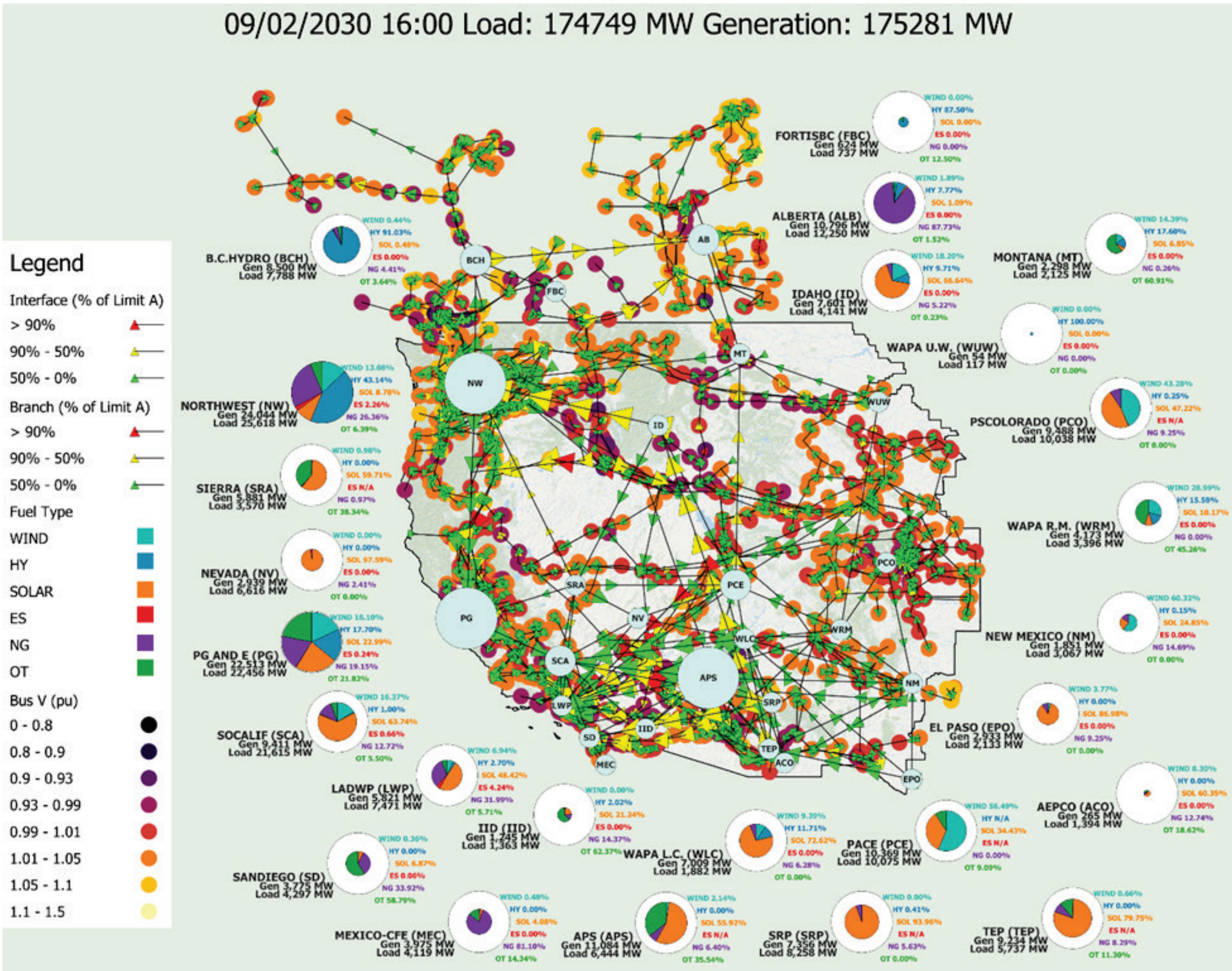

Figure B.11. AC-PF visualization for 2030/09/02 4:00 PM case

These visualizations were designed to support comprehension of the system state across the large geographic area in the WI by highlighting sub-regions of concern rather than problems with individual elements. The tool allows users to visualize generation mix by subregions with pie charts. Bus voltages levels are color-coded to differentiate voltage or frequency levels. Line loading and interface flow are clearly marked with different colored arrows to show directions and loading conditions.

Additionally, the dynamic behavior of the WECC bulk transmission system is anticipated to change with offshore wind integration and dynamic visualization capabilities are also useful. In this case, steady state conditions produced from the power flow analysis were fed to the DCAT tool to provide the initial conditions for dynamic simulation of cascading impacts from transmission line contingencies. The DCAT tool produced sets of time series data that capture the responses of the generators and the resulting variations to line flows, bus voltages, and bus frequencies. The goal of visualizing these results is to communicate the scale of the impacts of the line contingencies that are simulated. The tool accomplishes this task by producing images of the system as snapshots of the conditions over time. Figure B.12 shows an example snapshot of bus frequencies from a DCAT simulation of cascading line outages from an extreme earthquake event.

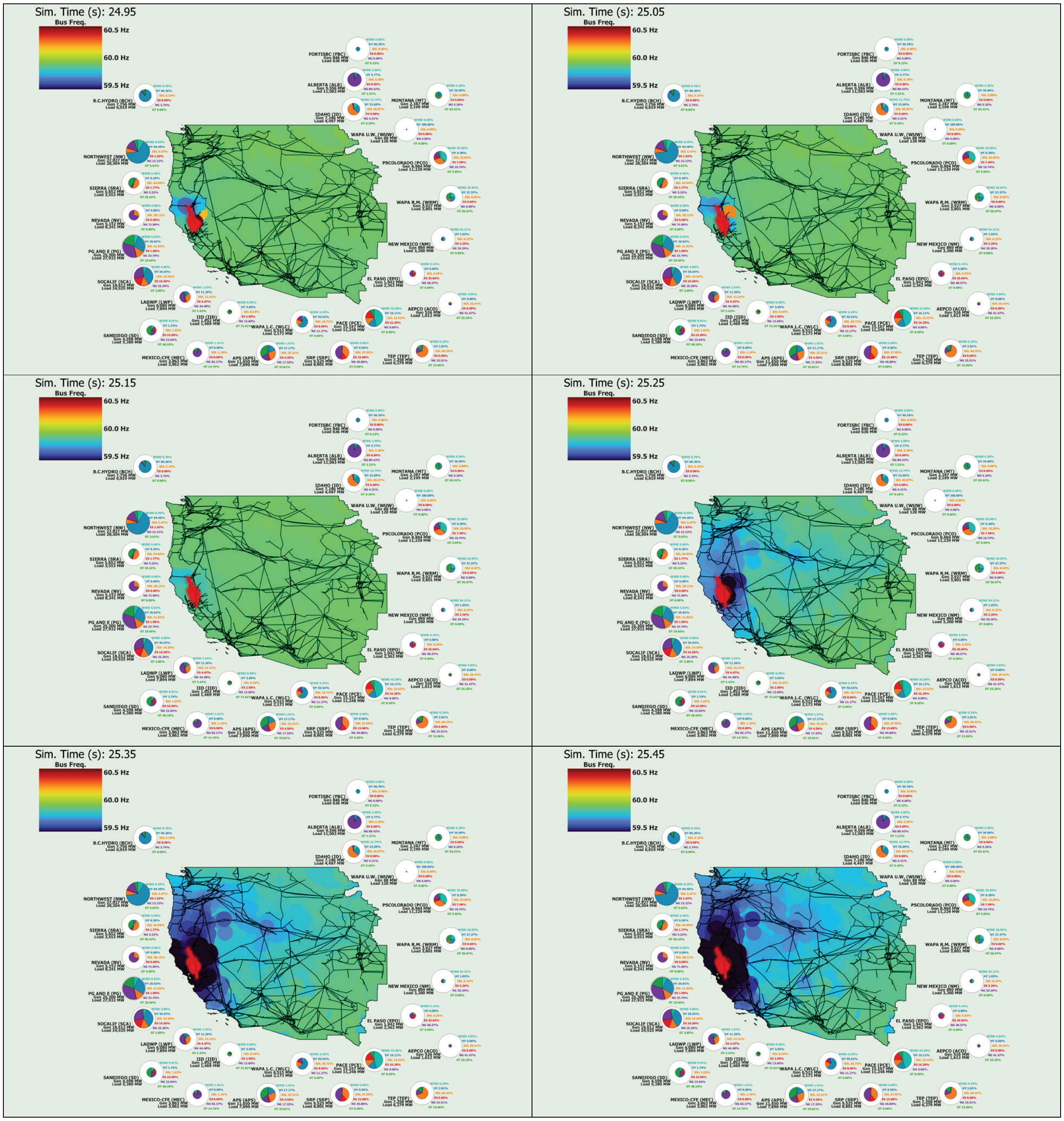

Figure B.12. Selected snapshots of DCAT simulation of an extreme earthquake event for 2030/07/16 6:00PM

These images were aggregated into GIF format so that the audience can comprehend the sequence of events from the system wide impacts perspective. Where large portions of the WECC system are colored with darker shades, the viewer can understand that the line contingency (or its cascading effects) led to dramatic, system wide adverse conditions.
The tool accomplishes its objectives by leveraging the python application programming interface (API) of QGIS, which is an open-source Geospatial Information System (GIS). The benefits of using QGIS is that it provides extensive customization of data layer styles and print layouts, which facilitates creating complex visualizations that can communicate multiple, big-picture

simulation outcomes. Additionally, the API allows automatic generation of the map images, which dramatically reduces the time to process the numerous, independent hourly cases resulting from the PCM process. Last, QGIS features many advanced vector geometry processing algorithms. By developing the visualization process using QGIS, future efforts to improve the application can explore the use of these algorithms in developing more intuitive visualizations of the AC-PF and DCAT data.

B.5 Dynamic Model Preparation

The dynamic model preparation process for large interconnected systems is time-consuming. To make dynamic model preparation easier, project scripts and procedures were used (Samaan et al. 2015). The initial step is to prepare the master dynamics file. The master dynamics file contains the majority of the dynamic models for a specific future year. This master dynamics file makes it easy to prepare dynamic files for different hours/operational conditions within a given year. As a result, this job consists of two major stages.

1. Create a master dynamics file for a future year.
2. Creating dynamic files for future operation conditions in a certain year.

Figure B.13 illustrates the process of preparing a dynamic model for any future planning case utilizing the master dynamic file. The following is a discussion of the preparation process, broken down into its individual stages:

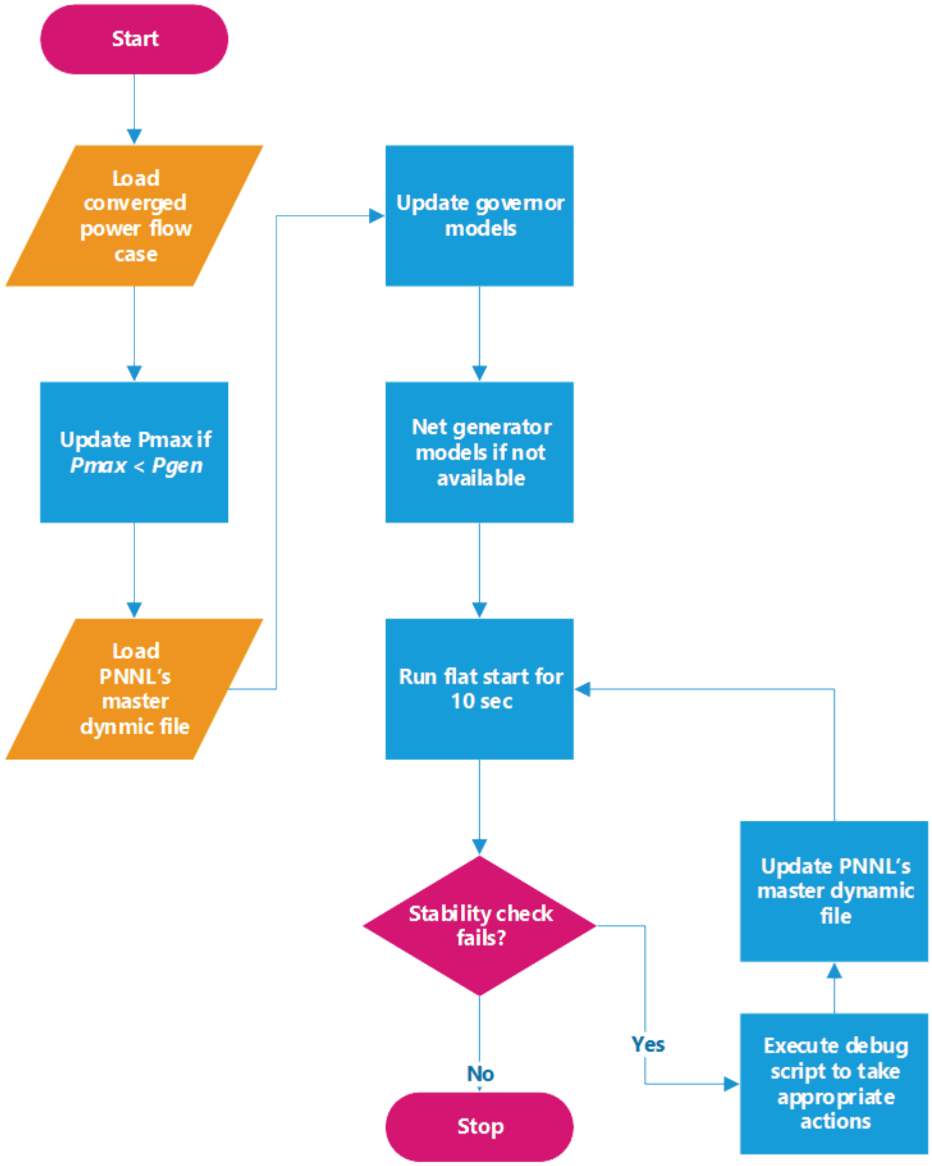

Figure B.13. Dynamic model preparation process

B.5.1 Preparation of master dynamics file for a specific future year

To prepare the master dynamics file, we first considered a sample hour/operating condition and obtained the converged AC power flow case and a dynamic file corresponding to a past year. We then proceeded to make the following changes to develop the master dynamics file as discussed below. We used PSLF in this work as the simulation software to develop a master dynamic file with a flat start.

B.5.1.1 Stage 1: Removal of duplicate models

In this step, the duplicate models in the existing dynamic file are identified by loading it in PSLF.

B.5.1.2 Stage 2: Adjust ID mismatch issues between the models in dynamics and steady state

In this step, the units that have ID mismatch errors are identified by loading the dynamics file into the PSLF. A script was implemented to automatically locate these units in the dynamics file and search for the corresponding unit in the power flow case. If it is identified in the power flow case, the ID mismatch error is resolved. If a unit is absent in the power flow case, it is considered an additional model in the dynamics file.

B.5.1.3 Stage 3: Addition of missing dynamic models corresponding to newly added units in power flow case for future year

In this step, the models that were missing from previous years or the new units for the upcoming year are incorporated into the dynamic file, following this process:

1. All missing units with “PMAX” exceeding 60 MW, regardless of their status, were taken into account for inclusion in the dynamic file. Currently, any units smaller than 60 MW are netted.
2. To replace a missing machine model, we searched for devices in the dynamics file with the same unit subtype and added the appropriate model from relevant samples.

B.5.1.4 Stage 4: prepare protection models:

For each generating unit, undervoltage, overvoltage, underfrequency, and overfrequency relays have been modeled. According to the new NERC Standard PRC-024-1, "Generator Frequency and Voltage Protective Relay Settings," the settings for generating units’ protection relays were chosen in DCAT (NERC n.d.).

B.5.1.5 Stage 5: Adjust the “MWCAP” of “GGOV” units based on power flow case

In this step, the proposed work adjusts the “MWCAP” value of the GGOV units by identifying the maximum of “MBase” and “PMAX” of the corresponding unit in power flow case. This is because the power flow case has units whose “MBase” is sometimes greater than “PMAX.” After identification, the “MWCAP” of “GGOV” is updated with the identified value plus 20 MW (as buffer) for better initialization.

B.5.1.6 Stage 6: Adjust “MVABase” mismatches between the models in dynamics and power flow case

In this step, the “MVABase” of all machine models are updated to with the corresponding value of the units from power flow case.

B.5.1.7 Stage 7: Remove extra models

Remove extra models from dynamics file which does not have a unit in power flow case.

B.5.1.8 Stage 8: Model input parameter tuning considering numerical stability

In this step, we do not modify the sensitive parameters of the dynamic models but rather adjust the input settings of the models to avoid any constraint violations.

B.6 Database Module for Contingency Results

The results discussed in this report derive from an extensive analysis, examining hundreds of power flow cases alongside thousands of contingencies to compare grid performance across numerous planning scenarios. The study team effectively employed the interactive visualization and database management system created in the NTP study project to visually investigate and analyze system behavior.

The research team employed Python automation scripts from NTP to effectively manage extensive power flow datasets generated by production cost models, power flow tools, and contingency analysis methods. These scripts employ QGIS to enable the automated creation of comprehensive, interactive maps that showcase power flow information, including the transmission grid layout, voltage profiles, and transmission line loading. Comprehensive back-to-back automation enables users to retrieve power flow information from solvers, typically found in binary files, process this data, and upload it to the database server. This facilitates the creation of GIS visualizations, including QGIS layers, and tailored QGIS projects for particular power flow cases or scenarios. The analytics module evaluates all simulated contingencies across various events and situations, enabling the user to select areas for more detailed analysis. This module facilitates future integration with widely recognized Big Data analytical and interactive visualization tools.

Figure B.14 displays a flowchart of the visualization automation process. The study team employed NTP's cloud-based GIS database architecture to take advantage of the strong and scalable infrastructure offered by AWS cloud services. This architecture employs a PostgreSQL database, an advanced object-relational database system recognized for its strong data management features.

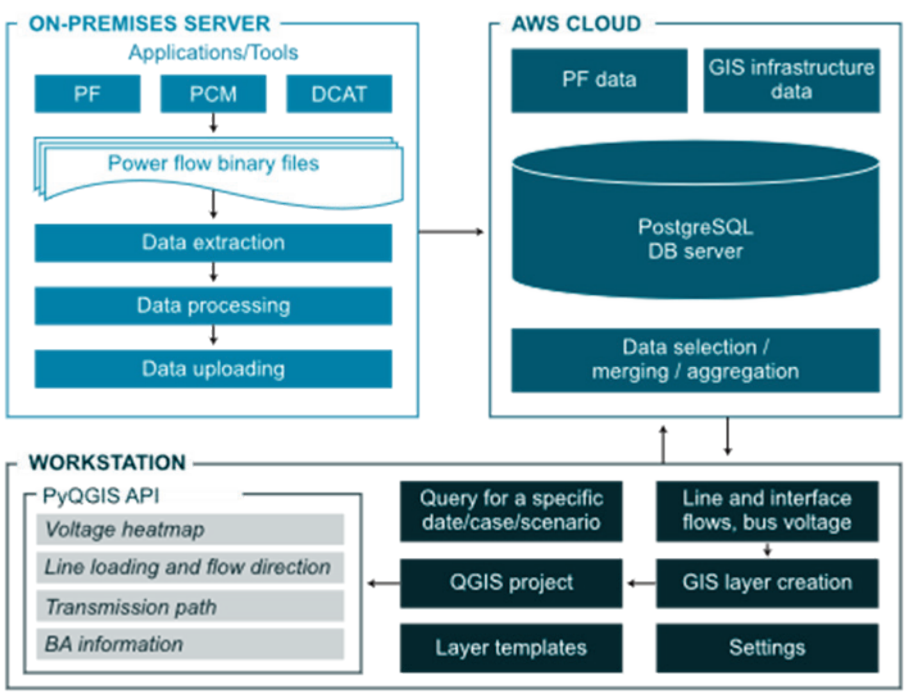

Figure B.14. Flowchart showing the automated process for analyzing and visualizing simulation results.

The database archived commercial GIS data concerning electricity infrastructure, the simulation outcomes from the production cost model, power flow, and contingency analyses, systematically indexing these results with specific identifiers like scenario, case, and date, thereby enhancing efficient data retrieval and organization. The PostgreSQL database on AWS offers robust data manipulation capabilities, facilitating quick data retrieval, aggregation, and the integration of datasets (e.g., combining power flow data with bus locations).

Appendix C – Department of Defense Siting Considerations

DoD Draft Language for

U.S. DOE-PNNL-NREL West Coast Offshore Wind Transmission Study &

BOEM-NREL Floating Offshore Wind Energy Costs and Opportunities in Washington State

The Department of Defense (DoD) is committed support energy development in a manner that is compatible with military activities. DoD collaborates with stakeholders to identify and avoid conflicts between proposed energy projects and current and anticipated future military requirements.

Washington is home to a number of military installations, including homeports for a large number of naval forces supporting national defense interests in the Pacific. At-sea training, testing, and routine operations rely the availability of adequate air, sea, and undersea space to safely and effectively execute their missions.

DoD coordinated with the study team to support mapping analysis for the siting of offshore wind transmission infrastructure. Analysis of the potential for impacts to at-sea readiness activities conducted offshore Washington is ongoing within DoD. Offshore wind has the potential to impact at-sea military operations, largely through the introduction of obstructions to air and sea space, and interference with radar, telemetry, and other range systems.

Early and ongoing coordination with the DoD to address any potential impacts is critical to achieve sustainable energy solutions and ensure viability of critical military training and testing activities, and operating areas.

Appendix D – Export System Costs

Export cable costs for both HVAC and HVDC lines (Figure D.1) were estimated based on a combination of recent feedback from industry and previously published studies. A 420 kV HVAC line was chosen for distances to points of interconnection shorter than 75 km in most instances, given that this choice is more economical than the HVDC line under that distance threshold (this is the point where cost curves intersect in Figure D.1). Longer HVAC also become less practical due to reactive power compensation needs.

These cost curves are the sum of components for each export system. From industry consultation, we assume costs similar to static cables for this study, since the vast majority of the length of each cable would be static, with the only dynamic portion being at the end near the platform. Based on recent talks with industry, we assume $3.5 M per km per 420 kV HVAC cable including installation, where installation is 30% of the cable cost. For a 1 GW HVAC system, there are 2 cables assumed, and one substation. The cables can carry 500 MW of real power each, and substations allow for 2 of these cables.

For the HVDC cable costs, we assumed $5.3M per km for a bipole 525 kV HVDC cable bundle with dedicated metallic return, which includes an 8% risk factor and 15% inflation rate from the costs outlined in Brinkman et al. (2024). The installation cost for the 525 kV HVDC cable is assumed to be 30% of the total cable cost. The cable bundle is assumed to be able to carry 2 GW, and there would be one offshore substation per cable bundle.

For HVAC, we assume substation costs (both onshore and offshore) of approximately $600M per 1 GW system (including platform costs), plus reactive power compensation cost of $0.54 M, per km, per GW (for shunt reactors at both ends). For HVDC, we assume substation costs of $1.9 b, including converter stations and platform costs.

For interlinking in a multi-terminal HVDC network, we assume that adding a small auxiliary platform hosting DC circuit breakers would cost $150M for a single additional cable coming from the wind energy area, and $242M for two additional cables. This includes the costs of the platform, and also the DC circuit breakers ($31M per pole, installed). These costs originate from Brinkman et al. (2024).

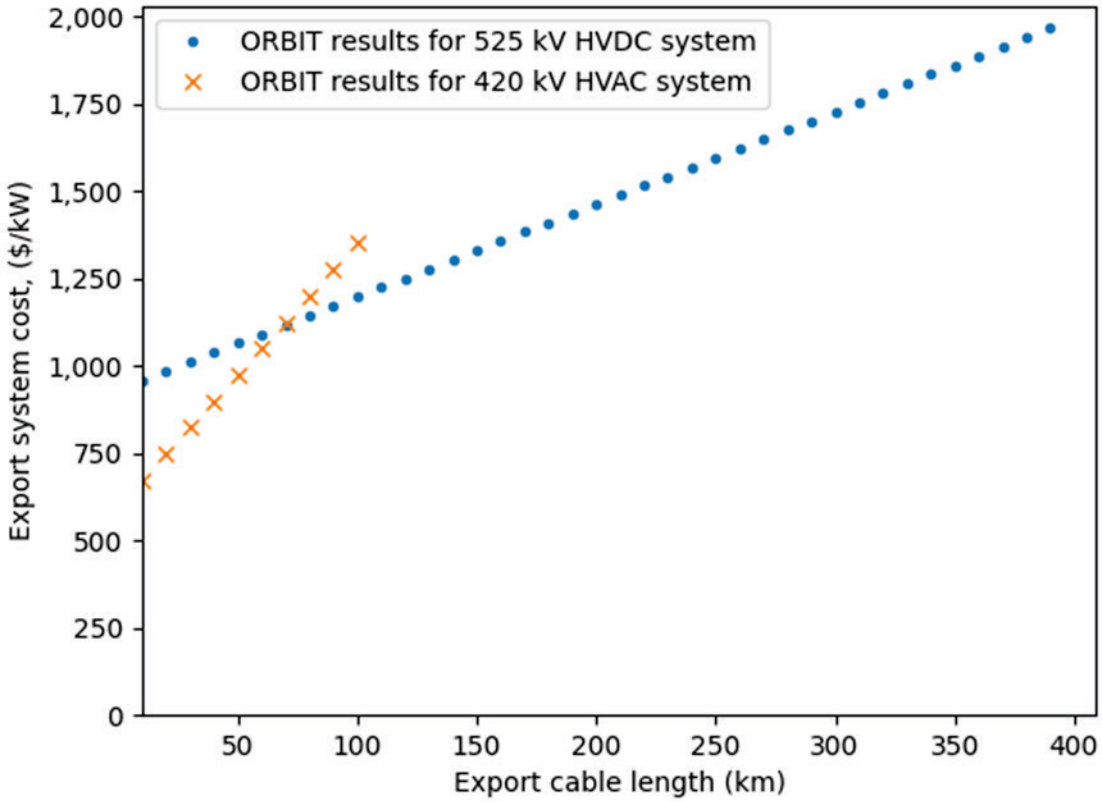

Figure D.1. Export system costs per kW for a 2 GW HVDC system, or a 1 GW HVAC system

The export system costs for the different cable types (in $/kW) are given below for 525 kV HVDC,

$$Cost = 2.65x + 932 \tag{5}$$

and for 420 kV HVAC:

$$Cost = 7.54x + 596 \tag{6}$$

where x is the export cable length in km.

Appendix E – Tradeoffs between Floating Substructure Topologies

There are several floating substructure choices that exist (Beiter et al. 2020a; Ojo et al. 2022), and each choice has its own benefits and drawbacks (Table E.1).

Table E.1. Tradeoffs between different substructure choices

Substructure type	Seabed footprint	Installation complexity
Tension Leg Platform	Lower than the listed alternatives	Mixed reviews- some say easier to install in deep water, others mention difficulty and high initial cost
Semisubmersible	Typically high but can be modified	Lower than many alternatives and lower sensitivity to water depth
Spar	About the same as a semisubmersible	Designed for use in deeper waters due to large draft, sensitive to weather

Three common choices tension leg platforms (TLP), semisubmersibles, and spars (Figure E.1). These choices all result in relatively similar loads on the wind turbine (Robertson and Jonkman n.d.). The spar buoy has ballast and deep draft to help maintain its stability. It requires assembly at sea in a deep water area sheltered from high waves, which can be hard to find. As such, more modifications to the spar buoy system are needed to make it commercially attractive (Beiter et al. 2020a). The semisubmersible design is dependent on buoyancy and surface area to maintain stability and has a definite advantage of being able to support the wind turbine before being connected to the mooring lines. This allows the turbine and substructure system to be assembled at port and towed to site or disconnected from their mooring lines at site and towed back to port for maintenance. The tension leg platform uses tension in the mooring lines to achieve stability, so is unstable until attachment of mooring lines. Once installed, it has a smaller seabed footprint, which can be preferential to certain stakeholders (Green et al. 2023). However, installation can be expensive and ways to reduce cost and installation difficulty are currently being examined.

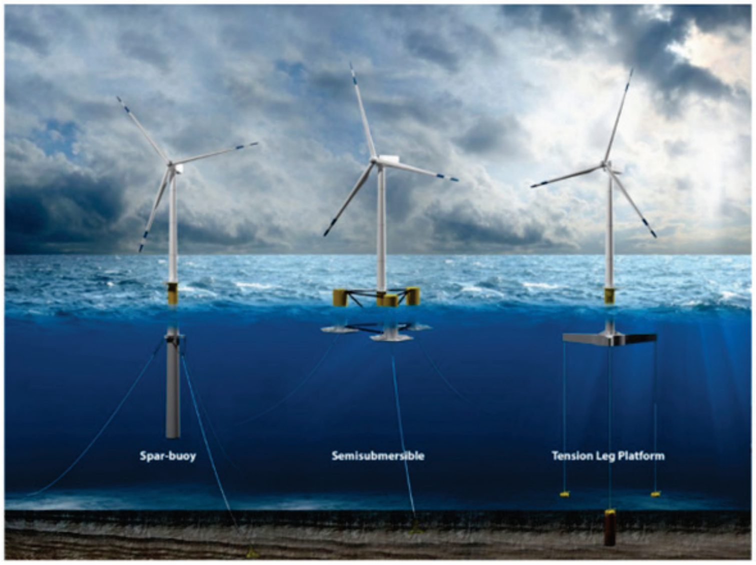

Figure E.1. Substructure types for floating offshore wind farms. Illustration by Josh Bauer, NREL

Mooring systems can vary in design and need to be compatible with the chosen substructure. The main configurations currently used in industry are the catenary mooring system and taut leg mooring system. The catenary system is more common in shallow waters, is the easiest to manufacture, and use drag-embedment anchors depending on anchoring points and system design. Taut leg mooring systems are pre-tensioned until taut, and have an angle of about 30-45 degrees (Corewind 2021). Mooring lines in deeper waters are longer and anchor installation is correspondingly more difficult, which increases station keeping costs. The layout of anchors in very deep water can also be more challenging because there is increased possibility for interference between neighboring turbines mooring systems. Shared mooring systems can be a way to reduce mooring system costs and problems with neighboring anchor interference. Shared mooring systems have mooring lines from the interior of the wind farm run directly between adjacent floating platforms instead of to anchors (Hall et al. 2022). This reduces the number of mooring lines to the seabed and therefore the total line length as well as the number of anchors. Connolly and Hall (2019) found cost savings for shared mooring systems at depths more than 500 m. The number of turbines suitable for each shared mooring system should also be analyzed as the number of turbines impacts accumulation of thrust loads (Goldschmidt and Muskulus 2015).

Appendix F – Economic Analysis

F.1 Regional Disaggregation Methodology

As interregional transmission enables more coordinated operation of low-cost generation resources, the distribution of operating costs within each region changes. For systemwide, analysis evaluating changes in operating costs are sufficient to quantify cost impacts across scenarios. When evaluating the benefit distribution among regions, a further consideration is needed to capture the transmission benefits of interregional trade to each region. The adjusted production cost (APC) metric is used to evaluate these benefits. The APC is the difference in total production costs adjusted for import costs and export revenues with and without a proposed transmission upgrade. This metric is used among independent system operators/regional transmission operators in the United States for transmission valuation and cost allocation including SPP, MISO, and PJM and is defined as follows:

$$APC = Production\ Costs + Purchase\ Costs - Generator\ Revenues \tag{7}$$

where,

$Purchase\ Costs$ = (Hourly Consumer Load + Storage Charging + Imports) × Locational Marginal Price

$Generator\ Revenues$ = Hourly Generation × Locational Marginal Price

A key benefit of the APC when trying to disaggregate transmission benefits is that it does not strictly rely on the physical location where costs are incurred to estimate costs and benefits. As a simple example, a new transmission upgrade may enable the development of low-cost generation capacity in one region (Region A) that can serve additional load in a neighboring region (Region B). Strictly looking at where costs are occurring, the new transmission line will increase capital and operating costs in Region A because it is building more capacity and generating more. By contrast, capital and operating costs will decrease in Region B because it is building less capacity and relying on imports to meet its load. However, Region A is also benefiting through increased sales of power to its neighbors. In addition, Region B is not getting these imports for free; it incurs some cost to purchase imported energy. By including an adjustment for import costs and export revenues, the APC can capture these benefits.

F.2 Stakeholder Disaggregation Methodology

The metrics used to estimate the benefits to generators, load-serving entities, and transmission owners are producer surplus, consumer surplus, and transmission rent. This methodology follows CAISO (2017) and Hogan (2018) for calculating these metrics using production cost modeling data. See Mankiw (2024) or Varian (1992) for a more general introduction to the metrics for economic market analysis. Producer surplus is defined as the difference between revenue received and operating costs. Graphically, this can be computed as the area above a supply curve and below the price received by the generators. Consumer surplus is defined as the difference between total load benefits and the load payments. Graphically, this can be computed as the area below a demand curve and above the price paid by load. Transmission rents (also called congestion rents) are defined as the difference between the load payments and generator revenue.

Generator benefits are estimated as producer surplus, the annual operating profits (revenue minus cost) to the generators. This metric does not incorporate the generation or transmission capital costs. The generator revenues and costs were obtained from the PCM simulations and are summed over all hours in the year and all generators. Generator revenue is estimated by multiplying the hourly LMP at the generator by the hourly dispatched generation—that is, generators are not compensated for generation curtailed in the model. The total benefits to generators are computed by summing over all generators *j* and hours *h* using the following equation 8:

$$Benefit_{gen} = \sum_{h=1}^{8760} \sum_{j=1}^{J} Benefit_{jh} = \sum_{h=1}^{8760} \sum_{j=1}^{J} LMP_{jh} \times Generation_{jh} - Cost_{jh} \tag{8}$$

Transmission owner benefits are estimated as the total congestion in the PCM simulations. There are two approaches that can be used to calculate transmission owner benefits. The first is multiplying the congestion price on a line by the flow on the line and summing over all lines. The second approach is by taking the difference between load payment and generator revenue. CAISO (2017) and has shown that these approaches give the same numerical value (eq. 9):

$$Benefit_{to} = \sum_{h=1}^{8760} \sum_{l=1}^{L} Load\ Payment_{lh} - \sum_{h=1}^{8760} \sum_{j=1}^{J} Generator\ Revenue_{jh} \tag{9}$$

Load-serving entity benefits are estimated using consumer surplus, the total load benefits minus the load payments. The total load benefits represent the overall economic benefit to all end-consumers from electricity use. The total load benefit is a large value to the consumers but is outside the scope of this study to estimate. This study estimates the change in benefits when comparing different transmission topologies, and this is leveraged to estimate load-serving entity benefits without requiring an estimate of total load benefits. When the total load benefit is equal across the scenarios being compared, their difference is zero, and the change in load-serving entity benefit simplifies to the avoided cost in load payments. The critical assumption required for the total load benefit to be equal across scenarios is that load demand is the same across the compared scenarios. This assumption is held true within the production cost modeling input assumptions. Load payments are obtained from the PCM simulations, where it is calculated by multiplying the hourly LMP by the hourly load and summing over all hours in the year and all load locations (eq. 10).

$$\Delta Benefit_{lse} = \Delta \sum_{h=1}^{8760} \sum_{l=1}^{L} LMP_{lh} \times Load_{lh} \tag{10}$$

An important result of this method of disaggregation is that the total benefits as defined by the sum of the network user benefits is equal to the avoided generator costs, so the total benefits are equal to the operating cost benefits as shown in the system-wide benefits section.

Pacific Northwest National Laboratory

902 Battelle Boulevard
P.O. Box 999
Richland, WA 99354
1-888-375-PNNL (7665)

www.pnnl.gov

National Renewable Energy Laboratory

15013 Denver West Parkway
Golden, CO 80401
(303) 275-3000